Characterization of HAdV-C5 E4orf6 as a negative regulator of E1B-55K SUMOylation

Dissertation

with the aim of achieving a doctoral degree at the Faculty of Mathematics, Informatics, and Natural Sciences,
Department of Biology,
University of Hamburg

submitted by
Marie Fiedler
October 2020, Hamburg

Tag der Disputation: 22.01.2021

Erster Gutachter: Prof. Dr. Thomas Dobner

Zweiter Gutachter: Prof. Dr. Wolfram Brune

Declaration on oath

I hereby declare on oath that I have written the present dissertation myself and have not used any sources or aids other than the ones indicated.

Hamburg

30.09.2020

Signature

HPI Heinrich Pette Institute
Leibniz Institute for Experimental Virology

HPI • Martinistraße 52 • D-20251 Hamburg

Dr. Timothy Soh, Ph.D.

Research group of
Quantitative and Molecular Virology

Phone: +49 (0) 40 48051-273
timothy.soh@leibniz-hpi.de

Hamburg, September 30, 2020

Marie Fiedler's Ph.D. thesis entitled "**Characterization of HAdV-C5 E4orf6 as a negative regulator of E1B 55K SUMOylation**" is written in fluent and proper English. I confirm that the language is clearly written and properly articulated.

Kind regards,

Table of content

Abbreviations

aa	amino acid
Ab	antibody
AdV	Adenovirus
bp	base pair
BRK	baby rat kidney cells
CAR	Coxsackie/Adenovirus-receptor
DAPI	4‘,6‘-diamidine-2'-phenylindole dihydrochloride
DDR	DNA damage response
DMEM	Dulbecco’s Modified Eagle Medium
ds	double-stranded
E. coli	*Escherichia coli*
EBV	Epstein-Barr Virus
et al.	and others (*et alii*, lat.)
ffu	fluorescence forming unit
fwd	forward
h.p.i.	hours post infection
h.p.t.	hours post transfection
HAdV	human Adenovirus
HCMV	human Cytomegalovirus
HPV	human Papillomavirus
HRP	horseradish Peroxidase
HSV-1	Herpes Simplex Virus Type 1
IFN	interferon
IgG	immunoglobulin G
ITR	inverted terminal repeat
KSHV	Kaposi´s Sarcoma Virus
kb	kilobase
kDa	kilodalton
MLTU	major late transcription unit
MOI	multiplicity of infection
NB	nuclear body
NES	nuclear export signal

NHEJ	non-homologous end joining
NPC	nuclear pore complex
orf	open reading frame
PAGE	polyacrylamide gel electrophoresis
PML	promyelocytic leukemia
PTM	post-translational modification
rev	reverse
RT	room temperature
SAE	SUMO activating enzyme
SENP	sentrin/ SUMO-specific protease
SEM	standard error of the mean
SCM	SUMO conjugation motif
SCS	SUMO conjugation site
SDS	sodium dodecyl sulfate
SIM	SUMO interacting motif
SUMO	small ubiquitin-like modifier
U	unit
vol	volume
wt	wild type
(v/v)	volume per volume
(w/v)	weight per volume

Abstract

The human adenovirus type 5 of species C (HAdV-C5) early region 1B-55 kDa (E1B-55K) is one of the key players in maintaining a replication competent cellular environment during infection. It prevents apoptosis, promotes late viral gene expression, and fights the DNA damage response. Its multifunctional properties are regulated primarily through posttranslational modifications (PTMs). These include most notably phosphorylations at highly conserved serine (S) and threonine (T) residues at the carboxy (C)-terminus as well as the conjugation of small ubiquitin like modifiers (SUMOs) to lysines (K) situated in the amino-terminal region of E1B-55K. SUMOylation is a reversible enzymatic reaction cascade, often usurped by viruses for protein regulation. Remarkably, phosphorylation positively influences E1B-55K SUMOylation. Several lines of evidence suggest that SUMO conjugation provides a molecular mechanism, controlling crucial functions of the viral protein. These include the repression of p53- and Sp100A-stimulated transcription via its intrinsic SUMO E3 ligase activity, proteolytic degradation of the chromatin remodeling factor Daxx and nucleo-cytoplasmic transport through CRM1-dependent and -independent export pathways. Intriguingly, SUMOylation seems to be negatively regulated by HAdV-C5 early region 4 open reading frame 6 (E4orf6). E1B-55K together with E4orf6 forms a cullin 5-based E3 ubiquitin ligase complex that induces proteasomal degradation of a variety of host restriction factors, induces a shut-off of host cell protein synthesis, and augments the production of late viral proteins. Since the reduction of E1B-55K SUMO levels by E4orf6 is an interesting internal regulatory mechanism which has not been described so far, this work aimed to establish E4orf6 as a negative regulator of E1B-55K SUMOylation and to determine how E4orf6 reduces E1B-55K SUMO levels. To further evaluate the role of E4orf6 in the regulation of SUMO-conjugation to E1B-55K, we investigated different virus mutants expressing E1B-55K proteins carrying amino acid exchanges in the SUMO conjugation sites in presence or absence of E4orf6. Here, Ni-NTA SUMO pulldown analysis of wild-type (wt) and mutant virus-infected SUMO overexpressing HeLa cells confirmed that E4orf6 substantially reduces the conjugation of SUMO to E1B-55K. The second part of this work is focused on revealing the mechanism used by E4orf6 to decrease E1B-55K SUMOylation. Therefore, we examined several steps of the SUMO cycle which may be targeted by E4orf6. Initially, it was tested whether the SUMO cycle is generally inhibited or whether only the SUMOylation of E1B-55K is

decreased. Here, early region 2A (E2A) was chosen as a representative for all other SUMO substrates and its SUMO levels have been analyzed in presence and absence of E4orf6, confirming an E1B-55K specific mechanism. By investigating E1B-55K SUMO conjugations with an unremovable SUMO mutant in presence and absence of E4orf6, we have shown that the attachment of SUMO to E1B-55K is inhibited by E4orf6. In conclusion with this finding, we have neither found evidence for an enhanced deSUMOylation by SENPs nor changes in the SUMO-phosphorylation crosstalk dependent on E4orf6. Finally, our experiments have shown that SUMO conjugation to E1B-55K is not reduced in an E1B-55K mutant lacking the E4orf6 binding region. These results indicate that complex formation between both viral proteins is a prerequisite to reduce SUMOylation. Affirming these data is the observation that co-localization of E1B-55K and SUMO 2 in infected A549 cells is enhanced in absence of E4orf6 and when an interaction between E1B-55K and E4orf6 is mutational prevented.

.

1 Introduction

1.1 Classification of Adenoviruses

Human Adenoviruses (HAdV) were isolated for the first time in 1953 from adenoid material by Wallace Rowe [1]. In 1954, these newly discovered viruses were identified as causative agents for respiratory and ocular diseases and termed adenoid degeneration (AD) agents, adenoid pharyngeal conjunctival (APC) agents and acute respiratory disease (ARD) agents, according to their clinical manifestations [2]. In 1956, they were summarized under the name adenoviruses (AdV) [3]. Today, they comprise a complete family named *Adenoviridae* [4]. Depending on their host specificity, this family is further categorized into five genera. *Mastadenoviridae* include AdVs, which infect mammals while *Aviadenoviridae* have birds as hosts. *Atadenoviridae* were isolated from reptiles, birds, ruminants and marsupials and *Siadenoviridae* have avian or amphibian hosts. The last genus is named *Ichtadenoviridae* and originates from fish (Fig. 1) [5–7]. HAdV are part of the genus *Mastadenoviridae*, which is further subdivided into seven species, termed A to G [8]. Currently, these species comprise more than 103 different types [9]. According to the international committee for virus taxonomy (ICTV), species designation is based on the phylogenetic distance, genome organization of the E3 region, G/C content, oncogenicity in rodents, host range, cross neutralization, ability to recombine, number of VA RNA genes, and hemagglutination properties [10]. Notably, types 1 to 51 were characterized predominantly by serological methods, while more recently identified types were categorized mainly via genomic analyses (Fig. 1) [9–14].

In 1962, the oncogenic potential of HAdV has been demonstrated for the first time. In this study, HAdV type 12 of species A (HAdV-A12) was identified as a causative agent for tumor formation in newborn hamsters [15]. These observations lead to the categorization of HAdV as a DNA tumor virus and in the following years, HAdV became a valuable model organism for the investigation of viral tumorigenesis.

Moreover, HAdV research contributed significantly to a better understanding of virus-host interactions and the identification of general molecular mechanisms. Among others, HAdV research led to important progress in understanding the antigen presentation to T cells and to the nobel prize-awarded discovery of mRNA splicing [16,17].

Most studies regarding virus infections were undertaken with HAdV-C2 and HAdV-C5, since they are non-oncogenic and are highly prevalent in the human population [18,19].

A further important aspect about HAdV is their clinical relevance as a drug. Due to their well-known biology, broad cell tropism, genetic stability, high gene transduction efficiency, and ease of large-scale production, HAdV derived vectors have been extensively studied for the treatment of genetic disorders, as oncolytic agents and as vaccines [20–25]. Currently, more than 20 % of all human gene therapy trials are conducted with HAdV derived vectors [22].

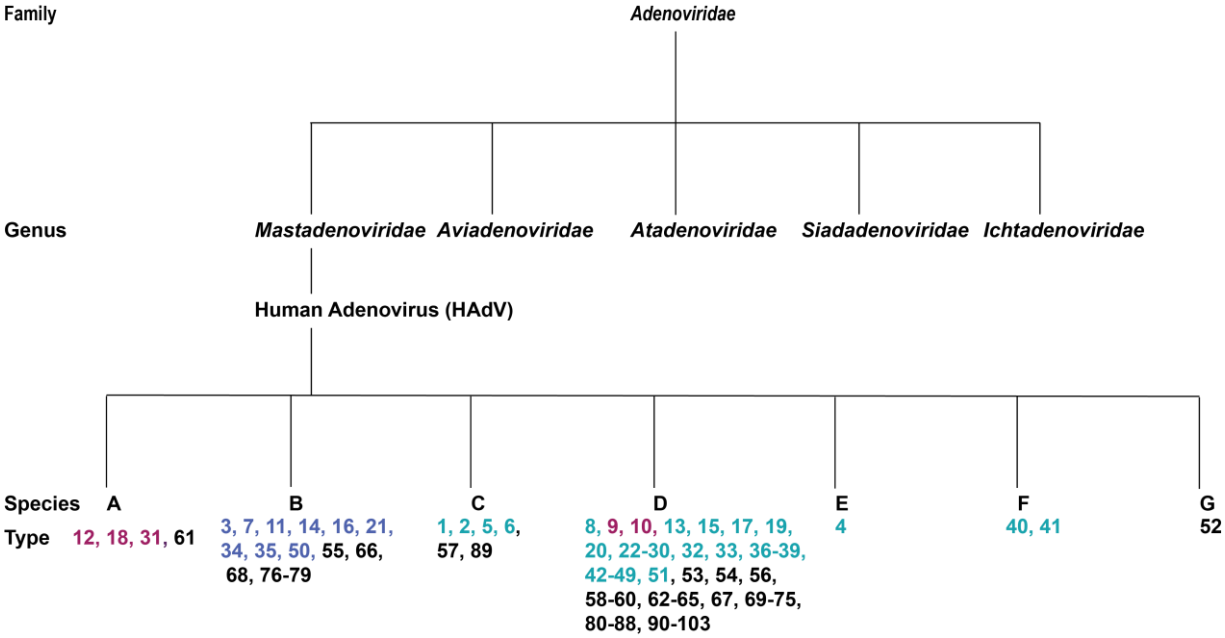

Fig. 1: Taxonomy tree of the family of *Adenoviridae*. The family of *Adenoviridae* is divided into five genera. The depicted taxonomy tree focuses specifically on HAdV, which belongs to the genus *Mastadenoviridae*. Currently, more than 103 HAdV types are known, which are classified into seven species (A to G). The oncogenic potential has been determined for types 1 to 51 and is indicated by the different colors of the type numbers: magenta is highly oncogenic, blue is weakly oncogenic, turquoise is non-oncogenic and the oncogenicity of the black written types has not been investigated yet [5,8,9,26–28].

1.2 Pathogenesis and treatment options

HAdV have a high prevalence in the human population since they have a broad tissue tropism and can infect several types of primary differentiated epithelial cells, postmitotic resting cells and cells derived from the nervous system [28–32]. Furthermore, they can be easily transmitted through the respiratory route, conjunctival inoculation, or the fecal-oral route [28]. Additionally, HAdV are very stable and can remain infectious for

several weeks in a dry environment. Hence, infection could also happen through contact with contaminated surfaces [33]. First HAdV infections commonly occur very early in life. Approximately 80 % of all children at the age of six have experienced a HAdV infection due to a lack of neutralizing antibodies [34]. Usually, an overcoming the infection leads to the acquisition of humoral immunity. Generally, epidemics have been documented for children and adults, who live or work in closed or crowded settings, like child care facilities, schools, hospitals, or military camps [35–37].

For healthy persons, HAdV infections are mostly asymptomatic or have a mild progression with self-limiting clinical manifestations like pneumonia (species A, E), cystitis (species A, B and E), keratoconjunctivitis (species D), or gastroenteritis (species F) [38–43]. Recently, a correlation between a HAdV-D36 infection and obesity has been investigated [44]. Notably, occasional epidemic outbreaks with fatal outcomes have been documented even in immunocompetent individuals [45–47]. However, HAdV are a major threat for immunocompromised individuals, like organ or allogenic stem cell transplant recipients, congenital immunodeficiency patients and individuals undergoing chemotherapy [14]. For these patients HAdV infections can cause life threatening diseases such as acute pneumonia, hemorrhagic enteritis, hemorrhagic cystitis, hepatitis, nephritis, encephalitis, myocarditis, or even multi-organ failure [28,48–51].

Besides acute infections, HAdV can persist in tonsillar lymphocytes, lung epithelial cells, the central nervous system, and the entire gastrointestinal tract, including intestinal T lymphocytes [18,28,29,52–56]. Problematically, a latent virus can be reactivated upon immunosuppression, often leading to severe diseases [14].

Currently, HAdV specific antivirals are not available. Admittedly, a food and drug administration (FDA)-approved live oral vaccine for the commonly occurring HAdV types 4 and 7 exists, but is restricted to U.S. military trainees [57,58]. In general, mildly progressing infections are treated symptomatically [59]. In case of serious HAdV infections, antiviral drugs like cidofovir, brincidofovir, or ribavirin can be given, but the efficacy against HAdV is low and often accompanied with strong side effects [60–67]. For individuals under immunosuppressive therapy, the reduction of treatment regimens has to be considered to allow a recovery of leucocytes [14]. Particularly, T-cell depletion has been identified as an important risk factor for the development of viremia [68–74].

Therefore, not to antiviral therapy responding patients have been treated with donor derived HAdV-specific T cells in clinical trials, however this is still an experimental approach [75]. Accordingly, the development of new treatment options is urgently needed to protect especially immunosuppressed patients from severe HAdV induced diseases.

1.3 Structure of HAdV particles

HAdV are non-enveloped, large viruses with a linear double stranded (ds) DNA genome [5]. The outer shell of the virus, the capsid, assembles to a pseudo T=25 icosahedron with a diameter of approximately 90 nm [76–78]. It is composed of the major structural proteins hexon (polypeptide II; 109 kDa), penton (polypeptide III; 63.3 kDa) and fiber (Polypeptide IV; 61.9 kDa) as well as the minor structural proteins IIIa (63.5 kDa), VI (23 kDa) VIII (15.4 kDa) and IX (14.4 kDa). The major structural proteins build the framework of the icosahedral capsid, which consists of 20 triangular facets and twelve vertices. Each facet is formed of twelve hexon trimers, while a vertex is constituted of a penton pentamer, also called penton base. Every base is associated with a non-covalently bound, protruding trimeric fiber [79–81]. The fiber is organized in an N-terminal tail, a long shaft, and a C-terminal knob region [82,83]. Since the major capsid proteins are the first peptides that interact with the host cell, their sequence variation as well as the physical size of the fiber determines the entry pathway and viral tropism [84]. The minor structural components (IIIa, VI, VIII, IX) are located between the hexons and pentons. They are considered as the capsid cement, since their main function is the stabilization of the viral shell [78,79,85–90]. The cement proteins are organized in two layers, an exterior consisting of protein IX and an interior composed of IIIa, VIII and VI. The outer cement proteins build a contiguous network, which surrounds the facets, while the inner cement proteins are associated in a complex, which connects the core to the shell via binding of core protein V to minor capsid proteins (Fig. 2) [88].

The capsid encloses the non-icosahedral particle core that contains the linear dsDNA genome and the core proteins V (41 kDa), VII (19 kDa), mu (µ; 11 kDa), IVa2 (50 kDa), the terminal protein (TP; 55 kDa) and the adenoviral protease (AVP; 23 kDa) [79,89,91–97]. Within the capsid, the viral DNA is organized in a condensed chromatin-like structure wrapped around histone-like protein VII [98,99]. Furthermore, the genome is associated with protein V and mu [79,87,97,98]. To create a condensed nucleosome, the proteins

interact with each other and the DNA [94,96,100]. Additionally, TP attaches covalently to the 5' end of the DNA [79,87,94–96]. Moreover, the core is filled with a few copies of AVP, which cleaves the pre-cursor versions of IIIa, VI, VII, VIII, as well as TP and mu for particle maturation [79,87,95,98,101–103].

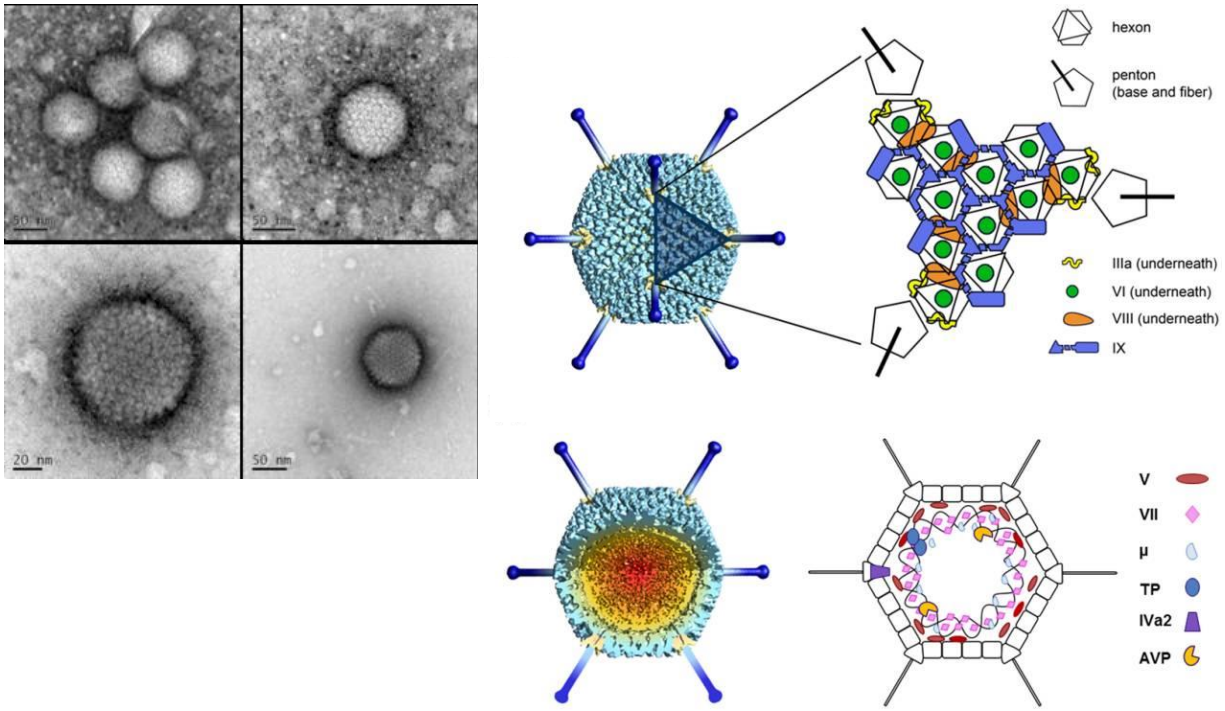

Fig. 2: Structure of the HAdV-C5 virion. The left illustration shows electron microscope images of the icosahedral structure of adenoviral virions (Department of Electron Microscopy, Heinrich Pette Institute, Leibniz Institute for Experimental Virology, Hamburg). On the right side, a schematic image of a HAdV-C5 particle is shown, depicting the organization of capsid, core and cement proteins according to San Martin *et al.* [80]. TP: terminal protein, AVP: adenoviral protease.

1.4 Genome organization

HAdV have a linear, ds DNA genome with a size of approximately 36 kbp [104]. At its ends, the DNA is flanked by several inverted terminal repeats (ITR) [5,32]. The terminal 1 to 50 bp contain the origin of replication (ori), whereby the first 18 bp form the minimal ori and the rest is considered as the auxiliary origin. Next to the left ITR and before the E1 coding region, the viral genome harbors a packaging sequence (ψ) that drives the encapsidation of the viral DNA [32,105,106]. In general, the genome organization of the different HAdV types is very similar and encodes approximately 40 structural and regulatory proteins [5]. It comprises the immediate early region E1A, the four early transcription units E1B, E2A, E3 and E4, the delayed early region encoding the proteins

IX and IVa2, and the major late transcription unit (MLTU) [32,107]. The transcription of the MLTU is mainly controlled by a single promoter. This promoter is termed major late promoter (MLP) and directs the synthesis of one late pre-mRNA. The late pre-mRNA gives rise to five late mRNAs, termed L1 to L5, by alternative polyadenylation and splicing. These mRNAs encode mainly structural proteins. All mRNAs harbor a tripartite leader (TPL) sequence, to which 3′ acceptor sites in the main MLTU body are spliced [32]. The TPL has a size of approximately 200 nucleotides and mainly encodes structural, core and capsid proteins. Moreover, it impacts the nuclear export, allows preferential translation of viral mRNAs by ribosome shunting, and stabilizes the late mRNAs [108–111]. Besides L1 to L5, virus-associated (VA) RNAI and VA RNAII are encoded by the MLTU. Notably, the HAdV genome can be transcribed from both DNA strands. At each 5' end, the DNA associates with TP, which is required for efficient DNA replication and packaging into progeny virions (Fig. 3) [32].

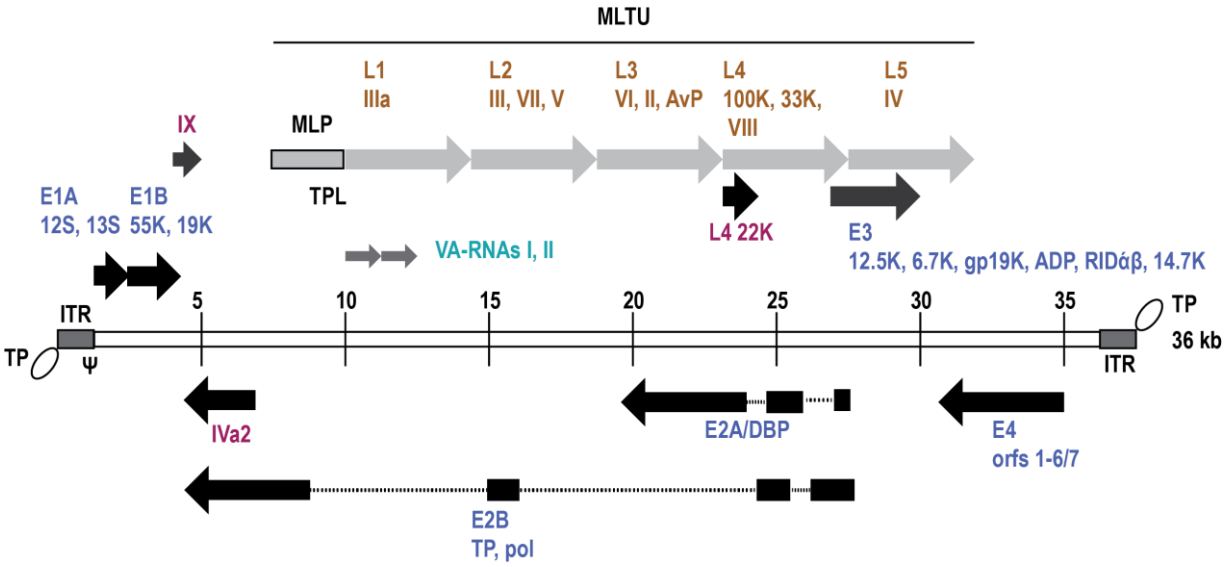

Fig. 3: Genome organization of HAdV-C5. Schematic representation of the HAdV-C5 genome. The genome is flanked by internal terminal repeat (ITR) sequences. At the 5' ends, the DNA is associated with the terminal protein (TP). Ψ indicates the packaging sequence. Arrows show the transcriptional direction of the indicated transcription units. The major late transcription unit (MLTU) comprises the late genes. Its transcription is controlled by the major late promoter (MLP). In front of the late genes, the genome harbors a tripartite leader (TPL) sequence. Names of encoded early gene products are written in blue, delayed gene products in magenta and late gene products in brown. The virus-associated RNAs (VA-RNAs) I and II are indicated in turquoise. (Adopted from Täuber & Dobner and Dimmock & Leppard [112,113]).

1.5 DNA replication

HAdV genome replication is very efficient, approximately one million copies can be produced within 40 h in one cell [32]. It requires the viral proteins encoded by the E2 transcription unit, the terminal protein (TP), AdV polymerase (AdV-pol) and the DNA binding protein (DBP/E2A), as well as the cellular transcription factors nuclear factor I (NFI), NFII, and octamer transcription factor 1 (Oct-1)/ NFIII [114,115].

In the first steps, NFI and Oct-1 are recruited to the auxiliary ori. Here, they form a preinitiation complex together with the viral proteins AdV-pol, pTP and DBP. The formation of the preinitiation complex requires various interactions among the constituents [32,114,115]. DNA synthesis itself is catalyzed by AdV-pol in a strand displacement mechanism, in which pTP serves as a protein primer. For DNA replication, dCMP is covalently attached to the precursor of TP (pTP) and pTP-C is formed. In parallel, DBP induces several structural changes of the DNA, while NFI and Oct-1 mediate substantial bending of the ori. Notably, DNA replication initiation occurs at base four of the template strand. Here, pTP-C is extended by adenine and thymine to the trinucleotide intermediate pTP-CAT. After synthesis, pTP-CAT jumps back three bases and pairs with the first three template residues, from where elongation continues. This mechanism is conserved among all HAdV and requires short repeat sequences of 2 to 4 bp within the first 10 bp of the genome. Directly after or during the back jump, the pre-initiation complex already starts to disassemble. The elongation of the pTP-CAT intermediate by AdV-pol is substantially supported by DBP and NF-II [32,114,115]. DBP is the major viral replication protein and fulfills several important tasks during viral DNA replication. Most of these activities rely on DBP's ability to change the DNA structure and destabilize the helix. In the initiation process, it stimulates AdV-pol as well as NFI binding to the DNA and reduces the K_m for the attachment of the first nucleotide to pTP. During elongation, it helps to unwind the DNA in an ATP independent manner and enhances the rate and processivity of AdV-pol. Additionally, it protects the ssDNA against nucleases [114]. NFII acts as a DNA topoisomerase and ensures the generation of a complete DNA strand [114]. In a round of replication, only one strand of the initial duplex genome is used as a template for the replication. Accordingly, a replication cycle results in a ds DNA molecule, consisting of a mother and daughter strand, as well as a displaced single strand. Only in the following cycle, the complementary strand to the

displaced single strand is generated. Therefore, the displaced strand forms a panhandle structure through annealing of its self-complementary ITRs. This structure is equal to the termini of the ds viral genome, hence the pre-initiation complex can form and initiate the synthesis of a second duplex. Newly produced duplex genomes could either be packaged into new virions or could be used as a template for a second round of replication [32,114,115].

For generation of progeny genomes, viral proteins, especially DBP, induce the formation of replication compartments (RCs), which are distributed all over the nucleus. They have a donut shape and are organized in an inner area, which contains the single stranded DNA and a peripheral zone, in which newly formed dsDNA molecules accumulate [116].

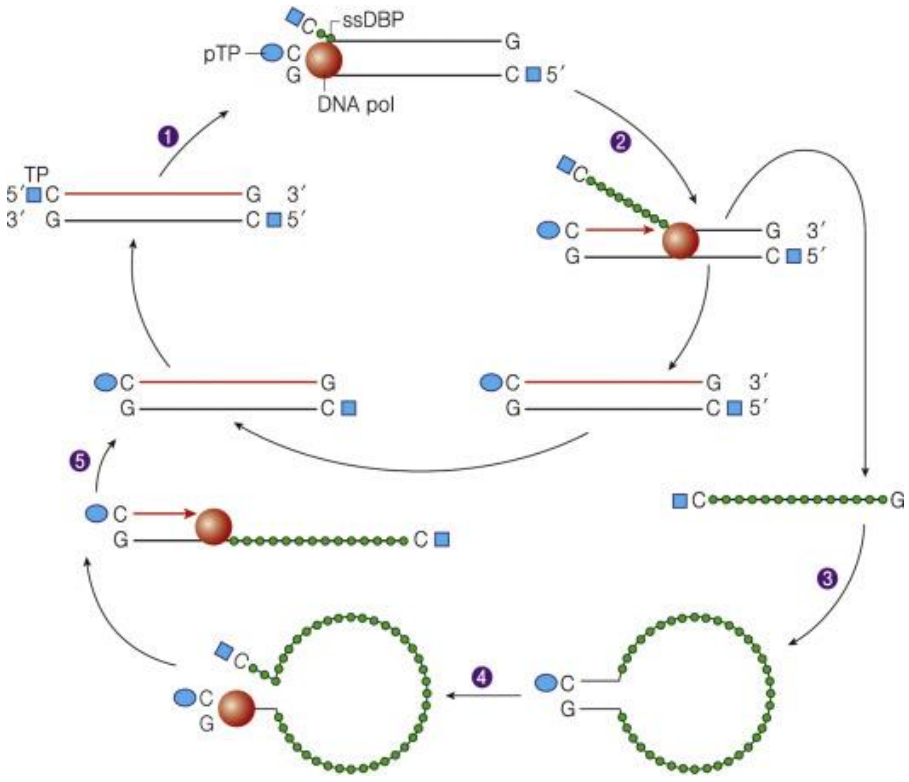

Fig. 4: Schematic illustration of HAdV DNA replication. AdV express their own DNA polymerase AdV-pol/E2B, which replicates the viral genome in a strand displacement mechanism. The replication cycle can be divided into 5 steps: Formation of the preinitiation complex and start of DNA amplification (1). Elongation of the first daughter strand and displacement of the single mother strand from the new synthesized duplex genome (2). Formation of the panhandle structure by the DBP covered single strand (3). Association of the pre-initiation complex with the panhandle and initiation of DNA replication of the second new ds genome (4). Release of the second duplex genome (5) (Adopted from Ryu *et al.* [117]).

1.6 The lytic replication cycle

HAdV mainly infect post mitotic, resting epithelial cells either of the respiratory or the gastrointestinal tract [118]. In cell culture, different tumor and primary cell lines can be infected. In these cells the virus can complete its lytic life cycle, while the infection of rodent cells results in an abortive infection and could lead to tumorigenesis [118,119]. This mechanism is described in more detail in section 1.7. Most studies investigating the replication of HAdV employed HAdV-C2 or HAdV-C5 in epithelial cell systems. Per definition, the HAdV life cycle is divided into an early and a late stage of infection [120]. The transition from the early to the late phase is initiated by the onset of DNA replication (Fig. 5). Early events comprise virus internalization, nuclear import of viral DNA and early gene expression, while the late phase is characterized by viral DNA replication, expression of late genes, progeny assembly and finally release (Fig. 5). In between early and late stage, the proteins IVa2 and IX are synthesized [121]. However, division of the adenoviral life cycle into two phases is often indistinct because at early time points low-level transcription of the MLTU occurs and some early genes are still expressed at late times post infection[32].

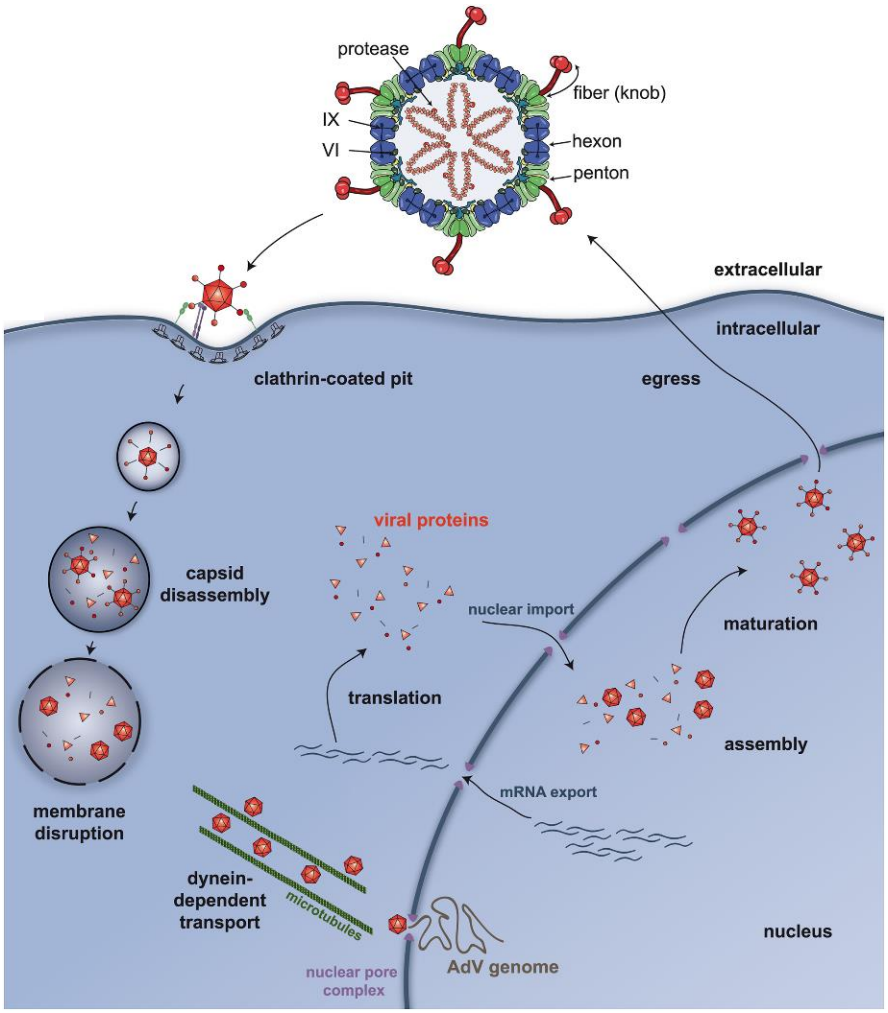

Fig. 5: Visualization of the HAdV-C5 life cycle in epithelial cells. The image shows the essential steps of the HAdV-C5 replication. After receptor binding, viral particles enter the cell via endocytosis. Acidification of the endosome leads to partial disassembly of the viral particle, whereby protein VI is released and induces endosomal lysis. Subsequently, the viral particle reaches the cytosol and is transported along the dynein network to the nucleus. Here, the virion docks to the NPC, dissociates completely and the viral DNA is released into the nucleus. Inside the nucleus, viral gene expression, DNA replication, and progeny assembly occur, while the viral mRNA is translated in the cytoplasm. One replication round ends with the rupture of the host cell and release of the newly synthesized viral particles. Reprinted from Kremer and Nemerow [122].

1.6.1 Virus entry and nuclear import of viral DNA

In the first step of infection, the virus binds to cellular surface receptors via the fiber knob. Most HAdV types use the coxsackievirus B and AdV receptor (CAR), which is a member of the immunoglobulin superfamily and normally forms tight junctions between polarized epithelial cells [123,124]. The interaction between fiber and CAR is mediated via a conserved AB loop on the lateral surface of the fiber knob [125]. A further prominent example for receptors utilized by HAdV is CD46. Especially, HAdV types of species B

use CD46 as primary entry receptor. This receptor is a member of the family of complement regulatory proteins and is ubiquitously expressed on different host tissues for example hematopoietic cells, which do not express CAR. HAdV types using CAR as entry receptor infect the cell via clathrin mediated endocytosis, whereas CD46 using HAdV types enter the cell through macropinocytosis. Moreover, several cell surface proteins like glycan GD1a, polysialic acid, heparin sulfate proteoglycans, CD80, CD86, desmoglein-2, MHC-I and VCAM-1 have been identified as alternative entry receptors, explaining the broad tissue tropism of HAdV [126]. Following primary receptor association, penton binds to αvβ3 and αvβ5 integrins, which are incorporated into the host cell membrane and initiates endocytosis of the virion. After internalization, the viral particle is enclosed by the endosome. The pH inside the endosome lowers during its maturation and initiates the dissociation of several vertex proteins such as IIIa, peripentonal hexons, penton, VI, VIII and the fiber extensions. Especially, freed protein VI and exposed pentons trigger the lysis of the endosomal membrane and the liberation of the partly uncoated virus into the cytoplasm. Subsequently, the particle is transported along the microtubule network to the nucleus [32,127–130]. Here, hexon docks to the nuclear pore complex (NPC) and binds additionally to the microtubule motor protein kinesin-1. The movement of kinesin-1 along the microtubules results in capsid disassembly and NPC permeabilization, facilitating the import of the uncoated viral DNA into the nucleus through porous NPCs [131]. Inside the nucleus, the viral genome remains associated with protein VII and winds around cellular histones. These interactions shield the linear dsDNA against the DNA damage repair responses until early viral proteins are synthesized, which then take over the DNA preservation [132].

1.6.2 Expression of early genes

After unwinding the DNA, viral gene expression starts with the E1 to E4 domains of the adenoviral genome (Fig. 3). HAdV exploit the cellular RNA polymerase II for the transcription of most of their genes, only the VA genes are transcribed by RNA polymerase III [32]. The main challenges for early viral peptides comprise the creation of a favorable environment in the host cell for progeny production, the activation of the cell cycle, the antagonism of antiviral defenses, and the production and recruitment of proteins, required for viral genome amplification [32].

The first expressed gene is E1A, whose transcription is controlled by a constitutively active enhancer [133,134]. During the early phase of infection, two major isoforms of E1A (E1A-12S and E1A-13S) are synthesized through alternative splicing. These isoforms differ mainly in one 46 aa domain, which is only present in E1A-13S [135,136]. Three further isoforms of E1A are produced during the late phase of infection, but no biological functions have been identified yet [137–139]. Early E1A proteins work as transcriptional regulators, whereby E1A-12S is generally considered as a transcriptional repressor, while E1A-13S mainly acts as a transcriptional activator. E1A-12S has been shown to alter the activity of ~10.000 cellular promoters and to induce a global redistribution of transcription factors as well as epigenetic modulators in order to drive cells to S-phase [140–143]. E1A-13S modulates the transcription of cell cycle regulating genes and activates the transcription of the remaining E1 to E4 encoded viral genes. The unique region of E1A-13S has been shown to be crucial for the activation of viral transcription units [143]. Remarkably, E1A proteins do not directly bind to DNA, but rather interact with cellular DNA binding factors that control gene expression [141,144–148]. Essential for S-phase entry and activation of early viral transcription is the binding of E1A to pRB family proteins, resulting in the release of activating E2F transcription factors from pRB proteins. Thus, these cellular factors can enhance the E2F-dependent transcription of early viral genes as well as cell cycle driving host genes [148–150]. Furthermore, it was found that simultaneous interactions with the closely related proteins p300 and CREB binding protein (CBP) are necessary for the stimulation of cell cycle progression [151,152]. Besides driving cell cycle and viral gene expression, E1A is also able to inactivate first intrinsic immune responses of the host by repressing the transcription of interferon (IFN)-induced genes [153]. Notably, E1A also has cytotoxic properties, which are mainly based on the activation and stabilization of the apoptosis inducing factor p53. Nevertheless, also p53 independent apoptotic pathways are stimulated by E1A [154–156].

Cell death, induced by E1A activities, is precluded by the E1 region encoded proteins E1B-55K and E1B-19K. Especially E1B-55K displays a variety of measures to avoid the expression of p53 responsive genes, leading to the interruption of apoptosis triggering signaling cascades (see chapter 1.13). E1B-19K mimics the anti-apoptotic protein BCL-2. This factor can suppress the release of cell death inducing effectors from mitochondria by binding to the apoptosis regulating molecules BAK and Bax [157,158].

Moreover, E1B-55K contributes significantly to the counteraction of antiviral defenses and DNA damage response mechanisms induced by promyelocytic leukemia nuclear body (PML NB) components (1.13).

A further important part of the early phase is the preparation for viral genome amplification. This includes the production of the E2 encoded proteins DBP, AdV-pol and TP, which drive the replication process. DBP is the major component of viral RCs and facilitates DNA replication [159]. Besides supporting genome amplification, it stabilizes viral mRNAs and directs transcription and translation of viral genes, to initiate the late phase [160–163]. AdV-pol acts as a DNA polymerase and catalyzes genome replication in a strand displacement reaction, while TP serves as a protein primer for the initiation of DNA replication (1.5) [164].

The E3 region of HAdV-C5 encodes the seven peptides E3-12.5K (gp12.5 kDa), E3-6.7K (CR1α), E3-19K (gp19K), E3-11.6K (adenoviral death protein (ADP); CR1β), E3-10.4K (RIDα), E3-14.9K (RIDβ), and E3-14.7K. These proteins mainly inhibit immune signaling and viral antigen presentation on the cell surface of infected cells to prevent growth arrest, apoptosis, and recognition by natural killer cells (NK) and cytotoxic T cells (CTL) [165–170]. Furthermore, E3-11.6K/ ADP accumulates at the final phase of infection and may ensure efficient cell lysis and viral egress [171].

The E4 transcription unit encodes at least seven different peptides termed according to their open reading frames E4orf1, E4orf2, E4orf3, E4orf3/4, E4orf4, E4orf6 and E4orf6/7. Little is known about the functions of E4orf1, E4orf2, and E4orf3/4, since they do not impact viral replication significantly. Notably, E4orf1 of HAdV-D9 was investigated regarding its contribution to the oncogenicity of this HAdV type [172]. In the context of infection, E4orf3 and E4orf6 play a more important role. At least one of them is needed to ensure efficient viral replication by preventing the activation of the DNA repair mechanisms [173–175]. Moreover, both proteins have redundant tasks in RNA processing, nuclear export of late viral mRNAs, and in shutting off host cell protein synthesis [175–182]. Essential for its functionality, E4orf3 assembles into a polymer and forms a track-like network within the nucleus. Thereby, antiviral acting PML NBs are dispersed and several of its components are sequestered into these structures [183,184]. Furthermore, E4orf3 facilitates heterochromatin formation at p53-responsive promoters

by histone trimethylation, resulting in a reduced expression of these genes [185]. The formation of an E3 ubiquitin ligase together with E1B-55K is crucial for the viral growth promoting effect of E4orf6. This complex degrades antiviral factors, enhances the export of viral late RNAs and induces a shut-off of host cell protein synthesis (see chapter 1.13.3). Independent of the interaction with E1B-55K, E4orf6 inhibits the tumor suppressor p53 and its functional relative p73 [186,187]. The E4orf4 protein, encoded by the following open reading frame, is not an essential protein but an important support factor that provides backup and reinforcement to other early proteins. It mediates the progression from early to late stage of HAdV infection by downregulation of the transcription of cellular genes, which interfere with viral replication and early HAdV genes [188,189]. Furthermore, it influences the cell cycle beneficially for replication, controls alternative splicing of viral mRNAs and regulates protein translation [190–193]. Besides, it blocks the DNA damage response (DDR) and at late stages it shows cell lysing abilities, which may help to ensure a proper viral spread [194–200]. Remarkably, most functions depend on its interaction with the cellular protein phosphatase 2A (PP2A) [201]. The last E4 protein is E4orf6/7, which results from a fusion between open reading frames 6 and 7. It mainly acts as a transcriptional activator of E2F responsive genes by binding to E2F transcription factors and stabilizing their interaction with responsive promoters. Thereby it affects genes involved in the cell cycle progression and viral DNA synthesis [174,202–204]. At late stages of infection the transcription of the E4 encoded genes is repressed by the accumulation of DBP and E4orf4 [176].

However, not only early genes are expressed at early stages of infection, but also the MLTU is weakly active at this time, leading to a production of L1-52/55K, which is later involved in virion assembly [136,140]. In addition, viral non-coding RNAs (VA RNAs) are expressed early in infection, but are extremely abundant at late stages of infection. These RNAs facilitate translation of late mRNAs and participate in the inhibition of the IFN response [205–208].

1.6.3 Induction of the late phase of infection

The start of viral DNA replication and expression of the MLTU indicate the transition from the early to the late phase of infection. Accumulation of E2 proteins leads to the induction of viral DNA synthesis. The transcription of the MLTU is mainly controlled by

the MLP [136,209]. Full activation of this promoter requires the intermediate proteins IVa2 and IX as well as the late proteins L4-22K and L4-33K [210–214]. Through viral genome accumulation, the expression of the intermediate proteins IX and IVa2 as well as the late proteins L4-22K and L4-33K is induced [215–217]. Notably, the transcription of these L4 genes is controlled by an individual promoter, which is embedded in the L4 transcription unit and therefore named L4P. This promoter enables the transcription of L4-22K and L4-33K before MLP activation [217]. The identification of L4P resolved the seemingly paradoxical requirement of L4 gene products for MLP stimulation. Besides genome accumulation, E1A, E4Orf3, IVa2 and p53 participate in the stimulation of L4P [217,218]. Additionally to transcriptional activation, L4-22K and L4-33K regulate the splicing of the MLTU mRNA transcript [210,219,220].

The MLTU encodes the majority of structural proteins and proteins involved in progeny assembly. At first, a primary MLTU transcript with a size of 28 kbp is produced [136,140]. Through differential splicing and polyadenylation, the late mRNAs L1 to L5 are generated. These mRNAs encode 15 late proteins [136,140]. The efficient production of viral late proteins is ensured by a shut-off of host cell protein synthesis. This includes the preferential export of viral late mRNAs initiated by the E4orf6/E1B-55K complex and L4-100K mediated ribosome-shunting towards viral mRNAs [221–223]. Moreover, L4-100K promotes viral replication through the prevention of granule-mediated cell killing [224].

1.6.4 Assembly and egress

The assembly of the HAdV capsid occurs in the nucleus, presumably in the periphery of RCs and is initiated by the accumulation of structural polypeptides and DNA replicates [225]. Most viruses follow one of two existing assembly concepts. In the first one, the viral capsid assembles around the genome (concomitant assembly), while in the second one the genome is introduced into preformed capsids (sequential assembly). How HAdV particles form is still under debate. Some publications emphasize that HAdV follow the sequential route [226–231] while others suggest the concomitant pathway [225,226].

Hexon capsomers and penton bases assemble in the cytoplasm and are separately transported into the nucleus. A hexon capsomer consists of a hexon trimer and requires L4-100K for formation. Here, L4-100K has a dual chaperone-like function, on the one hand it facilitates the folding of hexon monomers and on the other hand it serves as a scaffold for trimer formation [232,233]. The nuclear import of trimeric hexons is initiated by direct binding of hexon to protein VI [232–235]. The penton pentamer, also referred to as penton base, comprises seven pentons with a protruding fiber. Similarly to hexon, it assembles completely in the cytoplasm and is subsequently imported into the nucleus [96,229,236]. Within the nucleus, hexon capsomers and penton bases associate with the minor structural proteins (IIIa, VI, VIII, IX, AvP) and build the capsid shell [32,237,238]. During assembly, L1-52/55K was suggested to act as a scaffold protein, since it can be detected in the pro-virus, but not in mature virions. Nevertheless, it is not a *bona fide* scaffold protein [102,239].

New genomes are synthesized in nuclear RCs and associate with the core proteins pTP, V, VII and mu. Furthermore, they bind to the packaging factors IVa2, L1-52/55K, L4-33K, L4-22K and IIIa via the packaging sequence (ψ) at the left end of the ds DNA. Additionally, pTP is recruited to each 5’ end of the genome. Equipped with these proteins, the viral DNA is packaged into new virions [80,96]. Various studies displayed that each packaging factor is prerequisite for genome incorporation, although the exact roles have not been determined [213,240,249,241–248]. IVa2 has been suggested to serve as an ATPase, generating the required energy for the insertion of the genome into the capsid. In this potential process, L4-33K is supposed to act as a small terminase, which enhances ATPase function of IVa2 [242,243,250–252]. These assumptions support the idea of a sequential packaging process. The specific function of L4-22K is unknown, but both L4 proteins associate to individual complexes with IVa2 to promote DNA packaging [213,242–246]. Moreover, L1-52/55K was found to interact with IIIa, VII, and IVa2 and binds nonspecifically to the viral DNA to facilitate the incorporation of the genome into the capsid [245,247–249].

Complete maturation of new generated pro-virions require the cleavage of the immature forms of IIIa, L1-52/55K, VI, VII, VIII, mu and pTP by Avp [253–256].

Subsequently, the packaging factors are released from the pro-virus, resulting in conformational changes of the capsid and complete particle maturation [94].

Viral egress remains also enigmatic and only a few aspects of the process have been elucidated until today. One study demonstrates that the adenoviral protease destroys the mechanical integrity of the cell by cleaving cytokeratin K18 leading to a destroyed cellular filament that results in cell lysis [257]. A second focuses on ADP, which is cytotoxic and induces cell rupture as it accumulates in the late phase of infection [171]. Moreover, free penton proteins have been shown to interfere with CAR oligomerization at tight junctions of the cell, promoting the release of new synthesized viruses [258].

In total, the HAdV replication cycle takes 24h to 36h, depending on the cell line and ends with the egress of up to 10^4 newly synthesized viral particles per cell [32].

1.7 Oncogenic potential

In 1962, HAdV-A12 was found to induce tumors in newborn hamsters [15]. Since then, HAdV are classified as DNA tumor viruses and serve as an important model organism for the investigation of viral transformation. In the following years, several HAdV types have been tested for their capacity to transform primary rodent cells in cell culture and to induce tumors in rodents. So far, all tested types could transform primary rodent cells with a comparable efficiency [259]. However, their potential to cause malignancies in animals differs significantly [260,261]. Therefore, HAdV types 1 to 54 are classified as non-oncogenic, weakly oncogenic and highly oncogenic according to the frequency and required time for the initiation of tumor formation in rodents (Fig. 1) [10]. Remarkably, a rising number of studies displays the potential of HAdV to transform human cells. These comprise the cell lines human embryonic kidney cells (HEK293), human embryonic lung cells (HEL), and amniocytes [260,262–266]. Recently, Speiseder and co-workers showed that also human mesenchymal stroma cells (hMSCs) can be transformed by HAdV oncogenes [267]. Furthermore, HAdV DNA has been detected in low amounts in pediatric brain tumors, small-cell lung carcinomas, mantle cell lymphomas and human sarcomas [31,268–270]. However, no evidence for a clear correlation between HAdV infections and tumor development has been identified yet.

HAdV induced transformation is the result of an abortive infection, in which only certain genes are expressed, but no progeny production occurs. However, these gene products are sufficient to cause malignant changes in the infected cell. In general, HAdV induced transformation is thought to follow the classical concept of viral oncogenesis, whereby the oncogenes persist in the transformed cells and are constantly expressed [271]. Besides viral oncogene expression, transformed cells are characterized by morphological changes and loss of contact inhibition. Thus, they grow as multilayered colonies (foci) [272]. HAdV initiated transformation is a two-step process, which requires the cooperation of E1A with either E1B-55K or E1B-19K [24,32,271,273]. In the first step, E1A modulates cellular gene expression to drive cell proliferation and immortalization. However, as described in chapter 1.6.2 uncontrolled cell cycle progression induces apoptosis. Therefore, E1B-55K or E1B-19K are prerequisites for prevention of the pro-apoptotic functions of E1A and initiation of complete transformation. The oncogenic abilities of E1B-55K mainly rely on the direct interaction with p53, inhibition of p53-mediated transcription, and the nuclear export of p53 to perinuclear aggresomes [274,275].

Besides the E1 proteins, E4orf3 and E4orf6 can contribute to the transforming abilities of HAdV. Both E4 proteins synergize individually with E1A and E1B to increase the transformation efficiency [276–278]. Especially, the co-expression of E4orf6 with the E1 proteins leads to an increased tumorgenicity. Most probably, this is achieved through enhanced p53 inhibition caused by the E4orf6/E1B-55K E3 ubiquitin ligase complex and separate activities of E4orf6 [277,279]. In addition, E4orf3 and E4orf6 can cooperate with E1A to transform primary baby rat kidney (BRK) cells without the assistance of E1B-55K. Notably, cells transformed by E1A and either E4orf3 or E4orf6 often fail to express the viral oncogenes, indicating that transformation occurs through a hit-and-run mechanism, in which the viral oncogenes are only required as causative agents [280].

1.8 The SUMOylation cycle

SUMOylation is a reversible post translational modification (PTM) similar to ubiquitylation. SUMO was initially described in 1996 and until now, more than 1000 proteins have been identified as SUMO targets [281–283]. Within a three step enzymatic cascade, SUMOs are covalently linked to lysine (K) residues of target proteins and

thereby influence protein interactions, stability, localization, and function [284]. SUMOylation often occurs at SUMO conjugation motifs (SCMs), which consist of a hydrophobic aa (Ψ), the modification competent lysine, any aa (χ), and glutamine (E) or asparagine (D; ΨKχE/D). However, under stress conditions, SUMOylation frequently takes place at non-consensus sites on target proteins [283,285].

SUMO proteins are expressed in all eukaryotes, whereby lower eukaryotes encode at least one SUMO isoform while higher eukaryotes often express more paralogues [286]. In humans, five different isoforms have been identified so far. The main isoforms are SUMO 1 to SUMO 3, which are ubiquitously expressed and acknowledged as important regulators in various pathways like DNA damage repair (DDR), immune response, carcinogenesis, cell cycle progression, and apoptosis [286–288]. SUMO 1 shares only 50 % sequence identity with the other two major isoforms, whereas SUMO 2 and SUMO 3 are 97% identical. The latter two differ only in three N-terminal aa in their mature form and are therefore referred to as SUMO 2/3 [287,288]. In contrast to SUMO 1 to SUMO 3, little is known about the characteristics and functions of SUMO 4 and SUMO 5. The mRNA of SUMO 4 was found only in lymph nodes, kidneys, and spleen. However, it is not clear yet whether the mRNA is translated [289,290]. Nevertheless, mutations in a SUMO 4 coding gene have been associated with type I diabetes mellitus [291]. The expression of SUMO 5 seems to be restricted to testis and peripheral blood and it might enhance growth, but also destabilization of PML NBs [292].

Before the SUMO cascade starts, all SUMO proteins need to be processed by Sentrin/ SUMO-specific proteases (SENPs). Thereby, SENPs hydrolytically cleave the last four aa off the C-terminus of SUMO and expose a conserved di-glycine motif (GG) [288,293,294]. SUMO 1 as well as SUMO 2/3 can be attached to target proteins as single molecules. Yet, only SUMO 2/3 can additionally build polySUMO 2/3 chains, in which SUMO-SUMO linkage occurs through internal lysine residues. Nevertheless, SUMO 1 can bind to polySUMO 2/3 chains, where it functions as chain terminator [286,288]. The conjugation of SUMO 4 to target proteins under physiological conditions seems to be unlikely, since this isoform is resistant to SENP cleavage, whereby the transition to the mature form is prohibited [290]. A first study investigated the modification of PML by

SUMO 5, in which they stated that PML could be modified by polySUMO 5, at least in *in vitro* analysis [292].

After maturation, SUMO is selected among other ubiquitin-related modifiers, like ubiquitin or Nedd8, by the heterodimeric E1 enzyme complex consisting of SUMO E1 activating enzyme 1 (SAE1) and SAE2. Through adenylation, the C-terminal GG motif of SUMO is activated in an ATP consuming reaction that allows the formation of a highly reactive thioester bond between SUMO-GG and the conserved catalytic cysteine (C) of SAE2 (Fig. 6 step 1). [295,296].

Next, the E1 complex recruits the SUMO specific E2 enzyme ubiquitin carrier protein 9 (UBC9), which accepts SUMO and forms a SUMO-UBC9 thioester bond between its catalytic C and the C-terminal GG-motif of SUMO (Fig. 6 step 2) [297,298]. In contrast to ubiquitylation, in which more than twenty E2 enzymes have been identified, UBC9 is the sole known SUMO specific E2 enzyme [299,300].

After SUMO binding, UBC9 orchestrates the SUMO acceptor substrate and usually an E3 SUMO ligase to transfer SUMO to the target protein (Fig. 6 step 3) [284]. The single identified exception is Ran GTPase-activating protein 1 (RANGAP1), which can be modified without the support of an E3 SUMO ligase [301]. During the conjugation reaction, UBC9 is responsible for target recognition and the E3 SUMO ligase confers further substrate specificity and catalyzes the transfer. While E1 and E2 SUMO enzymes are unique, many unrelated proteins possess E3 SUMO ligase activity towards SUMO substrates [284]. The best characterized class of ligases is the Siz/ protein inhibitor of activated STAT (Siz/PIAS) family of really interesting new gene (RING)-related E3 ligases and Ran-binding protein 2 (RanBP2) [302]. Further classes comprise the polycomb group (PcG) protein Pc2, Histone deacetylase 4 (HDAC4), and zinc finger protein 451 (ZNF451) [303–305]. Additionally to the ligase function, some E3 SUMO ligases, such as ZNF451, act as a SUMO elongase, which extends SUMO2/3 chains [306]. Moreover, SUMOylation is connected to the ubiquitinylation cycle via SUMO-targeted ubiquitin ligases (STUbLs). These enzymes bind poly-SUMO chains to target polySUMOylated proteins for ubiquitination-dependent proteasomal degradation [307]. Two human STUbLs, RNF4 and RNF111 (Arkadia) have been identified until today [308–310]. SUMOylation is a highly dynamic and reversible process, allowing the fast

adaptation to environmental changes. Additionally to SUMO processing, deSUMOylation is catalyzed by SENPs [311,312]. Thereby, SENPs cleave the isopeptide bond between SUMO and the lysine residues of target proteins and depolymerize isopeptide linked poly SUMO chains (Fig. 6) [313,314].

How SUMOylation is regulated is incompletely understood yet. One mechanism is the removal of SUMO from target proteins by SENPs as explained above. A further possibility is the regulation at the level of attachment. SUMO conjugation can be affected by the environment of the SCM, for example by patches of negatively charged aa and alterations in the local charge, induced by phosphorylation of serine (S), threonine (T), and tyrosine (Y) residues [283,315,316]. Additionally, other PTMs such as ubiquitylation, acetylation, and methylation occur at lysine residues. Thus these PTMs compete with SUMO for the same acceptor sites. Also, binding to other macromolecules like DNA or proteins affects SUMOylation [283].

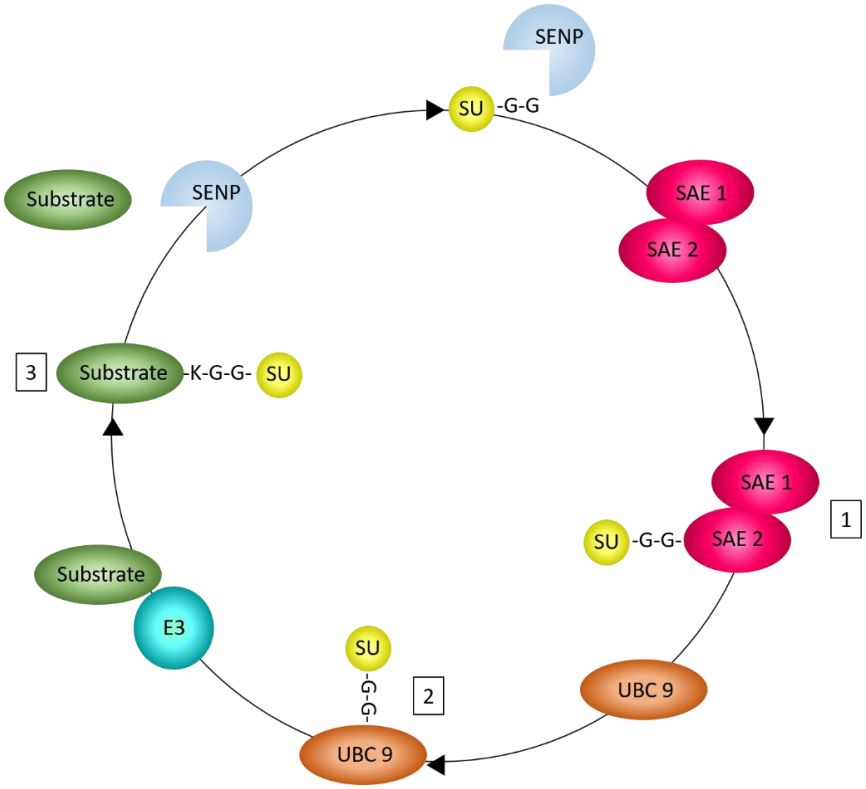

Fig. 6: Schematic illustration of the SUMO cycle. The transfer of SUMO to substrate proteins is a three step enzymatic cascade. Before the conjugation process starts, SUMO is matured via proteolytic cleavage by SENPs. These proteases cleave SUMO after a characteristic double glycine (GG) motif. In the first step of the cascade, SUMO binds to the E1 activating SAE1/2 complex via the GG motif (1). In the second step SUMO is transferred to the E2 SUMO conjugating enzyme UBC9 (2) and in the last step SUMO is conjugated to a lysine (K) residue of the substrate. In general, the attachment to a target protein is facilitated by an E3 SUMO ligase (3). SUMOylation is a highly dynamic process, which is rapidly reversed by SENPs. SUMO: small ubiquitin-like modifier, SAE: SUMO activating enzyme, Ubc9: ubiquitin carrier protein 9, SENP: Sentrin/ SUMO-specific protease. (Adopted from Everett *et al.* 2013 [317]).

1.9 Human SENPs

SENP proteases are central regulators of diverse cellular processes by ensuring a balanced SUMO conjugation and deconjugation. They cleave an isopeptide bond between SUMO and the ε-amino group of the lysine residue of the substrate. Furthermore, they induce maturation of SUMO proteins by clipping off SUMO precursors after a characteristic double G motif through hydrolysis of a peptide bond [313]. The human SENP family comprises seven members, SENP 1, SENP 2, SENP 3, SENP 5, SENP 6, SENP 7, and SENP 8, which all belong to the CA clan of cysteine proteases (Fig. 7) [313,318–320]. Human SENPs have a conserved catalytic domain at their C-terminal end, which exhibits 20 % to 60 % sequence identity. Furthermore, they share the same catalytic mechanism, involving a classical catalytic tirade, comprising a catalytically active cysteine (C), a histidine (H), and an asparagine (D) [318]. In contrast, the N-terminus of each SENP is unique and seems to be crucial for regulatory functions, substrate recognition and localization [321]. According to sequence homologies and phylogenetic analyses of the catalytic domains, human SENPs are further sub-grouped pairwise into SENP 1 and 2, SENP 3 and 5 as well as SENP 6 and 7 [313] (Fig. 7). In addition, SENP pairs localize to the same cellular structures, SENP 1 and 2 are enriched at the NPC and in PML NBs in interphase cells and move to the kinetochore during mitosis [322–327]. SENP 3 and 5 are mainly found in the nucleolus, but sub-fractions associate with mitochondria and chromatin [328–335]. SENP 6 and 7 were detected in the nucleoplasm and partly reside at chromatin [336–338]. In general, it is assumed that the localization of SENPs significantly influences their activity [318].

SENPs show preferences in processing and deconjugation for the different SUMO paralogues. SENP 1 and 2 show a high activity in maturing SUMO 1 to SUMO 3, whereby SENP 2 is mostly active on SUMO 2, followed by SUMO 1 and SUMO 3, while SENP 1 favors SUMO 1 over SUMO 2/3 [339–341]. SENP 3 hasn't been investigated for processing activities, but SENP 5 highly favors SUMO 2 [339,342]. Remarkably, SENP 6 and SENP 7 are almost inactive in SUMO hydrolyzation [339,343]. *In vitro* studies utilizing SUMOylated RANGAP1 as a model substrate revealed that SENP 1 and SENP 2 deconjugate SUMO 1 to SUMO 3 with a comparable efficiency, while SENP 3 and SENP 5 are very ineffective against SUMO 1 and preferentially remove SUMO 2/3 from

RANGAP1. SENP 6 and SENP 7 favorably cut SUMO 2-RANGAP1 linkages, but show the highest isopeptidase activity against SUMO-SUMO bonds (Fig. 7) [339,342–346].

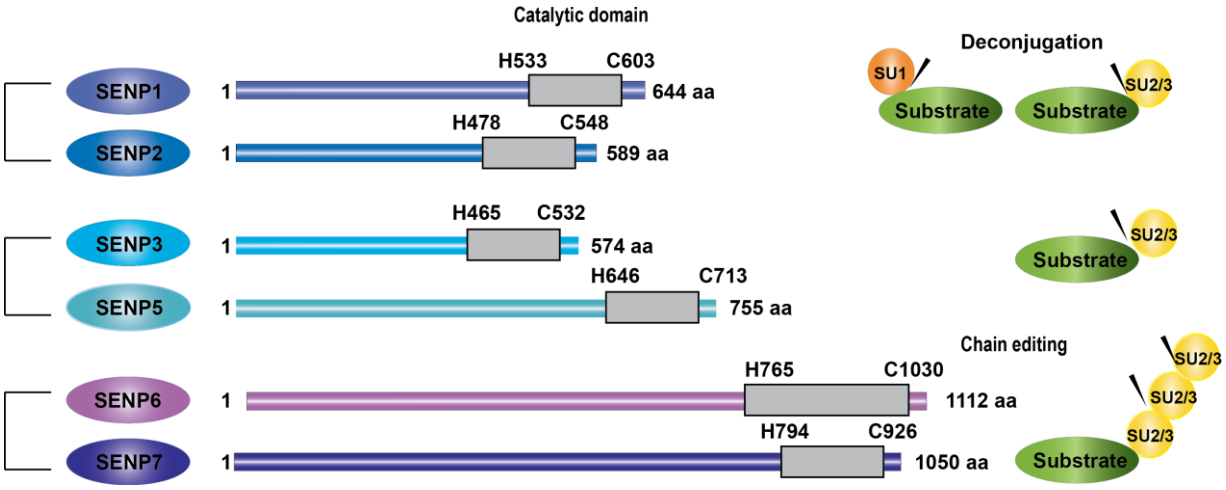

Fig. 7: Overview of the structure of human SENPs. SUMOylation is a reversible process. The rapid deconjugation is performed by SENP proteases. In humans, six SUMO specific SENP isoforms occur. Human SENPs belong to the CA clan of cysteine proteases. They share a conserved catalytic domain on the C-terminus, marked by the grey rectangles. Based on sequence comparison and phylogenetic analyses of the conserved catalytic domain. SENPs are evolutionary categorized pairwise. The figure depicts the pairwise evolutionary relationship between SENP 1 and SENP 2, SENP 3 and SENP 5, and SENP 6 and SENP 7. The N-terminus of each SENP is unique and determines the substrate selection and localization. Furthermore, the N-terminus is involved in the regulation of SENPs. SENP 1 and SENP 2 deconjugate SUMO 1 and SUMO 2/3 with comparable efficiency, while SENP 3 and SENP 5 preferentially cleave SUMO 2/3 from the substrate. SENP 6 and SENP 7 are able to clip-off SUMO 2/3, but most efficiently modify poly SUMO 2/3 chains by cleaving SUMO-SUMO linkages. (Adopted from Piller & Müller [318]). aa: amino acid, H: histidine, C: cysteine, SENP: Sentrin/ SUMO-specific protease, SU: SUMO.

1.10 PML NBs as a part of the antiviral immune response

PML NBs are also called nuclear domain-10 (ND10) or PML oncogenic domains (PODs) [347–349]. They associate to the nuclear matrix in the interchromatin space and are present in most mammalian cells [350]. PML NBs appear as discrete nuclear foci with a width of 0.2–1.0 µm. Dependent on the cell cycle phase, cell type and differentiation stage, cell nuclei comprise 2 to 30 PML NBs [351,352]. They consist of more than 165 permanently or transiently associated proteins, which mediate several pathways including cell cycle, apoptosis, senescence, p53 regulation, protein degradation, stress reactions, DNA damage responses, epigenetic mechanisms, and resistance to pathogens [348,353–356]. Upon a particular stimulus, these structures adapt dynamically to the requirements of the respective situation to protect the host cell. This is achieved through fast alterations in composition and mediation of protein activities [352,357]. The fundamental constituent of PML NBs is the PML protein. Since PML regulation is

dysfunctional in different cancer types, it has been assumed as a tumor suppressor [348,358]. Furthermore, it is essential for PML NB formation and recruitment of other PML NB factors [347–349]. In humans, seven isoforms of PML (I to VII) occur, which are generated through alternative splicing of one *pml* mRNA [359,360]. Additionally to PML, the transcription factor Sp100, the chromatin remodeler and apoptotic factor Daxx, the DNA repair protein blooms helicase (BLM) and small ubiquitin like modifier (SUMO) are examples for resident proteins in PML NBs [347,356,361]. Transient constituents comprise the Mre11-Rad50-NBS1 (MRN) DNA repair complex, p53, Rb proteins, ubiquitin specific protease 7 (USP7), the transcription factor ATRX, sentrin-specific protease 1 (SENP 1) and the activating acetyltransferase CREB binding protein (CBP) plus its relative p300 [356,361].

Many of these components have intrinsic anti-viral properties, such as inactivation of viral protein functions, repression of viral transcription and degradation of viral proteins, reflecting the important role of PML NBs within the antiviral immune response [362–366]. Moreover, PML NB components play a central part in further innate and intrinsic immune mechanisms. On the one hand, several PML NB proteins are upregulated by IFNs. On the other hand, some constituents have the potential to stimulate IFN as well as cytokine signaling themselves. For instance, PML, Sp100, Daxx, and ATRX expression is upregulated by IFNs, while PML itself is able to induce IFN and cytokine signaling [362,364]. In addition, PML NB components, especially the MRN complex, act as DNA damage as well as viral genome sensors, which activate the DNA damage response, including cell cycle arrest and apoptosis upon recognition [367–369]. Due to those multifaceted anti-viral properties, PML NBs are discussed as key restriction factors of viral infections [362,364]. Hence, many viruses evolved antagonistic strategies that destroy the integrity of whole nuclear structures or inhibit individual PML NB proteins [362,366,370–375]. For example, herpes simplex virus type 1 (HSV-1), Epstein–Barr virus (EBV) and human cytomegalovirus (HCMV) express the three early proteins, infected cell protein 0 (ICP0), EBV-determined nuclear antigen (EBNA5) and immediate early protein 1 (IE1), respectively. Those target the degradation of the antiviral factor Sp100 to inhibit its transcriptional repressive function and enhance viral gene expression [376,377]. Furthermore, ICP0 initiates the degradation of PML, thus disrupting PML NBs and enhancing viral replication, while HCMV expresses IE1 and IE2, which

are involved in the dispersion of PML NBs [377–379]. Additionally, the HCMV tegument protein pp71 was shown to initiate the degradation of Daxx to ensure efficient transcription of viral genes [380]. Remarkably, some viruses do not only inhibit PML NBs, but seem to use the PML NB hub to augment their own replication [381]. This assumption is based on the observation that several nuclear replicating viruses like HAdV, HCMV, herpesviruses, polyomavirus simian virus 40 (SV40), and papillomaviruses form their RCs directly next to PML NBs and recruit different PML NB components to their RCs [381–385].

The fast adaptation of the PML-network to various situations is significantly coordinated by SUMOylation of its constituents [386]. On the one hand, SUMOylation directs the recruitment and functions of PML NB associated proteins and on the other hand, it controls the structural organization of the nuclear domains. Most PML NB components can be SUMO modified or contain SUMO interacting motifs (SIMs), which allow the interaction with a variety of SUMO modified peptides. Due to the pivotal role of SUMOylation in the PML NB organization and the concentration of required SUMO-enzymes, these structures are considered as cellular SUMOylation hot spots [386]. Accordingly, it is not surprising that several pathogens employ the SUMO machinery to antagonize anti-viral PML NB activities [317,387,388].

1.11 Interactions of viral proteins with PML NBs and the SUMO system

Several studies showed that many DNA viruses need to control the anti-pathogenic activities of PML NBs to ensure efficient dissemination. Those viruses include *Adenoviridae, Herpesviridae, Papillomiaviridae, and Poxviridae,* but also RNA viruses like *Bunyaviridae, Coronaviridae, Flaviviridae, Orthomyxoviridae, Paramyxoviridae, Picornaviridae, and Retroviridae.* Bacteria like *Clostridium perfringens, Listeria monocytogenes,* and *Streptococcus pneumoniae* have this requirement as well [32]. Interestingly, some of these pathogens developed not only antagonistic features, but also evolved mechanisms to misuse these structures for their own advantage [317,351]. As PML NBs are heavily coordinated via SUMOylation, this PTM is an important target of these pathogens for the regulation of PML NBs [389]. Since PML NB formation and SUMOylation takes place in the nucleus, especially nuclear replicating DNA viruses have been intensively studied regarding their interaction with PML NB proteins and the

SUMO machinery [317,384]. Important examples for DNA viruses, interfering with the SUMO system to block the antiviral response or to mediate their own protein activities are listed in the table below (Tab. 1) [390]. In summary, these viruses either alter global SUMOylation or influence the SUMO modification of specific substrates, which is achieved through mediation of SUMO machinery components or the expression of own SUMO-enzymes. Furthermore, different viral proteins have been confirmed as SUMO targets, influencing their protein functionality, protein interactions, localization, or stability [317,388,390,391]. Interestingly, the chicken adenovirus type 1 (CELO), expresses GAM 1, a functional homologue to the HAdV-C5 gene products encoded by the E1 region, that induces the degradation of UBC 9 and SAE 1, thereby downregulating the global amount of SUMO conjugated proteins [392].

Tab. 1: Table of DNA virus proteins interacting with PML NB components and the SUMO machinery. Modified from Wilson [390].SCM: SUMO conjugating motif; SIM: SUMO interacting motif, +: SCM/ SIM containing, -: without SCM/ SIM.

Virus family	Virus	Protein	SCM	SIM	Effect
Parvovirus	AAV	Rep78	+	-	SUMOylation may stabilize Rep78
Papillomavirus	HPV	E1	+	-	Not determined
		E2	+	-	SUMOylation stabilizes E2
		E6	-	-	Blocks SUMOylation of PIASy substrates; Degrades Ubc9
		E7	-	-	Inhibits SUMOylation of pRB
		L2	+	+	Modulates L2 incorporation into capsids
Herpesvirus	HSV	ICP0	-	+	STUbL, relocalizes SENP 1
	VSV	ORF29p	+	-	Not determined
		OFR61	-	+	Possible STUbL
	CMV	IE1	+	-	SUMOylation prevents binding to STAT2 Regulates SUMOylation of IE2
		IE2-p86	+	+	SUMOylation enhances transactivation activities
		UL44	+	-	SUMOylation enhances DNA binding
		pp71	+	-	Increases SUMOylation of Daxx
	HHV6	IE1	+	-	Not determined
		IE2	-	-	Binds Ubc9
	EBV	BZFL1 (Z)	+	-	SUMOylation represses transactivation activity
		BGLF4/ pK	-	+	Decreases SUMOylation of BZLF1
		EBNA3B	+	-	Unclear

Virus family	Virus	Protein	SCM	SIM	Effect
		EBNA3C	+	+	SUMOylation affects nuclear distribution
		LF2	-	-	Enhances SUMOylation of Rta
		LMP1	-	-	Binds Ubc9 and increases SUMOylation generally and for specific substrates Inhibits SENP 2
		Rta (BRLF1)	+	-	SUMOylation may enhance transactivation activity; promotes association with RNF4
	KSHV	K-bZIP	+	+	SUMO E3 ligase; SUMOylation enhances repressive activity
		K-Rta	-	+	STUbL
		LANA1 (ORF63)	+	+	SIM facilitates interaction with host proteins
		LANA2 (vIRF3)	+	+	Enhances and represses SUMOylation of specific substrates
Poxvirus	Vaccina	A40R	+	-	SUMOylation solubilizes A40R
		E3	+	+	SUMOylation represses transactivation activity

1.12 HAdV proteins interfering with PML NB components and the SUMO machinery

Among DNA viruses, HAdV have been intensively investigated regarding their interaction with PML NBs, leading to the identification of multiple viral proteins interfering with PML NB components. PML NBs have a dual role in HAdV infections. On the one hand, HAdV counteract antiviral PML NB components. On the other hand, they use PML NBs as a site for viral DNA replication and some components contribute beneficially to viral replication [382,393,394]. The interference of HAdV proteins with PML NBs is frequently linked to the SUMOylation system. PML NBs are considered as hot spots for this post translational modification and many HAdV proteins use the SUMOylation facility provided by PML NBs to create a replication competent milieu [387].

The first protein expressed during HAdV infection is E1A. This peptide is known to regulate a variety of important processes, including transcription of viral and cellular genes, cell cycle movement, apoptosis, differentiation, transformation, and the immune

response. To that end, E1A alters the physical properties of PML NBs and interferes with their components. Through the expression of this viral protein, the number and size of PML NBs gets reduced. Moreover, it directly binds to PML II. This complex functions as a transcriptional activator for the adenoviral E2 genes and cellular gene expression. The latter requires further interaction with p300 [394]. Additionally, E1A binds to UBC9, the sole known E2 SUMO-conjugating enzyme. Remarkably, the interaction neither has impact on transformation of mouse-embryonic-fibroblasts, nor on global SUMOylation [395–397]. Nevertheless, it has been found that E1A inhibits the SUMO 1 modification of its interaction partner pRB, which is a component of PML NBs [398]. Intriguingly, this feature depends on the binding to UBC9 [398]. However, the role of pRB SUMOylation remains elusive.

The second HAdV protein, which interferes with PML NBs and the SUMO machinery is E4orf3. An essential function of this polymeric peptide is to prevent antiviral PML NB activities such as induction of the DDR or apoptosis. Therefore, it disrupts the integrity of PML NBs and rearranges them into track-like structures. Obligatory for the reorganization is its binding to PML II [374,399]. Although the mechanism is not completely understood, it is assumed that the PML NB reorganization contributes significantly to the counteraction of the multifaceted immune response of the host cell. Besides PML II, E4orf3 sequesters many other PML NB constituents and SUMO proteins into these tracks [184,369,400–403]. In most cases this is accompanied by an increase in their SUMO modification resulting in an inhibition or proteasomal degradation [404]For instance, it relocalizes and enhances the SUMOylation of the DNA repair proteins Mre11 and Nbs1 of the MRN complex, transcriptional intermediary factor 1 α (TIF-1α, TRIM24), TIF-1γ (TRIM33), and the general transcription factor II-I (TFII-I) [369,400–403,405–407]. In fact, E4orf3 functions as an E3 SUMO ligase and elongase for Tif-1γ and TFII-I, respectively [407]. Lately, Mre11 and Nbs1 have been identified as additional E4orf3 E3 SUMO ligase substrates [408]. Furthermore, the cellular E3 SUMO ligase PIAS3 is redistributed into these tracks depending on E4orf3 expression [409]. Moreover, E4orf3 also affects the SUMOylation of viral proteins. Recently, Sohn and Hearing showed that E4orf3 functions as an E3 SUMO ligase for E1B-55K SUMO 1 modification in viral infections if E4orf6 is not expressed. However, this effect was only observed with a multiplicity of infection (MOI) of 500 [408]. Also, E2A/DBP was recently shown to be SUMOylated at

several SCMs. In general, the SUMO modification of DBP stimulates viral replication, the localization of RCs next to E4orf3 induced tracks, DBP binding to Sp100A (only in infection) and PML [410]. A further protein, which is SUMOylated during HAdV infection is the core protein pV. Notably, its SUMOylation reduces virus growth [411]. Since the adenoviral protease belongs to the same type and shows structural similarities to ULP 1, the SENP of *Saccharomyces cerevisiae*, it was tested for its ability to deconjugate SUMO, but turned out to be inactive in that way [412]. Center of this work will be the regulation of the SUMOylation of E1B-55K. Thus, the current knowledge about the viral peptide and its interference with PML NB components and the SUMO system will be described in detail in the next chapter.

1.13 HAdV-C5 E1B-55K

1.13.1 Structural features and functional domains of E1B-55K

E1B-55K consists of 496 aa and has a molecular weight of 55 kDa. An overview about the functional domains is displayed in Fig. 8. Currently, it is not known to what extent E1B-55K is structured, but it seems to have an elongated organization and to be non-globular [413]. According to mutational analysis, E1B-55K might adopt a very complex three-dimensional conformation, which is prone to mutational inactivation. Already small insertions, deletions, or point mutations throughout the protein abolishes binding to partner proteins. Furthermore, it is mostly not possible to map precise binding sites on E1B-55K for interacting proteins, resulting in the assumption that interaction motifs consist of short sequences or single aa from different areas of the protein, which are brought into close proximity through folding of its IDR [414].

At the amino terminal end, from aa 83 to aa 91, E1B-55K has a well-defined nuclear export signal (NES; LYPELRRILTI) of the human immunodeficiency virus 1 (HIV 1) Rev type. The NES enables the protein to shuttle between the nucleus and the cytoplasm via the chromosomal maintenance 1 (CRM 1) export pathway. E1B-55K mutants, in which the leucine (L) residues of the NES have been altered to alanine (A) remain in the nucleus [415–417].

Next to the NES, from aa 101 to aa 106, a classical SCM (ΨKχE/D) is located with the major SUMO attachment site at K104 [418,419]. In close proximity to the SCM, a further SUMO acceptor site has been suggested at K101.

The region between aa 282 and aa 456 is especially rich in histidine (H) and cysteine (C) residues and resembles a zinc finger binding domain. Thus far, no evidence has been found about zinc-E1B-55K interactions and the functionality of the motif. However, C residues allow internal disulfide bond formation and among different polypeptides, stabilizing the protein structure as well as protein connections [420]. In order to promote viral replication and cellular transformation, E1B-55K cooperates with various peptides. Most of the identified binding sites lie within the H/C rich domain. Particularly well studied are the interactions with the tumor suppressor p53 and the viral protein E4orf6. Residues involved in E4orf6 binding are identified at A143 and aa 262 to aa 326 [421]. This domain, partly overlaps with the p53 interacting motif from aa 224 to aa 354 [422].

At the C-terminus E1B-55K is phosphorylated at serine 490 (S490), S491, and threonine 495 (T495) [423–425]. This area is designated as the C-terminal phosphorylation region (CPR).

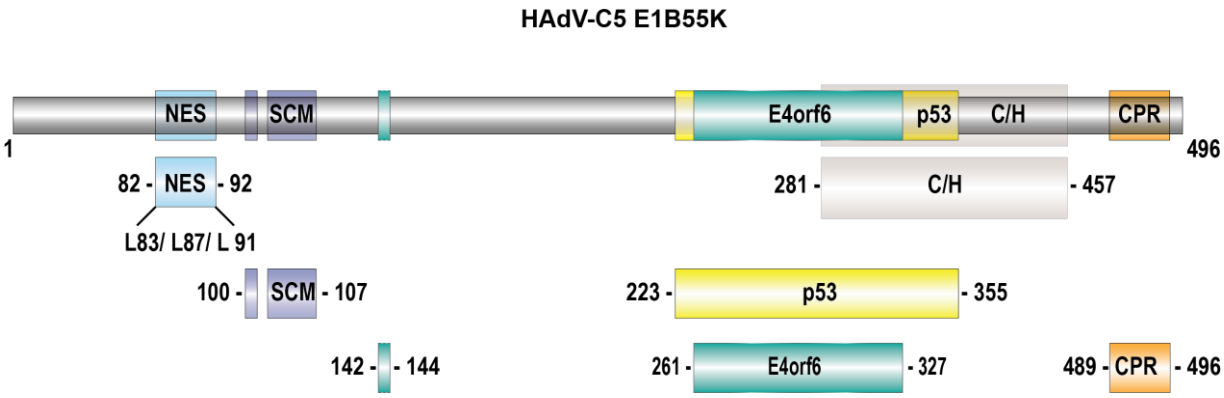

Fig. 8: Illustration of the functional domains and protein binding sites of HAdV-C5 E1B-55K. The image includes the nuclear export signal (NES) from aa 83 to aa 93 containing the leucine (L) residues 83, 87, and 91, which are mutated to alanine (A) to destroy the NES, the SUMO conjugation motif (SCM) from aa 101 to aa 106, including the SUMO conjugation site (SCS) at lysine (K) 104 and the close SCS at K101, the p53 binding region between aa 223 and aa 354, the E4orf6 binding site at A143 and the E4orf6 binding domain from aa 262 to aa 326, the cysteine/ histidine (C/H) rich area from aa 282 to aa 456, and the C-terminal phosphorylation region (CPR) from S490 to T495 [417–426].

1.13.2 Intracellular localization of E1B-55K

The intracellular localization of E1B-55K is generally heterogeneous and changes dynamically during the viral life cycle. It is influenced by the presence of other adenoviral proteins, cellular proteins and post-translational modifications (PTMs). In the early phase of infection, E1B-55K can be detected diffusely dispersed in the nucleus and in defined perinuclear aggregates in close proximity to microtubule organization centers (MTOC) [427]. Later, these cytoplasmic spots have been identified as aggresomes. These structures serve as a storage for misfolded and inactive proteins until they are degraded. Viruses regularly utilize aggresomes to inhibit anti-viral proteins [428]. The nuclear fraction of E1B-55K is mainly associated with PML NBs and E4orf3 induced PML-reorganizing tracks [429]. A further nuclear subpopulation can be detected in the nuclear matrix [430]. As virus replication progresses, E1B-55K moves to viral replication centers (RCs) and accumulates at perinuclear aggresomes [221,415,431,432]. It has been discussed if binding between E1B-55K and E4orf6 is required for the redistribution [221,415,431]. Without other viral proteins E1B-55K accumulates mainly in aggresomes [427,433]. However, export inhibitor studies revealed that E1B-55K continuously shuttles between the nucleus and the cytoplasm, independent of other viral proteins [427,433]. The nuclear export of E1B-55K is mediated by the cellular export factor CRM 1, which recognizes the NES of E1B-55K. A mutational destruction of the NES leads to a predominant nuclear localization of the viral peptide [415,419]. It is still unknown, how the import of E1B-55K is regulated, but nuclear localization correlates with proper C-terminal phosphorylation at S490, S491, and T495 as well as SUMOylation at K104 [419,425,434]. Also, E4orf3 might enhance nuclear localization [431].

1.13.3 Functions of E1B-55K

E1B-55K is an important modulator of adenoviral replication and contributes to oncogenic transformation [414]. During the productive viral life cycle, it acts at early and late stages affecting several processes such as cellular and viral gene expression, DNA damage responses, cell cycle control, induction of apoptosis, and antiviral immunity.

In the course of viral infection, E1B-55K associates with the viral protein E4orf6 and the cellular factors cullin 5, elongin B and C, the E2 ubiquitin-conjugating enzyme, as well as neddylated Rbx-1, in order to build an E3 ubiquitin ligase, which ubiquitylates

antiviral proteins leading to their proteasomal degradation (Fig. 9) [426,435]. Within this complex, E1B-55K is responsible for the recruitment of target proteins, whereas E4orf6 recruits the cellular factors, required for ligase assembly [426]. Moreover, E4orf6 prevents the deneddylation of cullin°5 by inhibiting the deneddylase SENP 8 resulting in an activation of the E3 ubiquitin ligase [436]. The first identified substrate of this complex is the tumor suppressor p53. This factor is activated by E1A and would induce apoptosis if not counteracted. Last few years, the number of verified substrates increased constantly. Numerous targets have regulatory functions within the DNA double strand break repair response and are PML NB components, such as the MRN-complex components Mre11 and Rad50, DNA ligase IV, survival-time associated PHD protein in ovarian cancer 1 (Spoc 1), blooms helicase (BLM), the acetyltransferase tat interacting protein 60 kDa (Tip60), X-linked α-thalassaemia retardation syndrome (ATRX), integrin α-3, and tankyrase 1 binding protein 1 (Tab182) [349,369,437–441]. Besides formation of an ubiquitin ligase, the E1B-55K/E4orf6 complex supports the splicing, export, and the stabilization of viral mRNAs. Simultaneously, it abrogates the generation of cellular proteins by inhibiting cellular DNA synthesis and the nuclear export of cellular mRNAs. Accordingly, this process has been named host cell shut-off [442–444].

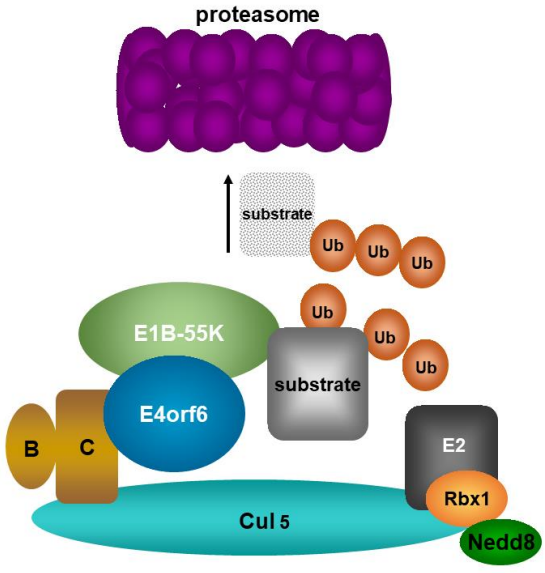

Fig. 9: Schematic illustration of the E1B-55K/E4orf6 E3 ubiquitin ligase complex. During HAdV-C5 infection E1B-55K and E4orf6 interact with the cellular factors cullin 5 (Cul5), elongin B and C (B/C), the E2 ubiquitin-conjugating enzyme, as well as the Nedd8 modified E3 ubiquitin-protein ligase Rbx-1 in order to build an E3 ubiquitin ligase complex. This E3 ubiquitin ligase transfers ubiquitin (ub) to antiviral substrates and thereby induces their proteasomal degradation.

One of the earliest identified properties of E1B-55K is its ability to inhibit the transcriptional activator p53. Many *in vitro* and transient expression analyses revealed that E1B-55K evolved several ways to inhibit p53-mediated transcription. First, E1B-55K binds to the tumor suppressor at its amino terminal transactivation domain, resulting in the sequestration of p53 to aggresomes [413,445–448]. In parallel, the interaction between E1B-55K and p53 increases the DNA binding capacity of the tumor suppressor and recruits E1B-55K to p53 responsive promoters. Here, E1B-55K functions as a transcriptional repressor of p53 dependent genes [413,446]. Furthermore, E1B-55K influences PTMs of p53. On the one hand, it acts as an E3 SUMO ligase towards p53 and enhances the SUMOylation of the tumor suppressor. Consequently, p53 is relocalized to PML NBs and exported to aggresomes more efficiently [449,450]. On the other hand, E1B-55K indirectly abrogates p53 acetylation by binding and thereby inhibiting the responsible acetyltransferase p300/ CREB binding protein associated factor (PCAF). Acetylation mediates the sequence-specific DNA binding capacity of p53 and thus facilitates the transactivation of p53 responsive promoters [451]. In combination, all these activities result in a very efficient inhibition of p53 regulated transcription and consequently in the abrogation of most p53 dependent anti-proliferative measures [452]. The capacity of E1B-55K to inhibit p53 dependent transcription strongly correlates with its transforming potential of primary baby rat kidney cells (pBRKs) [413,418,424,446,453,454]. However, whether these properties account for the viral replication promoting capacities of E1B-55K remains to be determined.

A further key ability of E1B-55K is the binding and inhibition of PML NB constituents. Dependent on the presence of other viral proteins and its PTMs, E1B-55K binds to different PML isoforms [455]. Remarkably, PML binding is essential for the co-localization of E1B-55K with PML NBs, the repression of p53-regulated transcriptional activation, induction p53 SUMOylation and oncogenic transformation of primary cells in cooperation with E1A [456]. Moreover, E1B-55K interferes with the activating transcription factor speckled protein of 100 kDa (Sp100), resulting in dissociation of the Sp100 isoforms B, C and HMG from PML NBs and in Sp100A SUMO conjugation. Sp100A is targeted through SUMOylation to the periphery of viral RCs, where it might amplify viral gene expression [183,393,457]. Furthermore, the ability of Sp100A to activate p53-mediated transcription is inhibited [457]. Recently, it has been demonstrated that E1B-55K binds

and induces the proteolytic degradation of the chromatin remodeling factor death domain-associated protein (Daxx), while the positive effect of Daxx on p53-regulated transcription is inactivated [458]. To initiate the proteasomal degradation of Daxx, E1B-55K recruits the SUMO-targeted ubiquitin ligase (STUbl) RNF4, which ubiquitylates SUMO modified Daxx and facilitates its depletion [459]. Remarkably, the degradation of Daxx does not require the presence of E4orf6, indicating that E1B-55K developed a second way to induce the proteasomal degradation of antiviral factors [458]. Furthermore, E1B-55K binds heterochromatin-associated transcription factor Kruppel-associated box associated protein 1 (Kap1) and reduces its SUMOylation, whereby epigenetic gene silencing on the viral genome might be minimized. In parallel, this interaction results in an increased SUMO modification of E1B-55K [460]. Additionally, the E2 SUMO enzyme Ubc9 has been identified as an interaction partner of E1B-55K [461].

1.13.4 Phosphorylation of E1B-55K

E1B-55K is phosphorylated at three residues at its C-terminus. In general, phosphorylation is an important tool for the cell to control protein functions. It is regulated by kinases and phosphatases. Kinases catalyze the transfer of a γ-phosphoryl group of ATP to an amino hydroxyl group of a protein substrate, while phosphatases facilitate the reverse reaction. Phosphorylation mainly occurs at serine, threonine and tyrosine residues and is associated with the activation and deactivation of enzymes and receptors [462]. E1B-55K is phosphorylated at three sites at its N-terminus (S490, S491, and T495) [423,424]. The phosphorylated serine residues of E1B-55K lie within a consensus sequence for casein kinase 2 (CK2; (S/TXXE/D), while the threonine is included in a casein kinase 1 (CK1) consensus site. However, CK2 is known for a broad substrate spectrum and phosphorylates all three residues during adenoviral infection [425]. Phenotypic analyses of E1B-55K phospho-mutants, in which all three phosphorylation sites were substituted either by aspartate (D) or alanine (A) revealed that phosphorylation at serine (S)490, serine (S) 491, and threonine (T) 495 is prerequisite for nuclear localization, aggresome formation, the transcriptional repression properties, and the ability to block E1A induced p53-mediated apoptosis [423,424]. Moreover, co-transfection experiments displayed that aa exchanges of serine (S)/ threonine (T) to alanine (A) inhibit the association of E1B-55K with p53, explaining the abrogated p53 repression [424,434]. Likewise, the interaction with MRN components

and DNA ligase IV is impaired, resulting in impaired proteasomal degradation without affected E1B-55K binding to E4orf6 [434]. In line with these observations, the phosphorylation deficient E1B-55K mutant lost its ability to transform pBRKs in combination with E1A [423,424]. Consistent with several studies about cross talk between different PTMs, phosphorylation promotes the SUMOylation of E1B-55K at K104 [461].

1.13.5 Regulation of E1B-55K functions via SUMOylation

SUMOylation is a very efficient and dynamic cellular mechanism for the modulation of protein functions and localization. Several viruses developed mechanisms to usurp the SUMO machinery to control their own proteins. Besides DBP and pV, E1B-55K has been identified as adenoviral SUMO targets. Mutational analysis identified K104 as the major acceptor site. This site is embedded in a classical SCM [418,461]. Notably, K104R is highly conserved among divergent HAdV types, indicating its relevance for protein functions [461]. In consecutive studies, our department investigated the K at position 101 as a putative minor SUMO attachment site. E1B-55K can be modified by SUMO 1 to SUMO 3 [408]. However, the composition of attached SUMO chains and the corresponding E3 SUMO ligase are still unknown.

As SUMOylation is known to determine the physiological as well as biological properties of proteins, E1B-55K SUMO mutants have been analyzed regarding protein-protein interactions, spatial distribution, and functionality. Remarkably, these investigations have demonstrated that SUMOylation regulates some, but not all functions of E1B-55K. Precisely, the efficient repression of p53-dependent transcription, the retention of p53 in PML NBs, its function as an E3 SUMO ligase towards p53, and consequently the transformation of pBRKs in cooperation with E1A is suppressed, if SUMOylation of E1B-55K is prevented [418,450]. Furthermore, the association with PML isoform V, but not with PML IV is disturbed [455]. However, in infection experiments other viral proteins influence the E1B-55K interaction with different PML isoforms. Currently, it is unknown whether these dissimilarities are based on E1B-55K SUMOylation changes [455]. Additionally, it has been revealed that binding, sequestration, and enhancement of Sp100A SUMOylation are dependent on E1B-55K`s own SUMOylation [457]. Moreover, the E4orf6 independent proteolytic degradation of Daxx requires the SUMOylation of E1B-55K at K104 [458]. Remarkably,

neither binding to Daxx nor UBC9 is impaired by a depleted SUMO modification of E1B-55K [418,463]. Lastly, the inhibition of SUMO modification inhibits the nuclear import of E1B-55K [461]. Hence, the altered subcellular localization of SUMO depletion mutants is assumed to be one of the reasons for their functional defects [418,461].

In line with the previously explained observations, augmented SUMOylation is accompanied by increased activity and predominant nuclear localization. For example, the disruption of the NES at the N-terminus of E1B-55K results in higher SUMOylation of the viral protein and in parallel increased pBRK transformation and repression of p53 induced transcriptional activation. Furthermore, this mutant displays a predominant localization at viral RCs in the nucleus [461].

Beyond that, little is known about the regulation of E1B-55K SUMOylation. On the one hand, phosphorylation has been shown to stimulate E1B-55K's SUMOylation [461]. On the other hand, nuclear localization of E1B-55K correlates with its SUMO modification [419,461]. However, whether nuclear localization is a prerequisite for SUMOylation or if SUMOylation targets E1B-55K to the nucleus is not clear yet. In addition, protein interactions influence SUMOylation of E1B-55K. For example, the viral protein E4orf6 has been discussed as a regulatory factor for E1B-55K SUMOylation. Virus mutants, harboring an E4orf6 deletion, show an increased SUMOylation of E1B-55K [430]. Besides E4orf6, interaction with the cellular protein Kap1 influences SUMOylation of E1B-55K. As explained above, the interaction of the two proteins results in an increased SUMOylation of E1B-55K, while SUMO modification of Kap1 is reduced [460]. Notably, E4orf6 has been suggested as an additional regulator of E1B-55K SUMOylation [430].

In summary, E1B-55K not only regulates antiviral activities of cellular proteins via modulation of their SUMOylation. It is also itself a target of the SUMO machinery, whose activity and nuclear localization correlate with its SUMO conjugation levels.

2 Material

2.1 Cells

2.1.1 Bacterial cells

Strain	Genotype
DH5α	supE44, ΔlacU169, (φ80dlacZΔM5), hsdR17, recA1, endA1, gyrA96, thi-1, relA1.
GB05red	(GB2005, araC-BAD- γβαA) lambda red operon and recA under P_{BAD} promotor were inserted at the *ybcC* locus.
GBred-gyrA462	(GB05red, *gyrA462*) GyrA mutation of Arg462Cys.

2.1.2 Mammalian cells

Cell line	Genotype	Reference
A549	Human lung carcinoma cell line.	DMSZ
H1299	Human lung carcinoma cell line, p53 negative.	ATCC
HeLa	Human cervix carcinoma cell line, p16-negative.	DMSZ
Hela SUMO 1	HeLa cells stably expressing N-terminally 6x His-tagged SUMO 1 under puromycin selection (2µg/ ml).	Ron Hay
HeLa SUMO 2	HeLa cells stably expressing N-terminally 6x His-tagged SUMO 2 under puromycin selection (2µg/ ml).	Ron Hay
pBRK	Primary baby rat kidney cells, freshly isolated from 3-5 days old Sprague Dawley rats (Janvier, France).	Ron Hay

2.2 Viruses

Adenovirus	Virus characteristics
H5pg4100 (HAdV-C5-wt)	Wild type HAdV-C5 carrying an 1863 bp deletion (nt 28602-30465) in the E3 open reading frame.
H5pm4102 (HAdV-C5 K104R)	HAdV-C5 mutant based on the H5pg4100 backbone with an additional mutation resulting in a K to R exchange at position 104 of E1B-55K (K104R).
H5pm4243 (HAdV-C5 K101R)	HAdV-C5 mutant based on the H5pg4100 backbone with an additional mutation resulting in a K to R exchange at position 101 of E1B-55K (K101R).
H5pm4244 (HAdV-C5 K101R K104R)	HAdV-C5 mutant based on the H5pg4100 backbone with an additional mutation resulting in a K to R exchange at position 101 and 104 of E1B-55K (K101/104R).

H5hh4301 (HAdV-C5 ΔE4orf6)	HAdV-C5 E4orf6 deletion mutant based on the H5pg4100 backbone with a point mutation in the E4orf6 open reading frame resulting in a stop codon at P66.
H5hh4303 (HAdV-C5 K104R ΔE4orf6)	HAdV-C5 E4orf6 deletion mutant (ΔE4orf6) based on H5pm4102.
H5hh4302 (HAdV-C5 K101R ΔE4orf6)	HAdV-C5 E4orf6 deletion mutant (ΔE4orf6) based on H5pm4243.
H5hh4304 (HAdV-C5 K101/104R ΔE4orf6)	HAdV-C5 E4orf6 deletion mutant (ΔE4orf6) based on H5pm4244.
H5hh2476 (HAdV-C5 A143)	HAdV-C5 mutant based on the H5pg4100 backbone with a mutation resulting in an insertion of the aa L, E, F, and Q behind A143 of E1B-55K.
H5hh2477 (HAdV-C5 A143 ΔE4orf6)	HAdV-C5 E4orf6 deletion mutant (ΔE4orf6) based on the H5hh2477.
H5pm4174 (HAdV-C5 delP)	HAdV-C5 E1B-55K mutant carrying three amino acid exchanges in the CK2 consensus (S490/91A, T495A) leading to a complete phosphorylation deficiency.
H5hh4326 (HAdV-C5 delP ΔE4orf6)	HAdV-C5 E4orf6 deletion mutant (ΔE4orf6) based on H5pm4174.
H5pm4175 (HAdV-C5 pM)	HAdV-C5 E1B-55K mutant carrying three amino acid exchanges in the CK2 consensus (S490/91D, T495D) resulting in a mimicked phosphorylation.
H5hh4327 (HAdV-C5 pM ΔE4orf6)	HAdV-C5 E4orf6 deletion mutant (ΔE4orf6) based on H5pm4175.

2.3 Nucleic acids

2.3.1 Oligonucleotides

Name	Sequence	Purpose
cmv	5’-CCC ACT GCT TAC TGG C-3’	Sequencing
pcDNA3-rev	5’-GGC ACC TTC CAG GGT CAA G-3’	Sequencing
E1-Box fwd 2454 bp	5’-CAA GGA TAA TTG CGC TAA TGA GC-3’	Sequencing
E1B-C-Terminus	5’-GGCCTCCGACTGTGGTTGCTTC-3’	Sequencing
Q90P fwd	5’-GAT GTG TTC CAA CAG CCG ACG GGA GGT TAG-3’	SDM
Q90P rev	5’-CTA ACC TCC CGT CGG CTG TTG GAA CAC ATC-3’	SDM
S490/491D T495D rescue	5’-AGC TGA GGC CCG ATC ACT TGG TGC TGG CCT GCA CCC GCG CTG AGT TTG GCG ATG ACG ATG AAG ATG AC GAT	RED rec.

	TGAG GTA CTG AAA TGT GTG GGC GTG GCT TAA GGG TGG GAA AGA ATA T-3’	
S490/491A T495A rescue	5’-AGC TGA GGC CCG ATC ACT TGG TGC TGG CCT GCA CCC GCG CTG AGT TTG GCG CTG CCG ATG AAG ATG CA-3’	RED rec
E1B phosphor ccdB amp fw	5’-AGC TGA GGC CCG ATC ACT TGG TGC TGG CCT GCA CCC GCG CTG AGT TTG GCG CCA GTA TAC ACT CCG CTA G-3’	RED rec
delP rescue	5‘-CTG GTC ATT AAG CTA AAA GCT AGA TTC CTA GCC TCC TCT GTA GCC TCA CAA GCA GCC CCA TAC GAT ATA AGT TG-3‘	RED rec
Seq E4orf6 p15AAd5 rev	5’-CTT TGA GAG AGT GGA TAT ACT AC-3’	Sequencing
Seq E4orf6 p15A Ad5 fw	5’-CAT ATT CTT AGG TGT TAT ATT C-3’	Sequencing
Seq E4orf6 p15AAd5 2. fwd	5’-CAA CTT GCG GTT GCT TAA C-3’	Sequencing
Seq E4orf6 p15A Ad5 2. rev	5’-CTG GTT TTG CTT CAG GAA ATA TG-3’	Sequencing
E4orf6 fwd 32246bp	5’-GCA GAT CTG TTT GTC ACG CC-3’	Sequencing
SENP 1 seq	5’-GCA TTT GGA TCC AAA GAT TCT GG-3’	Sequencing
SENP 2 seq	5’-CAA AAA GAG GAA AGA GAG AAG TAC C-3’	Sequencing
SENP 3 seq	5’-CTG TTG TCG TTT TGA CTC-3’	Sequencing
SENP 6 seq	5’-GAA TCA CAA GTG GAG CCT GAA ATT AAG-3’	Sequencing
SENP 7 seq	5’-CAG GAA ACA GCT ATG ACC-3’	Sequencing

2.3.2 Vector plasmids

#	Name	Reference
136	pcDNA3	DMSZ
152	pCMX3b-Flag	ATCC

2.3.3 Recombinant plasmids

Name	Vector	Insert	Reference
6x His SUMO 2.	pcDNA3	SUMO 2	R. Hay
SENP 1 flag	pcDNA3-flag	SENP1	S. Müller
SENP 2 flag	pcDNA3-flag	SENP2	S. Müller
SENP 3 flag	pCI-Flag	SENP3	S. Müller
SENP 6 flag	pCI-Flag	SENP6	S. Müller

SENP 7 flag	pCI-Flag	SENP 7	S. Müller
SENP 1 CAT flag	pcDNA3-flag	SENP1 CAT C603S	S. Müller
SENP 2 CAT flag	pcDNA3-flag	SENP2 CAT C548S	S. Müller
SENP 3 CAT flag	pCI-Flag -flag	SENP3 CAT C532S	S. Müller
SENP 6 CAT flag	pCI-Flag -flag	SENP6 CAT C1030S	S. Müller
SUMO2 Q90P	pcDNA3	SUMO 2 Q90P	This work
pcDNA-E1B-55K	pcDNA3	HAdV-C5 E1B-55K	Group database
pcDNA-K101R	pcDNA3	HAdV-C5 K101R	Group database
pcDNA-E4orf6	pcDNA3	HAdV-C5 E4orf6	Group database
p15A Ad5 E4orf6-	p15A	HAdV-C5 ΔE4orf6	Group database
p15A Ad5 E1B-55K delp E4orf6-	p15A	HAdVC5 E1B-55K S490/491A T495A/ ΔE4orf6	Group database
p15A Ad5 E1B-55K PM E4orf6-	p15A	HAdVC5 S490/491D T495D /ΔE4orf6	Group database

2.4 Antibodies

2.4.1 Primary antibodies

Name	Properties
2A6	Monoclonal mouse Ab against the N-terminus of HAdV-C5 E1B-55K (hybr. sup.).
4E8	Monoclonal rat Ab against the central region of HAdV-C5 E1B-55K (hybr. sup.).
RSA3	Monoclonal mouse Ab against the N-terminus of HAdV-C5 E4orf6 (hybr. sup.).
1807	Polyclonal rabbit Ab against HAdV-C5 E4orf6 (serum).
B6-8	Monoclonal mouse Ab against HAdV-C5 E2A (hybr. sup.).
Actin (AC-15)	Monoclonal mouse Ab against β-actin (Sigma-Aldrich, A5441).
6xis	Monoclonal mouse Ab against 6xHis-tag (Clontech, 631212).
Flag M2	Monoclonal mouse Ab against the flag tag (Sigma-Aldrich, F3165).
Flag 6F7	Monoclonal rat Ab against the flag tag (hybr. sup.).
SUMO 2/3	Monoclonal mouse Ab against SUMO 2/3 (MoBiTec, M114-3).
6A11	Monoclonal rat Ab against HAdV-C5 E4orf3 (hybr. sup.).

2.4.2 Secondary antibodies for immunoblotting

Name	Properties
HRP-anti-mouse IgG	Polyclonal horseradish peroxidase (HRP) conjugated Ab against mouse IgG (H+L $(ab')_2$ fragment, raised in goat (Jackson, 115-036-003).
HRP-anti-rat IgG	Polyclonal HRP conjugated Ab against rat IgG (H+L $(ab')_2$ fragment, raised in goat (Jackson, 112-036-003).
HRP-anti-rabbit IgG	Polyclonal HRP conjugated Ab against rabbit IgG (H+L $(ab')_2$ fragment, raised in goat (Jackson, 111-036-003).
HRP-anti-mouse IgG (light chain specific)	Polyclonal HRP conjugated Ab against the light chain of mouse IgG raised in goat (Jackson, 115-035-174).

2.4.3 Secondary antibodies for immunofluorescence analyses

Name	Properties
Alexa Fluor™ 488 anti-mouse	Polyclonal Alexa™488 conjugated Ab against mouse IgG (H+L, F(ab')2 fragment), raised in goat (Invitrogen, A-11001).
Alexa Flour™ 488 anti-rat	Polyclonal Alexa™488 conjugated Ab against rat IgG (H+L, F(ab')2 fragment), raised in goat (Invitrogen, A-11008).
Cy5 anti-rat	Polyclonal Cy5 conjugated Ab against rat IgG (H+L, F(ab')2 fragment), raised in goat (Dianova).

2.5 Standards and markers

Product	Companys
1 kb and 100bp DNA ladder	NEB
Page Ruler™ Prestained Protein Ladder	Thermo Scientific

2.6 Commercial systems

Product	Company
Plasmid Purification Mini, Midi, and Maxi Kit	Qiagen
QIAquick® Gel Extraction Kit	Qiagen
Protein Assay	BioRad
SuperSignal™ West Pico Chemilumininescent Substrate	Thermo Scientific
ProFection® Mammalian Transfection System	Promega

2.7 Chemicals, enzymes, reagents, equipment

All chemicals, enzymes, reagents, cell culture materials, general plastic material, and other equipment were obtained from the following companies: AppliChem, Biomol, BioRad, Biozym, Brand, Engelbrecht, Eppendorf, Falcon, Gibco BRL, Greiner, Hartenstein, Hellma, Ibidi, Invitrogen, Merck, New England Biolabs, Nunc, Pan, Promega, Protean, Qiagen, Roche, Sarstedt, Schleicher&Schuell, Sigma Aldrich, Stratagene and ThermoFisher Scientific, VWR, and Whatman.

2.8 Software and database

Software	Purpose	Reference
Acrobat 9 Pro	PDF data processing	Adobe
CLC Main Workbench 7	Sequence data processing	CLC bio
Filemaker Pro 14	Database management	Filemaker, Inc.
Illustrator C6	Layout processing	Adobe
Photoshop CS6	Layout processing	Adobe
Word 2016/365	Text processing	Microsoft
PowerPoint 2016/365	Layout processing	Microsoft
PubMed	Literature database, open sequence analysis	Open software (provided by NCBI)
Fiji	Image processing	imagej
Prism 5	Data graphing, statistical analysis	GraphPad
NIS-Elements	Imaging of confocal fluorescence images	Nikon
NIS-Elements Viewer 4.20	Imaging software	Nikon
Gene tool	Imaging of agarose gels and transformation assay plates	GBox-Systems (Syngene)
GPS-SUMO	*In silico* prediction of SCMs and SIMs	The cuckoo work group
Mendeley Desktop 1.19.6	Reference management	Mendeley Ltd.

3 Methods

3.1 Bacterial cells

3.1.1 Culture and storage

Bacterial cell cultures were grown as liquid or solid cultures. Liquid cultures consisted of sterile Luria-Bertani (LB) broth containing 100 µg/ml ampicillin and were inoculated with a single *Eschericha* (*E.) coli* colony. Afterwards, inoculated cultures were incubated for 24 h at 30 or 37 °C and 210 rpm in the Innova 4000 Incubator (New Brunswick). To inoculate solid cultures, *E. coli* cells were plated on LB-agar dishes, containing 100 µg/ml ampicillin and incubated for 24 h at 30 or 37 °C. From these plates, single colonies were picked and used for the inoculation of liquid cultures. For short-term storage *E. coli* cultures were kept at 4 °C. For long-term storage, liquid cultures were mixed 1:1 (v/v) with autoclaved glycerol and stored in CryoTubes™ (Sarstedt) at -80 °C.

LB-medium	10 g/l 5 g/l 5 g/l	tryptone yeast extract NaCl *autoclaved
antibiotic solution	100 mg/ml	ampicillin *sterile filtered *stored at -20 °C

3.1.2 Chemical transformation of *E. coli*

100 µl of chemical competent *E.coli* DH5α were gently thawed on ice and transferred into a pre-cooled polypropylene reaction tube (14 ml; Falcon) containing approximately 200 ng of plasmid DNA. Next, the cells were mixed carefully with the DNA by pipetting up and down. Afterwards, the cells were incubated for 30 min on ice, followed by a heat shock at 42 °C for 45 s in a water bath. Afterwards, the reaction mix was cooled for 2 min on ice. Then, 1 ml LB medium without antibiotics was added and the bacteria were incubated for 1 h at 37°C and 200 rpm (Inova 4000 Incubator, New Brunswick). Finally, the culture was centrifuged for 3 min at 4000 rpm and 4°C (Centrifuge 5417 R; Eppendorf) and the pelleted cells were resuspended in 100 µl LB medium and plated on LB dishes containing the appropriate antibiotic.

3.1.3 Preparation of electro-competent bacteria

At first, 5 ml LB medium were supplemented with appropriate antibiotics, inoculated with the desired bacterial strain and incubated overnight (Inova 4000 Incubator; New Brunswick). At the next day, 1.4 ml of LB medium plus appropriate antibiotics was inoculated with 30 µl of the pre-culture in a 1.5 ml reaction tube (Eppendorf) and incubated for 2 h at 37 °C and 850 rpm (Inova 4000 Incubator; New Brunswick). In parallel, ddH_2O was cooled on ice. After the incubation period, cells were prepared for electroporation. First, cells were centrifuged at 7800 g for 30 s at 2°C (Centrifuge 5417 R; Eppendorf) to remove the culture medium. Next, these cells were washed twice with pre-cooled ddH_2O. Therefore, the cell pellet was resolved in 1 ml ddH_2O by vortexing. After the first washing step, cells were pelleted via centrifugation at 9600 g for 30 s at 2 °C (Centrifuge 5417 R; Eppendorf). After the second washing step, cells were centrifuged at 11600 g for 30 s at 2 °C (Centrifuge 5417 R; Eppendorf). Each time, the ddH_2O was decanted carefully. After the second washing step, cells were resolved in pre-cooled 30 µl ddH_2O and immediately applied to electroporation.

3.1.4 Electroporation of bacteria

In advance, electroporation cuvettes (BioRad, 1mm) were pre-cooled on ice. Then, electro-competent bacteria were transferred to a pre-cooled electroporation cuvette (BioRad, 1mm) and supplemented with the DNA, which has to be electroporated. Electroporation was performed in a GenePulser machine (BIO-RAD Micro Pulser Program EC1: 1 pulse 1,8 kV) for approximately 5 ms. After the pulse, the cells were resuspended immediately in 600 µl of LB medium without antibiotics and transferred into 1.5 ml reaction tubes and incubated for 1 hour at 37°C (ThermoMixer®comfort; Eppendorf). Afterwards, cells were plated on LB agar containing appropriate antibiotics and incubated at 37°C overnight.

3.2 Mammalian cells

3.2.1 Maintenance and passaging of mammalian cell lines

All cell culture techniques were performed in special laminar cell culture flow hoods to ensure sterile conditions. Furthermore, mammalian cells were grown in monolayers on polystyrene cell culture dishes (Sarstedt/Falcon). As culture medium, Dulbeccos Modified Eagle Medium (DMEM, Gibco) containing 0.11 g/l sodium pyruvate was used

($DMEM_0$). Additionally, the DMEM was supplemented with 10 % FCS (PAN) and 1 % penicillin/ streptomycin solution (10000 U/ml penicillin; 10 mg/ml streptomycin in 0.9 % NaCl, PAN) by hand (standard medium). Before usage, culture medium was prewarmed to 37°C in a water bath. In case of HeLa SUMO 1 and HeLa SUMO 2 overexpressing cells, the DMEM was also supplemented with puromycin (1 µg/ml). Mammalian cells were cultivated at 37 °C in Hera Safe 6220 incubators (Heraeus) in a 5 % CO2 atmosphere.

For cell passaging, the media was removed, the cells were washed with phosphate buffered saline (PBS) and detached by a trypsin digest for 5-10 min at 37°C. To inactivate the trypsin again, standard medium was added and the cells were transferred to 50 ml tubes (Falcon) for centrifugation (2000 rpm, 3 min, Multifuge 3S-R; Heraeus). In the next step, the medium was aspirated and the pelleted cells were resuspended in fresh standard medium. Depending on the purpose, the cells were reseeded in a cell type specific ratio (1:5 – 1:20) or counted and re-plated for experiments (3.2.2).

3.2.2 Determination of the cell number

For experimental approaches, cells were counted with a Neubauer cell counter (Carl Roth). To avoid the counting of already dead cells, 50 µl of cell-suspension was mixed with 50 µl trypan blue solution to dye dead cells before counting. Next, 10 µl of the mix was pipetted onto the counting chamber and the number of cells was determined in a light microscope (Leica DMIL). The number of cells was calculated by the following formula:

$$\frac{cells}{ml} = counted\ cells * 2 * 10^4$$

PBS (pH 7,3)	140 mM	NaCl
	3 mM	KCl
	4 mM	Na_2HPO_4
	1,5 mM	KH_2PO_4
		*autoclave
trypan blue solution	0,15 % (w/v)	trypan blue
	0,85 % (w/v)	NaCl in H_2O

3.2.3 Storage and re-cultivation of mammalian cell lines

In order to store mammalian cells, the cells were trysinized and centrifuged as described above (3.2.1). Then, the cells were resuspended in FCS, supplemented with 10 % DMSO (v/v), and stored as 1 ml aliquots in 1.8 ml CryoTubes™ (Sarstedt) at -80°C in a freezer or in a liquid nitrogen tank. To ensure a gradually freezing the cells were cooled down to -80 °C in a Mr. Frosty (Zefa Laborservice).

To re-cultivate frozen cells, they were thawed in a water bath at 37°C, diluted in 10 ml standard culture medium and centrifuged with 2000 rpm for 3 min (Multifuge 3S-R; Heraeus). The pelleted cells were resuspended in an appropriate volume of standard DMEM and seeded on culture plates with a suitable size.

3.2.4 Transfection of mammalian cells

3.2.5 Polyethylenimine (PEI) transfection

Plasmid DNA can be introduced into mammalian cells via PEI transfection. PEI is a stable cationic polymer and is able to condense DNA into positively charged particles. These particles bind to anionic cell surfaces and can be endocytosed by the cell.

PEI was dissolved in dd H_2O (1 mg/ml) and the pH was adjusted to 7. 2 with 0.1 N HCl. Finally, the solution was sterilely filtered (pore size 0.45 µm, VWR) and stored at -80°C. Cells to be transfected were seeded 24 h before transfection. For transfection, the plasmid DNA was diluted in DMEM without supplements to 500 µl followed by the addition of PEI in a ratio of 1:10 (DNA: PEI, v/v). The mixture was shortly vortexed and incubated at RT for 20 min. In the meantime, the medium of the cells was removed and replaced with fresh DMEM without supplements ($DMEM_0$). For transfection, the cells were hardly covered with medium to avoid cell draining. Before adding the transfection mix dropwise to the cells, the probes were shortly centrifuged. The culture dishes were swirled gently and incubated for 4 h at standard culturing conditions. Afterwards, the medium was replaced by standard culture medium and the cells were propagated further for 24 – 48 h.p.t.

3.2.6 Calcium-phosphate transfection

Cells were seeded 24 h before transfection in 10 cm dishes. The next day, the DNA for each sample was diluted with ddH_2O to a final volume of 437.5 µl. Furthermore, 62 µl 2M $CaCl_2$ solution was added. Under aeration, each sample mix was added to 500 µl 2xHBS buffer.

Mixing DNA with calcium chloride in a buffered saline/phosphate solution leads to a co-precipitation of calcium-phosphate-DNA crystals. These crystals can be endocytosed by cells. Aeration of the phosphate buffer while adding the DNA-calcium chloride solution ensures the formation of very fine precipitates, which is important because clumped DNA will not adhere to or enter the cell efficiently. Since crystal formation is also pH depended, all reagents have to be warmed to RT before usage.

The transfection solution was incubated 30 min at RT. During this period, the medium of the cells was exchanged by 5 ml per 10 cm dish fresh standard culture medium. Afterwards, the transfection mix was dropped on the cells and the cells were incubated 6-8 h under standard cell culture conditions. Afterwards the transfection medium was exchanged by fresh standard medium, to avoid toxic effects of the transfection reagents.

3.2.7 Transfection with Lipofectamine® 2000

In two separate reaction tubes (Sarstedt) the DNA and 20 µl Lipofectamine® 2000 were diluted with $DMEM_0$, to a final volume of 500 µl each. Afterwards both solutions were unified, gently vortexed, and briefly centrifuged. Then, the transfection mixture was incubated for 20 min at RT. After incubation, the cells were washed once with $DMEM_0$, followed by a dropwise addition of the transfection mix to the cells. In case the medium was not enough to cover the cells further $DMEM_0$ was added. The culture dishes were shaken carefully and incubated at normal conditions for 6-8 h, whereby the plates were swirled every hour. Finally, the medium was changed to standard medium and incubated at standard propagation conditions.

3.2.8 Harvesting of mammalian cells

For harvesting adhesive cells, the culture medium was exchanged with ice cold PBS. Subsequently, the cells were detached carefully with a cell-scraper and transferred to a falcon tube. After a centrifugation step at 2000 rpm for 3 min (Multifuge 3S-R; Heraeus), the PBS was removed and the pelleted cells were replated or stored at -20 °C.

3.2.9 Transformation assay

In order to study the influence of overexpressed cellular proteins on the transformation potential of adenoviral onco-proteins, transformation assays with primary baby rat kidney cells (pBRKs) were performed. These cells were freshly isolated from 3 to 5 days old baby rats and cultured as described above. 48 h post isolation, the cells were seeded and 24 h later transfected via the calcium phosphate method. The transfected cells were cultured for 4-8 weeks, until multilayered colonies of transformed cells (foci) were visible and most untransformed cells died. During this time, the medium was changed once per week. The transformation efficiency was quantified by counting the emerged cell foci. Therefore, the foci were stained with a crystal violet solution (74 % dd H_2O 25 % methanol (v/v) 1% crystal violet (w/v).

3.3 DNA techniques

3.3.1 Preparation of plasmid DNA (maxi prep)

For the preparation of plasmid DNA from *E. coli*, 500 ml LB medium containing the appropriate antibiotic were inoculated with a single colony of pre-plated bacteria or 200 µl of a liquid pre-culture derived from a single bacteria colony. After 24 h of incubation at 30 C or 37°C and 210 rpm (Inova 4000 Incubator; New Brunswick), the cells were pelleted at 6000 rpm for 10 min at 4°C (Avanti J-E; Beckman & Coulter). Afterwards, plasmid DNA was prepared via Maxi Kit according to the manufacturers protocol (Qiagen).

3.3.2 Preparation of plasmid DNA (mini prep)

For the preparation of small amounts of plasmid DNA, for example for the generation of a new plasmids, 1 ml liquid LB cultures were inoculated with a single bacteria colony

or 20 µl of a liquid pre-culture derived from a single bacteria colony. Cells were incubated overnight at 30/37 °C and 210 rpm (Inova 4000 Incubator; New Brunswick). The next day, the cells were centrifuged at 6000 rpm for 3 min at 4 °C (Centrifuge 5417 R; Eppendorf). Afterwards, the supernatant was discarded and the cell pellet was resuspended in in 300 µl resuspension buffer P1 (Qiagen). Subsequently, 300 µl lysis buffer P2 were added and the pellet buffer solution was vigorously mixed to ensure proper cell lysis. After 5 min incubation at RT, cell lysis was stopped by adding 300 µl neutralization buffer P3 (Qiagen) and a 20 min incubation period on ice. In the next step, cell debris was separated via centrifugation at 13000 rpm for 5 min and 4 °C (Centrifuge 5417 R; Eppendorf). The DNA containing supernatant was transferred to 1.5 ml reaction tube (Eppendorf) and supplemented with one volume isopropanol. To precipitate the DNA, the solution was centrifuged at 130000 rpm for 30 min at 4 °C (Centrifuge 5417 R; Eppendorf). Subsequently, the supernatant was carefully discarded and the DNA pellet was washed with 70 % (v/v) ethanol and precipitated again via centrifugation at 13000 rpm for 10 min at 4°C (Centrifuge 5417 R; Eppendorf). Afterwards, the washing solutions was aspirated and the DNA pellet was air dried. Finally, the DNA pellet was dissolved in approximately 20 µl of ddH_2O.

3.3.3 Determination of nucleic acid concentration

DNA concentrations and purity were measured with a NanoDrop spectrophotometer (PEQLAB) at a wavelength of 260 nm. DNA purity was given by the calculation of the OD_{260}/OD_{280} ratio. A value of 1.8 indicates highly pure DNA.

3.3.4 Agarose gel electrophoresis and gel extraction

For gel electrophoreses 0.8 % (w/v) agarose gels (Seakem® LE agarose; Biozym) were casted. Therefore, 1 x TBE buffer was mixed with agarose and heated in a microwave to solve the agarose powder. Additionally, the solution was supplemented with 0.5 g/ml ethidium bromide (Roth) to stain nucleic acids and poured in a casting apparatus. For analysis the DNA samples were supplemented with 6x Loading buffer (NEB), loaded into the gel pockets and separated according to the size using a constant voltage of 5-10 V/cm in 1x TBE buffer. Pursuing to the expected DNA size a 100 bp or 1kb marker was chosen as a reference. The DNA was visualized and documented by exposing the ethidium bromide bound DNA with UV light of a wavelength of 312 nm in the UV

transilluminator (G-box system, Syngene) and using gene tool software for taking pictures. DNA bands designated to gel extraction were analyzed with a UV table and cut out with a scalpel. Later, the DNA was extracted using the QIAquick® Gel Extraction Kit (QIAGEN) according to the manufacturer's protocol.

3.3.5 Polymerase chain reaction (PCR)

For DNA amplification, a 50 µl reaction mix was prepared in 0.2 ml PCR tubes (Sarstedt) containing 25 ng DNA template, 125 ng forward and reverse primer, 1 µl dNTPs (1 mM each, NEB), 5 µl 10 x PCR reaction buffer, and the Pfu Ultra II DNA Polymerase (5 U/µl, Stratagene). Sterile water was added to reach the desired volume of 50 µl. The following PCR program was performed in a thermocycler (MJ Mini™ Personal Thermo Cycler, BioRad):

DNA denaturation	1 min	95 °C
Primer annealing	45 s	55-77°C
Extension	1 min/ kb 20-30 cycles	72°C
Final extension	10 min	72°C
Storage	hold	4 C

To control PCR efficiency as well as size of the amplified DNA fragment, 5 µl of the PCR product solution were analyzed via agarose gel analysis. Size and DNA yield were examined with the G:Box transilluminator system (SynGene).

3.3.6 Site-directed mutagenesis

Point mutations were introduced into DNA plasmids via site-directed mutagenesis PCR. Therefore, specific forward and reverse oligonucleotides were synthesized encoding the mutations to be introduced. These oligonucleotides were utilized for a PCR reaction according to the following the protocol:

DNA denaturation	1 min	95 °C
Primer annealing	45 s	55°C
Extension	45 s / kb 12-18 cycles	68 °C
Final extension	10 min	68°C
Storage	hold	4 C

Afterwards, the reaction mixture was applied to Dpn 1 (New England Biolabs) digestion for 2 h at 37 °C to destroy the methylated DNA template. Subsequently, 10 µl of the digested PCR mixture were investigated via agarose gel analyses to ensure the correct and efficient amplification of the DNA plasmid. Afterwards, 10 µl of the reaction mixture was transformed into chemical competent *E. coli* DH5α cells as described in 3.1.2. The next day, single colonies were picked and used for the inoculation of liquid LB medium. The inoculated cultures were incubated overnight. 24 h later, the DNA was isolated as described in 3.1.1 and controlled via agarose gel analysis and sequencing (3.3.8).

3.3.7 Enzymatic restriction

For enzymatic restriction analyses, the appropriate amount of DNA, which has to be analyzed, was mixed with the appropriate restriction enzyme, buffer and supplements according to the manufacturer's instructions (New England Biolabs; Roche). For analytical purposes, double or triple digests were performed if possible. Best enzyme-buffer combinations were determined with the online tool Double Digest Finder (NEB) (www.neb.com/tools-andresources).

3.3.8 Sequencing of plasmid DNA

For sequencing, 1-1.2 µg of purified DNA was mixed with 30 pmol of the appropriate oligonucleotide, adjusted to 12 µl with ddH_2O and send to the sequencing company SeqLab (Göttingen).

3.3.9 Generation of adenoviral recombinants via RED recombination

Isolation of the p15A ccdB amp box

In Advance, 5 ml LB medium, supplemented with ampicillin (100 µg/ml), was inoculated with *E. coli* GBred-gyrA462, containing the p15A ccdB amp plasmid, and incubated for 20 h at 37°C and 210 rpm (Innova 4000 Incubator, New Brunswick). The next day, the p15A ccdB amp plasmid was isolated from the culture as described in 3.3.2. To avoid background resulting from the presence of the parental plasmid during the first RED recombination, 1 µg of the p15A ccdB amp plasmid was digested with the restriction enzyme BseRI as described in 3.3.7. Afterwards, the DNA was purified via gel extraction (3.3.4). Here, the DNA was eluted in 100 µl ddH_2O.

Adding homologues overhangs to the p15A ccdB amp box via PCR

Viral mutagenesis is a two-step process. In the first step the ccdB amp box is inserted into the locus of interest by RED recombination. RED recombination is a homologous recombination system derived from phage lambda and requires approximately 50 bp of homologous sequence right and left of the mutation insertion site. Homologous sequences were added to the cddB amp cassette by PCR, utilizing oligonucleotides framing the location of the desired mutation (3.3.5).

First RED recombination

In preparation for the first RED recombination, 5 ml of LB medium, containing ampicillin (100 µg/ml) and chloramphenicol (15 µg/ml), were inoculated with *E. coli* GBred-gyrA462 and incubated overnight at 37°C and 210 rpm (Innova 4000 Incubator, New Brunswick). At the next day, 30 µl of the pre-culture were added to LB medium, supplemented with streptomycin (100 µg/ml) and incubated for 2 h at 37 °C and 800 rpm (ThermoMixer®comfort; Eppendorf). Afterwards, the RED recombination system was activated by the addition of 50 µl of sterile filtered 10 % (w/v) L-arabinose solution and incubation for 50 min at 37 °C and 800 rpm (ThermoMixer®comfort; Eppendorf). Next, the cells were made electro-competent as described in 3.1.3 and electroporated with 500 ng of the ccdB-amp PCR product and 500 ng of the target adenoviral genome containing plasmid (3.1.4). After recovery, cells were plated onto an ampicillin (100 µg/ml) and chloramphenicol (15 µg/ml) containing LB agar plate and incubated at 37°C for 20 h. At the following day, colonies were picked and used for the inoculation of 5 ml LB medium supplemented with ampicillin (100 µg/ml) and chloramphenicol (15 µg/ml). The bacterial culture was incubated overnight at 37°C and 210 rpm (Innova 4000 Incubator, New Brunswick). Plasmid DNA was prepared as described in 3.3.2. As control, 2 µg of DNA was investigated with an appropriate restriction enzyme (3.3.7). DNA that shows the correct restriction pattern was retransformed into GBred-gyrA462 to avoid a contamination with parental plasmid during the second red recombination. Therefore, 5 ml of LB medium, supplemented with streptomycin (100 ug/mL), were inoculated with *E. coli* strain GBred-gyrA462 and incubated for 16 h at 37°C and 210 rpm (Innova 4000 Incubator, New Brunswick). The next, day, 1.4 ml LB with streptomycin (100 µg/ ml) were inoculated with 30 µl of the GBred-gyrA462 overnight-culture and incubated for 2 h at 37 °C and 800 rpm

(ThermoMixer®comfort; Eppendorf). Afterwards, cells were made electro-competent (3.1.3) and electroporated with 500 ng of the newly synthesized and enzymatic restriction controlled p15A HAdV ccdB-Amp plasmid (3.1.4). Afterwards, electroporated bacteria were plated onto an ampicillin (100 µg/ml)/ chloramphenicol (15 µg/ml) containing LB agar plate and incubated at 37°C for 20 h.

Second RED recombination

At first, 5 ml LB medium supplemented with ampicillin (100 µg/ml) and chloramphenicol (15 µg/ml) was inoculated with one clone of the retransformants and incubated overnight at 37°C and 210 rpm (Innova 4000 Incubator, New Brunswick). At the same time, 5 ml of LB medium, supplemented with streptomycin (100 µg/ ml), was inoculated with *E. coli* GB05red and incubated for 16 h at 37°C and 210 rpm (Innova 4000 Incubator, New Brunswick).

At the following day, plasmid DNA of the retransformants was isolated as described in 3.3.2. Moreover, 1.4 ml LB plus streptomycin (100 µg/ml) was inoculated with 30 µl of the GB05red overnight culture and incubated for 2h at 37 °C and 800 rpm (ThermoMixer®comfort; Eppendorf). Afterwards, the RED recombination system was activated again by the addition of 10 % L-arabinose solution and incubation for 50 min at 37 °C and 210 rpm (ThermoMixer®comfort; Eppendorf). In the next step, cells were made electro-competent (3.1.3) and were electroporated with 500 ng of the isolated DNA, containing the adenoviral plasmid with the ccdB selection marker, and with 50 pmol of the rescue oligonucleotide (3.1.4). After recovery, electroporated cells were plated onto a LB plate agar plate containing chloramphenicol (15 µg/ml) and incubated for 20 h at 37 C.

At the next day, colonies were picked and used for the inoculation of 5 ml of LB medium, supplemented with chloramphenicol (15 µg/ml). These pre-cultures were incubated for 16 h at 37 °C and 210 rpm (Innova 4000 Incubator, New Brunswick). Again, plasmid DNA was isolated and 2 µg of plasmid DNA were applied to enzymatic restriction analysis (3.3.2 and 3.3.7). For final validation, three different restriction enzymes were utilized and the mutated region was sequenced (3.3.8). Validated bacmids, encoding the mutated HAdV genome were used for the generation of viral particles.

Transfection of bacmid DNA to generate viral particles

In advance, 293 cells were seeded in a 6 cm culture dish and grown to a density of 90 % (3.2.1). To generate infectious virus particles from recombinant bacmid DNA, 20 µg of bacmid DNA was linearized via SwaI and PacI digestion to separate the viral part of the bacmid from the bacterial DNA. After the SwaI digestion, the DNA was precipitated with 1/10 volume of 3 M sodium acetate (pH 5.2) and 1 volume of isopropanol, washed with 75 % ethanol and resolved in 50 µl ddH_2O. Following PacI digestion, the linearized bacmid DNA was transfected into the pre-seeded sub-confluent 293 cells via Lipofectamine transfection (3.2.7). The transfected cells were cultivated until they started to detach from the surface of the culture dish or for 5 days. Even if they did not detach after 5 days they were harvested (3.2.8). The gained cell pellet was washed with 5 ml PBS and lysed subsequently in 3 ml $DMEM_0$, supplemented with 10 % FCS, by 3 times freezing in liquid nitrogen and thawing at 37 °C in a water bath. Thereby, virus particles were released into the supernatant and separated from cell debris by centrifugation (4500 rpm, 10 min, RT). Afterwards, the particle containing supernatant was stored at -80 °C or used for the infection of sub-confluent A549 cells, seeded on a 15 cm cell culture dish, for further propagation of viral particles. Viral particles were released as described above and the obtained new virus stock was split to 5 aliquots and stored at -80 °C.

3.4 Handling Adenoviruses

3.4.1 Infection with Adenoviruses

Cells were seeded 24 h before infection so that they reach a confluence of approximately 80 % at the time of infection. For infection, the culture medium was removed, the cells were washed once with PBS, and fresh $DMEM_0$ was added. Virus stocks were diluted in $DMEM_0$ and the desired amount of viral particles was applied to the cells. The needed volume of the virus stock, containing the desired amount of viral particles, was calculated with the following formula:

$$Volume\ of\ virus\ stock\ \ [\mu l]$$

$$= \frac{multiplicity\ of\ infection\ (MOI)\ [ffu/cell]\ *\ number\ of\ cells}{virus\ titer\ [ffu]}$$

The cells were incubated for 2 h under standard culturing conditions. Afterwards, the infection medium was replaced with fresh culturing medium and the infected cells were propagated under standard culturing conditions until they were harvested at indicated time points.

3.4.2 Generation of high titer virus stocks

For the generation of high titer virus stocks, A549 cells were grown on 15 cm dishes and infected at a confluency of 80 % with an MOI of 20-50. As soon as the cells showed a cytopathic effect they were harvested and viral particles were released from the cells by three freeze and thaw cycles. Then the cell debris was removed by centrifugation (2,000 rpm, 5 min, RT; Multifuge 3 S-R; Heraeus) and the virus containing supernatant was supplemented with 10 % glycerol (v/v) and aliquoted. The virus aliquots were stored at -80°C.

3.4.3 Titration of virus stocks

For virus titration, $3*10^4$ A549 cells were seeded in a 6-well plate. The next day, the cells were infected with virus dilutions ranging from 10^{-1} to 10^{-5}. 24 h post infection the cells were fixed and permeablized with methanol. Afterwards, E2A was stained for immunofluorescence analysis as a marker for infected cells. For the staining, the E2A specific antibody B6-8 (1/10 in TBS-BG) and as a secondary antibody Alexa 488 (1/1000 in TBS-BG) were utilized. The stained cells were covered with PBS and the number of infected cells was determined via light microscopy (Leica DMIL) in order to calculate the resulting fluorescence forming units ([ffu/µl]). For the calculation, a lens specific factor depending on the objective magnification was multiplied with the number of infected cells and the virus dilution.

$$number\ of\ infected\ cells * objective\ factor * virus\ dilution = ffu/\mu l$$

Objective magnification	Resulting objective factor
40 x	6399
20 x	1600
10 x	389

3.5 Protein techniques

3.5.1 Preparation of total cell lysates

To prepare cell lysates, cells were harvested as described in 3.2.8. Depending on the amount of cells, cells were resuspended in 50 to 500 µl of pre-cooled RIPA buffer and incubated for 30 min on ice. For cell lysis, cells were vortexed for approximately 5 s every ten minutes during this incubation period. Afterwards, cells were sonified for 30 s at 4 °C (output 0.8, 0.8 impulse/ s, Branson Sonifier 450) to shear genomic DNA. To separate proteins from cell debris and insoluble cellular components, the probes were centrifuged at 11000 rpm for 3 min at 4 °C (Centrifuge 5417R; Eppendorf). In the following, total protein concentrations were measured by spectrometry (3.5.2). Depending on the assay requirement, protein concentrations were measured and adjusted to the same concentrations by the addition of RIPA buffer. For Western Blot analysis, lysates were denatured by the addition of 5x SDS buffer and heating at 98 °C for 3 min. Notably, detection of E4orf6 via Western Blot required heating at 60 °C for 12 min. Protein lysates were stored at -20 °C.

RIPA buffer	50 mM	Tris/HCl (pH 8)
	150 mM	NaCl
	5 mM	EDTA
	1 % (v/v)	Nonident P-40
	0.1 % (v/v)	SDS
	0.5 % (v/v)	Sodium desoxycholate
Protease inhibitors (freshly added)	1 mM	PMSF
	10 U/ ml	aprotinin
	1 µg/ ml	leupeptin
	1 µg/ ml	pepstatin
5x SDS buffer	100 mM	Tris/ HCl (pH (6.8)
	200 mM	DTT
	10 %(w/v)	SDS
	0.2 % (w/v)	Bromphenol blue

3.5.2 Determination of protein concentrations in solutions

Protein concentrations of total cell lysates were measured with a Bradford-based BioRad Protein-Assay. For sample preparation, 1 µl protein lysate was mixed with

800 µl ddH_20 and 200 µl supplied Bradford reagent (BioRad). After a 5 min incubation period, protein concentrations were determined by spectroscopy (SmartSpec Plus spectrometer, BioRad) at 595 nm. For calibration of the spectrometer, a standard curve was determined via the measurement of samples, containing a known concentration (1-16 µg/µl) of BSA.

3.5.3 Sodium dodecyl sulfate polyacrylamide gel electrophoresis (SDS PAGE)

SDS PAGE was used to separate proteins according to their molecular weight in a polyacrylamide gel. In advance, polyacrylamide gels consisting of a stacking phase and a separating phase were freshly poured in the SDS-PAGE system of Biometra according to the manufacturer´s instructions (Biometra multigel vertical gel electrophoresis system, Biometra). Depending on the size of the proteins to be detected, the separating phase of the gels was prepared with polyacrylamide concentrations of 10 % or 15 % utilizing the Biometra multigel vertical gel electrophoresis system (Biometra). Protein separation was performed at 15 mA/gel in TGS buffer. As a molecular weight standard, the PageRuler™ Prestained Protein Ladder Plus (Thermofisher) was used.

Acrylamide stock solution (30 %)	29 % (w/v) 1 % (w/v)	Acrylamide N N'Methylenbisacrylamide
Stacking gel (5%)	17 % (v/v) 120 mM 0.1 % (w/v) 0.1 % (v/v) 0.5 % (v/v)	Acrylamide stock solution Tris/HCl (pH 6.8) SDS APS Temed
10 % Separating gel	34 % (v/v) 250 mM 0.1 % 0.1 % 0.1 %	Acrylamide stock solution Tris/HCl (pH 8.8) SDS APS Temed

15 % Separating gel	50 % (v/v)	Acrylamide stock solution
	250 mM	Tris/HCl (pH 8.8)
	0.1% (w/v)	SDS
	0.1 %(v/v)	APS
	0.1 % (v/v)	Temed
TGS buffer	25 mM	Tris
	200 mM	Glycine
	0.1 % (w/v)	SDS

3.5.4 Western Blot

Via SDS PAGE separated proteins were transferred to nitrocellulose membranes with a pore size of 45 µm (GE Healthcare) via wet electroblotting. For the procedure, the TransBlot Electrophoretic Transfer Cell System (BioRad) was used according to the manufacturer's instructions. For protein transfer, towbin buffer was used and 400 mA were applied for 90 min. Afterwards, membranes were incubated in 5 % non-fat dry milk-PBS-tween solution (w/v; Frema) for at least 1 h at 4 °C on an orbital shaker (GFL) to saturate non-specific antibody binding sites. In the next step, the membranes were washed 3 times with PBS-tween for 10 min each time. Subsequently, the membranes were incubated with the respective primary antibody at 4 °C. Primary antibodies were diluted as indicated by the manufacturer. To ensure proper antibody binding, the membranes were gently moved by an orbital shaker during the incubation period. After 3 hours of incubation, membranes were washed as described above and incubated with the HRP-conjugated secondary antibody (Amersham) for 2 h at 4 °C. Secondary antibodies were diluted 1:10000 in 3 % non-fat dry milk PBS-tween solution (w/v in PBS-tween; Frema). After incubation with the secondary antibody, membranes were washed again. In the following, proteins were visualized on X-ray films (RP New Medical X-Ray Film; CEA), by the detection of the chemiluminescence signal emitted by HRP-conjugated proteins after applying the SuperSignal™ West Pico Chemiluminescent Substrate (Thermofisher) according to the manufacturer's instructions. X-ray films, were developed using the GBX Developer (Kodak) and digitalized. Illustrations were prepared utilizing Photoshop CS6 (Adobe) and Illustrator CS6 (Adobe).

Towbin buffer	25 mM	Tris/ HCl (pH 8.3)
	200 mM	Glycine
	0.05 % (w/v)	SDS
	20 %	Methanol
PBS-tween	0.1 % (v/v)	Tween20 in 1x PBS

3.5.5 Immunoprecipitation assay

At the beginning, 1 µg of total cell lysates from each sample were precleared by Pansorbin A addition and incubation for 1 h at 4 °C on a rotator. Afterwards, Pansorbin A was removed by centrifugation (600 g, 5 min, 4 °C; Centrifuge 5417R Eppendorf). In parallel, 1 µg of purified antibody or 100 µl/ mg sepharose for hybridoma supernatant was coupled to 3 mg of sepharose/ sample. After 1 h of incubation period, the antibody-coupled sepharose was washed 3 times with RIPA buffer. Subsequently, precleared protein lysates were mixed with the antibody coupled sepharose in 1.5 ml reaction tubes (Eppendorf). Immunoprecipitation was performed at 4 °C on a rotator (GFL) for at least 2 hours and centrifugation at 600 g for 5 min at 4 °C (Eppendorf 5417R). Additionally, sepharose coupled proteins were washed 3 times with 1.5 ml RIPA buffer. For denaturation and protein elution, the samples were mixed with 20 to 50 µl of 2 x SDS sample buffer and heated to 95 °C for 3 min. Finally, solubilized proteins were separated from the sepharose by centrifugation at 11000 g for 3 min (Eppendorf 5417R) and transferred to a new 1.5 ml reaction tube (Eppendorf). Until further investigations by SDS PAGE and Western Blot, samples were stored at -20 °C.

2x SDS buffer	100mM	Tris/ HCl (pH 6.8)
	4%	SDS
	200 mM	DTT
	0.2 % (w/v)	Bromphenol blue
	20 % (v/v)	Glycerol

3.5.6 Ni-NTA affinity chromatography

For Ni-NTA SUMO pulldown analysis, HeLa parental cells, SUMO 1 or SUMO 2 orverexpressing cells were infected or transfected (3.4.1 and 3.2.5). After 24 to 48 h, cells were harvested and washed with 5 ml per 10 cm dish pre-cooled PBS. Subsequently, these samples were split, whereby 0.5 ml per 10 cm dish of a sample

were applied to total cell lysate preparation (3.5.1) and 4.5 ml per 10 dish were used for Ni-NTA SUMO pulldown analysis. After centrifugation, the PBS of both sample types was aspirated and total cell lysate probes were stored at -20 °C until further investigations, while Ni-NTA pulldown samples were lysed in 5 ml per 10 cm dish guanidine hydrochloride (GuHCL) buffer. Until further investigations, these samples were frozen at -80 °C. In the next step, His-SUMO modified proteins were coupled to the Ni–NTA agarose. Therefore, Ni-NTA agarose beads were washed 3 times with GuHCl buffer. Afterwards, each Ni-NTA pulldown probe was supplemented with 50 µl Ni-NTA agarose beads (Thermo Scientific) and incubated overnight at 4 °C on a rotator (GFL). The next day, His-SUMO conjugates coupled to the Ni-NTA agarose were precipitated via centrifugation and washed once with GuHCL buffer, once with wash buffer 2 buffer, and once with wash buffer 3. Finally, His-SUMO conjugated proteins were eluted from the Ni-NTA agarose beads via addition of elution buffer and heating to 95 °C for 5 min. Samples were stored at -20 °C until further investigation via SDS PAGE and Western Blot.

GuHCl lysis buffer	6 M	GuHCl
	100 mM	Na_2HPO_4
	100 mM	NaH_2PO_4
	10 mM	Tris/ HCl (pH 8)
	20 mM	Imidazol
	5 mM	β-mercaptoethanol
Wash buffer 2, pH 8	8 mM	Urea
	100 mM	Na_2HPO_4
	100 mM	NaH_2PO_4
	10 mM	Tris/ HCl (pH 8)
	20 mM	Imidazol
	5 mM	β-mercaptoethanol
	250 mM	Tris/HCl (pH 8.8)
Wash buffer 3, pH 6.3	8 mM	Urea
	100 mM	Na_2HPO_4
	100 mM	NaH_2PO_4
	10 mM	Tris/ HCl (pH 6.3)
	20 mM	Imidazol
	5 mM	β-mercaptoethanol

Protease inhibitors (freshly added)	1 mM	PMSF
	10 U/ ml	aprotinin
	1 µg/ ml	leupeptin
	1 µg/ ml	pepstatin
Elution buffer	200 mM	Imidazol
	0.1 % (w/v)	SDS
	150 mM	Tris/ HCl (pH 6.3)
	30 %	Glycerol
	720 mM	β-mercaptoethanol
	0.01 % (w/v)	Bromphenol blue

3.5.7 Immunofluorescence analysis

Cells were seeded on 6 well plates containing glass coverslips. 24 h later, cells were transfected or infected. After the indicated incubation period, cells were fixed by the addition of 4 % PFA for 15 min at RT. In the following, cells were permeabilized with PBS-Triton. After 10 min of incubation, the supernatant was aspirated and the cells were blocked for 30 min with TBS-BG. Afterwards, the coverslips were incubated for 1 h with 50 µl/ coverslip of the indicated primary antibodies, which were diluted in PBS according to the manufacturer's instructions. Afterwards, the coverslips were washed 3 times with TBS-BG. Next, the indicated secondary antibodies were diluted 1/100 in PBS and were added to the samples. Additionally, the antibody dilution was supplemented with DAPI in a ratio of 1:5000. After incubation for 1 h, coverslips were washed three times with TBS-BG. Finally, coverslips were mounted on glass slides using glow medium. Digital images were acquired with a confocal spinning-disk microscope (Nikon Eclipse Ti-E stand; Yokagawa CSU-W1 spinning disk; 2x Andor888 EM-CCD camera; Nikon 100x NA 1.49 objective). Images were analyzed and cropped using Fiji and assembled with Illustrator CS6 (Adobe).

PBS-Triton	0.5 M	Triton X-100 in 1x PBS

4 Results

4.1 E4orf6 is a negative regulator of E1B-55K SUMOylation

E1B-55K SUMOylation is known to depend on phosphorylation and interactions with cellular proteins. Additionally, it has been suggested to be negatively regulated by its viral interaction partner E4orf6 [460,461]. Since SUMOylation controls many functions of E1B-55K this interaction appears to be an interesting internal viral regulatory mechanism. Thus, the first experimental part of this work focused on the verification of E4orf6 as a negative regulator of E1B-55K SUMOylation.

4.1.1 E4orf6 controls the SUMOylation of E1B-55K SUMO mutants during infection

The major SUMO acceptor site of E1B-55K is located at lysine K104, which is integrated within a classical SCM [418,461]. Next to K104, a putative SUMO site has been suggested at K101 of HAdV-C5-E1B-55K (Fig. 10).

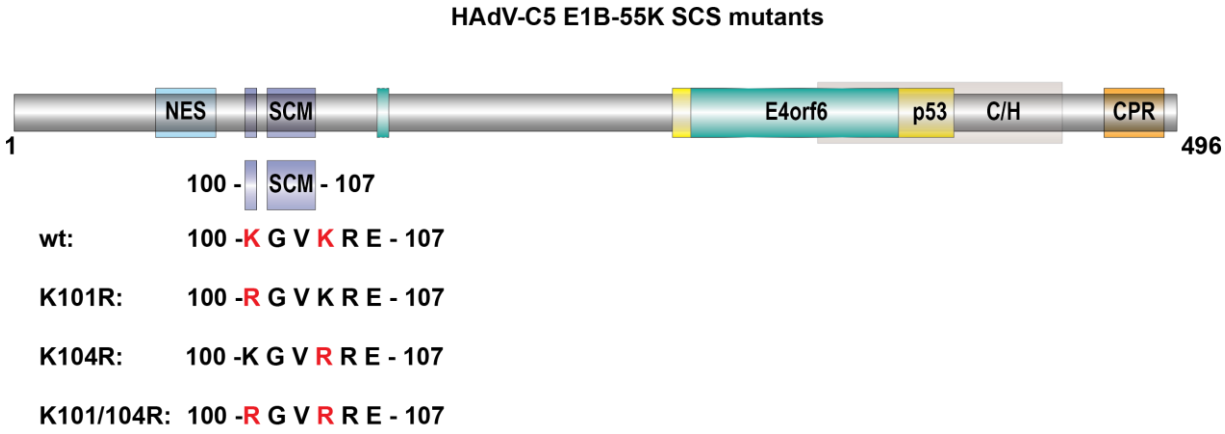

Fig. 10: Schematic representation of HAdV-C5 E1B-55K SUMO conjugation site mutants (SCS). These mutants carry lysine (K) to arginine (R) transitions at the SCS K101, K104, and K101 plus K104, respectively.

In this analysis, the E1B-55K SUMO modification of different virus mutants, expressing E1B-55K proteins carrying amino acid exchanges in one or both SCS (K101 and K104), in the presence or absence of E4orf6 shall be investigated to substantiate E4orf6 as a negative regulator of E1B-55K SUMOylation (Fig. 10). For simplification, the mutants were named according to their mutations and characterized in Tab. 2.

Tab. 2: List of E1B-55K/E4orf6 virus mutants.

Name	E1B-55K mutation	E4orf6 expression	SUMO level of E1B-55K
HAdV-C5-wt	wt	yes	Normal
HAdV-C5-ΔE4orf6	wt	no	To be determined
HAdV-C5-K101R	Prevention of SUMO modification at aa 101 by K to R mutation	yes	High
HAdV-C5-K101R ΔE4orf6	Prevention of SUMO modification at aa 101 by K to R mutation	no	To be determined
HAdV-C5-K104R	Prevention of SUMO modification at aa 104 by K to R mutation	yes	No modification
HAdV-C5-K104R ΔE4orf6	Prevention of SUMO modifiation at aa 104 by K to R mutation	no	To be determined
HAdV-C5-K101/104R	Prevention of SUMO modification at aa 101 and 104 by K to R mutation	yes	No modification
HAdV-C5-K101/104R ΔE4orf6	Prevention of SUMO modification at aa 101 and 104 by K to R mutation	no	To be determined

To examine the SUMOylation of E1B-55K mutants in presence and absence of E4orf6, Ni-NTA pulldown analysis were performed according to Tatham *et al.* 2009 [464]. To this end, HeLa parental cells and HeLa cells constitutively expressing either His-tagged SUMO 1 or His-tagged SUMO 2, were mock infected or infected with the indicated virus mutants. The cells were harvested 24 h.p.i. and His-SUMO modified proteins were isolated via Ni-NTA affinity chromatography [464]. In parallel, total cell lysates were prepared to control for equal protein concentrations. Differences in the SUMOylation levels of the E1B-55K mutants and protein steady state concentrations were visualized via SDS PAGE and immunoblotting (Fig. 11). In this experimental setup, SUMO conjugation is stabilized and modified proteins can be identified by a size shift, since they have a higher molecular weight in comparison to unmodified proteins.

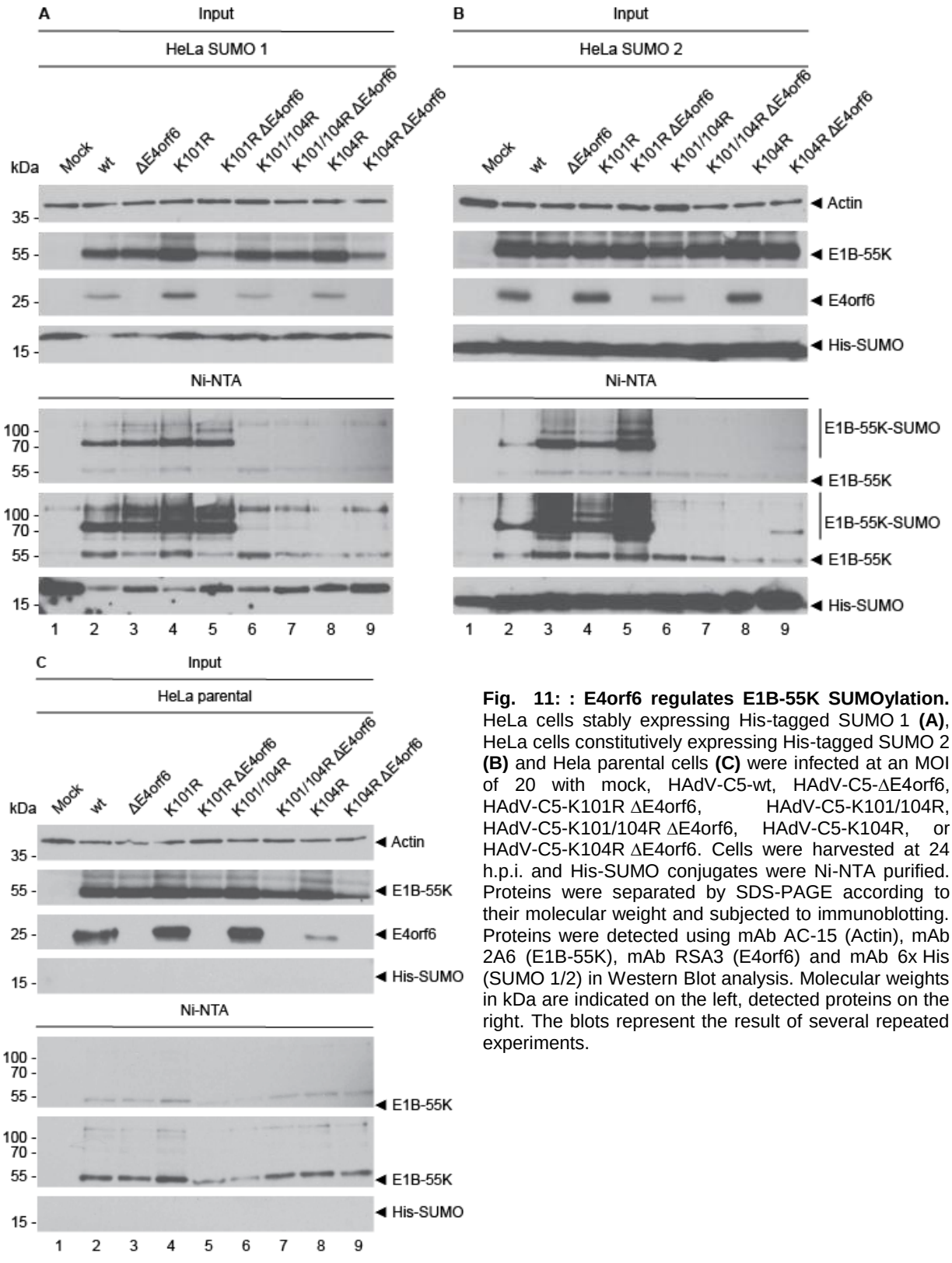

Fig. 11: : E4orf6 regulates E1B-55K SUMOylation. HeLa cells stably expressing His-tagged SUMO 1 **(A)**, HeLa cells constitutively expressing His-tagged SUMO 2 **(B)** and Hela parental cells **(C)** were infected at an MOI of 20 with mock, HAdV-C5-wt, HAdV-C5-ΔE4orf6, HAdV-C5-K101R ΔE4orf6, HAdV-C5-K101/104R, HAdV-C5-K101/104R ΔE4orf6, HAdV-C5-K104R, or HAdV-C5-K104R ΔE4orf6. Cells were harvested at 24 h.p.i. and His-SUMO conjugates were Ni-NTA purified. Proteins were separated by SDS-PAGE according to their molecular weight and subjected to immunoblotting. Proteins were detected using mAb AC-15 (Actin), mAb 2A6 (E1B-55K), mAb RSA3 (E4orf6) and mAb 6x His (SUMO 1/2) in Western Blot analysis. Molecular weights in kDa are indicated on the left, detected proteins on the right. The blots represent the result of several repeated experiments.

As expected, Western Blot analysis of Ni-NTA purified His-SUMO coupled proteins with E1B-55K specific antibodies showed that E1B-55K-wt as well as K101R were modified by SUMO 1 and SUMO 2 in presence of E4orf6, indicated by a ladder of E1B-55K specific bands above 70 kDa corresponding to conjugated SUMO moieties (E1B-55K-wt: Fig. 11 A and B lane 2; K101R: Fig. 11 A and B lane 4). Thereby, the SUMO 1 and SUMO 2 levels of K101R are increased in comparison to E1B-55K-wt (E1B-55K-wt: Fig. 11 A and B lane 2; K101R: Fig. 11 A and B lane 4). However, absence of E4orf6 resulted in modestly increased SUMO 1, and significantly higher SUMO 2 modification of E1B-55K-wt and K101R, respectively (HAdV-C5-ΔE4orf6: Fig. 11 A and B lane 3; HAdV-C5-K101R ΔE4orf6: Fig. 11 lane 5). In contrast, K101/104R and K104 were neither SUMO 1 nor SUMO 2 modified in cells infected with (K101/104R Fig. 11 A and B lane 6; K101/104R Fig. 11 A and B lane 8) or without (Fig. 11 A and B lane 7) E4orf6 expressing virus mutants. SUMO 1 modification of K104R was not detected in presence or absence of E4orf6 (Fig. 11 A lane). Remarkably, analysis of HAdV-C5-K104R ΔE4orf6 infected His-SUMO 2 cells revealed that K104R was modestly conjugated to SUMO 2 in the absence of E4orf6, while in presence of E4orf6 no SUMOylation of K104R occurred (Fig. 11 A and B lane 9 and lane 8). In infected HeLa parental cells, no His-SUMO modified E1B-55K variants were detected (Fig. 11 C). In sum, these results demonstrated that E4orf6 efficiently decreased SUMO 1 as well as SUMO 2 conjugation to E1B-55K-wt and K101R. Additionally, they showed that K104R can be modified by SUMO 2 during HAdV-C5-K104R ΔE4orf6 infections, confirming K101 as functional SCS of E1B-55K.Conclusively, the analysis of E1B-55K SUMO levels in cells infected with E4orf6 deficient virus mutants (ΔE4orf6) verified E4orf6 as a negative regulator of E1B-55K SUMOylation.

4.1.2 SUMOylation of E1B-55K does not influence binding to E4orf6

During infection, E1B-55K and E4orf6 interact with each other and form a complex in order to build an E3-ubiquitin ligase together with cellular proteins. This complex plays an important part in the counteraction of cellular antiviral measures. First, it induces the degradation of cellular proteins interfering with viral replication, and second, it facilitates the shut off of the host cell protein synthesis and selective export of viral mRNAs [465–467]. Since SUMOylation can cause alterations in protein interactions, it is conceivable that the SUMO status of E1B-55K influences its binding capacity towards E4orf6.

Furthermore, E1B-55K SUMOylation is known to influence the interaction to partner proteins as PML [456]. Therefore, the following investigation shall substantiate that the SUMOylation of E1B-55K does not influence its binding to E4orf6.

To address this issue, A549 cells were infected with HAdV-C5-wt, HAdV-C5-ΔE4orf6, HAdV-C5-K101R, HAdV-C5-K104R or HAdV-C5-K101/104R. At 24 h.p.i., cells were harvested, cell lysates were prepared and immediately subjected to immunoprecipitation (IP) analysis. Subsequently, the interaction between E1B-55K mutants and E4orf6 was visualized by SDS-PAGE and Western Blot (Fig. 12).

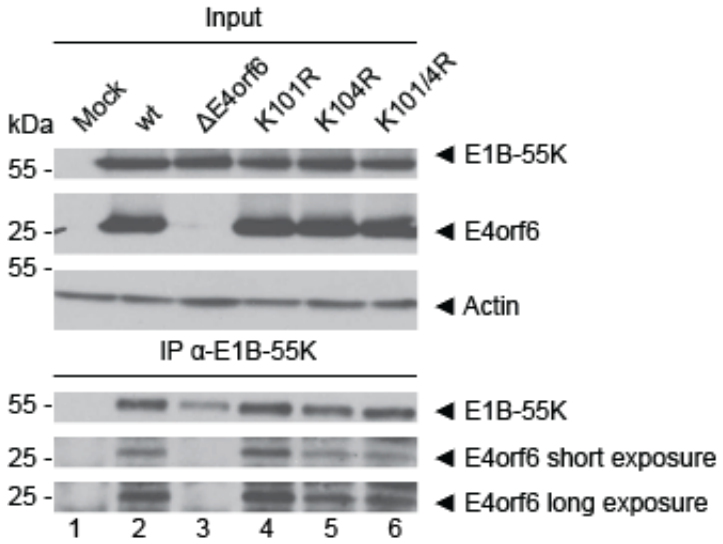

Fig. 12. SUMOylation of E1B-55K does not affect binding to E4orf6. A549 cells were infected with the indicated virus mutants at an MOI of 20 and harvested 24 h.p.i.. Afterwards, total-cell extracts were prepared and an IP of E1B-55K was performed using the 2A6 mouse mAb. Proteins were separated by SDS-PAGE and subjected to immunoblotting. Input levels of total-cell lysates and immunoprecipitated proteins were detected with the following antibodies: mAb 2A6 (E1B-55K), pAb 1807 (E4orf6) and mAb AC-15 (Actin). The molecular weights in kDa are indicated on the left and detected proteins on the right. The blots represent the results of several repeated experiments.

In these investigations, all tested mutants bound efficiently to E1B-55K, validating that the SUMOylation of E1B-55K or SCS mutations have no impact on complex formation between E1B-55K and E4orf6 (Fig. 12).

4.2 Investigating the mechanism of E4orf6 mediated reduction of E1B-55K SUMOylation

It is well established that viral proteins have the potential to regulate protein SUMOylation to promote virus replication. Hereby, several steps of the SUMO cycle can be attacked, resulting in alterations in SUMO conjugation either on single proteins or global level. The aim of the next part of this work was to determine the mechanism of E4orf6 to reduce E1B-55K SUMOylation to reveal internal viral control mechanisms that will complete the picture about the interference of HAdV-C5 proteins with host SUMOylation.

Based on the observation that phosphorylation, protein interactions and localization correspond with E1B-55K SUMOylation and the knowledge about viral strategies used to control protein SUMO modifications, four hypotheses were formulated, concerning the potential mechanism applied by E4orf6 to interfere with E1B-55K SUMOylation. The first goal was to elucidate whether E4orf6 inhibits the unique SUMO E1 or E2 enzymes and thereby causes a global reduction of SUMOylated proteins. The second idea suggested that E4orf6 might recruit SENPs to E1B-55K to enhance E1B-55K deSUMOylation. The next assumption implicated that E4orf6 might influence E1B-55K phosphorylation, which is known to regulate E1B-55K SUMOylation. Finally, the last idea emphasized a binding site competition between E4orf6 and SUMO proteins, respectively (Fig. 13). The following part of this work comprises the experimental prove of these hypotheses.

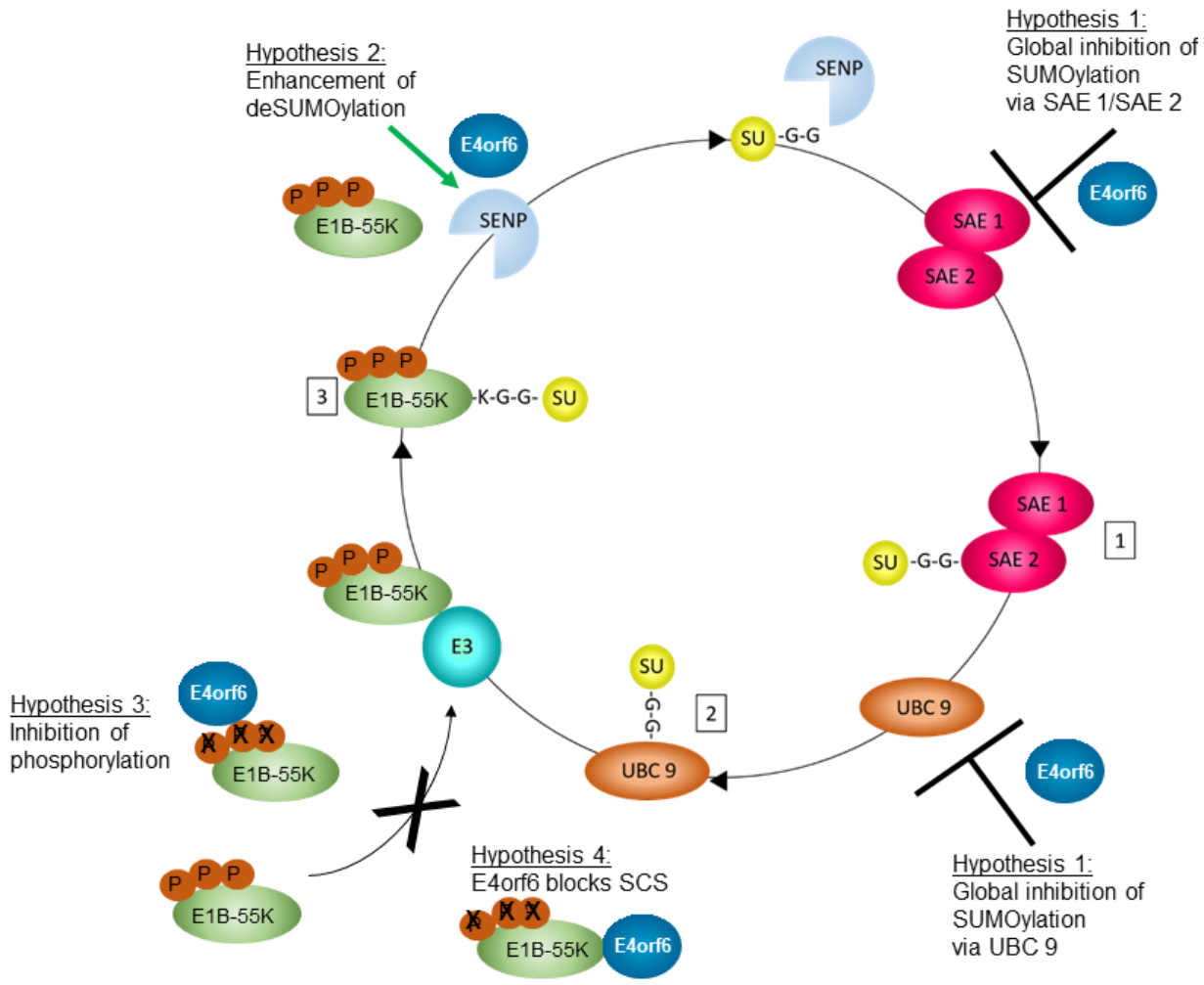

Fig. 13: Graphic illustration of potential mechanisms, applied by E4orf6 to reduce E1B-55K SUMO conjugation. E4orf6 decreases the SUMOylation of E1B-55K. In this illustration, potential E4orf6-mediated interference points with the SUMO cycle for E1B-55K SUMOylation reduction are depicted. The first presumption is the general inhibition of the SAE 1/SAE 2 complex and UBC 9, respectively (hypothesis 1). The second option is the enhanced deSUMOylation by SENPs (hypothesis 2). The third idea emphasized an inhibition of E1B-55K phosphorylation, simultaneously leading to reduced E1B-55K SUMO levels (hypothesis 3). The fourth hypothesis stated that the direct interaction between E1B-55K and E4orf6, causes a reduced SUMO conjugation due to a binding site competition (hypothesis 4).SU: SUMO, SENP: Sentrin/SUMO-specific protease, SAE: SUMO activating enzyme, UBC 9: ubiquitin carrier protein 9, P: phosphoryl group.

4.2.1 E4orf6 does not influence SUMO modification of E2A

To elucidate whether E4orf6 generally impedes SUMOylation or specifically reduces the SUMO modification of E1B-55K, for example by obstructing the unique E1 or E2 SUMO enzymes, the capacity of the E4 protein to reduce the SUMO levels of another representative SUMO substrate, the viral protein E2A, was tested. Recently, E2A has been identified as a SUMO target, which does not interact with E4orf6 [410]. The inhibition of the SUMO enzymes would affect all SUMO targets, as shown for the avian adenovirus CELO protein Gam 1 [392].

Accordingly, HeLa parental cells and HeLa cells overexpressing His-SUMO 2 were infected with HAdV-C5-wt or HAdV-C5-ΔE4orf6. Later on, samples were subjected to Ni-NTA pulldown analysis and changes in the SUMO levels of E2A have been visualized via immunoblotting. As a positive control, the SUMOylation of E1B-55K was depicted as well (Fig. 14). Immunoblotting of Ni-NTA pulldown probes from HAdV-C5-wt or HAdV-C5-ΔE4orf6 infected HeLa parental or HeLa SUMO 2 overexpressing cells showed, that E4orf6 expression slightly enhances E2A SUMOylation, while E1B-55K SUMO conjugation was enhanced in the absence of E4orf6 (Fig. 14 lane 5 and 6). This result suggests that E4orf6 does not deplete global SUMOylation, for example by impeding the unique E1 or E2 SUMO enzymes, as this would decrease SUMO conjugation to all substrates, including E2A. E4orf6 rather reduces E1B-55K SUMO levels specifically. Accordingly, E1B-55K specific mechanisms will be examined in the following parts of this work.

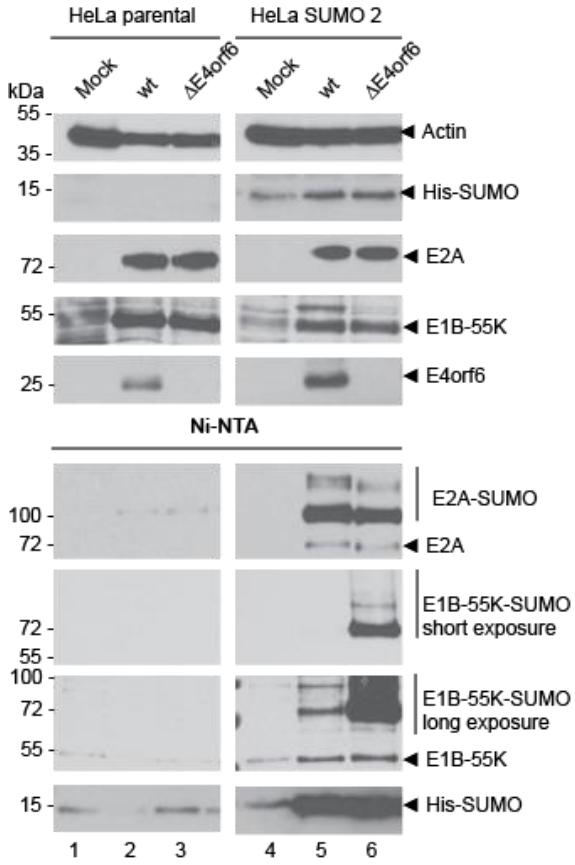

Fig. 14: E4orf6 does not reduce E2A SUMOylation. Hela parental cells or HeLa cells constitutively expressing His-tagged SUMO 2 were infected at a MOI of 20 with mock, HAdV-C5-wt or HAdV-C5-ΔE4orf6. At 24 h.p.i., the cells were harvested and His-SUMO 2 conjugates were subjected to Ni-NTA purification. In parallel total cell lysates were prepared. Proteins were separated by SDS-PAGE according to their molecular weight and subjected to immunoblotting. Proteins were detected using mAb AC-15 (Actin), mAb 2A6 (E1B-55K), mAb RSA3 (E4orf6), mAb B68 (E2A) and mAb 6x His (SUMO 1/2). Molecular weights in kDa are indicated on the left, detected proteins on the right. The blots represent the result of several repeated experiments.

4.2.2 Potential deSUMOylation of E1B-55K induced by E4orf6

In this sub-chapter, the role of SENPs regarding a potentially enhanced deSUMOylation of E1B-55K by E4orf6 was investigated using different approaches. In the SUMO cycle, SUMOylation is constantly reversed by SENPs. Humans express six SENP isoforms, namely, SENP 1, SENP 2, SENP 3, SENP 5, SENP 6, and SENP 7, all of which are able to act on SUMO and remove it from substrate proteins [313,319,320]. According to their evolutionary relationship, localization and substrate specificity, SENP 1 and SENP 2, SENP 3 and SENP 5, as well as SENP 6 and SENP 7 are further grouped pairwise [313,318]. Thus, at least one of each SENP pair is included in the experiments.

4.2.2.1 E4orf6 interacts with different human SENP isoforms

As described above, it was reflected on whether E4orf6 might recruit SENPs for the depletion of E1B-55K SUMOylation. A potential binding of E4orf6 to SENP isoforms might cause an indirect interaction between E1B-55K and these proteases, potentially resulting in a more efficient deSUMOylation of E1B-55K. Remarkably, E4orf6 has been already identified as a modulator of E1B-55K binding to different PML isoforms, making a similar effect on SENP isoforms possible (unpublished data). Thus, direct interactions between E4orf6 and one SENP of each resembling SENP pair was investigated in IP analysis.

For these experiments, H1299 cells were transfected with flag-tagged SENP isoforms 1 to 3 and isoforms 6 and 7, as well as E4orf6. Next, cell lysates were applied to IP analysis utilizing flag-tag specific antibodies. Afterwards, E4orf6-flag-SENP interactions were detected through immunostaining of E4orf6 (Fig. 15).

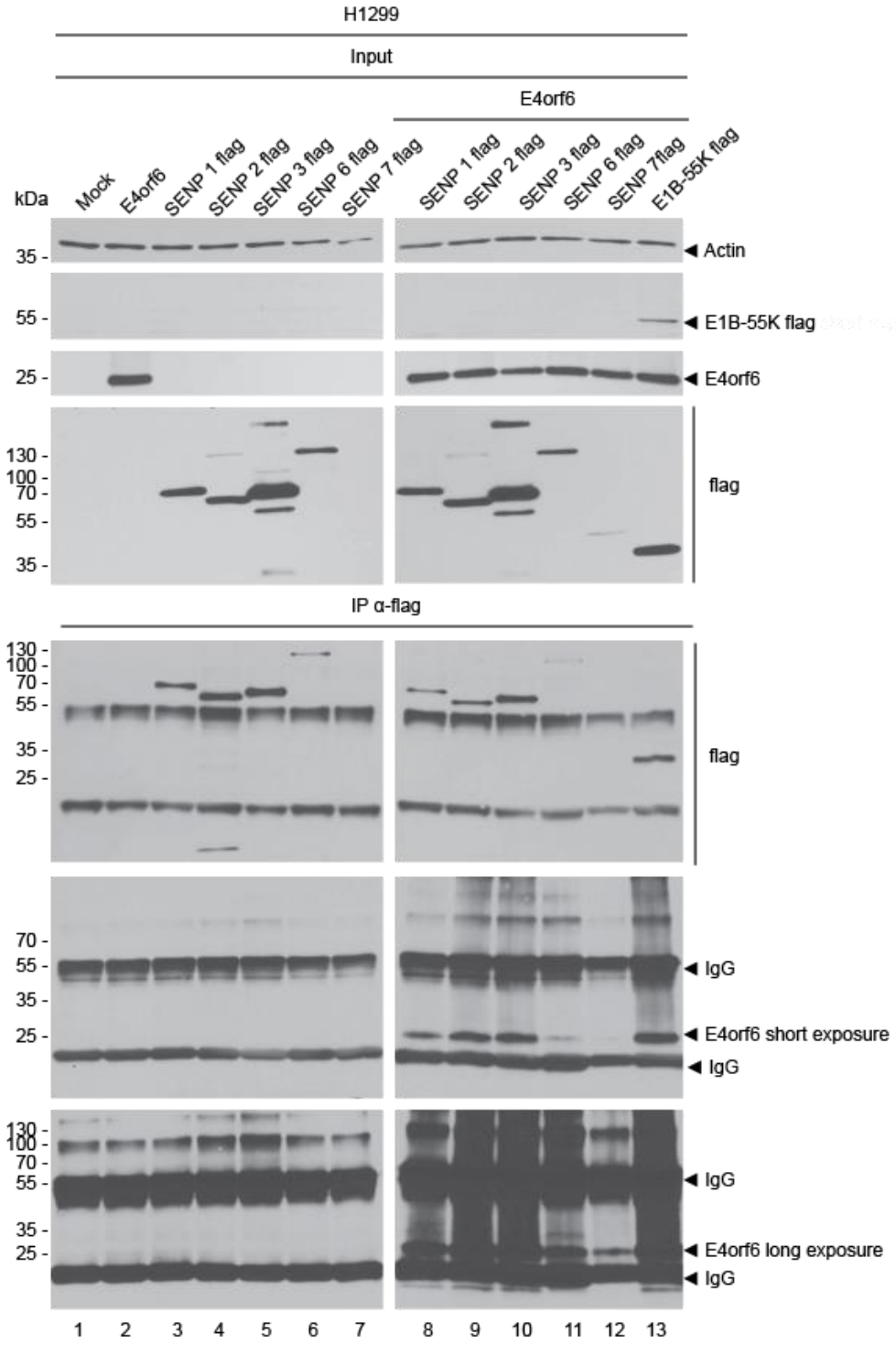

Fig. 15: E4orf6 binds different SENP isoforms. H1299 cells ($4*10^6$) were transfected with flag-tagged SENP isoforms 1 (4 µg), 2 (4 µg) 3 (4 µg), 6 (10 µg) or 7 (10 µg), respectively. In parallel, E4orf6 (4 µg) was transfected to investigate SENP-E4orf6 interactions. Immunoprecipitation of flag-tagged SENPs was performed using mAb M2 (flag), proteins were resolved by SDS PAGE and visualized by Western blotting. Co-precipitated proteins and input levels of total cell lysates were detected by using mAb RSA3 (E4orf6), mAb M2 (flag) and mAb AC-15 (Actin). Molecular weights in kDA are indicated on the left, while corresponding proteins are labeled on the right. The illustration represents the result of several repeated experiments.

Remarkably, E4orf6 bound to all tested SENP isoforms, but is itself not a SUMO target (SENP binding: Fig. 15 lanes 8 to 12; E4orf6 SUMOylation: data not published). Therefore, the interactions have another purpose than deSUMOylation of E4orf6. However, the observation that E4orf6 interacted with all tested SENP isoforms might be an indication for unspecific protein interactions mediated by the amino terminal region of the protein. E4orf6/7 shares the same 58 N-terminal aa and differs only in their C-terminal ends. Thus, the specificity of the association was examined in the following, by analyzing E4orf6/7 for binding SENP isoforms 1 to 3, 6, and 7 in IP analysis. Due to their homology, a different binding pattern of E4orf6/7 and E4orf6 towards the investigated protease isoforms would indicate a specific interaction between E4orf6 and the tested SENPs.

The co-immunoprecipitation assay depicted in Fig. 16 showed that E4orf6/7 was bound only to SENP 3 (Fig. 16 lane 13). Thus, a specific binding of E4orf6 to the tested SENP isoforms can be assumed. Additional validation can be found in the literature. E4orf6 interaction was also observed for E2F transcription factors E2F1 to E2F4 [468]. Presumably, binding of whole protein families is a special feature of E4orf6.

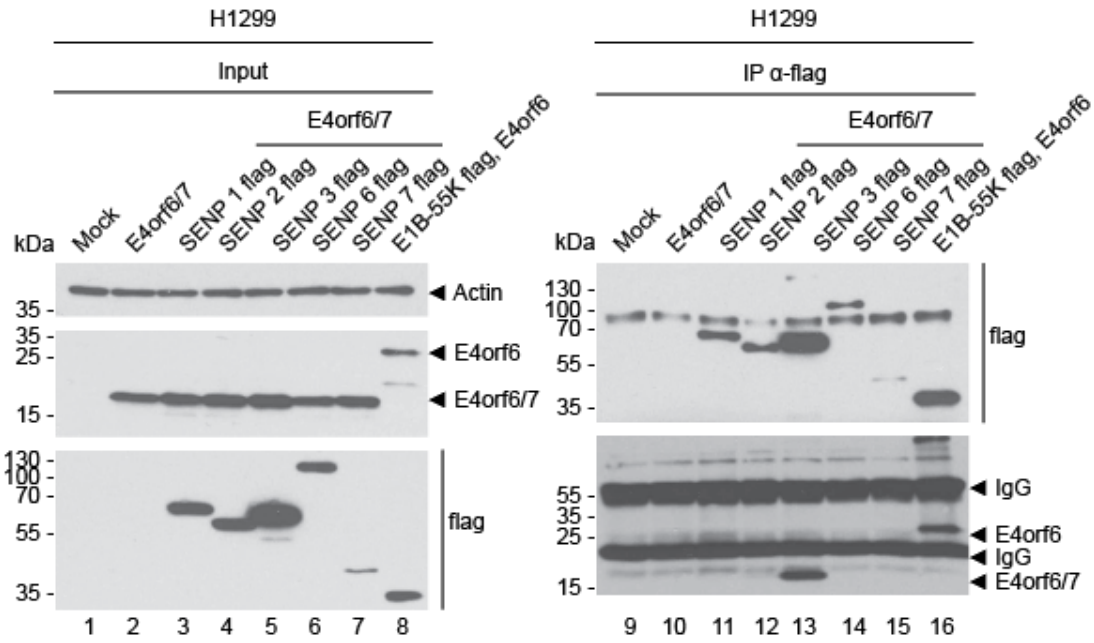

Fig. 16: E4orf6/7 interacts with SENP 3. H1299 cells ($4*10^6$) were transfected with the flag-tagged SENP isoform 1 to 3 (4 µg), 6 and 7 (10 µg) expressing plasmids and E4orf6/7 (4 µg). Immunoprecipitation of flag-tagged SENPs was performed using mAb M2 (flag), probes were resolved by SDS PAGE and visualized by Western blotting. Co-precipitated proteins and input levels of total cell lysates were detected by using mAb RSA3 (E4orf6/7 and E4orf6), mAb M2 (flag), and mAb AC-15 (Actin). Molecular weights in kDA are indicated on the left, while corresponding proteins are labeled on the right. The blots represent the result of several repeated experiments.

4.2.2.2 Localization changes of human SENPs during infection

In the next experiment, the localization of SENP 1 to 3 and 6 to 7 was investigated in HAdV-C5 infection, since the spatial distribution of SENPs has been identified as a key regulator of SENP target specificity [318].

H1299 cells were transfected with plasmids encoding SENP 1 to 3, 6, as well as 7. Twelve hours later, the transfected cells were infected with HAdV-C5-wt. As controls, cells were either transfected with SENP isoforms and mock infected or transfected with an empty flag-vector and infected with HAdV-C5. At 36 h.p.t. and 24 h.p.i., the cells were fixed for confocal immunofluorescence (IF) analysis and flag-tagged SENPs as well as the viral protein DBP, as a marker for infected cells, were stained. Cell nuclei were dyed with 4′, 6-diamidino-2-phenylindole (DAPI). Moreover, this analysis was conducted with flag-tagged SENP expressing constructs, since IF compatible SENP-specific antibodies are not available for the detection of endogenous SENPs. As a consequence, current knowledge about SENP localization is commonly based on exogenously expressed flag-tagged SENP isoforms. Unfortunately, E1B-55K staining was not possible in combination with flag-tag detection, since the available antibodies were cross-reactive. To show an indirect interaction, we choose to stain DBP, the major component of viral RCs, since SUMOylated E1B-55K is known to accumulate in these structures during the course of viral infections [221,419].

In mock infected cells, SENP 1 was diffusely disseminated in the nucleus and cytoplasm with partial accumulation in nuclear dots (Fig. 17 A c1-c4), whereas SENP 2 aggregated mainly in punctuate structures within the nucleus that has been shown to correspond to PML NBs (Fig. 17 A e1-e4) [318]. However, during HAdV-C5 infection, SENP 1 and SENP 2 co-localized with viral RCs, demarcated by DBP. Furthermore, both SENPs seemed to form E4orf3/PML resembling track-like structures (SENP 1: Fig. 17 A d1-d4; SENP 2: Fig. 17 f1-f4) [429]. SENP 3 was detected predominantly in the nucleoli (Fig. 17 A g1-g4), while SENP 6 and SENP 7 were diffusely disseminated in the nucleus (SENP 6: Fig. 17 A i1-i4; SENP 7: Fig. 17 A k1-k4). The distribution of these SENPs remained unaffected by HAdV-C5 infection (SENP 3: Fig. 17 A h1-h4, SENP 6: Fig. 17 A j1-j4; SENP 7: Fig. 17 A m1-m4).

In order to verify a relocalization of SENP 1 and SENP 2 to E4orf3 induced PML tracks, a second IF analysis was performed. Additionally, this staining can indicate a potential co-localization with E1B-55K, because beside partially localizing to the RCs later upon infection, E1B-55K binds E4orf3 and targets to E4orf3/PML tracks early during infection [429]. Consequently, H1299 cells were transfected and infected as described above. In the following, E4orf3 and the different flag-tagged SENP isoforms were detected in confocal IF analysis.

As already shown before, SENP 1 and SENP 2 co-localized with E4orf3/PML tracks upon HAdV-C5 infection, indicated by overlapping E4orf3 and SENP-flag signals (Fig. 17 B d1-d4, SENP 2: Fig. 17 f1-f4). Again, the localization of SENP 3, SENP 6 and SENP 7 did not change upon infection (SENP 3: Fig. 17 B h1-h4, SENP 6: Fig. 17 j1- j4, SENP 7: Fig. 17 m1-m4). In summary, these investigations indicate that the SENP isoforms SENP 1 and SENP 2 co-localize with adenoviral RCs and E4orf3/PML tracks. Since, those structures are known to be targeted by E1B-55K as well, a co-localization or interaction between E1B-55K and SENP 1 or SENP 2 is possible [419,429].

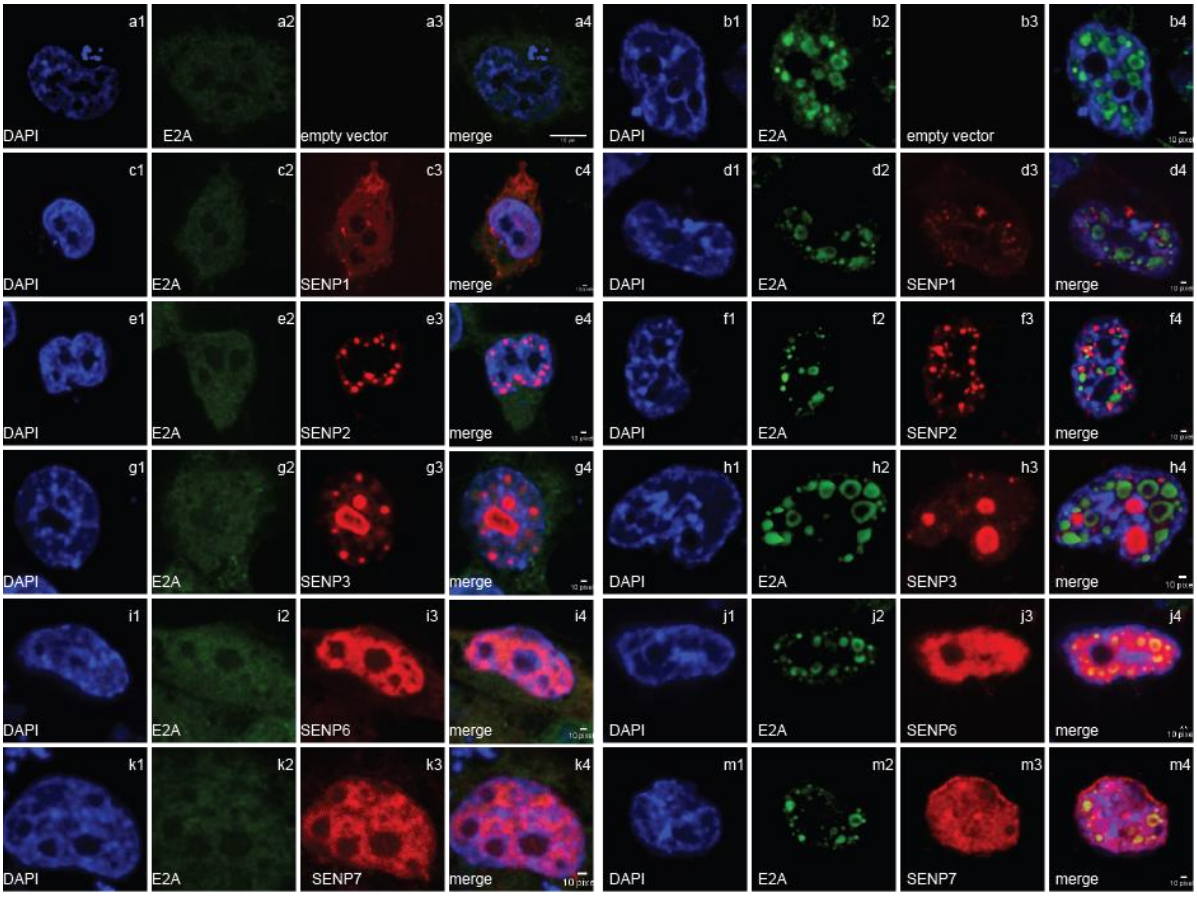

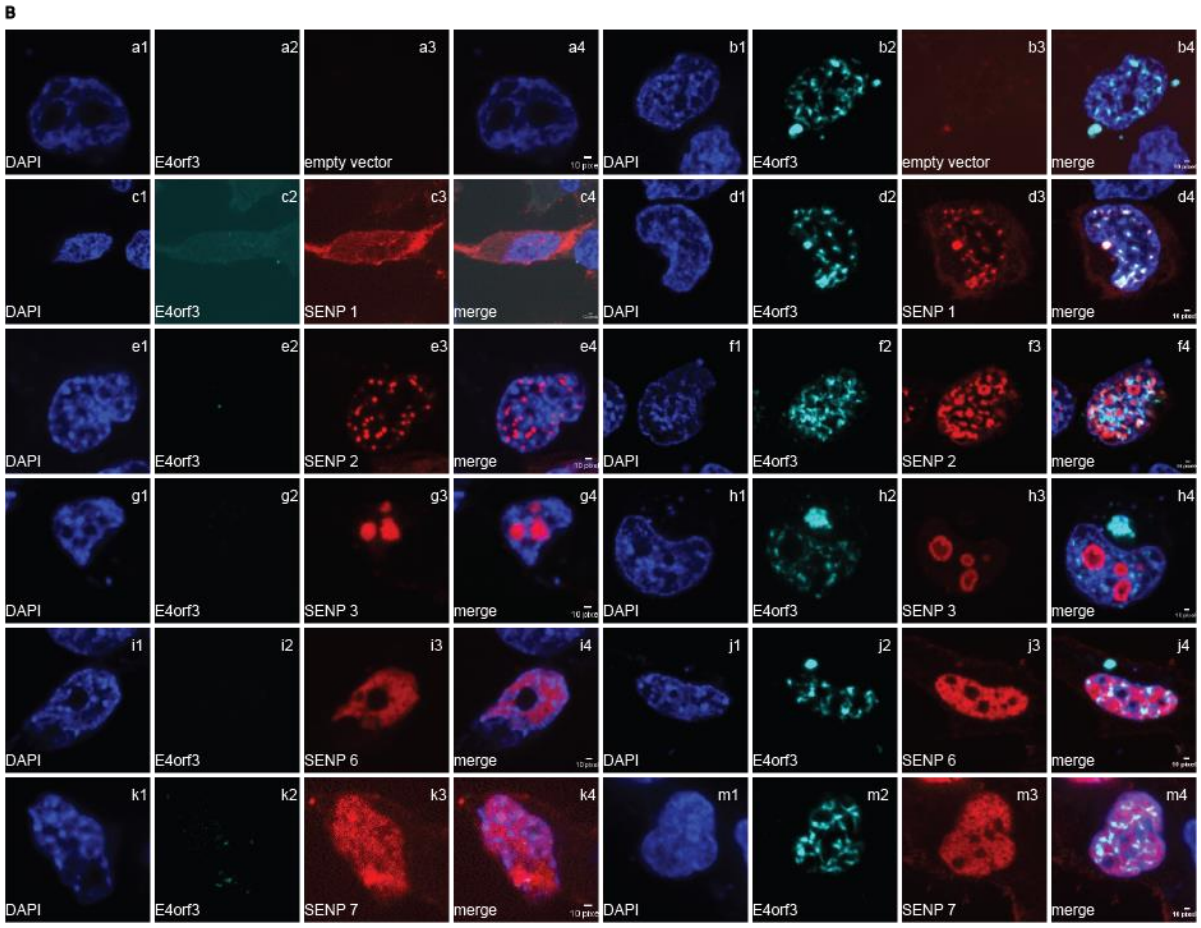

Fig. 17. SENP 1 and SENP 2 co-localize with viral RCs and E4orf3/PML track-like structures. H1299 cells ($3*10^4$) were seeded on a 6 well plate and transfected with 2 µg of plasmids encoding flag-tagged SENP 1 to SENP 3, SENP 6 and SENP 7. Twelve hours later, the cells were mock infected or infected with HAdV-C5-wt at an MOI of 20. At 24 h.p.i. cells were fixed with 4 % PFA and stained either with mAb mouse B6-8 (E2A/DBP) and pAb mouse Alexa™488 (green) as well as mAb rat 6F7 (flag SENP) and pAb rat Alexa™ 555 (**A**) or mAb rat 6A11 and pAb rat Cy5 (E4orf3) as well as mAb mouse M2 (flag SENP) and pAb mouse Alexa™555 (**B**). Cell nuclei were labeled with DAPI (blue). Afterwards they were analyzed by confocal microscopy. Each depicted phenotype has been found in at least 50 cells.

4.2.2.3 E1B-55K interaction with SENP 1 is independent of E4orf6

Besides co-localization, a second indication for a potential E4orf6-mediated deSUMOylation of E1B-55K by SENPs would be an E4orf6-dependent interaction between these proteins. In this context, IP analysis were performed to ascertain whether E1B-55K specifically interacts independently of E4orf6 with different SENP isoforms.

For the first analysis, H1299 cells were transfected with an E1B-55K expressing plasmid and plasmids encoding the flag-tagged SENP isoforms 1 to 3 and 6. Since

other viral proteins like E4orf3 might interfere with the binding between E1B-55K and the proteases, E1B-55K was transiently transfected in this experiment (Fig. 18).

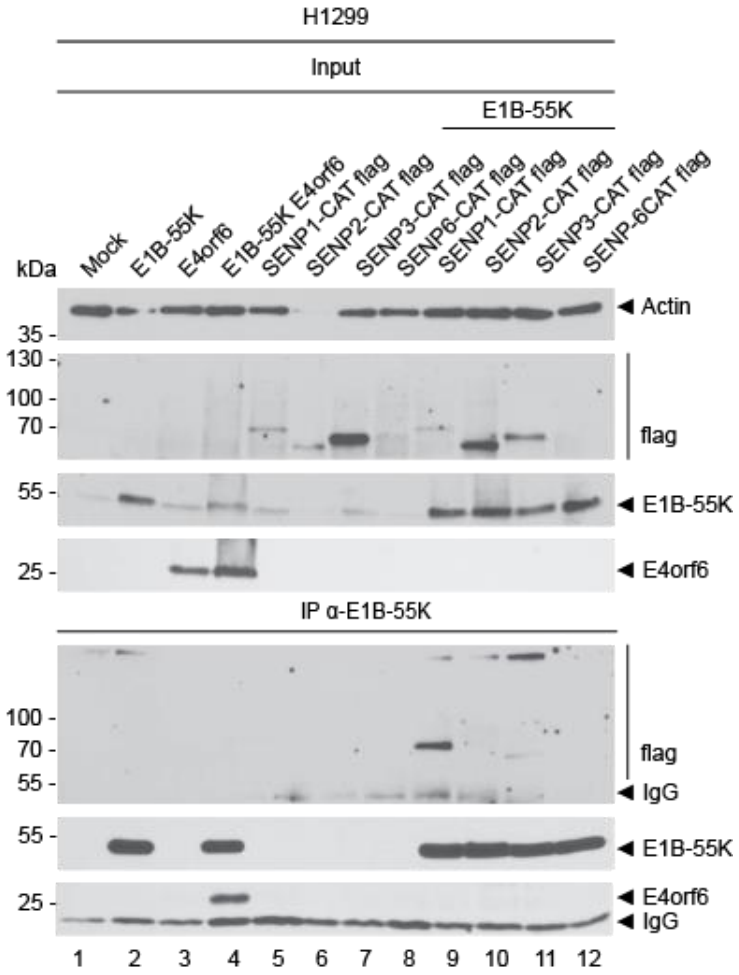

Fig. 18: E1B-55K interacts with SENP 1. H1299 cells ($4*10^6$) were transfected with plasmids encoding the catalytically inactive flag-tagged SENP isoforms 1, (4 µg), 2 (4µg), 3 (4 µg) and 6 (10 µg) and E1B-55K (4 µg). Immunoprecipitation of E1B-55K was performed using mAb 2A6 (E1B-55K), resolved by SDS PAGE and visualized by Western blotting. Coprecipitated proteins and input levels of total cell lysates were detected by using mAb 2A6 (E1B-55K), mAb RSA3 (E4orf6), mAb M2 (flag), and mAb AC-15 (Actin). Molecular weights in kDA are indicated on the left, while corresponding proteins are labeled on the right. The blots represent the result of several repeated experiments

After precipitation of E1B-55K conjugated proteins and subsequent staining for flag-tagged SENPs, no interaction between active SENPs and E1B-55K was detected (data not shown). However, deSUMOylation is a rapid process and SENP-target interactions are very instable. To steady these interactions, catalytically inactive SENP mutants were used for the repetition of the experiment. These mutations prevent the catalytically SUMO cleavage from modified proteins, and furthermore block the release of deSUMOylation targets from the proteases. Consequently, SENP-target interactions

are stabilized. Indeed, precipitation of E1B-55K and staining for flag-tagged catalytically inactive SENPs (CAT) revealed an interaction between SENP 1 CAT and E1B-55K, what is indicated by a SENP 1 CAT specific band at 70 kDa (Fig. 18 lane 9). In combination with the IF analysis (Fig. 17), this result suggested that E1B-55K might be targeted by SENP 1. Furthermore, a very faint interaction between SENP 3 was detected, indicating that E1B-55K might be also targeted by SENP 3 (Fig. 18 lane 11). However, according to the strength of interaction, SENP 1 might be the main SENP for E1B-55K deSUMOylation. As a successful positive control, an E4orf6 expressing plasmid was transfected in combination with E1B-55K, since the interaction of both proteins is well known and has been demonstrated in this work already (Fig. 18 lane 4). Admittedly, SENP 6 CAT expression was very weak and steady state concentrations were not shown here (Fig. 18 lane 4). However, SENP 1 CAT steady state concentrations were also very low, while the IP showed a solid enrichment of the protein (Fig. 18 lane 9). These observations, together with the co-localization assay (4.2.2.2), in which no changes in SENP 6 localization were detected, are indications against a potential interaction between E1B-55K and SENP 6.

4.2.2.4 E1B-55K is deSUMOylated by SENP 1 independently of E4orf6

As SENP 1 was identified as a binding partner of E1B-55K, it was reasonable to investigate whether this interaction results in an effective deSUMOylation of E1B-55K by SENP 1. Therefore, a Ni-NTA pulldown analysis was performed. In this assay Hela parental cells, HeLa SUMO 1 cells, or HeLa SUMO 2 cells were transfected with plasmids expressing E1B-55K, SENP 1, SENP 1 CAT, E1B-55K and SENP 1, or E1B-55K and SENP 1 CAT, respectively.

Precipitation of His-SUMO 1 and His-SUMO 2 modified proteins and specific staining for E1B-55K elucidated that SENP 1 reduced its SUMO1 and SUMO2 modification levels, while the co-expression of the catalytically inactive mutant SENP 1 CAT did neither affect SUMO 1 nor SUMO 2 modification of E1B-55K (Fig. 19). Furthermore, this experiment suggested that E4orf6 is not essential for an effective deSUMOylation of E1B-55K. However, it remains unclear whether E4orf6 enhances this process.

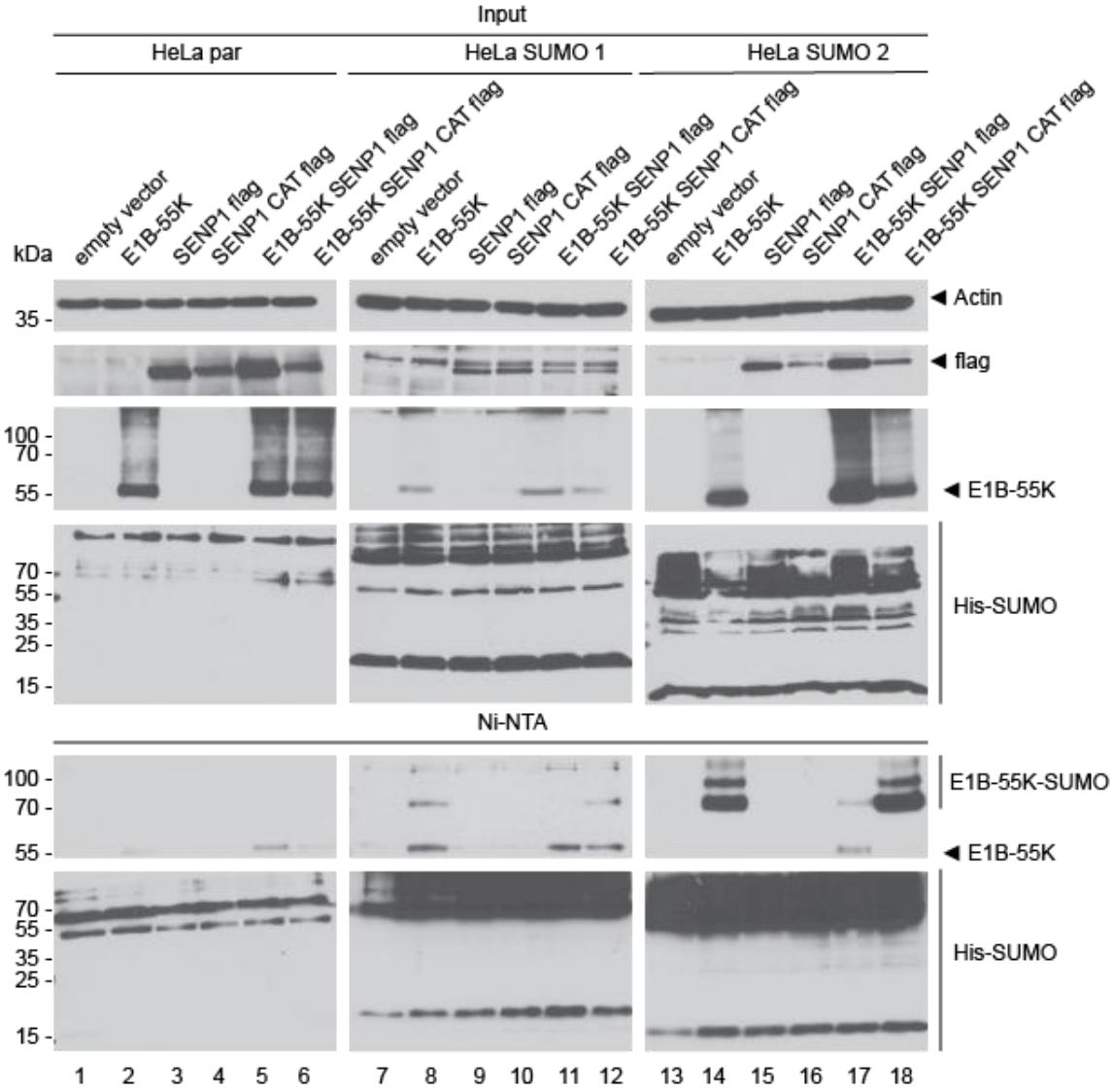

Fig. 19: E1B-55K is deSUMOylated by SENP 1. H1299 cells ($4*10^6$) were transiently transfected with E1B-55K (4 µg) and flag-tagged SENP 1 (4 µg) or SENP 1 CAT (4 µg) expressing plasmids. His-SUMO modified proteins were precipitated via Ni-NTA pulldown and total cell lysates were prepared. Precipitates and protein inputs were separated according to their molecular weight by SDS PAGE and visualized by immunoblotting. For specific protein detection mAb 2A6 (E1B-55K), mAb M2 (flag), mAb 6x His (SUMO 1/2) and mAb AC-15 (Actin) were used. Molecular weights in kDA are indicated on the left, while corresponding proteins are labeled on the right. The blots represent the result of several repeated experiments.

4.2.2.5 SENP 1 overexpression suppresses the focus-forming activity of E1A and E1B

Transformation of rodent cells by adenoviral oncogenes is a well-established system to study viral tumorigenesis. In this model system, HAdV genome encoded proteins of the E1A- and E1B-regions are sufficient to induce transformation of pBRK cells *in vitro*. Thereby, E1A induces constant cell proliferation resulting in cell immortalization, while E1B gene products are required to prevent apoptosis caused by E1A activities.

Different studies have shown that SUMOylation of E1B-55K is essential for its transforming abilities [418,454]. Hence, this system is a suitable tool to verify the efficient deSUMOylation of E1B-55K by SENP 1.

In order to investigate the effect of SENP 1 on the transforming abilities of the adenoviral oncogenes, freshly isolated pBRKs were transfected with E1A and E1B expressing plasmids alone and in combination with active and inactive SENP 1 expressing plasmids. Later, emerged foci were stained with crystal violet and the number of foci was counted on each plate. As controls, either K104R (negative) or K101R (positive) were transfected in combination with E1A.

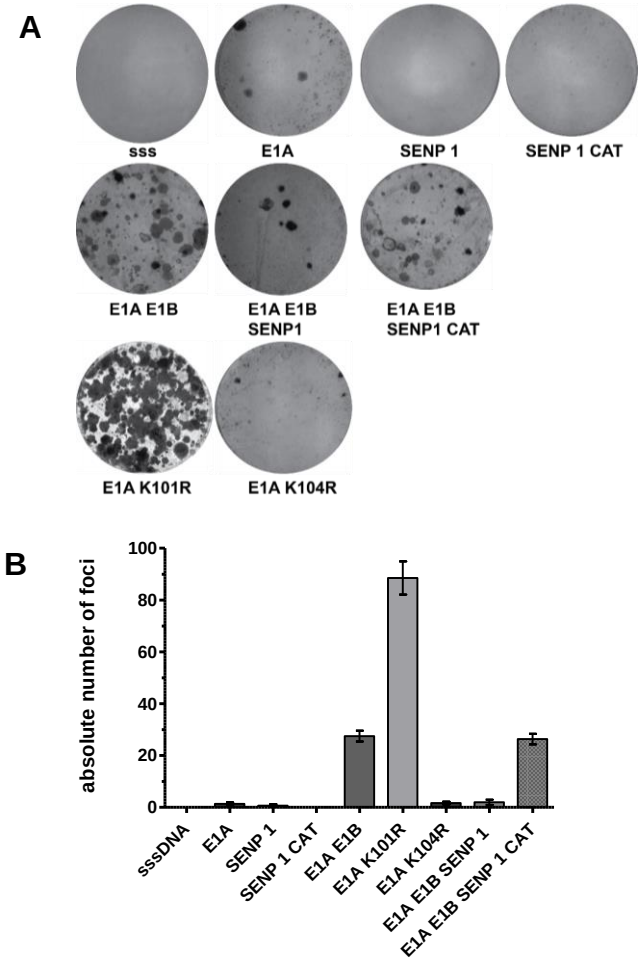

Fig. 20: Focus formation of HAdV-C5 E1B-55K K101R in pBRKs is increased. Primary BRK (pBRK) cells were transfected with 12 µg of plasmids encoding the E1-Box with HAdV-C5 E1A in combination with HAdV-C5 E1B-55K-wt, K101R, or K104R. 12 µg of SENP 1, or SENP 1 CAT were transfected as indicated together with the E1-Box. 12 µg of sssDNA were transfected as DNA carrier. The experiment was performed in triplicates. Therefore, one transfected 100 mm plate was split into three 100 mm plates at 48 h.p.t. The cells were kept in culture for eight weeks and afterwards, the plates were fixed with a crystal violet solution (25 % MeOH and 1 % crystal violet in H_2O) **(A)**. The foci of each plate were counted and the SEM was determined **(B)**. The illustration shows one representative experiment of four repeated assays. sssDNA: sheared salmon sperm DNA.

As expected, the expression of E1A and E1B resulted in an efficient transformation of pBRK cells, while the co-transfection of SENP 1 caused a significant decrease in the amount of foci (Fig. 20). In contrast, the co-expression of E1B/E1A and SENP 1 CAT led to a similar number of foci as E1A/E1B expression alone (Fig. 20). Furthermore, K101R showed an augmented transformation rate, while K104R almost lost the transformation capacity (Fig. 20). This result suggested, that SENP 1 is able to inhibit the E1A/E1B depended transformation of pBRKs by an efficient deSUMOylation of E1B-55K.

4.2.2.6 SENP binding capacity of E1B-55K is not influenced by E4orf6

In order to test whether E4orf6 influences the interaction of E1B-55K with SENPs, both proteins were transfected in H1299 cells in combination with the SENP CAT isoforms 1 to 3, and 6. Subsequently, immunoprecipitation assays were performed (Fig. 21).

In contrast to PML, the binding of E1B-55K to the SENPs was not changed upon E4orf6 expression. E1B-55K bound efficiently to SENP 1 CAT and very weak to SENP 3 CAT in presence (Fig. 21) and absence of E4orf6 (Fig. 18). This result emphasized that E4orf6 does not enhance the deSUMOylation of E1B-55K by recruitment of further SENPs, despite its own binding capacity towards SENP 1 to 3, 6, and 7, although it cannot be excluded yet.

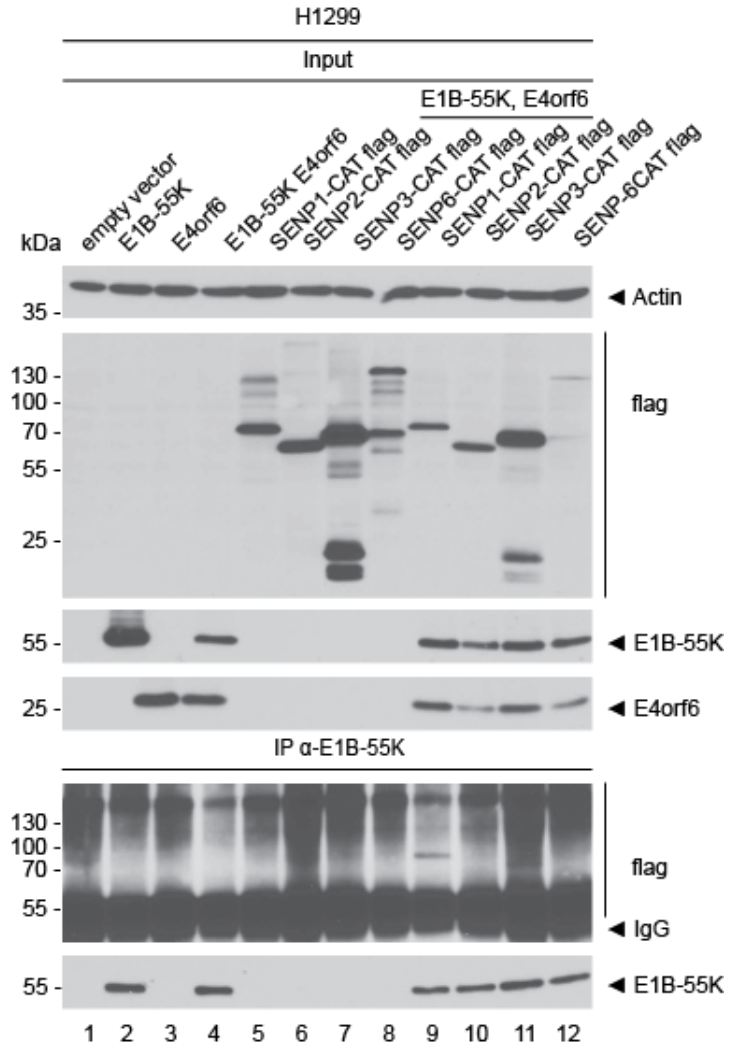

Fig. 21: E1B-55K binds to SENP 1 and SENP 3 in presence of E4orf6. H1299 cells ($4*10^6$) were transfected with the indicated catalytically inactive flag-tagged SENP isoforms 1 (4 µg), 2 (4 µg), 3 (4µg), 6 (10 µg), E4orf6 (4 µg) and E1B-55K (4 µg) expressing plasmids. Immunoprecipitation of E1B-55K was performed using mAb 2A6 (E1B-55K), co-precipitated proteins and input levels of total cell lysates were resolved by SDS PAGE and visualized by Western blotting, using the following Ab, mAb 2A6 (E1B-55K), mAb RSA3 (E4orf6), mAb M2 (flag), and mAb AC-15 (Actin). Molecular weights in kDA are indicated on the left, while corresponding proteins are labeled on the right. The blots represent the result of several repeated experiments.

4.2.2.7 E4orf6 decreases E1B-55K SUMOylation independently of SENPs

In the previous experiments, a potential deSUMOylation of E1B-55K by E4orf6 through the enhancement of SENP-E1B-55K interactions was investigated. However, E1B-55K bound to the same SENPs in presence and absence of E4orf6 and was not necessarily required for the deSUMOylation of E1B-55K by SENP 1. These results suggested that E4orf6 does not recruit an additional SENP for the removal of SUMO from E1B-55K, but did not exclude the possibility that E4orf6 might enhance the deSUMOylation of E1B-55K by SENP 1.

In order to solve this issue, the route through which SUMO attachment or deSUMOylation is affected by E4orf6 was analyzed on a higher level. To this end, a Ni-NTA pulldown with a SUMO 2 mutant, harboring a glutamine (Q) to proline (P) mutation at its SENP cleavage site at position 90 (Q90P), was performed. This mutation causes structural changes within SUMO 2, which prevent its introduction into the catalytic pocket of SENP proteases. Thereby, the removal of SUMO from target proteins is prohibited and stably SUMOylated proteins accumulate. However, neither SUMO maturation nor attachment to substrate proteins are affected. This SUMO mutant, as well as its SUMO 3 pendant SUMO T90P, are well established as potent tools in proteomic analyses aiming for the identification of new SUMO targets [290,469]. If E4orf6 inhibits the attachment of SUMO proteins to E1B-55K, the Q90P mutation of SUMO 2 will not influence the reductive effect of E4orf6 on E1B-55K SUMOylation. In contrast, an enhanced deSUMOylation should be blocked by the Q90P mutation and similar amounts of SUMOylated E1B-55K moieties will accumulate in presence and absence of E4orf6.

After cloning the His-tagged SUMO Q90P expressing plasmid (pHis-Q90P) via site directed mutagenesis, a Ni-NTA pulldown was performed, in which this SUMO mutant has been used as a bait. As prey, E1B-55K and K101R expressing plasmids were transfected, either alone or in combination with E4orf6, to analyze the effect of E4orf6 on the Q90P conjugation to E1B-55K and K101R. As controls, His-SUMO 2 was transfected with E1B-55K, K101R, E4orf6, E1B-55K plus E4orf6, and K101R plus E4orf6, respectively. Cell lysates were subsequently subjected to a Ni-NTA pulldown analysis and results have been illustrated in Western Blot (Fig. 22).

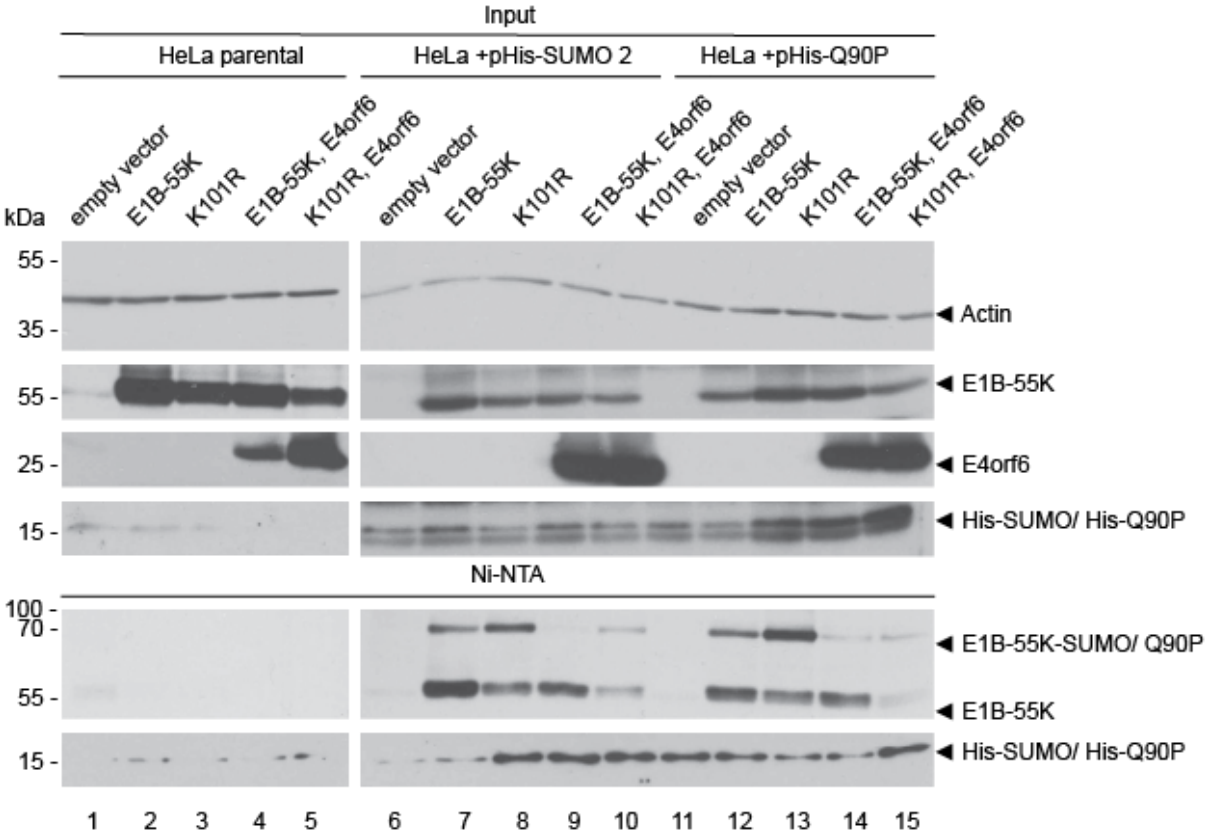

Fig. 22: E4orf6 inhibits SUMO attachment to E1B-55K. HeLa cells ($4*10^6$) were transiently transfected as indicated with plasmids encoding His-tagged SUMO 2 (10 µg), Q90P (10 µg), E1B-55K (4µg) and E4orf6 (4µg). His-SUMO modified proteins were precipitated via Ni-NTA pulldown. Precipitates and total cell lysates were separated according to their molecular weight by SDS PAGE and visualized by immunoblotting. For specific protein detection mAb 2A6 (E1B-55K), mAb RSA3 (E4orf6), mAb 6x His (SUMO 1/2) and mAb AC-15 (Actin) were used. Molecular weights in kDA are indicated on the left, while corresponding proteins are labeled on the right. The image represents the result of several repeated experiments.

As shown before in infection, E1B-55K and K101R were modified with SUMO 2, whereby K101R was slightly more SUMOylated than E1B-55K (Fig. 22 lane 7 and 8). Furthermore, the addition of E4orf6 resulted in reduced SUMO 2 levels of E1B-55K and K101R (Fig. 22 lanes 9 and 10). Similar to SUMO 2, Q90P was conjugated to E1B-55K and K101R (Fig. 22 lanes 6 to 10). Notably, Q90P conjugation of E1B-55K and K101R was decreased in presence of E4orf6 as well (Fig. 22 lanes 10 to 15). These results clearly demonstrated that E4orf6 does not enhance the deSUMOylation of E1B-55K, but rather inhibits the SUMO attachment to E1B-55K. Furthermore, it emphasized that the reductive effect of E4orf6 on E1B-55K is not influenced by other viral proteins, since E1B-55K and E4orf6 were transiently transfected alone in this experiment.

4.2.3 E4orf6 does not influence the crosstalk between E1B-55K phosphorylation and SUMOylation

E1B-55K is phosphorylated at its C-terminus (S490/491 and T495) by the kinase CK2 and SUMOylated at K101 and K104 [425]. Phosphorylation of E1B-55K has been identified as a regulator for E1B-55K SUMOylation [461]. Wimmer and co-workers suggested that phosphorylation is required for the activation of UBC 9, the single known E2 SUMO enzyme, which is essential for the transfer of SUMO to target proteins [461]. Since E1B-55K SUMOylation is dependent on its C-terminal phosphorylation, as we showed in the last experiment, that E4orf6 reduces the SUMO attachment to E1B-55K, it is conceivable that E4orf6 does not influence SUMOylation directly, but rather prevents phosphorylation and thereby inhibits SUMOylation indirectly. It is therefore tempting to speculate that E4orf6 might influence the phosphorylation of E1B-55K, which in turn would affect the SUMO conjugation to K101 and K104.

To evaluate whether E4orf6 regulates E1B-55K SUMOylation via phosphorylation, virus mutants needed to be generated in which the phospho-sites S490/491 and T495 were either exchanged by an arginine (R) or an asparagine (D) in combination with an E4orf6 deletion (Fig. 23). Arginine substitutions in the CPR of E1B-55K prevent the phosphorylation completely, while an exchange to asparagine mimics a constitutive phosphorylation [461,470]. Therefore, the virus mutants were named HAdV-C5-delP ΔE4orf6 (phospho deletion) and HAdV-C5-PM ΔE4orf6 (phospho mimic). Comparing delP and PM SUMO conjugation levels in presence and absence of E4orf6 shall reveal, whether E4orf6 renders E1B-55K SUMOylation through the inhibition of phosphorylation. If E4orf6 affects the phosphorylation of E1B-55K, no E4orf6 dependent changes in the SUMOylation of delP and PM are expected, while E4orf6 dependent alterations will refute this hypothesis.

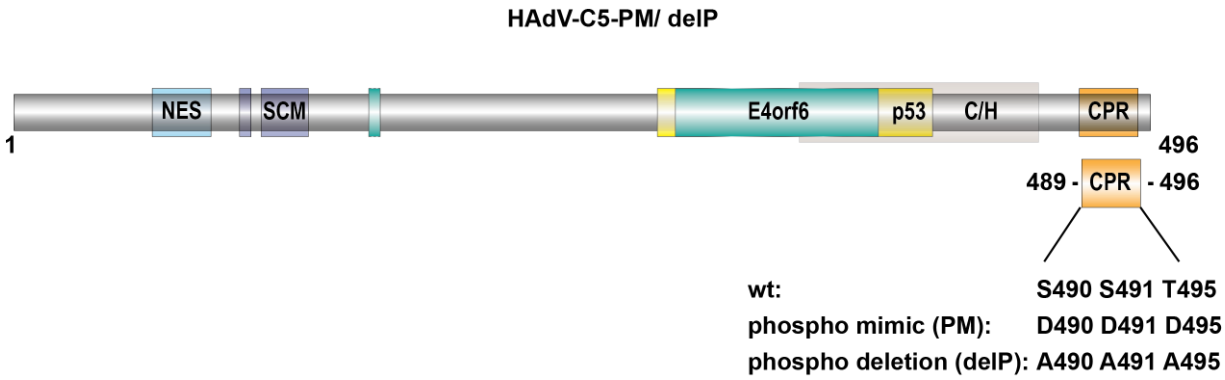

Fig. 23: Schematic illustration of E1B-5K phospho mimic (PM) and phospho deletion (delP) mutants. PM and delP are E1B-55K mutants carrying aa exchanges in the C-terminal phosphorylation region (CPR). Here, indicated serine (S) and threonine (T) residues are either exchanged by D (PM), constantly mimicking phosphorylation, or A (delP), abrogating E1B-55K phosphorylation.

In the beginning, HAdV-C5-delP ΔE4orf6 and HAdV-C5-PM ΔE4orf6 were generated. To this end, a RED recombination system was applied. This method has been developed for the generation of new HAdV libraries and relies on ccdB counter selection in combination with the RED recombination system derived from phage lambda [471,472]. A schematic overview of the cloning steps is illustrated in Fig. 24.

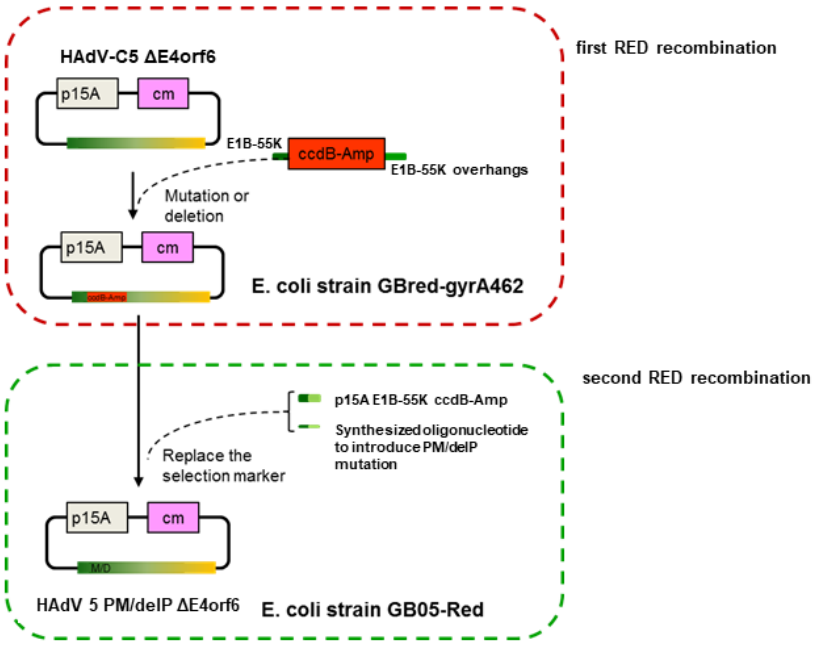

Fig. 24: Overview of the generation of HAdV-C5-PM ΔE4orf6 and HAdV-C5-delP ΔE4orf6 via a two-step RED recombination. A p15A plasmid backbone containing the HAdV-C5-ΔE4orf6 genome was used as a template. In the first RED recombination a ccdB-Amp selection cassette is introduced in the CPR region of E1B-55K. After isolation, the newly recombined p15A HAdV-C5-ΔE4orf6 ccdB Amp encoding plasmid was used as a template for the second RED recombination. Here, an oligonucleotide which hybridizes with the lagging strand DNA of the p15A plasmid at the CPD domain of E1B-55K containing either the PM or delP mutation is used to replace the ccdB-amp cassette and introduce the PM and delP mutation, respectively.

Prior to virus stock production, HAdV-C5-PM ΔE4orf6 and HAdV-C5-delP ΔE4orf6 encoding bacmids were analyzed via enzymatic digestion and mutated domains were sequenced. Correct bacmids were transfected into 293 cells applying the lipofectamine protocol and newly produced virus progenies were used to infect A549 cells to generate high titer virus stocks.

In the following, HAdV-C5-PM ΔE4orf6 and HAdV-C5-delP ΔE4orf6 as well as HAdV-C5-wt, HAdV-C5-ΔE4orf6, HAdV-C5-PM, and HAdV-C5-delP were applied to Ni-NTA pulldown analysis to evaluate the SUMO levels of E1B-55K variants in presence and absence of E4orf6 (Fig. 25).

As estimated, SUMO 2 conjugation of E1B-55K was reduced in presence of E4orf6 (Fig. 25 lanes 9 and 10). Remarkably, E4orf6 had a similar effect on PM and delP (Fig. 25 lane 11). In contrast to previous publications, delP was slightly SUMOylated (Fig. 25 lane 13) [461]. However, this might be explained by differences in the applied systems. Here, a cell line stably overexpressing SUMO 2 was used, which forces SUMOylation immensely, while Wimmer and colleagues transiently transfected SUMO 2 into H1299 cells, what generally results in lower SUMO levels. Nevertheless, the deletion of E4orf6 resulted in an increased SUMOylation of both phospho-mutants, evidently displaying that a change in phosphorylation was not the reason for the reduced SUMO levels of E1B-55K in presence of E4orf6 (Fig. 25 lanes 12 and 14).

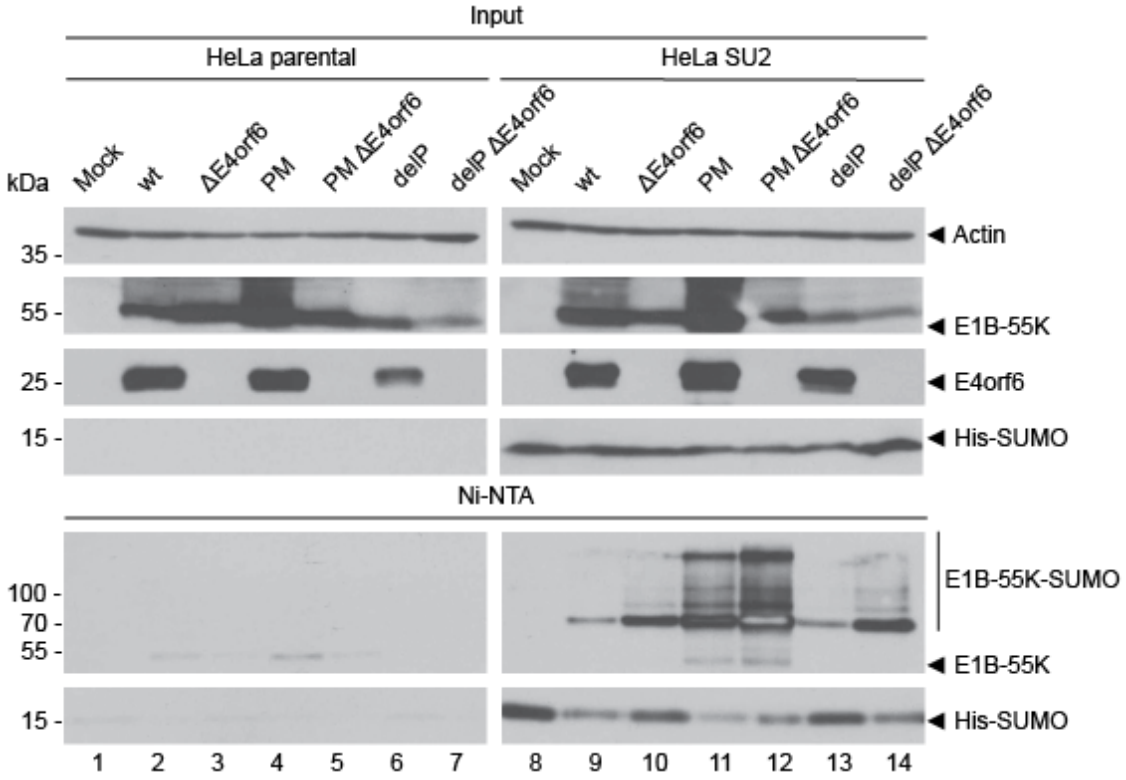

Fig. 25: E4orf6 does not regulate E1B-55K SUMOylation via phosphorylation. HeLa parental cells or HeLa cells constitutively expressing His-tagged SUMO 2 were infected at an MOI of 20 with mock, HAdV-C5-wt, HAdV-C5-ΔE4orf6, HAdV-C5-PM, HAdV-C5-PM-ΔE4orf6, HAdV-C5-delP or HAdV-C5-delP ΔE4orf6. At 24 h.p.i., the cells were harvested, total cell lysates were prepared and His-SUMO conjugates were Ni-NTA purified. Proteins were separated by SDS-PAGE according to their molecular weight and subjected to immunoblotting. Proteins were detected using mAb AC-15 (Actin), mAb 2A6 (E1B-55K), mAb RSA3 (E4orf6) and mAb 6x His (SUMO 1/2) in Western Blot analysis. Molecular weights in kDa are indicated on the left, detected proteins on the right. The blots represent the result of several repeated experiments.

4.2.4 Interaction between E1B-55K and E4orf6 is a requirement for reduced SUMOylation

In the last hypothesis it was assumed that binding of E4orf6 to E1B-55K interferes with the SUMOylation of E1B-55K, since direct protein-protein interactions have been described as potent regulators of PTMs for Kap1 or PML before [455,460]. For this examination, an E1B-55K mutant which is incapable of E4orf6 binding and behaves as similar as possible to HAdV-C5-wt in infection, needed to be identified first. Therefore, known E1B-55K mutants which do not interact with E4orf6 were examined for the required properties. In the following, this mutant shall be analyzed for SUMO level reductions of E1B-55K.

4.2.4.1 E1B-55K A143 binding to E4orf6 is significantly impaired

The screening for a suitable E1B-55K virus mutant incapable of E4orf6 binding comprised the examination of protein stability during viral infection, viral replication

efficacy, E1B-55K localization, p53 and Mre11 degradation as well as E4orf6 binding. Best results were obtained for a E1B-55K insertion mutant, termed A143, according to a binding inhibiting insertion of the four aa leucine (L), glutamic acid (E), phenylalanine (F) and glutamine (Q) at position A143 (Fig. 26) [473].

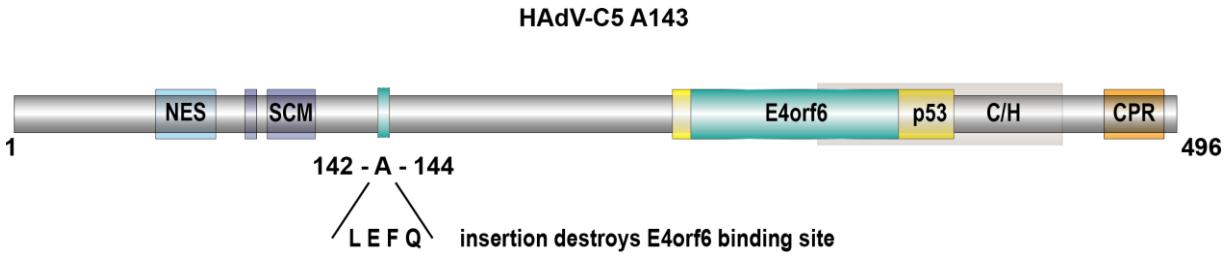

Fig. 26: Schematic illustration of the non-E4orf6 binding mutant A143. A143 is an E1B-55K mutant carrying an insertion of the aa leucine (L), glutamic acid (E), phenylalanine (F) and glutamine (Q) at position A143. This insertion affects E4orf6 binding.

Prior to the examination of the SUMOylation of A143, the binding deficiency of this mutant towards E4orf6 was verified in IP analysis (Fig. 27). Therefore, A549 cells were infected with mock, HAdV-C5, HAdV-C5-ΔE4orf6, and HAdV-C5-A143, respectively. At 24 h.p.i., the cells were harvested and cell lysates were prepared. Afterwards, the obtained probes were subjected to immunoprecipitation and immunoblotting.

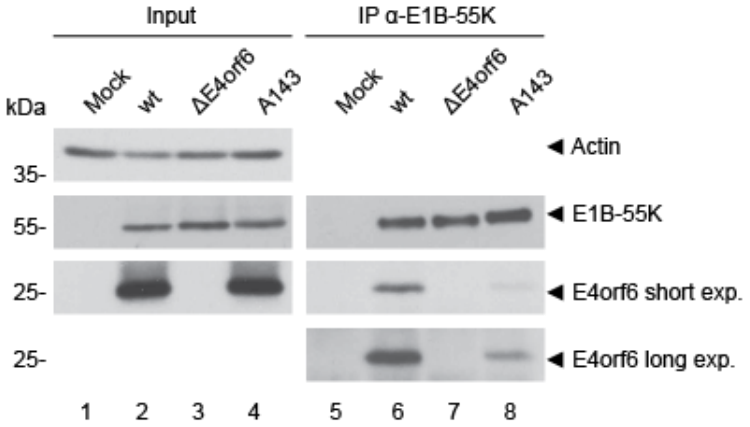

Fig. 27: A143 mutation reduces the binding capacity of E1B-55K towards E4orf6. A549 cells were infected with the indicated virus mutants at an MOI of 20 and harvested 24 h.p.i.. Afterwards, total-cell extracts were prepared and an IP of E1B-55K was performed using the 2A6 mouse mAb. Proteins were separated by SDS-PAGE and subjected to immunoblotting. Input levels of total-cell lysates and immunoprecipitated proteins were detected using mAb 2A6 (E1B-55K), mAb RSA3 (E4orf6) and mAb AC-15 (Actin). The molecular weights in kDa are indicated on the left and detected proteins on the right. The blots represent the result of several repeated experiments.

As anticipated, precipitation of E4orf6 was significantly decreased by the insertion of L, E, F, and Q at position A143 of E1B-55K, while E1B-55K-wt strongly bound to E4orf6 (Fig. 27 lane 8 and lane 6). However, the interaction between A143 and E4orf6 was not completely abolished (Fig. 27 lane 8, E4orf6 long exposure).

4.2.4.2 The interaction between E1B-55K and E4orf6 is required for E1B-55K SUMO level reductions

To test how the binding between E1B-55K and E4orf6 influences the SUMOylation of E1B-55K, the binding mutants HAdV-C5-A143 and HAdV-C5-A143 ΔE4orf6 were analyzed in SUMO pulldown experiments. Therefore, A549 cells were infected with mock, HAdV-C5-wt, HAdV-C5-ΔE4orf6, HAdV-C5-A143, and HAdV-C5-ΔE4orf6. Later on, infected cells were harvested and applied to SUMO pulldown analysis (Fig. 28).

As expected, SUMO modification of E1B-55K in presence of E4orf6 was modest, while in absence of E4orf6 it was significantly increased (Fig. 28 lane 7 and lane 8). Remarkably, A143 was higher SUMOylated than E1B-55K-wt (Fig. 28 lane 7 and lane 9) but did not reach the same band intensity as E1B-55K of HAdV-C5-ΔE4orf6 (Fig. 28 lane 8 and lane 9). Presumably, the remaining binding capacity between A143 and E4orf6 (Fig. 27) was sufficient to slightly impede A143 SUMO modification. In line with this, A143 was stronger modified with SUMO in the absence of E4orf6 (Fig. 28 lane 10). These findings support the hypothesis that E4orf6 competes with SUMO as well as E2 or E3 SUMO enzymes for E1B-55K binding sites.

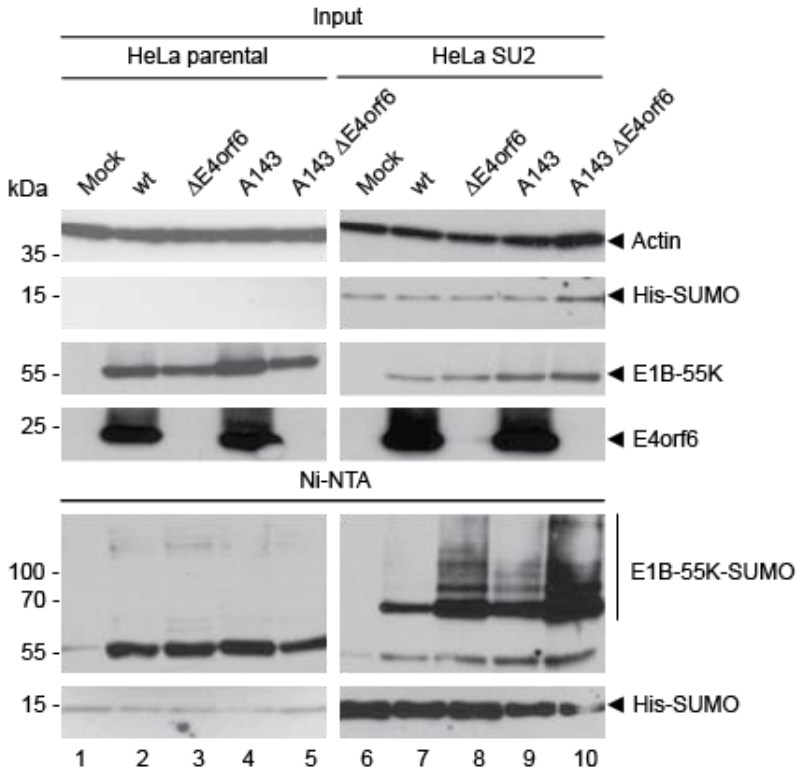

Fig. 28: Increased SUMOylation of E1B-55K A143. HeLa parental cells or HeLa cells constitutively expressing His-tagged SUMO 2 were infected at an MOI of 20 with mock, HAdV-C5-wt, HAdV-C5-ΔE4orf6, HAdV-C5-A143 or HAdV-C5-A143 ΔE4orf6. Cells were harvested at 24 h.p.i, total cell lysates prepared, and His-SUMO conjugates were Ni-NTA purified. Proteins were separated by SDS-PAGE according to their molecular weight and subjected to immunoblotting. Proteins were detected using mAb AC-15 (Actin), mAb 2A6 (E1B-55K), mAb RSA3 (E4orf6) and mAb 6x His (SUMO 1/2) in Western Blot analysis. Molecular weights in kDa are indicated on the left, detected proteins on the right. The blots represent the result of several repeated experiments.

4.2.5 E4orf6 decreases the co-localization of E1B-55K with SUMO 2

The localization pattern E1B-55K during HAdV-C5-wt infection has been described as very complex. The viral protein shuttles continuously between nucleus and cytoplasm [416,417]. Temporarily, it can be found in PML NBs, E4orf3 induced PML tracks as well as viral RCs. Furthermore, E1B-55K is diffusely disseminated in the nucleus and in perinuclear aggregates [221,418,419,430,450,461]. Determination of the spatial distribution of E1B-55K is only incompletely understood. However, previous studies have displayed a correlation between the localization of E1B-55K mutants and their SUMOylation. In these investigations, the highly SUMO modified E1B-55K mutants NES and PM tended to localize within the nucleus and associate with viral RCs, while the SUMOylation deficient E1B-55K mutant K104R accumulated mainly in cytoplasmic aggregates [418,419]. In this work, E4orf6 was substantiated as a negative regulator of E1B-55K SUMOylation that dependents on their interaction. As SUMOylation of E1B-55K

corresponds with its subcellular localization, it is conceivable that E4orf6 influences co-localization of E1B-55K and SUMO. Therefore, the co-localization of E1B-55K-wt, K101R, K104R, K101 K104R and A143 with SUMO 2 shall be investigated in presence and absence of E4orf6 in confocal IF analysis to further prove the previous results. Additionally, this analysis will support the notion that E1B-55K is modified *in vivo* by endogenous SUMO.

At first, A549, H1299 and HFF cells were infected with the indicated virus mutants, fixed at 24 h.p.i and immunostained for E1B-55K and endogenous SUMO 2. To evaluate whether E4orf6 influences the co-localization of E1B-55K and SUMO 2 proteins, the overlay signals of E1B-55K variants and SUMO 2 positive cells were quantified. Here, infected A549 cells were chosen to demonstrate the obtained results (Fig. 29).

In mock infected A549 cells, SUMO 2 was diffusely spread throughout the nucleus and accumulated in dots, which are presumably PML NBs (Fig. 29 A a1-a4). Upon infection with the indicated virus mutants, SUMO 2 was relocalized either to structures resembling viral E4orf3/PML tracks or viral RCs, as described in other studies for the localization of SUMO 2 during HAdV-C5-wt infections [409]. It is noteworthy, that viral RCs are known to change their shape depending on the stage of infection [116]. Earlier in infection, many donut shaped RCs spread all over the nucleus, while at later stages these structures coalesce and form huge aggregates [116].

In this experiment, SUMO 2 was detectable in donut shaped RCs as well as in aggregates resembling coalesced RCs (Fig. 29 A). Focusing on the co-localization of E1B-55K mutant proteins and SUMO 2, overlapping signals were observed mainly in RC-resembling structures (Fig. 29 A). During infection with the E4orf6 positive viruses HAdV-C5-wt and HAdV-C5-K101R, E1B-55K signals overlapped in 8 % of the counted cells with SUMO 2 signals (Fig. 29 A c1-c16, B) and K101R co-localized in 55 % of the cells with SUMO 2 (Fig. 29 A e1-e16, B). During HAdV-C5 ΔE4orf6 infection, E1B-55K co-localized in 29 % of the cells with SUMO 2 (Fig. 29 A d1-d16, B), while K101R signals of HAdV-C5-K101R ΔE4orf6 overlapped in 78 % of the counted cells (Fig. 29 A f1-f16, B). In summary, the deletion of E4orf6 caused an approximately 20 % increased co-localization of E1B-55K and K101R with SUMO 2 in viral RCs. To substantiate that, the interaction between E1B-55K and E4orf6 is responsible for the

lower co-localization between E1B-55K and SUMO 2, the E4orf6 binding deficient E1B-55K mutant A143 was analyzed in presence and absence of E4orf6. The examination of HAdV-C5-A143 and HAdV-C5-A143 ΔE4orf6 infected cells showed that the binding-deficient E1B-55K mutant protein co-localized in 26 % of the cells with SUMO 2 in presence of E4orf6 (Fig. 29 A g1-g16, B), while in absence of E4orf6, 33 % co-localization was revealed (Fig. 29 A h1-h16, B), resembling perfectly the results obtained in section 4.2.4.2. In contrast, the main proportions of K104R and K101/104R accumulated in cytoplasmic aggregates during infection with HAdV-C5-K104R, HAdV-C5-K104R ΔE4orf6, HAdV-C5-K101/104R and HAdV-C5-K101/104R ΔE4orf6, respectively (Fig. 29 A i1-8 (HAdV-C5-K104R), j1-j8 (HAdV-C5-K104R ΔE4orf6), k1-8 (HAdV-C5-K101/104R), m1-m8 (HAdV-C5-K101/104R ΔE4orf6), B). Notably, K101/K104R was neither SUMOylated in presence or absence of E4orf6, while K104R was slightly SUMO 2 modified in the absence of E4orf6, but not in presence of E4orf6 (4.1.1). Hence, both E1B-55K mutants did not assemble in viral RCs together with SUMO 2, since RC association correlated with a high SUMOylation. Occasionally, K104R and K101/104R formed nuclear dots, which randomly co-localized with SUMO 2. However, the deletion of E4orf6 did neither result in an increased nuclear accumulation of K104R and K101/104R nor in an association of K104R and K101/104R with SUMO 2 in viral RCs (Fig. 29 A i1-8 (HAdV-C5-K104R), j1-j8 (HAdV-C5-K104R ΔE4orf6), k1-8 (HAdV-C5-K101/104R), m1-m8 (HAdV-C5-K101/104R ΔE4orf6)). In control cells infected with an E1B-55K deficient virus, no E1B-55K specific signals were visible (Fig. 29 A pictures b1-b8). These results demonstrated on the one hand that E4orf6 influences the co-localization of E1B-55K with SUMO 2 and on the other hand that E4orf6 inhibits the localization of E1B-55K in viral RCs. Furthermore, analysis of HAdV-C5-A143 and HAdV-C5-A143 ΔE4orf6 infected cells showed that a binding between both proteins is required for the altered distribution of E1B-55K. These findings perfectly resemble the results from the previous experiments.

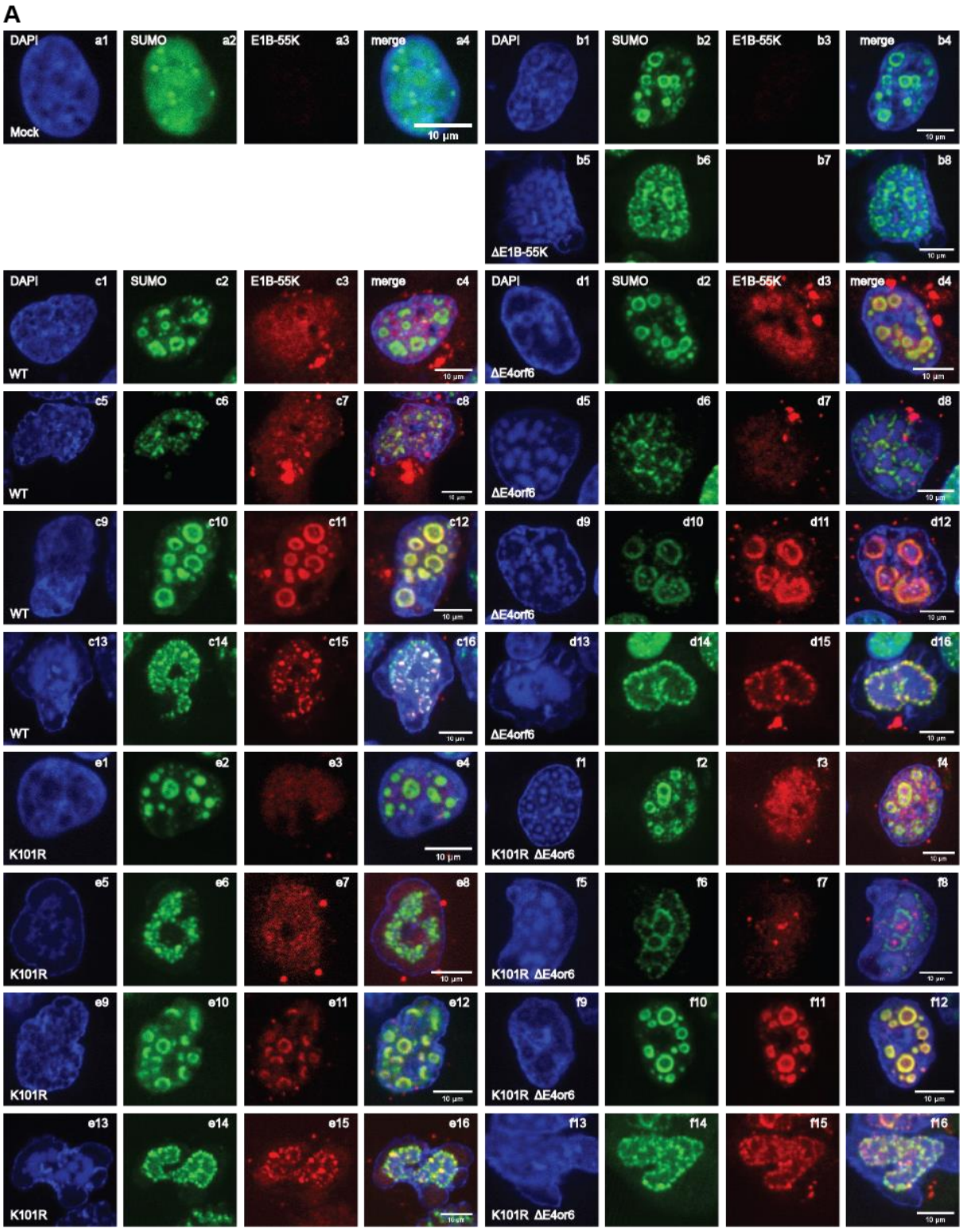
A
DAPI a1
SUMO a2
E1B-55K a3
merge a4
Mock
10 µm
DAPI b1
SUMO b2
E1B-55K b3
merge b4
b5
b6
b7
b8
ΔE1B-55K
DAPI c1
SUMO c2
E1B-55K c3
merge c4
WT
DAPI d1
SUMO d2
E1B-55K d3
merge d4
ΔE4orf6
c5
c6
c7
c8
WT
d5
d6
d7
d8
ΔE4orf6
c9
c10
c11
c12
WT
d9
d10
d11
d12
ΔE4orf6
c13
c14
c15
c16
WT
d13
d14
d15
d16
ΔE4orf6
e1
e2
e3
e4
K101R
f1
f2
f3
f4
K101R ΔE4or6
e5
e6
e7
e8
K101R
f5
f6
f7
f8
K101R ΔE4or6
e9
e10
e11
e12
K101R
f9
f10
f11
f12
K101R ΔE4or6
e13
e14
e15
e16
K101R
f13
f14
f15
f16
K101R ΔE4or6

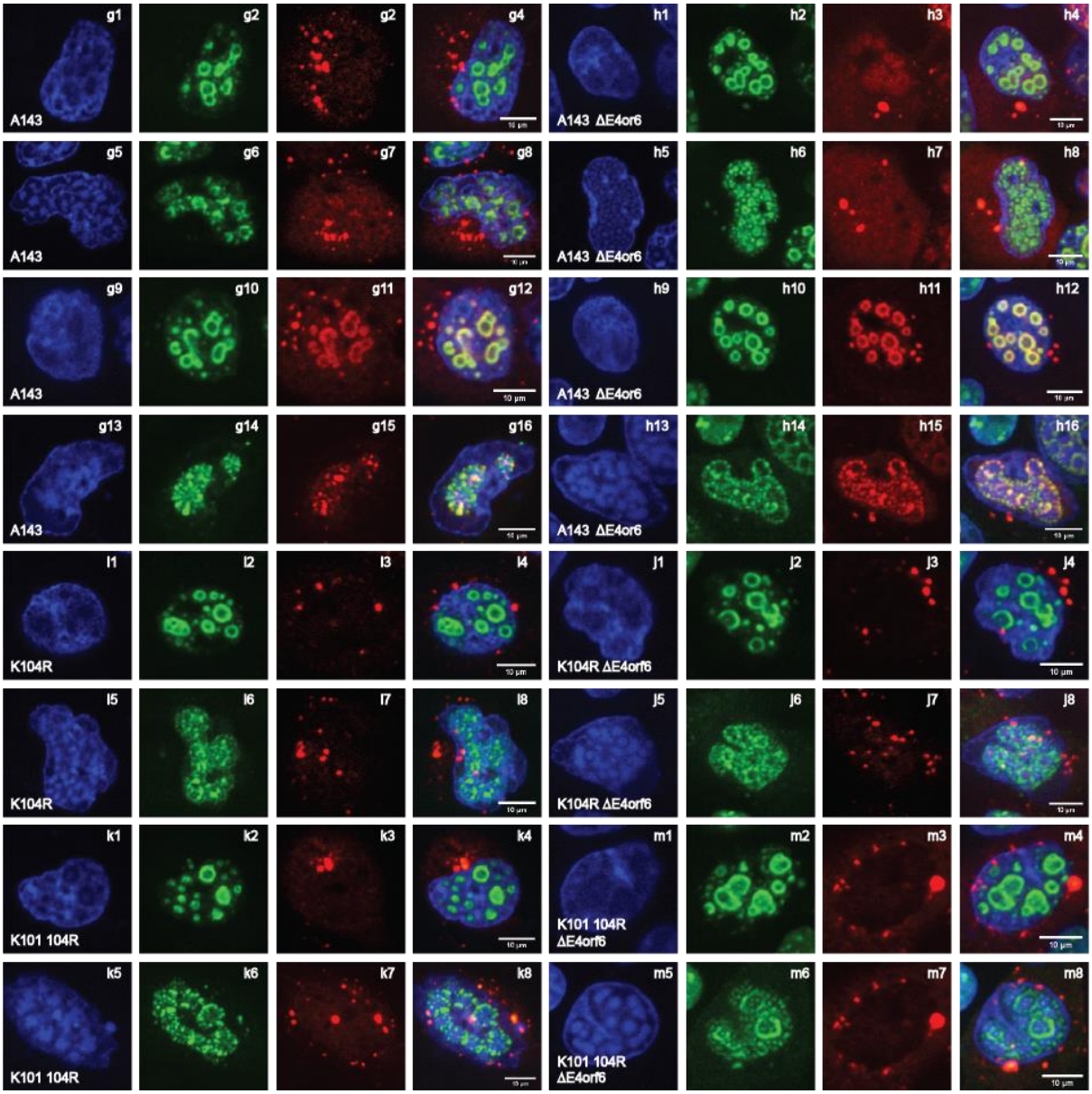
g1
A143
g2
g2
g4
h1
A143 ΔE4or6
h2
h3
h4
g5
A143
g6
g7
g8
h5
A143 ΔE4or6
h6
h7
h8
g9
A143
g10
g11
g12
h9
A143 ΔE4or6
h10
h11
h12
g13
A143
g14
g15
g16
h13
A143 ΔE4or6
h14
h15
h16
I1
K104R
I2
I3
I4
J1
K104R ΔE4orf6
J2
J3
J4
I5
K104R
I6
I7
I8
J5
K104R ΔE4orf6
J6
J7
J8
k1
K101 104R
k2
k3
k4
m1
K101 104R
ΔE4orf6
m2
m3
m4
k5
K101 104R
k6
k7
k8
m5
K101 104R
ΔE4orf6
m6
m7
m8

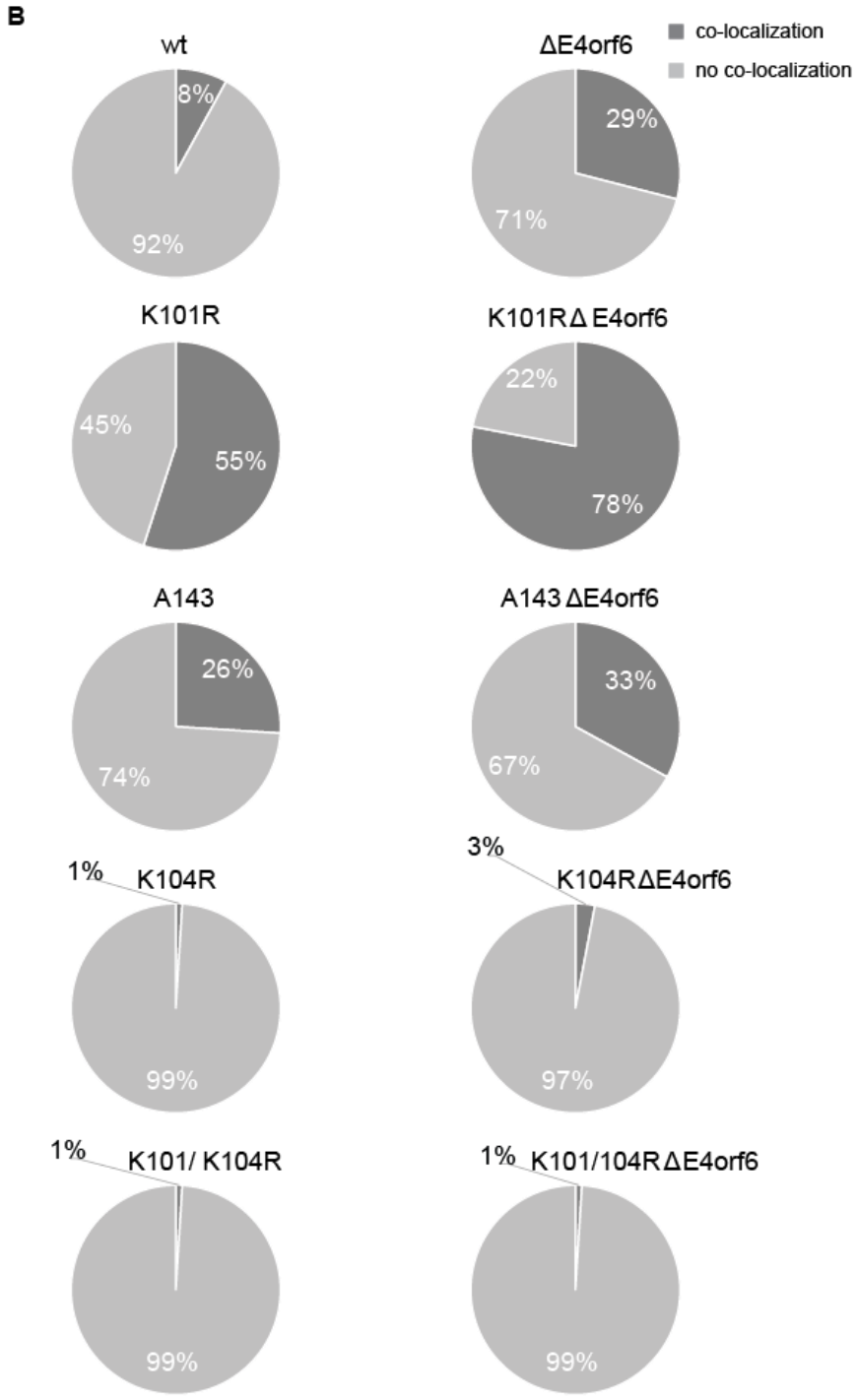

Fig. 29: E4orf6 influences the co-localization of E1B-55K and SUMO2. A) A549 cells were either mock infected or infected with the indicated virus mutants at an MOI of 20. At 24 h p.i. cells were fixed with 4% PFA and stained with mAb rat 4E8 (E1B-55K) and pAb rat Alexa™555 (red) as well as mAb mouse M114-3 (SUMO 2/3) and pAb mouse Alexa™488 (green). Cell nuclei were labeled with DAPI (blue). The pictures show the most frequent phenotypes of E1B-55K and SUMO 2, either showing no-colocalization of both proteins (images1-8) or depicting cells in which E1B-55K and SUMO specific signals overlay (images 9-16). **B)** Graphical overview about the quantification of the co-localization of E1B-55K and SUMO 2 in A459 cells. For each virus infection approximately 300 infected cells were counted and the amount of cells in which both proteins co-localize were determined and the respective numbers are indicated in percent.

5 Discussion

5.1 E1B-55K SUMOylation is modulated by E4orf6

Diverse viruses abuse the SUMO conjugation machinery for their own benefit. These include counteracting the immune responses leading to stimulation of viral replication and spread. One way to achieve this, they either change the SUMOylation of cellular proteins or use the SUMO machinery to regulate the functions of their own proteins. As many viral proteins, HAdV-C5 E1B-55K interferes with the cellular SUMO system in a dual way. On the one hand, it manipulates SUMO conjugation to cellular proteins like p53, Sp100A or Kap1. On the other hand, it can be N-terminally SUMOylated at K104 and at K101 [418,449,450,457,460]. Notably, SUMOylation at K104 is crucial for several functions, such as the E3 SUMO ligase activity towards p53, the enhancement of Sp100A SUMOylation, the repression of p53 dependent gene transcription, the E4orf6-independent induction of Daxx degradation, the binding to PML isoform V, its localization to PML NBs and, as a consequence, the transformation of primary baby rat kidney (BRK) cells in cooperation with E1A [418,455,457,463]. Moreover, higher E1B-55K SUMOylation levels correlate with nuclear localization and accumulation in viral RCs [419,461]. Regulation of E1B-55K SUMOylation is achieved via C-terminal phosphorylation or binding to Kap1 [460,461]. Furthermore, its interaction partner E4orf6 was suggested as a further regulating factor of E1B-55K SUMOylation [430]. Both proteins assemble a cul5 based E3 ubiquitin ligase complex, which in turn initiates the degradation of antiviral factors, and induces a shut-off of host cell protein synthesis, as well as the enhanced synthesis of late viral proteins [435,474–478]. As SUMOylation has been shown to augment the functionality of E1B-55K, downregulation of SUMO conjugation to E1B-55K by E4orf6 seems surprising at first. Therefore, we aimed to prove E4orf6 as a negative regulator of E1B-55K in the first part of this work. We investigated the SUMOylation of E1B-55K in infections with virus mutants carrying lysine to arginine exchanges at 101, 104, and 101 plus 104 in presence and absence of E4orf6. In this assay, we demonstrated that E4orf6 reduces the modification of E1B-55K and K101R with SUMO 1 as well as SUMO 2 (4.1.1). Furthermore, we quantified the co-localization events of E1B-55K SUMO mutants with SUMO 2 in presence and absence of E4orf6 in living cells. Here, we found an approximately 20 % increased co-localization of

E1B-55K or K101R and SUMO 2 in the absence of E4orf6 (4.2.5) Thus, both assays confirmed E4orf6 as a negative regulator of E1B-55K SUMOylation.

In previous studies focusing on EBV and Kaposi´s Sarcoma Virus (KSHV) protein regulation, it has been shown that these viruses have evolved the potential to coordinate their protein activities internally via SUMO level manipulation as well. The EBV immediate-early protein BZLF1 (Z) and KSHV basic region-leucine zipper (K-bZIP) act as transcription factors and mediate the switch between latent and lytic EBV and KSHV infections, respectively. This is achieved by repressing the transcription of early viral genes, and consequently, the induction of the lytic replication. Hereby, the transcriptional suppression and the establishment of the latent state is dependent on the SUMOylation of Z and K-bZIP. Intriguingly, SUMOylation is restricted by their viral interaction partners EBV protein kinase (EBV pK) and KSHV protein kinase (KSHV pK), facilitating the reactivation of lytic infections [479–482]. Together with our findings, these observations implicate that SUMO regulation among viral proteins is a common mechanism applied by many DNA tumor viruses to adapt to the environment. However, it has not been demonstrated yet, how EBV pK and KSHV pK regulate the SUMO conjugation to Z and k-bZIP, respectively. Currently, it is under debate whether HAdV can establish latency. Recent studies are rather emphasizing a persistence in lymphoid cells [18,55,483,484]. Therefore, it would be very suspenseful to study whether the regulation of E1B-55K SUMOylation by E4orf6 enables switching between lytic and persistent replication. These future investigations might also have clinical relevance, since HAdV persistence is of concern for allogeneic hematopoietic stem cell transplant recipients, as the reactivation of the virus might result in severe viremia or even death due to the impaired T-cell coordinated immune response of those patients [71,74,485–488]. Furthermore, HAdV are well known to induce sarcomas in rodents and transform pBRK cells in cell culture. Here, it is well established that the transformation of pBRKs is dependent on the presence of E1A and E1B-55K [24,489]. Furthermore, SUMOylation of E1B-55K is a prerequisite for the transformation of pBRKs [418]. However, it is not clear yet, if HAdV persistence is the pre-state of tumorigenesis in humans. So far, most reports demonstrated just the presence of HAdV in diverse human tumors such as lung, brain, liver, lung epithelium, and small-cell lung cancers, but were not able to show a correlation between the presence of HAdV and tumor development [31,269,489–491].

However, latest observations revealed that HAdV oncogenes have the potential to transform human cells. Speiseder *et al*. demonstrated the transformation of hMSCs by HAdV oncogenes E1A and E1B-55K [267]. Additionally, Kindsmüller and colleagues found persisting HAdV inside infiltrating T-lymphocytes derived from sarcoma tissues [268]. Hence, future investigations in newly available systems, such as primary cells, organoid tissue cultures or mouse models, are necessary to better understand the correlation between HAdV persistence, and tumor development in humans, as well as the role of E1B-55K SUMOylation and negative SUMO regulation by E4orf6 in these processes [492].

The main SCS of E1B-55K at K104 has been characterized intensively [418,419]. In addition to this SCS, mass spectrometry analyses from our department suggested a second SCS at K101. So far, however, investigations of E1B-55K mutants failed to prove K101 experimentally as a functional SCS. During the substantiation of E4orf6 as a negative regulator of E1B-55K SUMOylation, we were finally able to verify K101 as an active SCS of E1B-55K. This was achieved by analyzing the SUMOylation of K104R and K101/104R in absence of E4orf6 via Ni-NTA SUMO pulldown analysis (4.1.1). In these experiments, we demonstrated that the K104R mutant was SUMOylated at position K101 in the absence of E4orf6, but not in presence of E4orf6. In contrast, K101/104R was neither conjugated to SUMO in presence nor in absence of E4orf6, indicating that K101 and K104 are the only SCS of E1B-55K (4.1.1). Most probably, previous investigations failed to validate K101 as a SCS because SUMOylation of the K104R mutant was either investigated in transfection experiments, in which K104R localizes mainly in cytoplasmic aggregates, or in infections with E4orf6 expressing viruses [419,455,461]. In transfection experiments, SUMOylation of K104R was presumably prevented by the cytoplasmic retention of K104R, as SUMOylation occurs mainly in the nucleus [286]. In infection studies, SUMOylation at K101 was most likely suppressed by E4orf6, which has been confirmed as SUMOylation repressor in this work. However, even in an E4orf6 negative background SUMOylation of K104R was low and did not result in a significantly enhanced nuclear localization of the mutant, as demonstrated in our IF analysis. In summary, these results validate K104 as the major SCS of E1B-55K (4.2.5).

Taken together, these results substantiate E4orf6 as a negative regulator of E1B-55K SUMOylation. Nevertheless, it is clearly speculative at this point that E1B-55K SUMOylation is involved in the initiation of persistence or tumor development in humans. Furthermore, it has to be determined whether the E4orf6 mediated downregulation of E1B-55K SUMOylation interferes with this process.

5.2 Unraveling the mechanism of E4orf6 to reduce E1B-55K SUMOylation

We investigated potential mechanisms used by E4orf6 to reduce E1B-55Ks SUMOylation. Previously, several HAdV proteins have been identified to possess the potential of regulating SUMO conjugation to promote virus replication, underlining the general importance of the manipulation of the SUMO cycle for an efficient HAdV-C5 replication. To name a few examples besides E1B-55K, which has been already described, E4orf3 augments the SUMOylation of 51 cellular proteins [405]. It even acts as a SUMO ligase and elongase for the transcription factors TIF-1γ, TFI-II, as well as the MRN components Nbs1 and Mre11, respectively. These processes are part of HAdV-C5 countermeasures against the DDR and enhance transcription of late viral genes, controlled by the adenoviral intermediate promoter L4P [407,408]. Furthermore, E4orf3 might control SUMOylation via the sequestration of PIAS 3 to E4orf3/PML track-like structures [409]. Furthermore, proteomic analyses revealed that the overall SUMOylation is increased upon HAdV-C5 infection, at least in part in an E1B-55K and E4orf3 dependent mechanism [409]. In addition, E1A is known to prevent SUMOylation of pRB, and competes with mono-SUMOylated proteins for UBC 9 binding, thereby inhibiting SUMO chain elongations [395,396,493]. These examples show that HAdV proteins frequently usurp the SUMO system to promote an efficient replication via diverse mechanisms. Remarkably, it is a new observation that HAdV proteins regulate each other via their PTMs. As described in 5.1, other DNA tumor viruses use SUMOylation to regulate the activities of their proteins and to switch between latency and lytic replication. However, the utilized mechanisms have seldom been elucidated. Furthermore, most reports identified HAdV-C5 proteins as SUMOylation enhancers [390]. Studying a reductive mechanism will enlighten new capacities of HAdV-C5 to create a replication competent environment and possibly help to establish a new model for virus intern control mechanisms of protein functions. Thus, the SUMO reduction of E1B-55K by E4orf6 has been investigated in this work. To elucidate how E4orf6 reduces the

SUMOylation of E1B-55K, we examined four plausible hypotheses based on current knowledge about the regulation of protein SUMOylation. Here, we considered the different steps of the SUMO cycle, which might be attacked. First, we suggested a general inhibition of the SUMO system, which would affect all SUMO targets. Second, we estimated that E4orf6 enhances the deSUMOylation of E1B-55K. In the third hypothesis, we assumed that E4orf6 inhibits the phosphorylation of E1B-55K, resulting in the indirect regulation of E1B-55K SUMOylation. Lastly, we speculated that E4orf6 blocks the SUMO attachment process through the direct interaction between both viral factors.

5.2.1 E4orf6 reduces specifically the SUMOylation of E1B-55K

In the first hypothesis we asked whether E4orf6 inhibits the SUMO conjugation machinery via the inhibition of the unique E1 or E2 SUMO enzymes, as this mechanism has been found to be applied by diverse viral proteins. For example, GAM 1 of AdV CELO interrupts the SUMOylation system via the proteasomal degradation of SAE 1 and UBC 9. Thereby, GAM 1 promotes general gene transcription [392,494]. Moreover, the oncogenic E6 proteins of human Papillomavirus (HPV) type 16 and 18, which were considered as high risk cervical cancer inducers, have been found to bind UBC 9. As a consequence of this interaction, UBC 9 is degraded by the proteasome and global SUMOylation is downregulated [495]. Interestingly, E6 proteins of low risk HPV types had no effect on UBC 9 and conclusively on SUMOylation, emphasizing a potential link between UBC 9 deprivation and cervical cancer development [495]. To demonstrate whether E4orf6 decreases the E1B-55K SUMOylation specifically or if E4orf6 globally abrogates SUMO conjugation processes via inhibition of E1 or E2 SUMO enzymes, we investigated the SUMO levels of E2A as a representative SUMO target, in presence and absence of E4orf6. E2A was chosen because it has been demonstrated as being highly SUMO modified and it does not interact with E4orf6 [410]. Our studies showed that E2A SUMOylation is not changed by E4orf6 expression, indicating that none of the unique E1 or E2 SUMO enzymes is generally impaired by E4orf6, as an inhibition of these enzymes would also affect E2A (4.2.1). Leading us to the next hypotheses, which focused on E1B-55K specific mechanisms.

5.2.2 E4orf6 reduces the SUMO attachment to E1B-55K and does not enhance the deSUMOylation of E1B-55K by SENPs

As our second hypothesis, we assumed that E4orf6 reduces the SUMO levels of E1B-55K by enhancing deSUMOylation. SUMOylation is constantly reversed by SENPs. Humans express six SENP isoforms, SENP 1, 2, 3, 5, 6, and 7, which remove conjugated SUMO moieties from target proteins [313,319,320]. Notably, HAdV, vaccinia virus, fowlvirus, and african swine fever virus have been shown to encode SENP-resembling cysteine proteases. However, none of them is active against SUMO or SUMOylated proteins [391,412,496,497]. Nevertheless, the potential to regulate deSUMOylation processes seems to be a valuable tool for HAdV to manipulate the SUMO conjugation machinery. Thus, we examined the potential of E4orf6 to recruit cellular SENPs for the depletion of E1B-55K SUMOylation [391]. In previous investigations, it has been observed that ICP0 of HSV 1 binds SENP 1 and co-localizes with the protease in the nucleus. As a consequence, nuclear SUMO 1 levels are reduced and the SUMO 1 conjugation to substrates is prevented [498]. Moreover, latent membrane protein 1 (LMP1) of EBV was shown to inhibit SENP 2 via the induction of SENP 2 SUMOylation. Both studies showed that manipulation of SUMOylation via SENP interactions is advantageous for different DNA tumor viruses. Whereas, this work demonstrated that E4orf6 does not manipulate SENPs to reduce E1B-55K SUMOylation, but rather prevents SUMO attachment to E1B-55K (4.2.2.7). Therefore, E1B-55K modification by the SUMO mutant Q90P was investigated. E1B-55K modification by this mutant is not reversible via SENP cleavage as structural changes preclude the introduction of Q90P into the catalytic pocket of SENPs [290,469,499]. Consequently, we investigated explicit mechanisms which might reduce SUMO attachment to E1B-55K in the next experiments. Nevertheless, we found that SENPs interact with HAdV-C5 proteins, what is discussed in section 5.3, 5.4, and 5.5.

5.2.3 Phosphorylation of E1B-55K does not influence E4orf6 mediated inhibition of SUMOylation

An often observed phenomenon is crosstalk between different PTMs, such as acetylation, ubiquitinylation, or phosphorylation [500]. For example, former reports have shown that phosphorylation of the transcription factors myocyte enhancement factor 2 (MEF2) and heat-shock factor 1 (HSF1) facilitates their SUMO modification by

activation of the SUMO ligase function of UBC 9 [501]. Furthermore, the treatment of cells with CDK inhibitors results in a global downregulation of SUMO conjugation to SUMO substrates which are co-modified by phosphorylation [502]. Remarkably, it has already been shown that the SUMOylation of E1B-55K is dependent on its C-terminal phosphorylation at S490, S491, and S495 [461]. Thus, it might be reasonable that E4orf6 does not directly interfere with SUMO conjugation, but rather abrogates the phosphorylation of E1B-55K to affect its SUMOylation. Accordingly, we formulated our third hypothesis, in which we emphasized that E4orf6 impairs the phosphorylation of E1B-55K, resulting in an indirect negative regulation of E1B-55K SUMOylation. Presumably, E4orf6 inhibits the E1B-55K phosphorylating kinase CK2 or recruits a corresponding, but so far unknown phosphatase. Supporting this idea, earlier studies from our department suggested that E4orf6 binds to the phosphatase PP2A (unpublished data). In general, this phosphatase is known to interact with numerous viral proteins, such as truncated Epstein-Barr nuclear antigen leader protein (EBNA LP) of EBV, small T and middle T antigen of Polyomavirus, non-structural 5A (NS5A) of HCV, or E4orf4 of HAdV-C5, to accomplish viral life cycles [503–508]. To investigate if E4orf6 indirectly prevents SUMOylation via preventing its phosphorylation, we tested the effect of E4orf6 on two E1B-55K phospho-mutants, one constantly mimicking E1B-55K phosphorylation (PM) and a second one which is phosphorylation deficient (delP). This work showed that the SUMOylation of both E1B-55K mutants was decreased by E4orf6, implicating that E4orf6 does not regulate E1B-55K SUMOylation through phosphorylation (4.2.3). Thus, a further plausible interference point during SUMO attachment to e1B-55K was examined in the next part of this work.

5.2.4 Interaction between E1B-55K and E4orf6 is required for the reduction of E1B-55K SUMOylation

Finally, we addressed the question, whether the presence of E4orf6 is sufficient to reduce E1B-55K SUMO conjugation or if the binding between both proteins is required. Therefore, we analyzed the SUMOylation of the E4orf6 binding deficient E1B-55K mutant A143 during infection. In this assay, we found that the significantly reduced binding of A143 to E4orf6 is accompanied by an enhanced SUMO modification (4.2.4.2). Furthermore, the A143 insertion mutation resulted in a 26 % increased

co-localization with SUMO 2 in comparison to E1B-55K-wt (4.2.5). In agreement, these findings display that E4orf6 reduces the SUMOylation of E1B-55K via binding (Fig. 30).

Reduced E1B-55K SUMO levels might be explained by E4orf6 binding induced structural changes of E1B-55K. So far, very little is known about the three-dimensional structure of E1B-55K. Although, circular dichroism, NMR, and *in silico* analyses have suggested that the E1 protein is highly disordered at its N- and C- terminus, comprising the aa residues 1 to 146 and 385 to 496, respectively [509,510]. Additionally, the central part has been predicted to fold into a β-solenoid [509]. The SCSs of E1B-55K and the binding site A143 for E4orf6 are located in the C-terminal intrinsically disordered region (IDR). In general, IDRs are frequently subjected to PTMs. The high flexibility of these areas allows easy access to PTM sites for the catalytic domains of modifying enzymes [511]. Binding another protein can impair the conformational flexibility of IDRs and thereby preventing access to PTM sites for modifying enzymes [511]. Consequently, protein interactions can reduce PTM levels [511]. Probably, the association of E4orf6 with E1B-55K results in a loss of flexibility of the disordered C-terminus of E1B-55K, precluding the binding of E1B-55K to UBC 9 or the corresponding unknown E3 SUMO ligase, respectively. Yet, it seems more likely that E4orf6 blocks the interaction with the corresponding E3 SUMO ligase because the interaction between E1B-55K and UBC 9 has been demonstrated in infections with HAdV-C5-wt. As E1B-55K binds UBC 9 very efficiently in presence of E4orf6, the E4 protein does not seem to abrogate the binding capacity of E1B-55K towards UBC 9 significantly [461]. However, comparative analyses have not been performed so far. Notably, the HCMV protein immediate early 2 (IE2) regulates the SUMOylation of its viral interaction partner IE1 by competing with the corresponding E3 SUMO ligase PIAS1 for binding sites. This interaction occurs at the late stage of infection and results in a potentiation of the IE1 mediated repression of ISG activation [512]. In contrast to E1B-55K and E4orf6 binding, the IE1-IE2 interaction depends on the SUMOylation of IE2, while E4orf6 is not SUMO modified [512]. After identification of the corresponding E3 SUMO ligase for E1B-55K, it will be very interesting to examine whether the assumption that E4orf6 competes with the E3 SUMO ligase for E1B-55K binding is true. Remarkably, proteomic studies revealed more than 70 peptides, interacting with E1B-55K [513]. Probably, an E3 SUMO ligase is among these proteins.

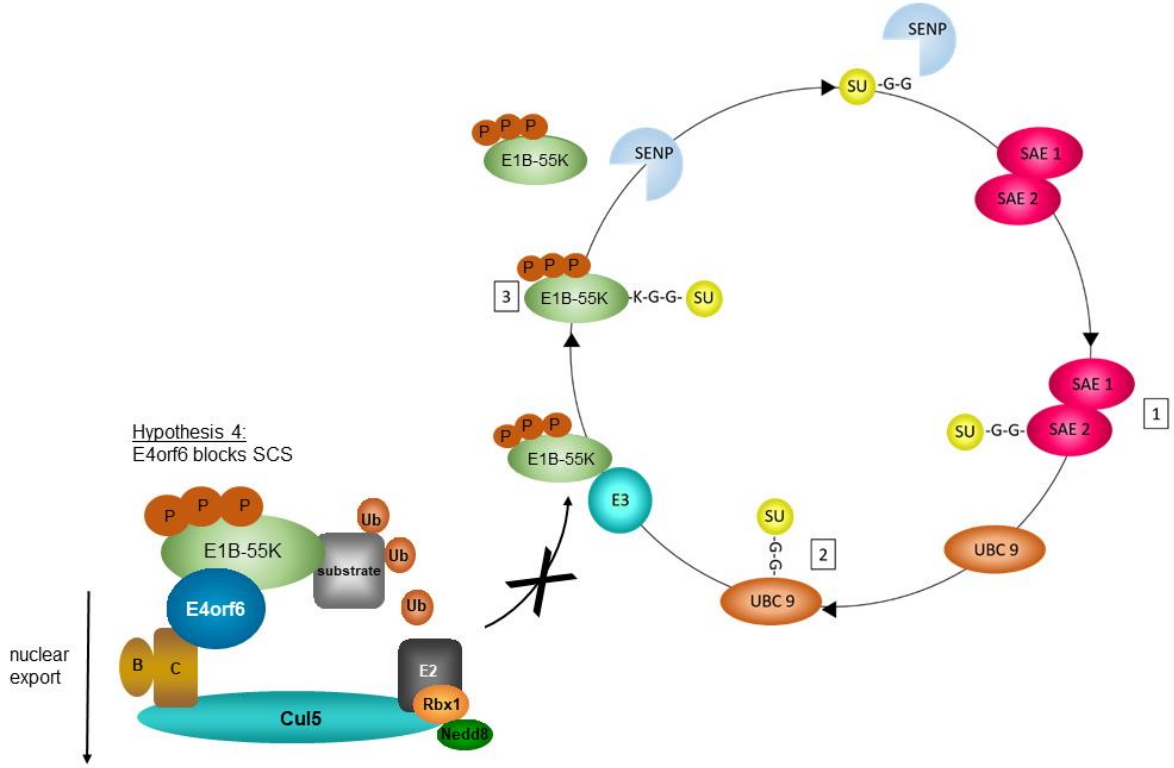

Fig. 30: Illustration of the E4orf6 mediated regulation of HAdV-C5 E1B-55K SUMOylation. E4orf6 decreases the SUMOylation of E1B-55K via interaction. E4orf6 might compete with the corresponding E3 SUMO enzyme for E1B-55K binding sites, presumably to favor the assembly of the viral E3 ubiquitin ligase and enhance the nuclear export of E1B-55K to stimulate late viral protein expression. SU: SUMO, SENP: Sentrin/ SUMO-specific protease, SAE: SUMO activating enzyme, UBC 9: ubiquitin carrier protein 9, P: phosphoryl group, GG: double glycine, K: lysine, Cul5: cullin 5, E2: Ubiquitin conjugating enzyme 2, B/C: elongin B and C, Ub: ubiquitin.

Moreover, our results define the current model about the interplay between E1B-55K activities and its cellular distribution more precisely. Previous studies emphasized the assumption that the complex localization pattern of E1B-55K depends on the time point of infection and is determined by its diverse protein-interactions and PTMs [427,429,432]. In contrast to our findings, this model suggested that E4orf6 is necessary to direct E1B-55K to viral RCs. Here, we showed that the co-localization of E1B-55K with SUMO 2, which accumulates in RCs during infection, is increased in the absence of E4orf6 (4.2.5). So far SUMO dependent properties of E1B-55K have been investigated only in transient transfection and transformation experiments. Thus, the role of SUMOylation during infection can only be included to the model with caution. Potentially, SUMOylation enables E1B-55K to bind PML IV and other SIM containing proteins which retain E1B-55K in the nuclear matrix and viral RCs, respectively. There, it might be especially important for counteracting anti-viral measures of Daxx, Sp100A and p53 [418,450,457,458]. Moreover, proper RC morphology depends on the expression of

E1B-55K, however, whether this function requires co-localization with RCS and SUMOylation of E1B-55K needs to be determined [409]. As soon as it binds E4orf6, transport of E1B-55K to viral RCs is reduced. Furthermore, Leppard and colleagues found that E4orf6 binding leads to detachment of E1B-55K from the nuclear matrix fraction, indicating that E4orf6 regulates E1B-55K localization via SUMOylation [430]. Furthermore, lower SUMOylation might result in a more efficient export of E1B-55K into the cytoplasm where K104 and K101/104R accumulate (4.2.5). An increased export of E1B-55K might facilitate simultaneously the export of late viral mRNAs and inhibition of the cellular mRNA export, processes which are facilitated by E1B-55K and E4orf6. Moreover, it seems conceivable that E4orf6 reduces the SUMOylation of E1B-55K to favor the assembly of the viral E3 ubiquitin ligase, shifting E1B-55K's functionality towards protein degradation. Future investigations, examining the SUMOylation and localization of E1B-55K and A143 over a progressing replication cycle might reveal whether different functions of E1B-55K can be associated with specific time points in infection and if the equilibrium between the functional fractions of E1B-55K shifts in a time-dependent manner and through E4orf6 regulation.

In summary, we validated E4orf6 as a negative regulator of E1B-55K SUMOylation and revealed that the interaction between both proteins causes the reduced SUMO attachment to E1B-55K. In our model, we assumed that SUMO attachment is prevented by a decreased accessibility for the corresponding E3 SUMO ligase to the SCSs of E1B-55K, due to a decreased flexibility of the IDR of E1B-55K. This region harbors both, the E4orf6 binding site as well as the SCSs. Additionally, we suggested that the reduced SUMOylation results in a functional switch, favoring the assembly of the E3 ubiquitin ligase and consequently protein degradation. Furthermore, we assumed that E4orf6 facilitates an enhanced nuclear export of the E1B-55K, which might result in an increased export of viral mRNAs and import of late viral proteins.

5.3 Relocalization of SENP 1 and SENP 2 during infection

The conjugation of SUMO to target proteins affects their activity, intracellular distribution, stability, and interaction with partner proteins. In general, SUMOylation can be triggered by cell cycle progression, differentiation, and stress stimuli such as DNA damage or viral infection [286]. For example, HAdV-C5 infection results in an enhanced

accumulation of SUMO 2 coupled proteins. During viral infection, SUMOylation is regulated on different levels, such as transcription, translation, or inhibition of different SUMO pathway components, such as degradation of E1 to E3 SUMO enzymes. How HAdV-C5 proteins influence cellular SUMOylation has been elucidated only in parts. Latest studies have demonstrated, that either E1B-55K or E4orf3 expression is necessary to increase global protein SUMOylation [409]. In line with this observation, both early proteins possess E3 SUMO ligase activity [403,449,450]. However, the observed changes on cellular and viral protein SUMOylation cannot be completely explained by this function, since E3 SUMO ligases generally have a high target specificity, but during HAdV-C5 infections a huge amount of proteins show an increased SUMO conjugation [514]. Furthermore, Sp100A SUMO conjugation is increased in an E1B-55K-dependent manner, but E1B-55K has not been verified as an E3 SUMO ligase for Sp100A [457]. In conclusion, E1B-55K and E4orf3 have to regulate SUMOylation via further, so far unknown mechanisms. In this work, we demonstrated, that E1B-55K covalently binds to SENP 1 and weakly to SENP 3. Moreover, E4orf3 co-localizes with SENP 1 and SENP 2 in E4orf3/PML tracks during HAdV-C5 infections (4.2.2.2 and 4.2.2.3). E1B-55K and SENP bindings can at least in part be explained by the observation that E1B-55K is targeted by SENP 1 for deSUMOylation as shown in 4.2.2.4 and 4.2.2.5. However, it cannot be excluded that this interaction also causes the inhibition of the SENPs. E4orf3 is not conjugated to SUMO (data not shown). Therefore, co-localization of these proteins must have another purpose than deSUMOylation of E4orf3. One possibility might be the functional inactivation of SENP 1 and SENP 2 via sequestration of the proteases in E4orf3/PML tracks. In previous studies, it has been demonstrated that the association of antiviral proteins with E4orf3/PML tracks is accompanied with their functional inactivation or proteasomal degradation, respectively [400,403,405–407]. Thus, it is conceivable that the E4orf3/PML track association of SENPs results in an impeded SUMO protease activity and conclusively leads to elevated amounts of SUMO modified proteins. Remarkably, a similar observation has been made for the EBV protein LMP 1. This viral regulator enhances the accumulation of SUMO conjugates in the cell, which supports the oncogenic function of LMP 1, enhances viral replication, and helps to counteract innate immune responses by targeting multiple steps of the SUMO cycle. On the one hand, hijacking UBC 9 seems to enhance the SUMOylation of cellular proteins [515]. On the other hand, LMP 1 reduces the ubiquitylation of SENP 2,

consequently altering its localization and inhibiting its activity, and thereby globally depleting cellular deSUMOylation events [515]. It will be very interesting for future investigations, if these interactions contribute to the enhanced SUMO modification of proteins upon HAdV-C5 infections.

A second consequence resulting from the sequestration of SENP 1 and SENP 2 in E4orf3 induced track-like structures might be the facilitation of PML NB dispersal. PML NBs are formed through PML dimerization and the recruitment of PML NB components, what depends on SUMOylation [347,516]. Therefore, two effects are possible. First, SENPs might be inhibited by the sequestration in PML/E4orf 3 tracks, resulting in an increased SUMOylation of PML NB components and more effective retention of antiviral factors. Moreover, an enhanced SUMOylation can also result in the recruitment of the STUbl RNF 4, which binds to SUMO chains of particular proteins and thereby induces their proteasomal degradation [517,518]. Second, the recruitment of active SENPs to facilitate the destabilization of PML NB structures is also possible. PML itself is SUMOylated at K65, K160, and K490, allowing the binding to SIM containing interaction partners [516–520]. Furthermore, PML carries a SIM, enabling the binding to SUMO conjugated proteins [521]. As both, SCSs and SIM, are involved in the recruitment of PML NB components, SUMO has been suggested as PML NB glue [522]. The accumulation of active SENP 1 and SENP 2 might reduce PML and PML NB component SUMOylation, resulting in destroyed SUMO/SIM interactions and thus destabilized PML NB structures. As a result, this reduced interaction potential between PML NB components might facilitate the reorganization of PML NBs into tracks, caused by E4orf3. PML NB reorganization is a common feature of nuclear replicating DNA viruses. One example is ICP0 of HSV 1, the viral protein acts as a STUbl and induces the proteasomal degradation of the PML NB components PML I to VI and Sp100, thereby supporting the dispersal of PML NBs [366,523–526]. Additionally, this viral protein has been shown to relocalize SENP 1 to the nucleus, where both proteins co-localize. As a consequence of this interaction, SUMO 1 levels decrease in the nucleus, and furthermore, the conjugation of SUMO 1 to PML is blocked. However, SENP 1 recruitment and nuclear removal of SUMO 1 are not sufficient to disrupt PML NBs alone, but have been suggested to be involved in PML NB dispersal [498,527–529]. Whether one or both suggestions about the role of SENP relocalization in E4orf3/PML tracks are

valid has to be examined in follow up experiments, for example by investigating the formation of E4orf3/PML tracks upon HAdV-C5 infections of SENP knock out cells. Intriguingly, SENP 6 does not seem to be influenced by HAdV-C5 E4orf3, although this SUMO protease is involved in the regulation of PML NB formation [530]. Furthermore, it is very interesting to speculate why both, SUMO ligases like PIAS 3 and SUMO proteases such as SENP 1 and SENP 2 are targeted by the same adenoviral protein.

An additional feature, resulting from the interaction of E1B-55K or E4orf3 with SENP 1 and SENP 2, respectively, might be the protection of viral RCs. In this work, we demonstrated that SENP 1 and SENP 2 associate partially with E2A-formed RCs (4.2.2.2), presumably thereby inhibiting E2A functions via deSUMOylation, since RC organization and effective progeny production highly depend on the SUMO conjugated E2A [410]. Notably, E1B-55K and E4orf3 have also been identified as important regulators of the RC structure, without elucidating the underlying mechanism [409]. Hence, we speculated that E1B 55K and E4orf3 protect E2A from deSUMOylation by inhibiting and re-localizing SENP 1 and SENP 2, respectively. A reduced SUMOylation of E2A might result in structural changes of RCs, as E2A might associate with RC components via their SIMs and requires SUMO modification for oligomerization, respectively. Moreover, the interaction and relocalization of SENPs might generally influence SUMO/SIM protein interactions contributing to RC organization. Nevertheless, further examinations, as SENP localization studies upon infections with E4orf3 or E1B-55K deficient virus mutants or SENP binding mutants, are necessary to substantiate these assumptions. Moreover, it will be interesting to see how these interactions determine cellular and viral protein SUMOylation and how they affect the organization of viral compartments such as E4orf3/PML tracks and viral RCs. Notably, SENP 1 and SENP 2 are the only SENPs which are active on SUMO 1, potentially indicating the importance for regulating SUMO 1 association to substrates for HAdV-C5 replication.

Taken together, SENPs seem to interfere with HadV-C5 infection. However, it is clearly preliminary to speculate about the functional consequences of these interaction and relocalization processes. Nevertheless, the fact that major HadV-C5 regulatory proteins, such as E2A, E1B-55K, and E4orf3 co-localize or interact with these enzymes during infection highlights the importance of these processes.

5.4 E4orf6 interacts with different SENP isoforms

A further important regulatory protein which has been identified as an interaction partner of SENPs is E4orf6 (4.2.2.1). The best studied function of E4orf6 during HAdV-C5 infection is the formation of a cullin 5/Rbx-1 based E3 ubiquitin ligase, together with E1B-55K. This complex initiates the proteasomal degradation of antiviral PML NB components and the enhancement of late viral protein production [369,435,437–439,441,474,531]. Moreover, the E1B-55K/E4orf6 complex facilitates the selective nuclear export of late viral mRNAs, and enhances the nuclear import of viral proteins via the induction of a shut-off of host cell protein synthesis [442,443,477,532,533]. So far it remains elusive, how the selective export and import processes are managed. Interestingly, SENP 1 and SENP 2 are involved in the organization of nucleoporine homeostasis and functionality of the nuclear pore complex [323–326,534]. In this work, we identified E1B-55K and E4orf6 as interaction partners of SENP 1 (4.2.2.1 and 4.2.2.3). Additionally, E4orf6 was shown to associate with SENP isoforms SENP 1, SENP 2, SENP 3, SENP 6 and SENP 7 (4.2.2.1). Presumably, interactions between the viral proteins and SENP 1 or SENP 2, respectively, might help to manipulate nuclear import and export processes to favor the transport of viral late mRNAs and late viral proteins, by disturbing SENP 1- and SENP 2-mediated NPC organization. Moreover, a potential removal of SENP 1 from the NPC by HAdV proteins, might help to protect the linear HAdV dsDNA genome against the DNA double-strand break repair, as SENP 1 displacement has been shown to inhibit non-homologous end joining (NHEJ) during DNA double-strand break (DSB) repair mechanisms [535].

It has been assumed that only 50 % of expressed E4orf6 associates in the E1B-55K/E4orf6 complex [221,421,536,537]. Therefore, also E1B-55K independent functions seem to be relevant for viral replication. The knowledge about these functions is sparse, however the few known properties are often associated with the manipulation of transcriptional activation or repression. For instance, E4orf6 inhibits pro-apoptotic functions of p53 by preventing the transactivation of p53 dependent genes [186]. Moreover, E4orf6 stabilizes unprocessed viral late RNAs in the nucleus. Thereby it provides correct splicing of viral late transcripts and supports late viral protein production [182,538]. Additionally, the E4 protein interacts with HoxB7 to enhance viral early gene transcription, and supports E1A by activating E2F dependent transcription

[539,540]. Recently, E4orf6 has been shown to downregulate the expression of the deNEDDylase SENP 8, and thereby, increasing the NEDDylation of cullin 5, consequently activating the viral E3 ubiquitin ligase. In contrast to the other SENP family members, this cysteine protease is active on NEDD8, but not on SUMO paralogues [436]. In this thesis, E4orf6 has been identified as a specific interaction partner of the human SENP family members SENP 1, SENP 2, SENP 3, SENP 6 and SENP 7 (4.2.2.1). Still, our findings demonstrate that these interactions do not contribute to the negative effect of E4orf6 on E1B-55K SUMO conjugation (4.2.2.7). Nevertheless, these interactions might be the first hint, leading to a revelation of novel potentials of E4orf6, as SENPs regulate several pathways important for controlling virus replication. These pathways include stress signaling, PML NB assembly, pre-ribosome formation, chromatin remodeling and gene expression, genomic integrity control, inflammatory signaling including adaptive immune responses, downregulation of transcription, and cell cycle progression [318]. As already mentioned, especially transcriptional control mechanisms might be affected, according to the role of E4orf6 as a transcriptional regulator. In general, SUMOylation is associated with transcriptional repression [286]. Therefore, the interaction between E4orf6 and the tested SENPs might contribute to the transcriptional control function of E4orf6. Notably, E4orf6 and SENPs have common targets, such as HOX genes. For example, SENP 3 has been identified as an activator of HOX gene transcription. In a separate investigation, the expression of HoxB7 has been shown to trigger HAdV replication [539]. Additionally, HoxB7 is an interaction partner of E4orf6 [539]. A potential conjunction between these observations could be analyzed in further researches.

Moreover, within this work, we identified E4orf6/7 as an interaction partner of SENP 3 (4.2.2.1). During infection, E4orf6/7 promotes the expression of the E2A transcription unit and other E2F regulated cellular genes [203,541]. Furthermore, E4orf6/7 is known to be conjugated to SUMO at K68 and might be targeted by SENP 3 for deSUMOylation (unpublished data). Indeed, SENP 3 accumulates mainly in nucleoli, but sub fractions associate with chromatin, where the transcriptional activator E4orf6/7 localizes [542].

In summary, these data showed for the first time that E4orf6 interacts with cellular SENPs. Since E4orf6 is not SUMOylated, these interactions have another purpose than

deSUMOylation of E4orf6. Albeit, it is still speculative that these interactions contribute to already known functions of the viral protein, like support of late viral protein production in combination with E1B-55K and transcription mediation or potential new functions, such as protection of the viral genome.

5.5 Interaction between E1B-55K and SENP 1 results in the deSUMOylation of E1B-55K

The enigma of SUMOylation, how the small amount of SUMO conjugating and deconjugating enzymes regulates the modification of thousands of so far identified substrate proteins lasted for many years. Recently, Jentsch and Psakhye were able to postulate an issue solving concept, in which they stated that each conjugating or deconjugating enzyme controls the SUMO modification status of larger protein groups. [318,543,544]. According to this concept, these protein groups are further part of functional networks, which are physically associated in macromolecular complexes, such as the NPC, PML NBs, DNA repair foci, or the nucleolus [543,544].

In this work, we have demonstrated in IP experiments that E1B-55K binds to SENP 1 (4.2.2.3). Furthermore, we have confirmed E1B-55K as a SENP 1 substrate for deSUMOylation in Ni-NTA SUMOylation analyses and transformation assays (4.2.2.4 and 4.2.2.5). These observations are in line with the theory of Jentsch and Psakhye, as SENP 1 also deSUMOylates Kap1, which is an interaction partner of E1B-55K. Similar to E1B-55K, Kap1 and SENP 1 localize to the PML NBs [460]. Distinct SENP family members are known to dynamically localize to nuclear sub-domains and act on co-localizing proteins. Thus, localization has been suggested as an important factor for SENP target specificity. Localization in turn, and consequently, the activity of SENPs, is determined by alternative splicing mechanisms and PTMs. Consequently, these control mechanisms are suggested as key regulators of SENP target specificity [318]. SENP 1 and SENP 2 are enriched at the NPC and in PML NBs in interphase cells, while the nuclear envelope breakdown in mitosis causes a re-localization to the kinetochore [323,325,326,534]. SENP 3 and SENP 5 are prominently in nucleoli. However, subfractions can be found at chromatin or mitochondria [297,329,331–335,545]. SENP 6 and SENP 7 concentrate in the nucleoplasm, where they at least partially reside at chromatin[337,343–345]. Notably, SENP 1 and E1B-55K localize to similar structures, such

as PML NBs, viral RCs, or E4orf3/PML tracks. Additionally, E1B-55K shuttles continuously between nucleus and cytoplasm, therefore it has to pass the NPC, where SENP 1 is known to reside [323,417,534]. Additionally, we and others showed that E1B-55K can be conjugated to SUMO 1, SUMO 2 and SUMO 3 (4.1.1) [418,461]. Therefore, it is reasonable that the viral protein is targeted by a SENP, which is capable of removing all SUMO isoforms. In future, analyses of E1B-55K SUMOylation in a SENP 1 knock out cell line, will help to substantiate E1B-55K as a SENP 1 substrate. Moreover, it will be interesting to see, whether SENP 1 interacts with E1B-55K proteins from other HAdV species and if this interaction correlates with their SUMOylation levels and functionality, as our department focuses also on the analysis of E1B-55K SUMOylation from different HAdV species. Notably, the interaction of SENP 1 and E1B-55K might be also responsible for the reduction of the SUMOylation of Kap1 by E1B-55K. As already described, Kap1 is a binding partner of E1B-55K. This interaction results in decreased SUMO levels of Kap1 and raises E1B-55K SUMO levels. Nevertheless, the underlying mechanism is still elusive [460]. Furthermore, we demonstrated a weak binding between E1B-55K and SENP 3 (4.2.2.3). Presumably, both proteins meet at chromatin, as E1B-55K is directed to p53 dependent promotors by p53 and subfractions of SENP 3 associate with the genome [329,331–335,413,545,546]. As the main proportion of SENP 3 localizes to the nucleoli, this interaction is not very frequent, explaining the weak signals in the Western Blot (4.2.2.3). Here, fluorescence-activated cell sorting-Förster´s resonance energy transfer (FACS-fret) analysis would help to substantiate this interaction [547].

Taken together, our results identified E1B-55K as an interaction partner and SENP 1 target. Together with previous observations, demonstrating the deSUMOylation of Kap1 by SENP 1, our results fit well in the concept of Jentsch and Psakhye that functional clusters are targeted by the same SENP. Furthermore, both proteins localize to similar structures during infection, supporting the assumption that SENP target specificity is determined by co-localization. This further explains the weak interaction between SENP 3 and E1B-55K, since only subfractions of both proteins localize at chromatin.

All in all, these findings clearly show that HAdV-C5 proteins interact with cellular SENPs. The consequences described above are still assumptions and very interesting for future investigations, as the knowledge about consequences of virus protein-SENP interactions is very limited so far. Furthermore, investigating these interactions might help to develop new therapeutics, for instance against virus induced cancer development. Currently, SENP inhibitors are discussed as supplements to chemotherapies and expression levels seem to be biomarkers for tumor progression prognosis [548,549].

6 Literature

1. Rowe, W. P., Huebner, R. J., Gilmore, L. K., Parrott, R. H. & Ward, T. G. Isolation of a Cytopathogenic Agent from Human Adenoids Undergoing Spontaneous Degeneration in Tissue Culture. *Exp. Biol. Med.* **84**, 570–573 (1953).
2. Hillemann, M. R. & Werner, J. H. Recovery of new agent from patients with acute respiratory illness. *Proc. Soc. Exp. Biol. Med.* **85**, 183–188 (1954).
3. Enders, J. F. *et al.* "Adenoviruses": Group name proposed for new respiratory-tract viruses. *Science (80-.).* **124**, 119–120 (1956).
4. Benko, M. Renewed taxonomy of adenoviruses reflects evolutionary relations. Literature review. *Magy. Allatorvosok Lapja* (2004).
5. Davison, A. J., Benko, M. & Harrach, B. Genetic content and evolution of adenoviruses. *Journal of General Virology* (2003) doi:10.1099/vir.0.19497-0.
6. Benkö, M. & Harrach, B. A proposal for a new (third) genus within the family Adenoviridae. *Arch. Virol.* (1998) doi:10.1007/s007050050335.
7. Benkő, M. *et al.* First Molecular Evidence for the Existence of Distinct Fish and Snake Adenoviruses. *J. Virol.* (2002) doi:10.1128/jvi.76.19.10056-10059.2002.
8. Harrach, B., Benko, M. & Both, G. Family Adenoviridae. In virus Taxonomy. *Oxford:Elsevier* (2011) doi:http://dx.doi.org/10.1016/B978-0-12-384684-6.00009-4.
9. Kosulin, K. Intestinal HAdV Infection: Tissue Specificity, Persistence, and Implications for Antiviral Therapy. *Viruses* (2019) doi:10.3390/v11090804.
10. International Committee on Taxonomy of Viruses. *Virus Taxonomy: Classification and Nomenclature of Viruses*. *Ninth Report of the International Committee on Taxonomy of Viruses* (2012). doi:10.1016/B978-0-12-384684-6.00057-4.
11. Bailey, A. & Mautner, V. Phylogenetic relationships among adenovirus serotypes. *Virology* (1994) doi:10.1006/viro.1994.1664.
12. Jones, M. S. *et al.* New Adenovirus Species Found in a Patient Presenting with Gastroenteritis. *J. Virol.* (2007) doi:10.1128/jvi.02650-06.
13. Rosen, L. A hemagglutination-inhibition technique for typing adenoviruses. *Am. J. Epidemiol.* (1960) doi:10.1093/oxfordjournals.aje.a120085.
14. Lion, T. Adenovirus infections in immunocompetent and immunocompromised patients. *Clin. Microbiol. Rev.* (2014) doi:10.1128/CMR.00116-13.
15. Yabe, Y., Trentin, J. J. & Taylor, G. Cancer Induction in Hamsters by Human Type 12 Adenovirus. Effect of Age and of Virus Dose. *Proc. Soc. Exp. Biol. Med.* (1962) doi:10.3181/00379727-111-27786.
16. Berget, S. M., Moore, C. & Sharp, P. A. Spliced segments at the 5' terminus of adenovirus 2 late mRNA. *Proc. Natl. Acad. Sci. U. S. A.* (1977) doi:10.1073/pnas.74.8.3171.
17. Greber, U. F., Arnberg, N., Wadell, G., Benko, M. & Kremer, E. J. Adenoviruses - from pathogens to therapeutics: A report on the 10th International Adenovirus Meeting. *Cell. Microbiol.* (2013) doi:10.1111/cmi.12031.
18. Garnett, C. T., Erdman, D., Xu, W. & Gooding, L. R. Prevalence and Quantitation of Species C Adenovirus DNA in Human Mucosal Lymphocytes. *J. Virol.* (2002) doi:10.1128/jvi.76.21.10608-10616.2002.
19. Al Qurashi, Y. M. A., Guiver, M. & Cooper, R. J. Sequence typing of adenovirus from samples from hematological stem cell transplant recipients. *J. Med. Virol.* (2011) doi:10.1002/jmv.22204.
20. Crystal, R. G. Adenovirus: The first effective in vivo gene delivery vector. *Human*

Gene Therapy (2014) doi:10.1089/hum.2013.2527.
21. Breyer, B. *et al.* Adenoviral Vector-Mediated Gene Transfer for Human Gene Therapy. *Curr. Gene Ther.* (2006) doi:10.2174/1566523013348689.
22. Lee, C. S. *et al.* Adenovirus-mediated gene delivery: Potential applications for gene and cell-based therapies in the new era of personalized medicine. *Genes and Diseases* (2017) doi:10.1016/j.gendis.2017.04.001.
23. Tang, D. C. C., Zhang, J., Toro, H., Shi, Z. & Van Kampen, K. R. Adenovirus as a carrier for the development of influenza virus-free avian influenza vaccines. *Expert Review of Vaccines* (2009) doi:10.1586/erv.09.1.
24. Endter, C. & Dobner, T. Cell transformation by human adenoviruses. *Current Topics in Microbiology and Immunology* (2004) doi:10.1007/978-3-662-05599-1_6.
25. Shaw, A. R. & Suzuki, M. Immunology of Adenoviral Vectors in Cancer Therapy. *Molecular Therapy - Methods and Clinical Development* (2019) doi:10.1016/j.omtm.2019.11.001.
26. Doszpoly, A. *et al.* Partial characterization of a new adenovirus lineage discovered in testudinoid turtles. *Infect. Genet. Evol.* (2013) doi:10.1016/j.meegid.2013.03.049.
27. Hage, E., Liebert, U. G., Bergs, S., Ganzenmueller, T. & Heim, A. Human mastadenovirus type 70: A novel, multiple recombinant species D mastadenovirus isolated from diarrhoeal faeces of a haematopoietic stem cell transplantation recipient. *J. Gen. Virol.* (2015) doi:10.1099/vir.0.000196.
28. Wold, W. S. M. & Ison, M. G. Adenoviruses. in *Fields Virology: Sixth Edition* (2013).
29. Kosulin, K. *et al.* Persistence and reactivation of human adenoviruses in the gastrointestinal tract. *Clin. Microbiol. Infect.* (2016) doi:10.1016/j.cmi.2015.12.013.
30. Sharma, A. *et al.* Regulation of the Coxsackie and adenovirus receptor expression is dependent on cystic fibrosis transmembrane regulator in airway epithelial cells. *Cell. Microbiol.* (2017) doi:10.1111/cmi.12654.
31. Kosulin, K. *et al.* Investigation of Adenovirus Occurrence in Pediatric Tumor Entities. *J. Virol.* (2007) doi:10.1128/jvi.00355-07.
32. Berk, A. J. Adenoviridae. in *Fields Virology: Sixth Edition* (2013). doi:10.1201/9781351071642-21.
33. Hara, J., Okamoto, S., Minekawa, Y., Yamazaki, K. & Kase, T. Survival and disinfection of adenovirus type 19 and enterovirus 70 in ophthalmic practice. *Jpn. J. Ophthalmol.* (1990).
34. Hong, J.-Y. *et al.* Lower Respiratory Tract Infections due to Adenovirus in Hospitalized Korean Children: Epidemiology, Clinical Features, and Prognosis. *Clin. Infect. Dis.* (2001) doi:10.1086/320146.
35. Moura, P. O. *et al.* Molecular epidemiology of human adenovirus isolated from children hospitalized with acute respiratory infection in São Paulo, Brazil. *J. Med. Virol.* (2007) doi:10.1002/jmv.20778.
36. Kajon, A. E. *et al.* Molecular Epidemiology of Adenovirus Type 4 Infections in US Military Recruits in the Postvaccination Era (1997–2003). *J. Infect. Dis.* (2007) doi:10.1086/518442.
37. Chang, S. Y. *et al.* A community-derived outbreak of adenovirus type 3 in children in Taiwan between 2004 and 2005. *J. Med. Virol.* (2008) doi:10.1002/jmv.21045.
38. Shauer, A. *et al.* Acute viral myocarditis: Current concepts in diagnosis and

treatment. *Israel Medical Association Journal* (2013).
39. De Ory, F. *et al.* Viral infections of the central nervous system in Spain: A prospective study. *J. Med. Virol.* (2013) doi:10.1002/jmv.23470.
40. Chhabra, P. *et al.* Etiology of viral gastroenteritis in children. *J. Infect. Dis.* (2013) doi:10.1093/infdis/jit254.
41. Rocholl, C., Gerber, K., Daly, J., Pavia, A. T. & Byington, C. L. Adenoviral infections in children: the impact of rapid diagnosis. *Pediatrics* (2004) doi:10.1016/j.annemergmed.2004.07.442.
42. Mameli, C. & Zuccotti, G. V. The impact of viral infections in children with community-acquired pneumonia. *Current Infectious Disease Reports* (2013) doi:10.1007/s11908-013-0339-z.
43. King, D. *et al.* Adenovirus-associated epidemic keratoconjunctivitis outbreaks - Four States, 2008-2010. *Morb. Mortal. Wkly. Rep.* (2013).
44. Ponterio, E. & Gnessi, L. Adenovirus 36 and obesity: An overview. *Viruses* (2015) doi:10.3390/v7072787.
45. Savón, C. *et al.* A myocarditis outbreak with fatal cases associated with adenovirus subgenera C among children from Havana City in 2005. *J. Clin. Virol.* (2008) doi:10.1016/j.jcv.2008.05.012.
46. Carr, M. J. *et al.* Deaths associated with human adenovirus-14p1 infections, europe, 2009-2010. *Emerg. Infect. Dis.* (2011) doi:10.3201/1708.101760.
47. Potter, R. N., Cantrell, J. A., Mallak, C. T. & Gaydos, J. C. Adenovirusassociated deaths in us military during postvaccination period, 1999-2010. *Emerg. Infect. Dis.* (2012) doi:10.3201/eid1803.111238.
48. Lindemans, C. A., Leen, A. M. & Boelens, J. J. How I treat adenovirus in hematopoietic stem cell transplant recipients. *Blood* (2010) doi:10.1182/blood-2010-04-259291.
49. Wigger, H. J. & Blanc, W. A. Fatal hepatic and bronchial necrosis in adenovirus infection with thymic alymphoplasia. *N. Engl. J. Med.* (1966) doi:10.1056/NEJM196610202751603.
50. Myerowitz, R. L. *et al.* Fatal disseminated adenovirus infection in a renal transplant recipient. *Am. J. Med.* (1975) doi:10.1016/0002-9343(75)90267-3.
51. Kojaoghlanian, T., Flomenberg, P. & Horwitz, M. S. The impact of adenovirus infection on the immunocompromised host. *Reviews in Medical Virology* (2003) doi:10.1002/rmv.386.
52. Green, M., Wold, W. S. M., Mackey, J. K. & Rigden, P. Analysis of human tonsil and cancer DNAs and RNAs for DNA sequences of group C (serotypes 1, 2, 5, and 6) human adenoviruses. *Proc. Natl. Acad. Sci. U. S. A.* (1979) doi:10.1073/pnas.76.12.6606.
53. Garnett, C. T. *et al.* Latent Species C Adenoviruses in Human Tonsil Tissues. *J. Virol.* (2009) doi:10.1128/jvi.02392-08.
54. Adrian, T., Schäfer, G., Cooney, M. K., Fox, J. P. & Wigand, R. Persistent enteral infections with adenovirus types 1 and 2 in infants: No evidence of reinfection. *Epidemiol. Infect.* (1988) doi:10.1017/S0950268800029393.
55. Roy, S. *et al.* Adenoviruses in lymphocytes of the human gastro-intestinal tract. *PLoS One* (2011) doi:10.1371/journal.pone.0024859.
56. Hogg, J. C. Role of latent viral infections in chronic obstructive pulmonary disease and asthma. *American journal of respiratory and critical care medicine* (2001) doi:10.1164/ajrccm.164.supplement_2.2106063.
57. Kuschner, R. A. *et al.* A phase 3, randomized, double-blind, placebo-controlled

study of the safety and efficacy of the live, oral adenovirus type 4 and type 7 vaccine, in U.S. military recruits. *Vaccine* (2013) doi:10.1016/j.vaccine.2013.04.035.

58. Hoke, C. H. & Snyder, C. E. History of the restoration of adenovirus type 4 and type 7 vaccine, live oral (Adenovirus Vaccine) in the context of the Department of Defense acquisition system. *Vaccine* (2013) doi:10.1016/j.vaccine.2012.12.029.
59. Khanal, S., Ghimire, P. & Dhamoon, A. S. The repertoire of adenovirus in human disease: The innocuous to the deadly. *Biomedicines* (2018) doi:10.3390/biomedicines6010030.
60. Morfin, F. *et al.* In vitro susceptibility of adenovirus to antiviral drugs is species-dependent. *Antivir. Ther.* (2005).
61. Ljungman, P. *et al.* Cidofovir for adenovirus infections after allogeneic hematopoietic stem cell transplantation: A survey by the Infectious Diseases Working Party of the European Group for Blood and Marrow Transplantation. *Bone Marrow Transplant.* (2003) doi:10.1038/sj.bmt.1703798.
62. Morfin, F. *et al.* Differential susceptibility of adenovirus clinical isolates to cidofovir and ribavirin is not related to species alone. *Antivir. Ther.* (2009).
63. Hirsch, H. H. *et al.* Fourth European conference on infections in leukaemia (ECIL-4): Guidelines for diagnosis and treatment of human respiratory syncytial virus, parainfluenza virus, metapneumovirus, rhinovirus, and coronavirus. *Clinical Infectious Diseases* (2013) doi:10.1093/cid/cis844.
64. Naesens, L. *et al.* Antiadenovirus activities of several classes of nucleoside and nucleotide analogues. *Antimicrob. Agents Chemother.* (2005) doi:10.1128/AAC.49.3.1010-1016.2005.
65. Hartline, C. B. *et al.* Ether Lipid-Ester Prodrugs of Acyclic Nucleoside Phosphonates: Activity against Adenovirus Replication In Vitro. *J. Infect. Dis.* (2005) doi:10.1086/426831.
66. Paolino, K. *et al.* Eradication of disseminated adenovirus infection in a pediatric hematopoietic stem cell transplantation recipient using the novel antiviral agent CMX001. *J. Clin. Virol.* (2011) doi:10.1016/j.jcv.2010.10.016.
67. Florescu, D. F. *et al.* Safety and Efficacy of CMX001 as Salvage Therapy for Severe Adenovirus Infections in Immunocompromised Patients. *Biol. Blood Marrow Transplant.* (2012) doi:10.1016/j.bbmt.2011.09.007.
68. Feuchtinger, T., Lang, P. & Handgretinger, R. Adenovirus infection after allogeneic stem cell transplantation. *Leukemia and Lymphoma* (2007) doi:10.1080/10428190600881157.
69. Myers, G. D. *et al.* Reconstitution of adenovirus-specific cell-mediated immunity in pediatric patients after hematopoietic stem cell transplantation. *Bone Marrow Transplant.* (2007) doi:10.1038/sj.bmt.1705645.
70. Heemskerk, B. *et al.* Immune Reconstitution and Clearance of Human Adenovirus Viremia in Pediatric Stem-Cell Recipients. *J. Infect. Dis.* (2005) doi:10.1086/427513.
71. Guérin-El Khourouj, V. *et al.* Quantitative and Qualitative CD4 T Cell Immune Responses Related to Adenovirus DNAemia in Hematopoietic Stem Cell Transplantation. *Biol. Blood Marrow Transplant.* (2011) doi:10.1016/j.bbmt.2010.09.010.
72. Zandvliet, M. L. *et al.* Simultaneous isolation of CD8+ and CD4+ T cells specific for multiple viruses for broad antiviral immune reconstitution after allogeneic stem

cell transplantation. *J. Immunother.* (2011) doi:10.1097/CJI.0b013e318213cb90.
73. Feuchtinger, T. *et al.* Detection of adenovirus-specific T cells in children with adenovirus infection after allogeneic stem cell transplantation. *Br. J. Haematol.* (2005) doi:10.1111/j.1365-2141.2004.05331.x.
74. Zandvliet, M. L. *et al.* Combined cd8+ and cd4+ adenovirus hexon-specific T cells associated with viral clearance after stem cell transplantation as treatment for adenovirus infection. *Haematologica* (2010) doi:10.3324/haematol.2010.022947.
75. Leen, A. M. & Rooney, C. M. Adenovirus as an emerging pathogen in immunocompromised patients. *British Journal of Haematology* (2005) doi:10.1111/j.1365-2141.2004.05218.x.
76. Horne, R. W., Brenner, S., Waterson, A. P. & Wildy, P. The icosahedral form of an adenovirus. *Journal of Molecular Biology* (1959) doi:10.1016/S0022-2836(59)80011-5.
77. CASPAR, D. L. & KLUG, A. Physical principles in the construction of regular viruses. *Cold Spring Harb. Symp. Quant. Biol.* (1962) doi:10.1101/SQB.1962.027.001.005.
78. Stewart, P. L., Burnett, R. M., Cyrklaff, M. & Fuller, S. D. Image reconstruction reveals the complex molecular organization of adenovirus. *Cell* (1991) doi:10.1016/0092-8674(91)90578-M.
79. Liu, H. *et al.* Atomic structure of human adenovirus by Cryo-EM reveals interactions among protein networks. *Science (80-.).* (2010) doi:10.1126/science.1187433.
80. Martín, C. S. Latest insights on adenovirus structure and assembly. *Viruses* (2012) doi:10.3390/v4050847.
81. Russell, W. C. Adenoviruses: Update on structure and function. *Journal of General Virology* (2009) doi:10.1099/vir.0.003087-0.
82. Nicklin, S. A., Wu, E., Nemerow, G. R. & Baker, A. H. The influence of adenovirus fiber structure and function on vector development for gene therapy. *Molecular Therapy* (2005) doi:10.1016/j.ymthe.2005.05.008.
83. Van Raaij, M. J., Mitrakl, A., Lavigne, G. & Cusack, S. A triple β-spiral in the adenovirus fibre shaft reveals a new structural motif for a fibrous protein. *Nature* (1999) doi:10.1038/44880.
84. Zhang, Y. & Bergelson, J. M. Adenovirus Receptors. *J. Virol.* (2005) doi:10.1128/jvi.79.19.12125-12131.2005.
85. Stewart, P. L., Fuller, S. D. & Burnett, R. M. Difference imaging of adenovirus: bridging the resolution gap between X-ray crystallography and electron microscopy. *EMBO J.* (1993) doi:10.1002/j.1460-2075.1993.tb05919.x.
86. Saban, S. D., Silvestry, M., Nemerow, G. R. & Stewart, P. L. Visualization of α-Helices in a 6-Ångstrom Resolution Cryoelectron Microscopy Structure of Adenovirus Allows Refinement of Capsid Protein Assignments. *J. Virol.* (2006) doi:10.1128/jvi.01652-06.
87. Reddy, V. S., Natchiar, S. K., Stewart, P. L. & Nemerow, G. R. Crystal structure of human adenovirus at 3.5 Å resolution. *Science (80-.).* (2010) doi:10.1126/science.1187292.
88. Kundhavai Natchiar, S., Venkataraman, S., Mullen, T. M., Nemerow, G. R. & Reddy, V. S. Revised Crystal Structure of Human Adenovirus Reveals the Limits on Protein IX Quasi-Equivalence and on Analyzing Large Macromolecular Complexes. *J. Mol. Biol.* (2018) doi:10.1016/j.jmb.2018.08.011.
89. Reddy, V. S. & Nemerow, G. R. Structures and organization of adenovirus

cement proteins provide insights into the role of capsid maturation in virus entry and infection. *Proc. Natl. Acad. Sci. U. S. A.* (2014) doi:10.1073/pnas.1408462111.

90. Reddy, V. S. & Nemerowb, G. R. Reply to Campos: Revised structures of adenovirus cement proteins represent a consensus model for understanding virus assembly and disassembly. *Proceedings of the National Academy of Sciences of the United States of America* (2014) doi:10.1073/pnas.1417014111.
91. Maizel, J. V., White, D. O. & Scharff, M. D. The polypeptides of adenovirus. II. Soluble proteins, cores, top components and the structure of the virion. *Virology* (1968) doi:10.1016/0042-6822(68)90122-0.
92. Russell, W. C., Laver, W. G. & Sanderson, P. J. Internal components of adenovirus. *Nature* (1968) doi:10.1038/2191127a0.
93. Chatterjee, P. K., Vayda, M. E. & Flint, S. J. Identification of proteins and protein domains that contact DNA within adenovirus nucleoprotein cores by ultraviolet light crosslinking of oligonucleotides 32P-labelled in vivo. *J. Mol. Biol.* (1986) doi:10.1016/0022-2836(86)90477-8.
94. Mangel, W. F. & Martín, C. S. Structure, function and dynamics in adenovirus maturation. *Viruses* (2014) doi:10.3390/v6114536.
95. Benevento, M. *et al.* Adenovirus composition, proteolysis, and disassembly studied by in-depth qualitative and quantitative proteomics. *J. Biol. Chem.* (2014) doi:10.1074/jbc.M113.537498.
96. Ahi, Y. S. & Mittal, S. K. Components of adenovirus genome packaging. *Frontiers in Microbiology* (2016) doi:10.3389/fmicb.2016.01503.
97. Takahashi, E., Cohen, S. L., Tsai, P. K. & Sweeney, J. A. Quantitation of adenovirus type 5 empty capsids. *Anal. Biochem.* (2006) doi:10.1016/j.ab.2005.11.014.
98. Pérez-Berná, A. J. *et al.* Distribution of DNA-condensing protein complexes in the adenovirus core. *Nucleic Acids Res.* (2015) doi:10.1093/nar/gkv187.
99. Ortega-Esteban, A. *et al.* Mechanics of Viral Chromatin Reveals the Pressurization of Human Adenovirus. *ACS Nano* (2015) doi:10.1021/acsnano.5b03417.
100. Vayda, M. E., Rogers, A. E. & Flint, S. J. The structure of nucleoprotein cores released from adenovirions. *Nucleic Acids Res.* (1983) doi:10.1093/nar/11.2.441.
101. Rancourt, C., Keyvani-Amineh, H., Sircar, S., Labrecque, P. & Weber, J. M. Proline 137 is critical for adenovirus protease encapsidation and activation but not enzyme activity. *Virology* (1995) doi:10.1006/viro.1995.1240.
102. Perez-Berna, A. J. *et al.* Processing of the L1 52/55k Protein by the Adenovirus Protease: a New Substrate and New Insights into Virion Maturation. *J. Virol.* (2014) doi:10.1128/jvi.02884-13.
103. Condezo, G. N. *et al.* Structures of Adenovirus Incomplete Particles Clarify Capsid Architecture and Show Maturation Changes of Packaging Protein L1 52/55k. *J. Virol.* (2015) doi:10.1128/jvi.01453-15.
104. Flint, J. Organization of the Adenoviral Genome. in *Adenovirus: Basic Biology to Gene Therapy* (1999).
105. Gräble, M. & Hearing, P. cis and trans requirements for the selective packaging of adenovirus type 5 DNA. *J. Virol.* (1992) doi:10.1128/jvi.66.2.723-731.1992.
106. Hearing, P., Samulski, R. J., Wishart, W. L. & Shenk, T. Identification of a repeated sequence element required for efficient encapsidation of the adenovirus type 5 chromosome. *J. Virol.* (1987) doi:10.1128/jvi.61.8.2555-2558.1987.

107. Weinmann, R., Raskas, H. J. & Roeder, R. G. Role of DNA dependent RNA polymerases II and III in transcription of the adenovirus genome late in productive infection. *Proc. Natl. Acad. Sci. U. S. A.* (1974) doi:10.1073/pnas.71.9.3426.
108. Dolph, P. J., Huang, J. T. & Schneider, R. J. Translation by the adenovirus tripartite leader: elements which determine independence from cap-binding protein complex. *J. Virol.* (1990) doi:10.1128/jvi.64.6.2669-2677.1990.
109. Dolph, P. J., Racaniello, V., Villamarin, A., Palladino, F. & Schneider, R. J. The adenovirus tripartite leader may eliminate the requirement for cap-binding protein complex during translation initiation. *J. Virol.* (1988) doi:10.1128/jvi.62.6.2059-2066.1988.
110. Huang, W. & Flint, S. J. The Tripartite Leader Sequence of Subgroup C Adenovirus Major Late mRNAs Can Increase the Efficiency of mRNA Export. *J. Virol.* (1998) doi:10.1128/jvi.72.1.225-235.1998.
111. Logan, J. & Shenk, T. Adenovirus tripartite leader sequence enhances translation of mRNAs late after infection. *Proc. Natl. Acad. Sci. U. S. A.* (1984) doi:10.1073/pnas.81.12.3655.
112. Täuber, B. & Dobner, T. Adenovirus early E4 genes in viral oncogenesis. *Oncogene* (2001) doi:10.1038/sj/onc/1204914.
113. Dimmock, N. J., Easton, A. J. & Leppard, K. N. *Introduction to Modern Virology*. *The effects of brief mindfulness intervention on acute pain experience: An examination of individual difference* (2015).
114. Hoeben, R. C. & Uil, T. G. Adenovirus DNA replication. *Cold Spring Harb. Perspect. Biol.* (2013) doi:10.1101/cshperspect.a013003.
115. Liu, H., Naismith, J. H. & Hay, R. T. Adenovirus DNA replication. *Current Topics in Microbiology and Immunology* (2003) doi:10.1007/978-1-4684-7935-5_7.
116. Hidalgo, P. & Gonzalez, R. A. Formation of adenovirus DNA replication compartments. *FEBS Lett.* (2019) doi:10.1002/1873-3468.13672.
117. Ryu, W. S. *Molecular Virology of Human Pathogenic Viruses*. *Molecular Virology of Human Pathogenic Viruses* (2016). doi:10.1016/c2013-0-15172-0.
118. Radko, S., Jung, R., Olanubi, O. & Pelka, P. Effects of adenovirus type 5 E1A isoforms on viral replication in arrested human cells. *PLoS One* (2015) doi:10.1371/journal.pone.0140124.
119. Liebermann, H., Mentel, R., Döhner, L., Modrow, S. & Seidel, W. Inhibition of cell adhesion to the virus by synthetic peptides of fiber knob of human adenovirus serotypes 2 and 3 and virus neutralisation by anti-peptide antibodies. *Virus Res.* (1996) doi:10.1016/S0168-1702(96)01369-X.
120. Chow, L. T., Lewis, J. B. & Broker, T. R. RNA transcription and splicing at early and intermediate times after adenovirus-2 infection. *Symp. Quant. Biol.* (1979) doi:10.1101/sqb.1980.044.01.044.
121. Bridge, E. & Pettersson, U. Nuclear organization of replication and gene expression in adenovirus-infected cells. *Current Topics in Microbiology and Immunology* (1995) doi:10.1007/978-3-642-79496-4_7.
122. Kremer, E. J. & Nemerow, G. R. Adenovirus Tales: From the Cell Surface to the Nuclear Pore Complex. *PLoS Pathogens* (2015) doi:10.1371/journal.ppat.1004821.
123. Roelvink, P. W. *et al.* The Coxsackievirus-Adenovirus Receptor Protein Can Function as a Cellular Attachment Protein for Adenovirus Serotypes from Subgroups A, C, D, E, and F. *J. Virol.* (1998) doi:10.1128/jvi.72.10.7909-7915.1998.

124. Cohen, C. J. *et al.* The coxsackievirus and adenovirus receptor is a transmembrane component of the tight junction. *Proc. Natl. Acad. Sci. U. S. A.* (2001) doi:10.1073/pnas.261452898.
125. Roelvink, P. W., Lee, G. M., Einfeld, D. A., Kovesdi, I. & Wickham, T. J. Identification of a conserved receptor-binding site on the fiber proteins of CAR-recognizing adenoviridae. *Science (80-.).* (1999) doi:10.1126/science.286.5444.1568.
126. Arnberg, N. Adenovirus receptors: Implications for targeting of viral vectors. *Trends in Pharmacological Sciences* (2012) doi:10.1016/j.tips.2012.04.005.
127. Bremner, K. H. *et al.* Adenovirus Transport via Direct Interaction of Cytoplasmic Dynein with the Viral Capsid Hexon Subunit. *Cell Host Microbe* (2009) doi:10.1016/j.chom.2009.11.006.
128. Leopold, P. L. *et al.* Dynein- and microtubule-mediated translocation of adenovirus serotype 5 occurs after endosomal lysis. *Hum. Gene Ther.* (2000) doi:10.1089/10430340050016238.
129. Wiethoff, C. M., Wodrich, H., Gerace, L. & Nemerow, G. R. Adenovirus Protein VI Mediates Membrane Disruption following Capsid Disassembly. *J. Virol.* (2005) doi:10.1128/jvi.79.4.1992-2000.2005.
130. Kelkar, S. *et al.* A Common Mechanism for Cytoplasmic Dynein-Dependent Microtubule Binding Shared among Adeno-Associated Virus and Adenovirus Serotypes. *J. Virol.* (2006) doi:10.1128/jvi.00481-06.
131. Strunze, S. *et al.* Kinesin-1-mediated capsid disassembly and disruption of the nuclear pore complex promote virus infection. *Cell Host Microbe* (2011) doi:10.1016/j.chom.2011.08.010.
132. Karen, K. A. & Hearing, P. Adenovirus Core Protein VII Protects the Viral Genome from a DNA Damage Response at Early Times after Infection. *J. Virol.* (2011) doi:10.1128/jvi.02540-10.
133. Berk, A. J., Lee, F., Harrison, T., Williams, J. & Sharp, P. A. Pre-early adenovirus 5 gene product regulates synthesis of early viral messenger RNAs. *Cell* (1979) doi:10.1016/0092-8674(79)90333-7.
134. Jones, N. & Shenk, T. An adenovirus type 5 early gene function regulates expression of other early viral genes. *Proc. Natl. Acad. Sci. U. S. A.* (1979) doi:10.1073/pnas.76.8.3665.
135. Berk, A. J. & Sharp, P. A. Structure of the adenovirus 2 early mRNAs. *Cell* (1978) doi:10.1016/0092-8674(78)90252-0.
136. Shaw, A. R. & Ziff, E. B. Transcripts from the adenovirus-2 major late promoter yield a single early family of 3′ coterminal mRNAs and five late families. *Cell* (1980) doi:10.1016/0092-8674(80)90568-1.
137. Miller, M. S. *et al.* Characterization of the 55-Residue Protein Encoded by the 9S E1A mRNA of Species C Adenovirus. *J. Virol.* (2012) doi:10.1128/jvi.06399-11.
138. Stephens, C. & Harlow, E. Differential splicing yields novel adenovirus 5 E1A mRNAs that encode 30 kd and 35 kd proteins. *EMBO J.* (1987) doi:10.1002/j.1460-2075.1987.tb02467.x.
139. Ulfendahl, P. J. *et al.* A novel adenovirus-2 E1A mRNA encoding a protein with transcription activation properties. *EMBO J.* (1987) doi:10.1002/j.1460-2075.1987.tb02468.x.
140. Nevins, J. R. & Wilson, M. C. Regulation of adenovirus-2 gene expression at the level of transcriptional termination and RNA processing. *Nature* (1981) doi:10.1038/290113a0.

141. Ferrari, R. *et al.* Adenovirus small E1A employs the lysine acetylases p300/CBP and tumor suppressor RB to repress select host genes and promote productive virus infection. *Cell Host Microbe* (2014) doi:10.1016/j.chom.2014.10.004.
142. Ferrari, R. *et al.* Epigenetic reprogramming by adenovirus e1a. *Science (80-.).* (2008) doi:10.1126/science.1155546.
143. Pelka, P., Ablack, J. N. G., Fonseca, G. J., Yousef, A. F. & Mymryk, J. S. Intrinsic Structural Disorder in Adenovirus E1A: a Viral Molecular Hub Linking Multiple Diverse Processes. *J. Virol.* (2008) doi:10.1128/jvi.00104-08.
144. Liu, F. & Green, M. R. A specific member of the ATF transcription factor family can mediate transcription activation by the adenovirus E1a protein. *Cell* (1990) doi:10.1016/0092-8674(90)90686-9.
145. Liu, F. & Green, M. R. Promoter targeting by adenovirus E1a through interaction with different cellular DNA-binding domains. *Nature* (1994) doi:10.1038/368520a0.
146. Pelka, P. *et al.* Adenovirus E1A Directly Targets the E2F/DP-1 Complex. *J. Virol.* (2011) doi:10.1128/jvi.00539-11.
147. Horwitz, G. A. *et al.* Adenovirus small e1a alters global patterns of histone modification. *Science (80-.).* (2008) doi:10.1126/science.1155544.
148. Ferrari, R. *et al.* Reorganization of the host epigenome by a viral oncogene. *Genome Res.* (2012) doi:10.1101/gr.132308.111.
149. Whyte, P. *et al.* Association between an oncogene and an anti-oncogene: the adenovirus E1A proteins bind to the retinoblastoma gene product. *Nature* (1988) doi:10.1038/334124a0.
150. Sha, J., Ghosh, M. K., Zhang, K. & Harter, M. L. E1A Interacts with Two Opposing Transcriptional Pathways To Induce Quiescent Cells into S Phase. *J. Virol.* (2010) doi:10.1128/jvi.02131-09.
151. Ferreon, J. C., Martinez-Yamout, M. A., Dyson, H. J. & Wright, P. E. Structural basis for subversion of cellular control mechanisms by the adenoviral E1A oncoprotein. *Proc. Natl. Acad. Sci. U. S. A.* (2009) doi:10.1073/pnas.0906770106.
152. Wang, H. G., Moran, E. & Yaciuk, P. E1A promotes association between p300 and pRB in multimeric complexes required for normal biological activity. *J. Virol.* (1995) doi:10.1128/jvi.69.12.7917-7924.1995.
153. Reich, N., Pine, R., Levy, D. & Darnell, J. E. Transcription of interferon-stimulated genes is induced by adenovirus particles but is suppressed by E1A gene products. *J. Virol.* (1988) doi:10.1128/jvi.62.1.114-119.1988.
154. Pötzer, B. M., Stiewe, T., Parssanedjad, K., Rega, S. & Esche, H. E1A is sufficient by itself to induce apoptosis independent of p53 and other adenoviral gene products. *Cell Death Differ.* (2000) doi:10.1038/sj.cdd.4400618.
155. Lowe, S. W. & Earl Ruley, H. Stabilization of the p53 tumor suppressor is induced by adeno virus 5 E1A and accompanies apoptosis. *Genes Dev.* (1993) doi:10.1101/gad.7.4.535.
156. Li, Z. *et al.* Adenoviral E1A targets Mdm4 to stabilize tumor suppressor p53. *Cancer Res.* (2004) doi:10.1158/0008-5472.CAN-04-2419.
157. Cuconati, A., Degenhardt, K., Sundararajan, R., Anschel, A. & White, E. Bak and Bax Function To Limit Adenovirus Replication through Apoptosis Induction. *J. Virol.* (2002) doi:10.1128/jvi.76.9.4547-4558.2002.
158. Chiou, S. K., Tseng, C. C., Rao, L. & White, E. Functional complementation of the adenovirus E1B 19-kilodalton protein with Bcl-2 in the inhibition of apoptosis

in infected cells. *J. Virol.* (1994) doi:10.1128/jvi.68.10.6553-6566.1994.
159. Chang, L. S. & Shenk, T. The adenovirus DNA-binding protein stimulates the rate of transcription directed by adenovirus and adeno-associated virus promoters. *J. Virol.* (1990) doi:10.1128/jvi.64.5.2103-2109.1990.
160. Cleghon, V., Voelkerding, K., Morin, N., Delsert, C. & Klessig, D. F. Isolation and characterization of a viable adenovirus mutant defective in nuclear transport of the DNA-binding protein. *J. Virol.* (1989) doi:10.1128/jvi.63.5.2289-2299.1989.
161. Ginsberg, H. S., Ensinger, M. J., Kauffman, R. S., Mayer, A. J. & Lundholm, U. Cell transformation: a study of regulation with types 5 and 12 adenovirus temperature sensitive mutants. *Symp. Quant. Biol.* (1974) doi:10.1101/sqb.1974.039.01.054.
162. Nicolas, J. C., Sarnow, P., Girard, M. & Levine, A. J. Host range temperature-conditional mutants in the adenovirus DNA binding protein are defective in the assembly of infectious virus. *Virology* (1983) doi:10.1016/0042-6822(83)90474-9.
163. Zijderveld, D. C. & van der Vliet, P. C. Helix-destabilizing properties of the adenovirus DNA-binding protein. *J. Virol.* (1994) doi:10.1128/jvi.68.2.1158-1164.1994.
164. Binger, M. H., Flint, S. J. & Rekosh, D. M. Expression of the gene encoding the adenovirus DNA terminal protein precursor in productively infected and transformed cells. *J. Virol.* (1982) doi:10.1128/jvi.42.2.488-501.1982.
165. Burgert, H. G. & Kvist, S. An adenovirus type 2 glycoprotein blocks cell surface expression of human histocompatibility class I antigens. *Cell* (1985) doi:10.1016/S0092-8674(85)80079-9.
166. McSharry, B. P. *et al.* Adenovirus E3/19K Promotes Evasion of NK Cell Recognition by Intracellular Sequestration of the NKG2D Ligands Major Histocompatibility Complex Class I Chain-Related Proteins A and B. *J. Virol.* (2008) doi:10.1128/jvi.02251-07.
167. Gooding, L. R., Elmore, L. W., Tollefson, A. E., Brady, H. A. & Wold, W. S. M. A 14,700 MW protein from the E3 region of adenovirus inhibits cytolysis by tumor necrosis factor. *Cell* (1988) doi:10.1016/0092-8674(88)90154-7.
168. Schneider-Brachert, W. *et al.* Inhibition of TNF receptor 1 internalization by adenovirus 14.7K as a novel immune escape mechanism. *J. Clin. Invest.* (2006) doi:10.1172/JCI23771.
169. Lichtenstein, D. L., Toth, K., Doronin, K., Tollefson, A. E. & Wold, W. S. M. Functions and mechanisms of action of the adenovirus E3 proteins. *International Reviews of Immunology* (2004) doi:10.1080/08830180490265556.
170. Li, Y. *et al.* Identification of a cell protein (FIP-3) as a modulator of NF-κB activity and as a target of an adenovirus inhibitor of tumor necrosis factor α-induced apoptosis. *Proc. Natl. Acad. Sci. U. S. A.* (1999) doi:10.1073/pnas.96.3.1042.
171. Tollefson, A. E. *et al.* The adenovirus death protein (E3-11.6K) is required at very late stages of infection for efficient cell lysis and release of adenovirus from infected cells. *J. Virol.* (1996) doi:10.1128/jvi.70.4.2296-2306.1996.
172. Javier, R. T. Adenovirus type 9 E4 open reading frame 1 encodes a transforming protein required for the production of mammary tumors in rats. *J. Virol.* (1994) doi:10.1128/jvi.68.6.3917-3924.1994.
173. Evans, J. D. & Hearing, P. Distinct Roles of the Adenovirus E4 ORF3 Protein in Viral DNA Replication and Inhibition of Genome Concatenation. *J. Virol.* (2003) doi:10.1128/jvi.77.9.5295-5304.2003.

174. Huang, M. M. & Hearing, P. The adenovirus early region 4 open reading frame 6/7 protein regulates the DNA binding activity of the cellular transcription factor, E2F, through a direct complex. *Genes Dev.* (1989) doi:10.1101/gad.3.11.1699.
175. Bridge, E. & Ketner, G. Redundant control of adenovirus late gene expression by early region 4. *J. Virol.* (1989) doi:10.1128/jvi.63.2.631-638.1989.
176. Weitzman, M. D. & Ornelles, D. A. Inactivating intracellular antiviral responses during adenovirus infection. *Oncogene* (2005) doi:10.1038/sj.onc.1209063.
177. Täuber, B. & Dobner, T. Molecular regulation and biological function of adenovirus early genes: The E4 ORFs. *Gene* (2001) doi:10.1016/S0378-1119(01)00722-3.
178. Shepard, R. N. & Ornelles, D. A. Diverse Roles for E4orf3 at Late Times of Infection Revealed in an E1B 55-Kilodalton Protein Mutant Background. *J. Virol.* (2004) doi:10.1128/jvi.78.18.9924-9935.2004.
179. Sarnow, P., Hearing, P., Anderson, C. W., Reich, N. & Levine, A. J. Identification and characterization of an immunologically conserved adenovirus early region 11,000 Mr protein and its association with the nuclear matrix. *J. Mol. Biol.* (1982) doi:10.1016/0022-2836(82)90389-8.
180. Huang, M. M. & Hearing, P. Adenovirus early region 4 encodes two gene products with redundant effects in lytic infection. *J. Virol.* (1989) doi:10.1128/jvi.63.6.2605-2615.1989.
181. Nordqvist, K. & Akusjarvi, G. Adenovirus early region 4 stimulates mRNA accumulation via 5' introns. *Proc. Natl. Acad. Sci. U. S. A.* (1990) doi:10.1073/pnas.87.24.9543.
182. Nordqvist, K., Ohman, K. & Akusjärvi, G. Human adenovirus encodes two proteins which have opposite effects on accumulation of alternatively spliced mRNAs. *Mol. Cell. Biol.* (1994) doi:10.1128/mcb.14.1.437.
183. Carvalho, T. *et al.* Targeting of adenovirus E1A and E4-ORF3 proteins to nuclear matrix-associated PML bodies. *J. Cell Biol.* (1995) doi:10.1083/jcb.131.1.45.
184. Doucas, V. *et al.* Adenovirus replication is coupled with the dynamic properties of the PML nuclear structure. *Genes Dev.* (1996) doi:10.1101/gad.10.2.196.
185. Soria, C., Estermann, F. E., Espantman, K. C. & Oshea, C. C. Heterochromatin silencing of p53 target genes by a small viral protein. *Nature* (2010) doi:10.1038/nature09307.
186. Dobner, T., Horikoshi, N., Rubenwolf, S. & Shenk, T. Blockage by adenovirus E4orf6 of transcriptional activation by the p53 tumor suppressor. *Science (80-.).* (1996) doi:10.1126/science.272.5267.1470.
187. Higashino, F., Pipas, J. M. & Shenk, T. Adenovirus E4orf6 oncoprotein modulates the function of the p53-related protein, p73. *Proc. Natl. Acad. Sci. U. S. A.* (1998) doi:10.1073/pnas.95.26.15683.
188. Müller, U., Kleinberger, T. & Shenk, T. Adenovirus E4orf4 protein reduces phosphorylation of c-Fos and E1A proteins while simultaneously reducing the level of AP-1. *J. Virol.* (1992) doi:10.1128/jvi.66.10.5867-5878.1992.
189. Bondesson, M., Ohman, K., Manervik, M., Fan, S. & Akusjärvi, G. Adenovirus E4 open reading frame 4 protein autoregulates E4 transcription by inhibiting E1A transactivation of the E4 promoter. *J. Virol.* (1996) doi:10.1128/jvi.70.6.3844-3851.1996.
190. Kanopka, A., Muhlemann, O. & Akusjarvi, G. Inhibition by SR proteins splicing of a regulated adenovirus pre-mRNA. *Nature* (1996) doi:10.1038/381535a0.
191. Nilsson, C. E. *et al.* The adenovirus E4-ORF4 splicing enhancer protein interacts

with a subset of phosphorylated SR proteins. *EMBO J.* (2001) doi:10.1093/emboj/20.4.864.
192. Mui, M. Z. *et al.* Identification of the Adenovirus E4orf4 Protein Binding Site on the B55α and Cdc55 Regulatory Subunits of PP2A: Implications for PP2A Function, Tumor Cell Killing and Viral Replication. *PLoS Pathog.* (2013) doi:10.1371/journal.ppat.1003742.
193. Wersto, R. P., Rosenthal, E. R., Seth, P. K., Eissa, N. T. & Donahue, R. E. Recombinant, Replication-Defective Adenovirus Gene Transfer Vectors Induce Cell Cycle Dysregulation and Inappropriate Expression of Cyclin Proteins. *J. Virol.* (1998) doi:10.1128/jvi.72.12.9491-9502.1998.
194. Nebenzahl-Sharon, K. *et al.* Biphasic Functional Interaction between the Adenovirus E4orf4 Protein and DNA-PK. *J. Virol.* (2019) doi:10.1128/jvi.01365-18.
195. Brestovitsky, A., Nebenzahl-Sharon, K., Kechker, P., Sharf, R. & Kleinberger, T. The Adenovirus E4orf4 Protein Provides a Novel Mechanism for Inhibition of the DNA Damage Response. *PLoS Pathog.* (2016) doi:10.1371/journal.ppat.1005420.
196. Nebenzahl-Sharon, K. *et al.* An Interaction with PARP-1 and Inhibition of Parylation Contribute to Attenuation of DNA Damage Signaling by the Adenovirus E4orf4 Protein. *J. Virol.* (2019) doi:10.1128/jvi.02253-18.
197. Gautam, D. & Bridge, E. The Kinase Activity of Ataxia-Telangiectasia Mutated Interferes with Adenovirus E4 Mutant DNA Replication. *J. Virol.* (2013) doi:10.1128/jvi.00376-13.
198. Livne, A., Shtrichman, R. & Kleinberger, T. Caspase Activation by Adenovirus E4orf4 Protein Is Cell Line Specific and Is Mediated by the Death Receptor Pathway. *J. Virol.* (2001) doi:10.1128/jvi.75.2.789-798.2001.
199. Robert, A. *et al.* Distinct cell death pathways triggered by the adenovirus early region 4 ORF 4 protein. *J. Cell Biol.* (2002) doi:10.1083/jcb.200201106.
200. Li, S. *et al.* The adenovirus E4orf4 protein induces growth arrest and mitotic catastrophe in H1299 human lung carcinoma cells. *Oncogene* (2009) doi:10.1038/onc.2008.393.
201. Kleinberger, T. Biology of the adenovirus E4orf4 protein: from virus infection to cancer cell death. *FEBS Letters* (2019) doi:10.1002/1873-3468.13704.
202. Marton, M. J., Baim, S. B., Ornelles, D. A. & Shenk, T. The adenovirus E4 17-kilodalton protein complexes with the cellular transcription factor E2F, altering its DNA-binding properties and stimulating E1A-independent accumulation of E2 mRNA. *J. Virol.* (1990) doi:10.1128/jvi.64.5.2345-2359.1990.
203. Obert, S., O'Connor, R. J., Schmid, S. & Hearing, P. The adenovirus E4-6/7 protein transactivates the E2 promoter by inducing dimerization of a heteromeric E2F complex. *Mol. Cell. Biol.* (1994) doi:10.1128/mcb.14.2.1333.
204. Raychaudhuri, P., Bagchi, S., Neill, S. D. & Nevins, J. R. Activation of the E2F transcription factor in adenovirus-infected cells involves E1A-dependent stimulation of DNA-binding activity and induction of cooperative binding mediated by an E4 gene product. *J. Virol.* (1990) doi:10.1128/jvi.64.6.2702-2710.1990.
205. Ma, Y. & Mathews, M. B. Structure, function, and evolution of adenovirus-associated RNA: a phylogenetic approach. *J. Virol.* (1996) doi:10.1128/jvi.70.8.5083-5099.1996.
206. Kidd, A. H., Garwicz, D. & Öberg, M. Human and simian adenoviruses: Phylogenetic inferences from analysis of VA RNA genes. *Virology* (1995)

doi:10.1006/viro.1995.1049.
207. Carnero, E., Sutherland, J. D. & Fortes, P. Adenovirus and miRNAs. *Biochimica et Biophysica Acta - Gene Regulatory Mechanisms* (2011) doi:10.1016/j.bbagrm.2011.05.004.
208. Aparicio, O. *et al.* Adenovirus VA RNA-derived miRNAs target cellular genes involved in cell growth, gene expression and DNA repair. *Nucleic Acids Res.* (2009) doi:10.1093/nar/gkp1028.
209. Ziff, E. B. & Evans, R. M. Coincidence of the promoter and capped 5′ terminus of RNA from the adenovirus 2 major late transcription unit. *Cell* (1978) doi:10.1016/0092-8674(78)90070-3.
210. Farley, D. C., Brown, J. L. & Leppard, K. N. Activation of the Early-Late Switch in Adenovirus Type 5 Major Late Transcription Unit Expression by L4 Gene Products. *J. Virol.* (2004) doi:10.1128/jvi.78.4.1782-1791.2004.
211. Lutz, P., Rosa-Calatrava, M. & Kedinger, C. The product of the adenovirus intermediate gene IX is a transcriptional activator. *J. Virol.* (1997) doi:10.1128/jvi.71.7.5102-5109.1997.
212. Ostapchuk, P., Anderson, M. E., Chandrasekhar, S. & Hearing, P. The L4 22-Kilodalton Protein Plays a Role in Packaging of the Adenovirus Genome. *J. Virol.* (2006) doi:10.1128/jvi.00123-06.
213. Ali, H., LeRoy, G., Bridge, G. & Flint, S. J. The Adenovirus L4 33-Kilodalton Protein Binds to Intragenic Sequences of the Major Late Promoter Required for Late Phase-Specific Stimulation of Transcription. *J. Virol.* (2007) doi:10.1128/jvi.01584-06.
214. Backström, E., Kaufmann, K. B., Lan, X. & Akusjärvi, G. Adenovirus L4-22K stimulates major late transcription by a mechanism requiring the intragenic late-specific transcription factor-binding site. *Virus Res.* (2010) doi:10.1016/j.virusres.2010.05.013.
215. Iftode, C. & Flint, S. J. Viral DNA synthesis-dependent titration of a cellular repressor activates transcription of the human adenovirus type 2 IVa2 gene. *Proc. Natl. Acad. Sci. U. S. A.* (2004) doi:10.1073/pnas.0407786101.
216. Huang, W., Kiefer, J., Whalen, D. & Flint, S. J. DNA synthesis-dependent relief of repression of transcription from the adenovirus type 2 IVa2 promoter by a cellular protein. *Virology* (2003) doi:10.1016/S0042-6822(03)00431-8.
217. Morris, S. J., Scott, G. E. & Leppard, K. N. Adenovirus Late-Phase Infection Is Controlled by a Novel L4 Promoter. *J. Virol.* (2010) doi:10.1128/jvi.00107-10.
218. Wright, J. & Leppard, K. N. The Human Adenovirus 5 L4 Promoter Is Activated by Cellular Stress Response Protein p53. *J. Virol.* (2013) doi:10.1128/jvi.01924-13.
219. Törmänen, H., Backström, E., Carlsson, A. & Akusjärvi, G. L4-33K, an adenovirus-encoded alternative RNA splicing factor. *J. Biol. Chem.* (2006) doi:10.1074/jbc.M607601200.
220. Morris, S. J. & Leppard, K. N. Adenovirus Serotype 5 L4-22K and L4-33K Proteins Have Distinct Functions in Regulating Late Gene Expression. *J. Virol.* (2009) doi:10.1128/jvi.02455-08.
221. Ornelles, D. A. & Shenk, T. Localization of the adenovirus early region 1B 55-kilodalton protein during lytic infection: association with nuclear viral inclusions requires the early region 4 34-kilodalton protein. *J. Virol.* (1991) doi:10.1128/jvi.65.1.424-429.1991.
222. Yueh, A. & Schneider, R. J. Selective translation initiation by ribosome jumping

in adenovirus- infected and heat-shocked cells. *Genes Dev.* (1996) doi:10.1101/gad.10.12.1557.
223. Yueh, A. & Schneider, R. J. Translation by ribosome shunting on adenovirus and hsp70 mRNAs facilitated by complementarity to 18S rRNA. *Genes Dev.* (2000) doi:10.1101/gad.14.4.414.
224. Andrade, F. *et al.* Adenovirus L4-100K assembly protein is a Granzyme B substrate that potently inhibits Granzyme B-mediated cell death. *Immunity* (2001) doi:10.1016/S1074-7613(01)00149-2.
225. Condezo, G. N. & San Martín, C. Localization of adenovirus morphogenesis players, together with visualization of assembly intermediates and failed products, favor a model where assembly and packaging occur concurrently at the periphery of the replication center. *PLoS Pathog.* (2017) doi:10.1371/journal.ppat.1006320.
226. Zhang, W. & Imperiale, M. J. Requirement of the Adenovirus IVa2 Protein for Virus Assembly. *J. Virol.* (2003) doi:10.1128/jvi.77.6.3586-3594.2003.
227. Sundquist, B., Everitt, E., Philipson, L. & Hoglund, S. Assembly of Adenoviruses. *J. Virol.* (1973) doi:10.1128/jvi.11.3.449-459.1973.
228. D'Halluin, J. C., Martin, G. R., Torpier, G. & Boulanger, P. A. Adenovirus type 2 assembly analyzed by reversible cross-linking of labile intermediates. *J. Virol.* (1978) doi:10.1128/jvi.26.2.357-363.1978.
229. Horwitz, M. S., Scharff, M. D. & Maizel, J. V. Synthesis and assembly of adenovirus 2. I. Polypeptide synthesis, assembly of capsomeres, and morphogenesis of the virion. *Virology* (1969) doi:10.1016/0042-6822(69)90006-3.
230. Ishibashi, M. & Maizel, J. V. The polypeptides of adenovirus. V. Young virions, structural intermediate between top components and aged virions. *Virology* (1974) doi:10.1016/0042-6822(74)90181-0.
231. Khittoo, G. & Weber, J. Genetic analysis of adenovirus type 2 VI. A temperature-sensitive mutant defective for DNA encapsidation. *Virology* (1977) doi:10.1016/0042-6822(77)90064-2.
232. Cepko, C. L. & Sharp, P. A. Assembly of adenovirus major capsid protein is mediated by a nonvirion protein. *Cell* (1982) doi:10.1016/0092-8674(82)90134-9.
233. Hong, S. S. *et al.* The 100K-chaperone protein from adenovirus serotype 2 (subgroup C) assists in trimerization and nuclear localization of hexons from subgroups C and B adenoviruses. *J. Mol. Biol.* (2005) doi:10.1016/j.jmb.2005.06.070.
234. Morin, N. & Boulanger, P. Hexon trimerization occurring in an assembly-defective, 100k temperature-sensitive mutant of adenovirus 2. *Virology* (1986) doi:10.1016/0042-6822(86)90367-3.
235. Wodrich, H. *et al.* Switch from capsid protein import to adenovirus assembly by cleavage of nuclear transport signals. *EMBO J.* (2003) doi:10.1093/emboj/cdg614.
236. Velicer, L. F. & Ginsberg, H. S. Synthesis, Transport, and Morphogenesis of Type 5 Adenovirus Capsid Proteins. *J. Virol.* (1970) doi:10.1128/jvi.5.3.338-352.1970.
237. Weber, J. & Philipson, L. Protein composition of adenovirus nucleoprotein complexes extracted from infected cells. *Virology* (1984) doi:10.1016/0042-6822(84)90168-5.
238. Zhang, W. & Arcos, R. Interaction of the adenovirus major core protein precursor,

pVII, with the viral DNA packaging machinery. *Virology* (2005) doi:10.1016/j.virol.2005.01.048.
239. Hasson, T. B., Ornelles, D. A. & Shenk, T. Adenovirus L1 52- and 55-kilodalton proteins are present within assembling virions and colocalize with nuclear structures distinct from replication centers. *J. Virol.* (1992) doi:10.1128/jvi.66.10.6133-6142.1992.
240. Zhang, W. & Imperiale, M. J. Interaction of the Adenovirus IVa2 Protein with Viral Packaging Sequences. *J. Virol.* (2000) doi:10.1128/jvi.74.6.2687-2693.2000.
241. Tyler, R. E., Ewing, S. G. & Imperiale, M. J. Formation of a Multiple Protein Complex on the Adenovirus Packaging Sequence by the IVa2 Protein. *J. Virol.* (2007) doi:10.1128/jvi.02097-06.
242. Ahi, Y. S., Vemula, S. V. & Mittal, S. K. Adenoviral E2 IVa2 protein interacts with L4 33K protein and E2 DNA-binding protein. *J. Gen. Virol.* (2013) doi:10.1099/vir.0.049346-0.
243. Ahi, Y. S. *et al.* Adenoviral L4 33K forms ring-like oligomers and stimulates ATPase activity of IVa2: Implications in viral genome packaging. *Front. Microbiol.* (2015) doi:10.3389/fmicb.2015.00318.
244. Ewing, S. G., Byrd, S. A., Christensen, J. B., Tyler, R. E. & Imperiale, M. J. Ternary Complex Formation on the Adenovirus Packaging Sequence by the IVa2 and L4 22-Kilodalton Proteins. *J. Virol.* (2007) doi:10.1128/jvi.01470-07.
245. Wohl, B. P. & Hearing, P. Role for the L1-52/55K Protein in the Serotype Specificity of Adenovirus DNA Packaging. *J. Virol.* (2008) doi:10.1128/jvi.00040-08.
246. Wu, K., Orozco, D. & Hearing, P. The Adenovirus L4-22K Protein Is Multifunctional and Is an Integral Component of Crucial Aspects of Infection. *J. Virol.* (2012) doi:10.1128/jvi.01463-12.
247. Ma, H.-C. & Hearing, P. Adenovirus Structural Protein IIIa Is Involved in the Serotype Specificity of Viral DNA Packaging. *J. Virol.* (2011) doi:10.1128/jvi.00467-11.
248. Perez-Romero, P., Tyler, R. E., Abend, J. R., Dus, M. & Imperiale, M. J. Analysis of the Interaction of the Adenovirus L1 52/55-Kilodalton and IVa2 Proteins with the Packaging Sequence In Vivo and In Vitro. *J. Virol.* (2005) doi:10.1128/jvi.79.4.2366-2374.2005.
249. Gustin, K. E., Lutz, P. & Imperiale, M. J. Interaction of the adenovirus L1 52/55-kilodalton protein with the IVa2 gene product during infection. *J. Virol.* (1996) doi:10.1128/jvi.70.9.6463-6467.1996.
250. Ostapchuk, P., Almond, M. & Hearing, P. Characterization of Empty Adenovirus Particles Assembled in the Absence of a Functional Adenovirus IVa2 Protein. *J. Virol.* (2011) doi:10.1128/jvi.02538-10.
251. Roy, A., Bhardwaj, A., Datta, P., Lander, G. C. & Cingolani, G. Small terminase couples viral DNA binding to genome-packaging ATPase activity. *Structure* (2012) doi:10.1016/j.str.2012.05.014.
252. Suna, S. *et al.* Structure and function of the small terminase component of the DNA packaging machine in T4-like bacteriophages. *Proc. Natl. Acad. Sci. U. S. A.* (2012) doi:10.1073/pnas.1110224109.
253. Gotten, M. & Weber, J. M. The adenovirus protease is required for virus entry into host cells. *Virology* (1995) doi:10.1006/viro.1995.0022.
254. Greber, U. F., Webster, P., Weber, J. & Helenius, A. The role of the adenovirus protease on virus entry into cells. *EMBO J.* (1996) doi:10.1002/j.1460-

2075.1996.tb00525.x.
255. Weber, J. Genetic analysis of adenovirus type 2 III. Temperature sensitivity of processing viral proteins. *J. Virol.* (1976) doi:10.1128/jvi.17.2.462-471.1976.
256. Webster, A. & Kemp, G. The active adenovirus protease is the intact L3 23K protein. *J. Gen. Virol.* (1993) doi:10.1099/0022-1317-74-7-1415.
257. Chen, P. H., Ornelles, D. A. & Shenk, T. The adenovirus L3 23-kilodalton proteinase cleaves the amino-terminal head domain from cytokeratin 18 and disrupts the cytokeratin network of HeLa cells. *J. Virol.* (1993) doi:10.1128/jvi.67.6.3507-3514.1993.
258. Walters, R. W. *et al.* Adenovirus fiber disrupts CAR-mediated intercellular adhesion allowing virus escape. *Cell* (2002) doi:10.1016/S0092-8674(02)00912-1.
259. Trentin, J. J., Yabe, Y. & Taylor, G. The quest for human cancer viruses. *Science (80-.).* (1962) doi:10.1126/science.137.3533.835.
260. Graham, F. L., Smiley, J., Russell, W. C. & Nairn, R. Characteristics of a human cell line transformed by DNA from human adenovirus type 5. *J. Gen. Virol.* (1977) doi:10.1099/0022-1317-36-1-59.
261. Branton, P. E. & Rowe, D. T. Stabilities and interrelations of multiple species of human adenovirus type 5 early region 1 proteins in infected and transformed cells. *J. Virol.* (1985).
262. Whittaker, J. L., Byrd, P. J., Grand, R. J. & Gallimore, P. H. Isolation and characterization of four adenovirus type 12-transformed human embryo kidney cell lines. *Mol. Cell. Biol.* (1984) doi:10.1128/mcb.4.1.110.
263. van den Heuvel, S. J. *et al.* p53 shares an antigenic determinant with proteins of 92 and 150 kilodaltons that may be involved in senescence of human cells. *J. Virol.* (1992) doi:10.1128/jvi.66.1.591-595.1992.
264. Byrd, P., Brown, K. W. & Gallimore, P. H. Malignant transformation of human embryo retinoblasts by cloned adenovirus 12 DNA. *Nature* (1982) doi:10.1038/298069a0.
265. Fallaux, F. J. *et al.* Characterization of 911: A new helper cell line for the titration and propagation of early region 1-deleted adenoviral vectors. *Hum. Gene Ther.* (1996) doi:10.1089/hum.1996.7.2-215.
266. Schiedner, G., Hertel, S. & Kochanek, S. Efficient transformation of primary human amniocytes by E1 functions of Ad5: Generation of new cell lines for adenoviral vector production. *Hum. Gene Ther.* (2000) doi:10.1089/104303400750001417.
267. Speiseder, T. *et al.* Efficient Transformation of Primary Human Mesenchymal Stromal Cells by Adenovirus Early Region 1 Oncogenes. *J. Virol.* (2017) doi:10.1128/jvi.01782-16.
268. Kosulin, K., Hoffmann, F., Clauditz, T. S., Wilczak, W. & Dobner, T. Presence of Adenovirus Species C in Infiltrating Lymphocytes of Human Sarcoma. *PLoS One* (2013) doi:10.1371/journal.pone.0063646.
269. Kuwano, K. *et al.* Detection of group C adenovirus DNA in small-cell lung cancer with the nested polymerase chain reaction. *J. Cancer Res. Clin. Oncol.* (1997) doi:10.1007/BF01240120.
270. Kosulin, K. *et al.* Screening for adenoviruses in haematological neoplasia: High prevalence in mantle cell lymphoma. *Eur. J. Cancer* (2014) doi:10.1016/j.ejca.2013.10.013.
271. Graham, F. L. Transformation by and Oncogenicity of Human Adenoviruses. in

The Adenoviruses (1984). doi:10.1007/978-1-4684-7935-5_9.
272. Bernards, R., Houweling, A., Schrier, P. I., Bos, J. L. & Van Der Eb, A. J. Characterization of cells transformed by Ad5/Ad12 hybrid early region I plasmids. *Virology* (1982) doi:10.1016/0042-6822(82)90042-3.
273. Bernards, R. & Van der Eb, A. J. Adenovirus: Transformation and oncogenicity. *BBA - Gene Structure and Expression* (1984) doi:10.1016/0167-4781(84)90029-0.
274. White, E. Regulation of apoptosis by adenovirus E1A and E1B oncogenes. *Semin. Virol.* (1998) doi:10.1006/smvy.1998.0155.
275. Rao, L. *et al.* The adenovirus E1A proteins induce apoptosis, which is inhibited by the E1B 19-kDa and Bcl-2 proteins. *Proc. Natl. Acad. Sci. U. S. A.* (1992) doi:10.1073/pnas.89.16.7742.
276. Moore, M., Horikoshi, N. & Shenk, T. Oncogenic potential of the adenovirus E4orf6 protein. *Proc. Natl. Acad. Sci. U. S. A.* (1996) doi:10.1073/pnas.93.21.11295.
277. Nevels, M., Rubenwolf, S., Spruss, T., Wolf, H. & Dobner, T. The adenovirus E4orf6 protein can promote E1A/E1B-induced focus formation by interfering with p53 tumor suppressor function. *Proc. Natl. Acad. Sci. U. S. A.* (1997) doi:10.1073/pnas.94.4.1206.
278. Nevels, M. *et al.* Transforming Potential of the Adenovirus Type 5 E4orf3 Protein. *J. Virol.* (1999) doi:10.1128/jvi.73.2.1591-1600.1999.
279. Nevels, M., Spruss, T., Wolf, H. & Dobner, T. The adenovirus E4orf6 protein contributes to malignant transformation by antagonizing E1A-induced accumulation of the tumor suppressor protein p53. *Oncogene* (1999) doi:10.1038/sj.onc.1202284.
280. Nevels, M., Täuber, B., Spruss, T., Wolf, H. & Dobner, T. “Hit-and-Run” Transformation by Adenovirus Oncogenes. *J. Virol.* (2001) doi:10.1128/jvi.75.7.3089-3094.2001.
281. Matunis, M. J., Coutavas, E. & Blobel, G. A novel ubiquitin-like modification modulates the partitioning of the Ran-GTPase-activating protein RanGAP1 between the cytosol and the nuclear pore complex. *J. Cell Biol.* **135**, 1457–1470 (1996).
282. Mahajan, R., Delphin, C., Guan, T., Gerace, L. & Melchior, F. A small ubiquitin-related polypeptide involved in targeting RanGAP1 to nuclear pore complex protein RanBP2. *Cell* **88**, 97–107 (1997).
283. Hendriks, I. A. & Vertegaal, A. C. O. A comprehensive compilation of SUMO proteomics. *Nat. Rev. Mol. Cell Biol.* **17**, 581–595 (2016).
284. Geiss-Friedlander, R. & Melchior, F. Concepts in sumoylation: a decade on. *Nat. Rev. Mol. Cell Biol.* **8**, 947–956 (2007).
285. Tatham, M. H. *et al.* Polymeric Chains of SUMO-2 and SUMO-3 Are Conjugated to Protein Substrates by SAE1/SAE2 and Ubc9. *J. Biol. Chem.* **276**, 35368–35374 (2001).
286. Flotho, A. & Melchior, F. *Sumoylation: A regulatory protein modification in health and disease*. *Annual Review of Biochemistry* vol. 82 357–385 (Annual Reviews , 2013).
287. Hay, R. T. SUMO: A History of Modification. *Mol. Cell* **18**, 1–12 (2005).
288. Saitoh, H. & Hinchey, J. Functional Heterogeneity of Small Ubiquitin-related Protein Modifiers SUMO-1 *versus* SUMO-2/3. *J. Biol. Chem.* **275**, 6252–6258 (2000).

289. Bohren, K. M., Nadkarni, V., Song, J. H., Gabbay, K. H. & Owerbach, D. A M55V Polymorphism in a Novel *SUMO* Gene (*SUMO-4*) Differentially Activates Heat Shock Transcription Factors and Is Associated with Susceptibility to Type I Diabetes Mellitus. *J. Biol. Chem.* **279**, 27233–27238 (2004).
290. Owerbach, D., McKay, E. M., Yeh, E. T. H., Gabbay, K. H. & Bohren, K. M. A proline-90 residue unique to SUMO-4 prevents maturation and sumoylation. *Biochem. Biophys. Res. Commun.* **337**, 517–520 (2005).
291. Wang, C.-Y., Yang, P., Li, M. & Gong, F. Characterization of a negative feedback network between SUMO4 expression and NFκB transcriptional activity. *Biochem. Biophys. Res. Commun.* **381**, 477–481 (2009).
292. Liang, Y.-C. *et al.* SUMO5, a Novel Poly-SUMO Isoform, Regulates PML Nuclear Bodies. *Sci. Rep.* **6**, 26509 (2016).
293. Rosas-Acosta, G., Russell, W. K., Deyrieux, A., Russell, D. H. & Wilson, V. G. A universal strategy for proteomic studies of SUMO and other ubiquitin-like modifiers. *Mol. Cell. Proteomics* **4**, 56–72 (2005).
294. Vertegaal, A. C. O. *et al.* Distinct and Overlapping Sets of SUMO-1 and SUMO-2 Target Proteins Revealed by Quantitative Proteomics. *Mol. Cell. Proteomics* **5**, 2298–2310 (2006).
295. Desterro, J. M., Rodriguez, M. S., Kemp, G. D. & Hay, R. T. Identification of the enzyme required for activation of the small ubiquitin-like protein SUMO-1. *J. Biol. Chem.* **274**, 10618–24 (1999).
296. Johnson, E. S., Schwienhorst, I., Dohmen, R. J. & Blobel, G. The ubiquitin-like protein Smt3p is activated for conjugation to other proteins by an Aos1p/Uba2p heterodimer. *EMBO J.* **16**, 5509–19 (1997).
297. Okuma, T., Honda, R., Ichikawa, G., Tsumagari, N. & Yasuda, H. In VitroSUMO-1 Modification Requires Two Enzymatic Steps, E1 and E2. *Biochem. Biophys. Res. Commun.* **254**, 693–698 (1999).
298. Desterro, J. M., Thomson, J. & Hay, R. T. Ubch9 conjugates SUMO but not ubiquitin. *FEBS Lett.* **417**, 297–300 (1997).
299. Johnson, E. S. & Blobel, G. Ubc9p Is the Conjugating Enzyme for the Ubiquitin-like Protein Smt3p. *J. Biol. Chem.* **272**, 26799–26802 (1997).
300. Hershko, A. & Ciechanover, A. THE UBIQUITIN SYSTEM. *Annu. Rev. Biochem.* **67**, 425–479 (1998).
301. Bernier-Villamor, V., Sampson, D. A., Matunis, M. J. & Lima, C. D. Structural basis for E2-mediated SUMO conjugation revealed by a complex between ubiquitin-conjugating enzyme Ubc9 and RanGAP1. *Cell* **108**, 345–56 (2002).
302. Pichler, A., Gast, A., Seeler, J. S., Dejean, A. & Melchior, F. The nucleoporin RanBP2 has SUMO1 E3 ligase activity. *Cell* **108**, 109–20 (2002).
303. Eisenhardt, N. *et al.* A new vertebrate SUMO enzyme family reveals insights into SUMO-chain assembly. *Nat. Struct. Mol. Biol.* **22**, 959–967 (2015).
304. Cappadocia, L., Pichler, A. & Lima, C. D. Structural basis for catalytic activation by the human ZNF451 SUMO E3 ligase. *Nat. Struct. Mol. Biol.* **22**, 968–975 (2015).
305. Kagey, M. H., Melhuish, T. A. & Wotton, D. The Polycomb Protein Pc2 Is a SUMO E3. *Cell* **113**, 127–137 (2003).
306. Pichler, A., Fatouros, C., Lee, H. & Eisenhardt, N. SUMO conjugation – a mechanistic view. *Biomol. Concepts* **8**, 13–36 (2017).
307. Sriramachandran, A. M. & Dohmen, R. J. SUMO-targeted ubiquitin ligases. *Biochimica et Biophysica Acta - Molecular Cell Research* (2014)

doi:10.1016/j.bbamcr.2013.08.022.
308. Erker, Y. *et al.* Arkadia, a Novel SUMO-Targeted Ubiquitin Ligase Involved in PML Degradation. *Mol. Cell. Biol.* (2013) doi:10.1128/mcb.01019-12.
309. Poulsen, S. L. *et al.* RNF111/Arkadia is a SUMO-targeted ubiquitin ligase that facilitates the DNA damage response. *J. Cell Biol.* (2013) doi:10.1083/jcb.201212075.
310. Tatham, M. H. *et al.* RNF4 is a poly-SUMO-specific E3 ubiquitin ligase required for arsenic-induced PML degradation. *Nat. Cell Biol.* (2008) doi:10.1038/ncb1716.
311. Gong, L., Millas, S., Maul, G. G. & Yeh, E. T. H. Differential Regulation of Sentrinized Proteins by a Novel Sentrin-specific Protease. *J. Biol. Chem.* **275**, 3355–3359 (2000).
312. Li, S.-J. & Hochstrasser, M. A new protease required for cell-cycle progression in yeast. *Nature* **398**, 246–251 (1999).
313. Hickey, C. M., Wilson, N. R. & Hochstrasser, M. *Function and regulation of SUMO proteases*. *Nature Reviews Molecular Cell Biology* vol. 13 755–766 (Nature Publishing Group, 2012).
314. Nayak, A. & Müller, S. SUMO-specific proteases/isopeptidases: SENPs and beyond. *Genome Biol.* **15**, (2014).
315. Yang, S.-H., Galanis, A., Witty, J. & Sharrocks, A. D. An extended consensus motif enhances the specificity of substrate modification by SUMO. *EMBO J.* **25**, 5083–93 (2006).
316. Hietakangas, V. *et al.* PDSM, a motif for phosphorylation-dependent SUMO modification. *Proc. Natl. Acad. Sci. U. S. A.* **103**, 45–50 (2006).
317. Everett, R. D., Boutell, C. & Hale, B. G. Interplay between viruses and host sumoylation pathways. *Nature Reviews Microbiology* (2013) doi:10.1038/nrmicro3015.
318. Kunz, K., Piller, T. & Müller, S. SUMO-specific proteases and isopeptidases of the SENP family at a glance. *J. Cell Sci.* **131**, (2018).
319. Mukhopadhyay, D. & Dasso, M. Modification in reverse: the SUMO proteases. *Trends in Biochemical Sciences* (2007) doi:10.1016/j.tibs.2007.05.002.
320. Yeh, E. T. H., Gong, L. & Kamitani, T. Ubiquitin-like proteins: New wines in new bottles. *Gene* (2000) doi:10.1016/S0378-1119(00)00139-6.
321. Hay, R. T. SUMO-specific proteases: a twist in the tail. *Trends in Cell Biology* (2007) doi:10.1016/j.tcb.2007.08.002.
322. Jiang, M., Chiu, S. Y. & Hsu, W. SUMO-specific protease 2 in Mdm2-mediated regulation of p53. *Cell Death Differ.* (2011) doi:10.1038/cdd.2010.168.
323. Chow, K. H., Elgort, S., Dasso, M. & Ullman, K. S. Two distinct sites in Nup153 mediate interaction with the SUMO proteases SENP1 and SENP2. *Nucl. (United States)* (2012) doi:10.4161/nucl.20822.
324. Goeres, J. *et al.* The SUMO-specific isopeptidase SENP2 associates dynamically with nuclear pore complexes through interactions with karyopherins and the Nup107-160 nucleoporin subcomplex. *Mol. Biol. Cell* (2011) doi:10.1091/mbc.E10-12-0953.
325. Hang, J. & Dasso, M. Association of the human SUMO-1 protease SENP2 with the nuclear pore. *J. Biol. Chem.* (2002) doi:10.1074/jbc.M201799200.
326. Zhang, H., Saitoh, H. & Matunis, M. J. Enzymes of the SUMO Modification Pathway Localize to Filaments of the Nuclear Pore Complex. *Mol. Cell. Biol.* (2002) doi:10.1128/mcb.22.18.6498-6508.2002.

327. Cubeñas-Potts, C., Goeres, J. D. & Matunis, M. J. SENP1 and SENP2 affect spatial and temporal control of Sumoylation in mitosis. *Mol. Biol. Cell* (2013) doi:10.1091/mbc.E13-05-0230.
328. Castle, C. D., Cassimere, E. K. & Denicourt, C. LAS1L interacts with the mammalian Rix1 complex to regulate ribosome biogenesis. *Mol. Biol. Cell* (2012) doi:10.1091/mbc.E11-06-0530.
329. Haindl, M., Harasim, T., Eick, D. & Muller, S. The nucleolar SUMO-specific protease SENP3 reverses SUMO modification of nucleophosmin and is required for rRNA processing. *EMBO Rep.* (2008) doi:10.1038/embor.2008.3.
330. Raman, N., Nayak, A. & Muller, S. mTOR Signaling Regulates Nucleolar Targeting of the SUMO-Specific Isopeptidase SENP3. *Mol. Cell. Biol.* (2014) doi:10.1128/mcb.00801-14.
331. Yun, C. *et al.* Nucleolar protein B23/nucleophosmin regulates the vertebrate SUMO pathway through SENP3 and SENP5 proteases. *J. Cell Biol.* (2008) doi:10.1083/jcb.200807185.
332. Nayak, A., Reck, A., Morsczeck, C. & Müller, S. Flightless-I governs cell fate by recruiting the SUMO isopeptidase SENP3 to distinct HOX genes. *Epigenetics Chromatin* (2017) doi:10.1186/s13072-017-0122-8.
333. Gong, L. & Yeh, E. T. H. Characterization of a family of nucleolar SUMO-specific proteases with preference for SUMO-2 or SUMO-3. *J. Biol. Chem.* (2006) doi:10.1074/jbc.M511658200.
334. Nishida, T., Tanaka, H. & Yasuda, H. A novel mammalian Smt3-specific isopeptidase 1 (SMT3IP1) localized in the nucleolus at interphase. *Eur. J. Biochem.* (2000) doi:10.1046/j.1432-1327.2000.01729.x.
335. Zunino, R., Braschi, E., Xu, L. & McBride, H. M. Translocation of SenP5 from the nucleoli to the mitochondria modulates DRP1-dependent fission during mitosis. *J. Biol. Chem.* (2009) doi:10.1074/jbc.M901902200.
336. Bawa-Khalfe, T. *et al.* Differential expression of SUMO-specific protease 7 variants regulates epithelial-mesenchymal transition. *Proc. Natl. Acad. Sci. U. S. A.* (2012) doi:10.1073/pnas.1209378109.
337. Maison, C. *et al.* The SUMO protease SENP7 is a critical component to ensure HP1 enrichment at pericentric heterochromatin. *Nat. Struct. Mol. Biol.* (2012) doi:10.1038/nsmb.2244.
338. Romeo, K. *et al.* The SENP7 SUMO-Protease presents a module of two HP1 interaction motifs that locks HP1 protein at pericentric heterochromatin. *Cell Rep.* (2015) doi:10.1016/j.celrep.2015.01.004.
339. Kolli, N. *et al.* Distribution and paralogue specificity of mammalian deSUMOylating enzymes. *Biochem. J.* (2010) doi:10.1042/BJ20100504.
340. Reverter, D. & Lima, C. D. A basis for SUMO protease specificity provided by analysis of human Senp2 and a Senp2-SUMO complex. *Structure* (2004) doi:10.1016/j.str.2004.05.023.
341. Shen, L. *et al.* SUMO protease SENP1 induces isomerization of the scissile peptide bond. *Nat. Struct. Mol. Biol.* (2006) doi:10.1038/nsmb1172.
342. Mikolajczyk, J. *et al.* Small Ubiquitin-related Modifier (SUMO)-specific proteases: Profiling the specificities and activities of human SENPs. *J. Biol. Chem.* (2007) doi:10.1074/jbc.M702444200.
343. Lima, C. D. & Reverter, D. Structure of the human SENP7 catalytic domain and poly-SUMO deconjugation activities for SENP6 and SENP7. *J. Biol. Chem.* (2008) doi:10.1074/jbc.M805655200.

344. Mukhopadhyay, D. *et al.* SUSP1 antagonizes formation of highly SUMO2/3-conjugated species. *J. Cell Biol.* (2006) doi:10.1083/jcb.200510103.
345. Shen, L. N., Geoffroy, M. C., Jaffray, E. G. & Hay, R. T. Characterization of SENP7, a SUMO-2/3-specific isopeptidase. *Biochem. J.* (2009) doi:10.1042/BJ20090246.
346. Alegre, K. O. & Reverter, D. Swapping small ubiquitin-like modifier (SUMO) isoform specificity of SUMO proteases SENP6 and SENP7. *J. Biol. Chem.* (2011) doi:10.1074/jbc.M111.268847.
347. Ishov, A. M. *et al.* PML is critical for ND10 formation and recruits the PML-interacting protein Daxx to this nuclear structure when modified by SUMO-1. *J. Cell Biol.* (1999) doi:10.1083/jcb.147.2.221.
348. Salomoni, P. & Pandolfi, P. P. The role of PML in tumor suppression. *Cell* (2002) doi:10.1016/S0092-8674(02)00626-8.
349. Melnick, A. & Licht, J. D. Deconstructing a disease: RARα, its fusion partners, and their roles in the pathogenesis of acute promyelocytic leukemia. *Blood* (1999) doi:10.1182/blood.v93.10.3167.410k44_3167_3215.
350. Parada, L. A. & Misteli, T. Chromosome positioning in the interphase nucleus. *Trends in Cell Biology* (2002) doi:10.1016/S0962-8924(02)02351-6.
351. Möller, A. & Schmitz, M. L. Viruses as Hijackers of PML Nuclear Bodies. *Archivum Immunologiae et Therapiae Experimentalis* (2003).
352. Dellaire, G. & Bazett-Jones, D. P. PML nuclear bodies: Dynamic sensors of DNA damage and cellular stress. *BioEssays* (2004) doi:10.1002/bies.20089.
353. Trotman, L. C. *et al.* Identification of a tumour suppressor network opposing nuclear Akt function. *Nature* (2006) doi:10.1038/nature04809.
354. Bernardi, R. *et al.* PML inhibits HIF-1α translation and neoangiogenesis through repression of mTOR. *Nature* (2006) doi:10.1038/nature05029.
355. Dellaire, G., Farrall, R. & Bickmore, W. A. The Nuclear Protein Database (NPD): Sub-nuclear localisation and functional annotation of the nuclear proteome. *Nucleic Acids Research* (2003) doi:10.1093/nar/gkg018.
356. van Damme, E., Laukens, K., Dang, T. H. & van Ostade, X. A manually curated network of the pml nuclear body interactome reveals an important role for PML-NBs in SUMOylation dynamics. *Int. J. Biol. Sci.* (2010) doi:10.7150/ijbs.6.51.
357. Muratani, M. *et al.* Metabolic-energy-dependent movement of PML bodies within the mammalian cell nucleas. *Nat. Cell Biol.* (2002) doi:10.1038/ncb740.
358. Zhong, S., Salomoni, P. & Pandolfi, P. P. The transcription role of PML and the nuclear body. *Nature Cell Biology* (2000) doi:10.1038/35010583.
359. Jensen, K., Shiels, C. & Freemont, P. S. PML protein isoforms and the RBCC/TRIM motif. *Oncogene* (2001) doi:10.1038/sj.onc.1204765.
360. Yoshida, H. *et al.* PML-Retinoic Acid Receptor α Inhibits PML IV Enhancement of PU.1-Induced C/EBPε Expression in Myeloid Differentiation. *Mol. Cell. Biol.* (2007) doi:10.1128/mcb.02422-06.
361. Negorev, D. & Maul, G. G. Cellular proteins localized at and interacting within ND10/PML nuclear bodies/PODs suggest functions of a nuclear depot. *Oncogene* (2001) doi:10.1038/sj.onc.1204764.
362. Scherer, M. & Stamminger, T. Emerging Role of PML Nuclear Bodies in Innate Immune Signaling. *J. Virol.* (2016) doi:10.1128/jvi.01979-15.
363. Reichelt, M. *et al.* Entrapment of viral capsids in nuclear PML cages is an intrinsic antiviral host defense against Varicella-zoster virus. *PLoS Pathog.* (2011) doi:10.1371/journal.ppat.1001266.

364. Tavalai, N. & Stamminger, T. Interplay between herpesvirus infection and host defense by PML nuclear bodies. *Viruses* (2009) doi:10.3390/v1031240.
365. Dutrieux, J. *et al.* PML/TRIM19-Dependent Inhibition of Retroviral Reverse-Transcription by Daxx. *PLoS Pathog.* (2015) doi:10.1371/journal.ppat.1005280.
366. Boutell, C. *et al.* A viral ubiquitin ligase has substrate preferential sumo targeted ubiquitin ligase activity that counteracts intrinsic antiviral defence. *PLoS Pathog.* (2011) doi:10.1371/journal.ppat.1002245.
367. Weiden, M. D. & Ginsberg, H. S. Deletion of the E4 region of the genome produces adenovirus DNA concatemers. *Proc. Natl. Acad. Sci. U. S. A.* (1994) doi:10.1073/pnas.91.1.153.
368. Boyer, J., Rohleder, K. & Ketner, G. Adenovirus E4 34k and E4 11k inhibit double strand break repair and are physically associated with the cellular DNA-dependent protein kinase. *Virology* (1999) doi:10.1006/viro.1999.9866.
369. Stracker, T. H., Carson, C. T. & Weilzman, M. D. Adenovirus oncoproteins inactivate the Mre11-Rad50-NBs1 DNA repair complex. *Nature* (2002) doi:10.1038/nature00863.
370. Lee, H.-R. *et al.* Ability of the Human Cytomegalovirus IE1 Protein To Modulate Sumoylation of PML Correlates with Its Functional Activities in Transcriptional Regulation and Infectivity in Cultured Fibroblast Cells. *J. Virol.* (2004) doi:10.1128/jvi.78.12.6527-6542.2004.
371. Ling, P. D., Tan, J., Sewatanon, J. & Peng, R. Murine Gammaherpesvirus 68 Open Reading Frame 75c Tegument Protein Induces the Degradation of PML and Is Essential for Production of Infectious Virus. *J. Virol.* (2008) doi:10.1128/jvi.02752-07.
372. Full, F. *et al.* Kaposi's Sarcoma Associated Herpesvirus Tegument Protein ORF75 Is Essential for Viral Lytic Replication and Plays a Critical Role in the Antagonization of ND10-Instituted Intrinsic Immunity. *PLoS Pathog.* (2014) doi:10.1371/journal.ppat.1003863.
373. Tsai, K., Thikmyanova, N., Wojcechowskyj, J. A., Delecluse, H. J. & Lieberman, P. M. EBV tegument protein BNRF1 disrupts DAXX-ATRX to activate viral early gene transcription. *PLoS Pathog.* (2011) doi:10.1371/journal.ppat.1002376.
374. Ou, H. D. *et al.* A structural basis for the assembly and functions of a viral polymer that inactivates multiple tumor suppressors. *Cell* (2012) doi:10.1016/j.cell.2012.08.035.
375. Ullman, A. J. & Hearing, P. Cellular Proteins PML and Daxx Mediate an Innate Antiviral Defense Antagonized by the Adenovirus E4 ORF3 Protein. *J. Virol.* (2008) doi:10.1128/jvi.00723-08.
376. Kim, Y.-E. *et al.* Human Cytomegalovirus Infection Causes Degradation of Sp100 Proteins That Suppress Viral Gene Expression. *J. Virol.* (2011) doi:10.1128/jvi.00758-11.
377. Gu, H. & Roizman, B. The degradation of promyelocytic leukemia and Sp100 proteins by herpes simplex virus 1 is mediated by the ubiquitin-conjugating enzyme UbcH5a. *Proc. Natl. Acad. Sci. U. S. A.* (2003) doi:10.1073/pnas.1533420100.
378. Chelbi-Alix, M. K. & De Thé, H. Herpes virus induced proteasome-dependent degradation of the nuclear bodies-associated PML and Sp100 proteins. *Oncogene* (1999) doi:10.1038/sj.onc.1202366.
379. Ahn, J. H. & Hayward, G. S. The major immediate-early proteins IE1 and IE2 of human cytomegalovirus colocalize with and disrupt PML-associated nuclear

bodies at very early times in infected permissive cells. *J. Virol.* (1997) doi:10.1128/jvi.71.6.4599-4613.1997.

380. Hwang, J. & Kalejta, R. F. Proteasome-dependent, ubiquitin-independent degradation of Daxx by the viral pp71 protein in human cytomegalovirus-infected cells. *Virology* (2007) doi:10.1016/j.virol.2007.05.037.
381. Tavalai, N. & Stamminger, T. New insights into the role of the subnuclear structure ND10 for viral infection. *Biochimica et Biophysica Acta - Molecular Cell Research* (2008) doi:10.1016/j.bbamcr.2008.08.004.
382. Ishov, A. M. & Maul, G. G. The periphery of nuclear domain 10 (ND10) as site of DNA virus deposition. *J. Cell Biol.* (1996) doi:10.1083/jcb.134.4.815.
383. Maul, G. G., Ishov, A. M. & Everett, R. D. Nuclear domain 10 as preexisting potential replication start sites of herpes simplex virus type-1. *Virology* (1996) doi:10.1006/viro.1996.0094.
384. Everett, R. D. DNA viruses and viral proteins that interact with PML nuclear bodies. *Oncogene* (2001) doi:10.1038/sj.onc.1204759.
385. Maul, G. G. Nuclear domain 10, the site of DNA virus transcription and replication. *BioEssays* (1998) doi:10.1002/(SICI)1521-1878(199808)20:8<660::AID-BIES9>3.0.CO;2-M.
386. Bernardi, R. & Pandolfi, P. P. Structure, dynamics and functions of promyelocytic leukaemia nuclear bodies. *Nature Reviews Molecular Cell Biology* (2007) doi:10.1038/nrm2277.
387. Sohn, S. Y. & Hearing, P. Adenovirus early proteins and host sumoylation. *mBio* (2016) doi:10.1128/mBio.01154-16.
388. Wimmer, P., Schreiner, S. & Dobner, T. Human Pathogens and the Host Cell SUMOylation System. *J. Virol.* (2012) doi:10.1128/jvi.06227-11.
389. Müller, S., Matunis, M. J. & Dejean, A. Conjugation with the ubiquitin-related modifier SUMO-1 regulates the partitioning of PML within the nucleus. *EMBO J.* (1998) doi:10.1093/emboj/17.1.61.
390. Wilson, V. G. Viral interplay with the host sumoylation system. *Adv. Exp. Med. Biol.* (2017) doi:10.1007/978-3-319-50044-7_21.
391. Wimmer, P. & Schreiner, S. Viral Mimicry to Usurp Ubiquitin and SUMO Host Pathways. *Viruses* **7**, 4854–72 (2015).
392. Boggio, R., Colombo, R., Hay, R. T., Draetta, G. F. & Chiocca, S. A mechanism for inhibiting the SUMO pathway. *Mol. Cell* (2004) doi:10.1016/j.molcel.2004.11.007.
393. Berscheminski, J. *et al.* Sp100 Isoform-Specific Regulation of Human Adenovirus 5 Gene Expression. *J. Virol.* (2014) doi:10.1128/jvi.00469-14.
394. Berscheminski, J., Groitl, P., Dobner, T., Wimmer, P. & Schreiner, S. The Adenoviral Oncogene E1A-13S Interacts with a Specific Isoform of the Tumor Suppressor PML To Enhance Viral Transcription. *J. Virol.* (2013) doi:10.1128/jvi.02023-12.
395. Hateboer, G. *et al.* mUBC9, a novel adenovirus E1A-interacting protein that complements a yeast cell cycle defect. *J. Biol. Chem.* (1996) doi:10.1074/jbc.271.42.25906.
396. Yousef, A. F. *et al.* Identification of a molecular recognition feature in the E1A oncoprotein that binds the SUMO conjugase UBC9 and likely interferes with polySUMOylation. *Oncogene* (2010) doi:10.1038/onc.2010.226.
397. Eskiw, C. H., Dellaire, G., Mymryk, J. S. & Bazett-Jones, D. P. Size, position and dynamic behavior of PML nuclear bodies following cell stress as a paradigm for

supramolecular trafficking and assembly. *J. Cell Sci.* (2003) doi:10.1242/jcs.00758.
398. Ledl, A., Schmidt, D. & Müller, S. Viral oncoproteins E1A and E7 and cellular LxCxE proteins repress SUMO modification of the retinoblastoma tumor suppressor. *Oncogene* (2005) doi:10.1038/sj.onc.1208539.
399. Patsalo, V. *et al.* Biophysical and functional analyses suggest that adenovirus E4-ORF3 protein requires higher-order multimerization to function against promyelocytic leukemia protein nuclear bodies. *J. Biol. Chem.* (2012) doi:10.1074/jbc.M112.344234.
400. Evans, J. D. & Hearing, P. Relocalization of the Mre11-Rad50-Nbs1 Complex by the Adenovirus E4 ORF3 Protein Is Required for Viral Replication. *J. Virol.* (2005) doi:10.1128/jvi.79.10.6207-6215.2005.
401. Yondola, M. A. & Hearing, P. The Adenovirus E4 ORF3 Protein Binds and Reorganizes the TRIM Family Member Transcriptional Intermediary Factor 1 Alpha. *J. Virol.* (2007) doi:10.1128/jvi.02629-06.
402. Vink, E. I., Yondola, M. A., Wu, K. & Hearing, P. Adenovirus E4-ORF3-dependent relocalization of TIF1α and TIF1γ relies on access to the Coiled-Coil motif. *Virology* (2012) doi:10.1016/j.virol.2011.10.033.
403. Sohn, S.-Y. & Hearing, P. Adenovirus Regulates Sumoylation of Mre11-Rad50-Nbs1 Components through a Paralog-Specific Mechanism. *J. Virol.* (2012) doi:10.1128/jvi.01273-12.
404. Forrester, N. A. *et al.* Adenovirus E4orf3 Targets Transcriptional Intermediary Factor 1 for Proteasome-Dependent Degradation during Infection. *J. Virol.* (2012) doi:10.1128/jvi.06583-11.
405. Sohn, S.-Y., Bridges, R. G. & Hearing, P. Proteomic Analysis of Ubiquitin-Like Posttranslational Modifications Induced by the Adenovirus E4-ORF3 Protein. *J. Virol.* (2015) doi:10.1128/jvi.02892-14.
406. Bridges, R. G., Sohn, S. Y., Wright, J., Leppard, K. N. & Hearing, P. The adenovirus E4-ORF3 protein stimulates SUMOylation of general transcription factor TFII-I to direct proteasomal degradation. *MBio* (2016) doi:10.1128/mBio.02184-15.
407. Sohn, S. Y. & Hearing, P. The adenovirus E4-ORF3 protein functions as a SUMO E3 ligase for TIF-1γ sumoylation and poly-SUMO chain elongation. *Proc. Natl. Acad. Sci. U. S. A.* (2016) doi:10.1073/pnas.1603872113.
408. Sohn, S. Y. & Hearing, P. Mechanism of Adenovirus E4-ORF3-Mediated SUMO Modifications. *MBio* (2019) doi:10.1128/mBio.00022-19.
409. Higginbotham, J. M. & O'Shea, C. C. Adenovirus E4-ORF3 Targets PIAS3 and Together with E1B-55K Remodels SUMO Interactions in the Nucleus and at Virus Genome Replication Domains. *J. Virol.* (2015) doi:10.1128/jvi.01091-15.
410. Stubbe, M. *et al.* Viral DNA binding protein SUMOylation promotes PML nuclear body localization next to viral replication centers. *MBio* (2020) doi:10.1128/mBio.00049-20.
411. Freudenberger, N., Meyer, T., Groitl, P., Dobner, T. & Schreiner, S. HAdV protein V core protein is targeted by the host SUMOylation machinery to limit essential viral functions. *J. Virol.* (2017) doi:10.1128/jvi.01451-17.
412. Balakirev, M. Y., Jaquinod, M., Haas, A. L. & Chroboczek, J. Deubiquitinating function of adenovirus proteinase. *J. Virol.* **76**, 6323–31 (2002).
413. Martin, M. E. D. & Berk, A. J. Adenovirus E1B 55K Represses p53 Activation In Vitro. *J. Virol.* (1998) doi:10.1128/jvi.72.4.3146-3154.1998.

414. Blackford, A. N. & Grand, R. J. A. Adenovirus E1B 55-Kilodalton Protein: Multiple Roles in Viral Infection and Cell Transformation. *J. Virol.* (2009) doi:10.1128/jvi.02417-08.
415. Dobbelstein, M., Roth, J., Kimberly, W. T., Levine, A. J. & Shenk, T. Nuclear export of the E1B 55-kDa and E4 34-kDa adenoviral oncoproteins mediated by a rev-like signal sequence. *EMBO J.* (1997) doi:10.1093/emboj/16.14.4276.
416. Dosch, T. *et al.* The Adenovirus Type 5 E1B-55K Oncoprotein Actively Shuttles in Virus-Infected Cells, Whereas Transport of E4orf6 Is Mediated by a CRM1-Independent Mechanism. *J. Virol.* (2001) doi:10.1128/jvi.75.12.5677-5683.2001.
417. Krätzer, F. *et al.* The adenovirus type 5 E1B-55K oncoprotein is a highly active shuttle protein and shuttling is independent of E4orf6, p53 and Mdm2. *Oncogene* (2000) doi:10.1038/sj.onc.1203395.
418. Endter, C., Kzhyshkowska, J., Stauber, R. & Dobner, T. SUMO-1 modification required for transformation by adenovirus type 5 early region 1B 55-kDa oncoprotein. *Proc. Natl. Acad. Sci. U. S. A.* (2001) doi:10.1073/pnas.191361798.
419. Kindsmüller, K. *et al.* Intranuclear targeting and nuclear export of the adenovirus E1B-55K protein are regulated by SUMO1 conjugation. *Proc. Natl. Acad. Sci. U. S. A.* (2007) doi:10.1073/pnas.0702158104.
420. Härtl, B., Zeller, T., Blanchette, P., Kremmer, E. & Dobner, T. Adenovirus type 5 early region 1B 55-kDa oncoprotein can promote cell transformation by a mechanism independent from blocking p53-activated transcription. *Oncogene* (2008) doi:10.1038/sj.onc.1211039.
421. Rubenwolf, S., Schütt, H., Nevels, M., Wolf, H. & Dobner, T. Structural analysis of the adenovirus type 5 E1B 55-kilodalton-E4orf6 protein complex. *J. Virol.* (1997) doi:10.1128/jvi.71.2.1115-1123.1997.
422. Kao, C. C., Yew, P. R. & Berk, A. J. Domains required for in vitro association between the cellular p53 and the adenovirus 2 E1B 55k proteins. *Virology* (1990) doi:10.1016/0042-6822(90)90148-K.
423. Teodoro, J. G. *et al.* Phosphorylation at the carboxy terminus of the 55-kilodalton adenovirus type 5 E1B protein regulates transforming activity. *J. Virol.* (1994) doi:10.1128/jvi.68.2.776-786.1994.
424. Teodoro, J. G. & Branton, P. E. Regulation of p53-dependent apoptosis, transcriptional repression, and cell transformation by phosphorylation of the 55-kilodalton E1B protein of human adenovirus type 5. *J. Virol.* (1997) doi:10.1128/jvi.71.5.3620-3627.1997.
425. Ching, W., Dobner, T. & Koyuncu, E. The Human Adenovirus Type 5 E1B 55-Kilodalton Protein Is Phosphorylated by Protein Kinase CK2. *J. Virol.* (2012) doi:10.1128/jvi.06066-11.
426. Blanchette, P. *et al.* Both BC-Box Motifs of Adenovirus Protein E4orf6 Are Required To Efficiently Assemble an E3 Ligase Complex That Degrades p53. *Mol. Cell. Biol.* (2004) doi:10.1128/mcb.24.21.9619-9629.2004.
427. Liu, Y., Shevchenko, A., Shevchenko, A. & Berk, A. J. Adenovirus Exploits the Cellular Aggresome Response To Accelerate Inactivation of the MRN Complex. *J. Virol.* (2005) doi:10.1128/jvi.79.22.14004-14016.2005.
428. Johnston, J. A., Ward, C. L. & Kopito, R. R. Aggresomes: A cellular response to misfolded proteins. *J. Cell Biol.* (1998) doi:10.1083/jcb.143.7.1883.
429. Leppard, K. N. & Everett, R. D. The adenovirus type 5 E1b 55K and E4 Orf3 proteins associate in infected cells and affect ND10 components. *J. Gen. Virol.* (1999) doi:10.1099/0022-1317-80-4-997.

430. Lethbridge, K. J., Scott, G. E. & Leppard, K. N. Nuclear matrix localization and SUMO-1 modification of adenovirus type 5 E1b 55K protein are controlled by E4 Orf6 protein. *Journal of General Virology* (2003) doi:10.1099/vir.0.18820-0.
431. Goodrum, F. D., Shenk, T. & Ornelles, D. A. Adenovirus early region 4 34-kilodalton protein directs the nuclear localization of the early region 1B 55-kilodalton protein in primate cells. *J. Virol.* (1996) doi:10.1128/jvi.70.9.6323-6335.1996.
432. Marshall, L. J. *et al.* RUNX1 Permits E4orf6-Directed Nuclear Localization of the Adenovirus E1B-55K Protein and Associates with Centers of Viral DNA and RNA Synthesis. *J. Virol.* (2008) doi:10.1128/jvi.00043-08.
433. White, E. & Cipriani, R. Role of adenovirus E1B proteins in transformation: altered organization of intermediate filaments in transformed cells that express the 19-kilodalton protein. *Mol. Cell. Biol.* (1990) doi:10.1128/mcb.10.1.120.
434. Schwartz, R. A. *et al.* Distinct Requirements of Adenovirus E1b55K Protein for Degradation of Cellular Substrates. *J. Virol.* (2008) doi:10.1128/jvi.00925-08.
435. Querido, E. *et al.* Degradation of p53 by adenovirus E4orf6 and E1B55K proteins occurs via a novel mechanism involving a Cullin-containing complex. *Genes Dev.* (2001) doi:10.1101/gad.926401.
436. Guo, H. *et al.* Adenovirus oncoprotein E4orf6 triggers Cullin5 neddylation to activate the CLR5 E3 ligase for p53 degradation. *Biochem. Biophys. Res. Commun.* (2019) doi:10.1016/j.bbrc.2019.07.028.
437. Schreiner, S. *et al.* SPOC1-Mediated Antiviral Host Cell Response Is Antagonized Early in Human Adenovirus Type 5 Infection. *PLoS Pathog.* (2013) doi:10.1371/journal.ppat.1003775.
438. Baker, A., Rohleder, K. J., Hanakahi, L. A. & Ketner, G. Adenovirus E4 34k and E1b 55k Oncoproteins Target Host DNA Ligase IV for Proteasomal Degradation. *J. Virol.* (2007) doi:10.1128/jvi.00029-07.
439. Orazio, N. I., Naeger, C. M., Karlseder, J. & Weitzman, M. D. The Adenovirus E1b55K/E4orf6 Complex Induces Degradation of the Bloom Helicase during Infection. *J. Virol.* (2011) doi:10.1128/jvi.02134-10.
440. Chalabi Hagkarim, N. *et al.* Degradation of a Novel DNA Damage Response Protein, Tankyrase 1 Binding Protein 1, following Adenovirus Infection. *J. Virol.* (2018) doi:10.1128/jvi.02034-17.
441. Gupta, A., Jha, S., Engel, D. A., Ornelles, D. A. & Dutta, A. Tip60 degradation by adenovirus relieves transcriptional repression of viral transcriptional activator EIA. *Oncogene* (2013) doi:10.1038/onc.2012.534.
442. Beltz, G. A. & Flint, S. J. Inhibition of HeLa cell protein synthesis during adenovirus infection. Restriction of cellular messenger RNA sequences to the nucleus. *J. Mol. Biol.* (1979) doi:10.1016/0022-2836(79)90081-0.
443. Blanchette, P. *et al.* Control of mRNA Export by Adenovirus E4orf6 and E1B55K Proteins during Productive Infection Requires E4orf6 Ubiquitin Ligase Activity. *J. Virol.* (2008) doi:10.1128/jvi.02309-07.
444. Woo, J. L. & Berk, A. J. Adenovirus Ubiquitin-Protein Ligase Stimulates Viral Late mRNA NuclearExport. *J. Virol.* (2007) doi:10.1128/jvi.01725-06.
445. Sarnow, P. *et al.* Adenovirus early region 1B 58,000-dalton tumor antigen is physically associated with an early region 4 25,000-dalton protein in productively infected cells. *J. Virol.* (1984) doi:10.1128/jvi.49.3.692-700.1984.
446. Yew, P. R., Liu, X. & Berk, A. J. Adenovirus E1B oncoprotein tethers a transcriptional repression domain to p53. *Genes Dev.* (1994)

doi:10.1101/gad.8.2.190.
447. Zantema, A. *et al.* Localization of the E1 B proteins of adenovirus 5 in transformed cells, as revealed by interaction with monoclonal antibodies. *Virology* (1985) doi:10.1016/0042-6822(85)90421-0.
448. Garcia-Mata, R., Gao, Y. S. & Sztul, E. Hassles with taking out the garbage: Aggravating aggresomes. *Traffic* (2002) doi:10.1034/j.1600-0854.2002.30602.x.
449. Muller, S. & Dobner, T. The adenovirus E1B-55K oncoprotein induces SUMO modification of p53. *Cell Cycle* (2008) doi:10.4161/cc.7.6.5495.
450. Pennella, M. A., Liu, Y., Woo, J. L., Kim, C. A. & Berk, A. J. Adenovirus E1B 55-Kilodalton Protein Is a p53-SUMO1 E3 Ligase That Represses p53 and Stimulates Its Nuclear Export through Interactions with Promyelocytic Leukemia Nuclear Bodies. *J. Virol.* (2010) doi:10.1128/jvi.01442-10.
451. Liu, Y., Colosimo, A. L., Yang, X.-J. & Liao, D. Adenovirus E1B 55-Kilodalton Oncoprotein Inhibits p53 Acetylation by PCAF. *Mol. Cell. Biol.* (2000) doi:10.1128/mcb.20.15.5540-5553.2000.
452. Fischer, M. Census and evaluation of p53 target genes. *Oncogene* **36**, 3943–3956 (2017).
453. Yew, P. R. & Berk, A. J. Inhibition of p53 transactivation required for transformation by adenovirus early 1B protein. *Nature* (1992) doi:10.1038/357082a0.
454. Endter, C., Härtl, B., Spruss, T., Hauber, J. & Dobner, T. Blockage of CRM1-dependent nuclear export of the adenovirus type 5 early region 1B 55-kDa protein augments oncogenic transformation of primary rat cells. *Oncogene* (2005) doi:10.1038/sj.onc.1208170.
455. Wimmer, P. *et al.* SUMO modification of E1B-55K oncoprotein regulates isoform-specific binding to the tumour suppressor protein PML. *Oncogene* (2010) doi:10.1038/onc.2010.284.
456. Wimmer, P. *et al.* PML isoforms IV and v contribute to adenovirus-mediated oncogenic transformation by functionally inhibiting the tumor-suppressor p53. *Oncogene* (2016) doi:10.1038/onc.2015.63.
457. Berscheminski, J. *et al.* Sp100A is a tumor suppressor that activates p53-dependent transcription and counteracts E1A/E1B-55K-mediated transformation. *Oncogene* (2016) doi:10.1038/onc.2015.378.
458. Schreiner, S. *et al.* Proteasome-Dependent Degradation of Daxx by the Viral E1B-55K Protein in Human Adenovirus-Infected Cells. *J. Virol.* (2010) doi:10.1128/jvi.00074-10.
459. Müncheberg, S. *et al.* E1B-55K-Mediated Regulation of RNF4 SUMO-Targeted Ubiquitin Ligase Promotes Human Adenovirus Gene Expression. *J. Virol.* (2018) doi:10.1128/jvi.00164-18.
460. Bürck, C. *et al.* KAP1 Is a Host Restriction Factor That Promotes Human Adenovirus E1B-55K SUMO Modification. *J. Virol.* (2016) doi:10.1128/jvi.01836-15.
461. Wimmer, P. *et al.* Cross-talk between phosphorylation and SUMOylation regulates transforming activities of an adenoviral oncoprotein. *Oncogene* (2013) doi:10.1038/onc.2012.187.
462. Ardito, F., Giuliani, M., Perrone, D., Troiano, G. & Lo Muzio, L. The crucial role of protein phosphorylation in cell signaling and its use as targeted therapy (Review). *Int. J. Mol. Med.* **40**, 271–280 (2017).
463. Schreiner, S. *et al.* Adenovirus Type 5 Early Region 1B 55K Oncoprotein-

Dependent Degradation of Cellular Factor Daxx Is Required for Efficient Transformation of Primary Rodent Cells. *J. Virol.* (2011) doi:10.1128/jvi.00440-11.

464. Tatham, M. H., Rodriguez, M. S., Xirodimas, D. P. & Hay, R. T. Detection of protein SUMOylation in vivo. *Nat. Protoc.* (2009) doi:10.1038/nprot.2009.128.
465. Schreiner, S., Wimmer, P. & Dobner, T. Adenovirus degradation of cellular proteins. *Future Microbiology* (2012) doi:10.2217/fmb.11.153.
466. Cheng, C. Y. *et al.* The E4orf6/E1B55K E3 Ubiquitin Ligase Complexes of Human Adenoviruses Exhibit Heterogeneity in Composition and Substrate Specificity. *J. Virol.* (2011) doi:10.1128/jvi.01890-10.
467. Blanchette, P. & Branton, P. E. Manipulation of the ubiquitin-proteasome pathway by small DNA tumor viruses. *Virology* (2009) doi:10.1016/j.virol.2008.10.005.
468. Dallaire, F. *et al.* The Human Adenovirus Type 5 E4orf6/E1B55K E3 Ubiquitin Ligase Complex Can Mimic E1A Effects on E2F. *mSphere* (2016) doi:10.1128/msphere.00014-15.
469. Békés, M. *et al.* The dynamics and mechanism of SUMO chain deconjugation by SUMO-specific proteases. *J. Biol. Chem.* (2011) doi:10.1074/jbc.M110.205153.
470. Groitl, P. & Dobner, T. Construction of adenovirus type 5 early region 1 and 4 virus mutants. *Methods Mol. Med.* (2007) doi:10.1385/1-59745-166-5:29.
471. Wang, H. *et al.* Improved seamless mutagenesis by recombineering using ccdB for counterselection. *Nucleic Acids Res.* (2014) doi:10.1093/nar/gkt1339.
472. Zhang, W. *et al.* An Engineered Virus Library as a Resource for the Spectrum-wide Exploration of Virus and Vector Diversity. *Cell Rep.* (2017) doi:10.1016/j.celrep.2017.05.008.
473. Yew, P. R., Cheng Kao, C. & Berk, A. J. Dissection of functional domains in the adenovirus 2 early 1b 55k polypeptide by suppressor-linker insertional mutagenesis. *Virology* (1990) doi:10.1016/0042-6822(90)90147-J.
474. Harada, J. N., Shevchenko, A., Shevchenko, A., Pallas, D. C. & Berk, A. J. Analysis of the Adenovirus E1B-55K-Anchored Proteome Reveals Its Link to Ubiquitination Machinery. *J. Virol.* (2002) doi:10.1128/jvi.76.18.9194-9206.2002.
475. Babiss, L. E., Ginsberg, H. S. & Darnell, J. E. Adenovirus E1B proteins are required for accumulation of late viral mRNA and for effects on cellular mRNA translation and transport. *Mol. Cell. Biol.* (1985) doi:10.1128/mcb.5.10.2552.
476. Bridge, E. & Ketner, G. Interaction of adenoviral E4 and E1b products in late gene expression. *Virology* (1990) doi:10.1016/0042-6822(90)90088-9.
477. Halbert, D. N., Cutt, J. R. & Shenk, T. Adenovirus early region 4 encodes functions required for efficient DNA replication, late gene expression, and host cell shutoff. *J. Virol.* (1985) doi:10.1128/jvi.56.1.250-257.1985.
478. Leppard, K. N. & Shenk, T. The adenovirus E1B 55 kd protein influences mRNA transport via an intranuclear effect on RNA metabolism. *EMBO J.* (1989) doi:10.1002/j.1460-2075.1989.tb08360.x.
479. Hagemeier, S. R. *et al.* Sumoylation of the Epstein-Barr Virus BZLF1 Protein Inhibits Its Transcriptional Activity and Is Regulated by the Virus-Encoded Protein Kinase. *J. Virol.* (2010) doi:10.1128/jvi.02369-09.
480. Murata, T. *et al.* Transcriptional repression by sumoylation of Epstein-Barr virus BZLF1 protein correlates with association of histone deacetylase. *J. Biol. Chem.* (2010) doi:10.1074/jbc.M109.095356.
481. Campbell, M. & Izumiya, Y. Post-translational modifications of Kaposi's sarcoma-associated herpesvirus regulatory proteins - SUMO and KSHV. *Front. Microbiol.*

(2012) doi:10.3389/fmicb.2012.00031.
482. Liao, W., Tang, Y., Lin, S.-F., Kung, H.-J. & Giam, C.-Z. K-bZIP of Kaposi's Sarcoma-Associated Herpesvirus/Human Herpesvirus 8 (KSHV/HHV-8) Binds KSHV/HHV-8 Rta and Represses Rta-Mediated Transactivation. *J. Virol.* (2003) doi:10.1128/jvi.77.6.3809-3815.2003.
483. Lion, T. Adenovirus persistence, reactivation, and clinical management. *FEBS Letters* (2019) doi:10.1002/1873-3468.13576.
484. Radke, J. R. & Cook, J. L. Human adenovirus infections: Update and consideration of mechanisms of viral persistence. *Current Opinion in Infectious Diseases* (2018) doi:10.1097/QCO.0000000000000451.
485. Mynarek, M. *et al.* Patient, virus, and treatment-related risk factors in pediatric adenovirus infection after stem cell transplantation: Results of a routine monitoring program. *Biol. Blood Marrow Transplant.* (2014) doi:10.1016/j.bbmt.2013.11.009.
486. Chakrabarti, S. *et al.* Adenovirus infections following allogeneic stem cell transplantation: Incidence and outcome in relation to graft manipulation, immunosuppression, and immune recovery. *Blood* (2002) doi:10.1182/blood-2002-02-0377.
487. Kaeuferle, T., Krauss, R., Blaeschke, F., Willier, S. & Feuchtinger, T. Strategies of adoptive T -cell transfer to treat refractory viral infections post allogeneic stem cell transplantation. *Journal of Hematology and Oncology* (2019) doi:10.1186/s13045-019-0701-1.
488. Tzannou, I. *et al.* Off-the-shelf virus-specific T cells to treat BK virus, human herpesvirus 6, cytomegalovirus, Epstein-Barr virus, and adenovirus infections after allogeneic hematopoietic stem-cell transplantation. *J. Clin. Oncol.* (2017) doi:10.1200/JCO.2017.73.0655.
489. Branton, P. E., Bayley, S. T. & Graham, F. L. Transformation by human adenoviruses. *BBA - Reviews on Cancer* (1984) doi:10.1016/0304-419X(84)90007-6.
490. Kuwano, K. *et al.* Detection of adenovirus E1A DNA in pulmonary fibrosis using nested polymerase chain reaction. *Eur. Respir. J.* (1997) doi:10.1183/09031936.97.10071445.
491. Tatsis, N. *et al.* Adenoviral vectors persist in vivo and maintain activated CD8+ T cells: Implications for their use as vaccines. *Blood* (2007) doi:10.1182/blood-2007-02-062117.
492. Rodríguez, E. *et al.* Humanized Mice Reproduce Acute and Persistent Human Adenovirus Infection. *J. Infect. Dis.* (2017) doi:10.1093/infdis/jiw499.
493. Knipscheer, P., Van Dijk, W. J., Olsen, J. V., Mann, M. & Sixma, T. K. Noncovalent interaction between Ubc9 and SUMO promotes SUMO chain formation. *EMBO J.* (2007) doi:10.1038/sj.emboj.7601711.
494. Boggio, R., Passafaro, A. & Chiocca, S. Targeting SUMO E1 to ubiquitin ligases: A viral strategy to counteract sumoylation. *J. Biol. Chem.* (2007) doi:10.1074/jbc.M700889200.
495. Heaton, P. R., Deyrieux, A. F., Bian, X. L. & Wilson, V. G. HPV E6 proteins target Ubc9, the SUMO conjugating enzyme. *Virus Res.* (2011) doi:10.1016/j.virusres.2011.04.001.
496. Kane, E. M. & Shuman, S. Vaccinia virus morphogenesis is blocked by a temperature-sensitive mutation in the I7 gene that encodes a virion component. *J. Virol.* (1993) doi:10.1128/jvi.67.5.2689-2698.1993.

497. Andrés, G., Alejo, A., Simón-Mateo, C. & Salas, M. L. African swine fever virus protease, a new viral member of the SUMO-1-specific protease family. *J. Biol. Chem.* (2001) doi:10.1074/jbc.M006844200.
498. Bailey, D. & O'Hare, P. Herpes simplex virus 1 ICPO co-localizes with a SUMO-specific protease. *Journal of General Virology* (2002) doi:10.1099/0022-1317-83-12-2951.
499. Malakhov, M. P. *et al.* SUMO fusions and SUMO-specific protease for efficient expression and purification of proteins. *J. Struct. Funct. Genomics* (2004) doi:10.1023/B:JSFG.0000029237.70316.52.
500. Cesaro, L., Pinna, L. A. & Salvi, M. A Comparative Analysis and Review of lysyl Residues Affected by Posttranslational Modifications. *Curr. Genomics* (2015) doi:10.2174/1389202916666150216221038.
501. Mohideen, F. *et al.* A molecular basis for phosphorylation-dependent SUMO conjugation by the E2 UBC9. *Nat. Struct. Mol. Biol.* (2009) doi:10.1038/nsmb.1648.
502. Hendriks, I. A. *et al.* Site-specific mapping of the human SUMO proteome reveals co-modification with phosphorylation. *Nat. Struct. Mol. Biol.* (2017) doi:10.1038/nsmb.3366.
503. Garibal, J. *et al.* Truncated Form of the Epstein-Barr Virus Protein EBNA-LP Protects against Caspase-Dependent Apoptosis by Inhibiting Protein Phosphatase 2A. *J. Virol.* (2007) doi:10.1128/jvi.02435-06.
504. Kleinberger, T. & Shenk, T. Adenovirus E4orf4 protein binds to protein phosphatase 2A, and the complex down regulates E1A-enhanced junB transcription. *J. Virol.* (1993) doi:10.1128/jvi.67.12.7556-7560.1993.
505. Shtrichman, R., Sharf, R., Barr, H., Dobner, T. & Kleinberger, T. Induction of apoptosis by adenovirus E4orf4 protein is specific to transformed cells and requires an interaction with protein phosphatase 2A. *Proc. Natl. Acad. Sci. U. S. A.* (1999) doi:10.1073/pnas.96.18.10080.
506. Dilworth, S. M. Polyoma virus middle T antigen and its role in identifying cancer-related molecules. *Nature Reviews Cancer* (2002) doi:10.1038/nrc946.
507. Benjamin, T. L. Polyoma virus: Old findings and new challenges. *Virology* (2001) doi:10.1006/viro.2001.1124.
508. Georgopoulou, U., Tsitoura, P., Kalamvoki, M. & Mavromara, P. The protein phosphatase 2A represents a novel cellular target for hepatitis C virus NS5A protein. *Biochimie* (2006) doi:10.1016/j.biochi.2005.12.003.
509. Tejera, B. *et al.* The human adenovirus type 5 E1B 55kDa protein interacts with RNA promoting timely DNA replication and viral late mRNA metabolism. *PLoS One* (2019) doi:10.1371/journal.pone.0214882.
510. Sieber, T. *et al.* Intrinsic disorder in the common N-terminus of human adenovirus 5 E1B-55K and its related E1BN proteins indicated by studies on E1B-93R. *Virology* (2011) doi:10.1016/j.virol.2011.07.012.
511. Van Der Lee, R. *et al.* Classification of intrinsically disordered regions and proteins. *Chemical Reviews* (2014) doi:10.1021/cr400525m.
512. Kim, E. T. *et al.* Analysis of human cytomegalovirus-encoded SUMO targets and temporal regulation of SUMOylation of the immediate-early proteins IE1 and IE2 during infection. *PLoS One* (2014) doi:10.1371/journal.pone.0103308.
513. Hidalgo, P., Ip, W. H., Dobner, T. & Gonzalez, R. A. The biology of the adenovirus E1B 55K protein. *FEBS Letters* (2019) doi:10.1002/1873-3468.13694.
514. Gareau, J. R. & Lima, C. D. The SUMO pathway: Emerging mechanisms that

shape specificity, conjugation and recognition. *Nature Reviews Molecular Cell Biology* (2010) doi:10.1038/nrm3011.
515. Selby, T. L. *et al.* The Epstein-Barr Virus Oncoprotein, LMP1, Regulates the Function of SENP2, a SUMO-protease. *Sci. Rep.* (2019) doi:10.1038/s41598-019-45825-5.
516. Zhong, S. *et al.* Role of SUMO-1-modified PML in nuclear body formation. *Blood* (2000) doi:10.1182/blood.v95.9.2748.009k31a_2748_2752.
517. Lallemand-Breitenbach, V. *et al.* Arsenic degrades PML or PML-RARα through a SUMO-triggered RNF4/ ubiquitin-mediated pathway. *Nat. Cell Biol.* (2008) doi:10.1038/ncb1717.
518. Sahin Umut, U. *et al.* Oxidative stress-induced assembly of PML nuclear bodies controls sumoylation of partner proteins. *J. Cell Biol.* (2014) doi:10.1083/jcb.201305148.
519. Kamitani, T. *et al.* Identification of three major sentrinization sites in PML. *J. Biol. Chem.* (1998) doi:10.1074/jbc.273.41.26675.
520. Brand, P., Lenser, T. & Hemmerich, P. Assembly dynamics of PML nuclear bodies in living cells. *PMC Biophys.* (2010) doi:10.1186/1757-5036-3-3.
521. Hecker, C. M., Rabiller, M., Haglund, K., Bayer, P. & Dikic, I. Specification of SUMO1- and SUMO2-interacting motifs. *J. Biol. Chem.* (2006) doi:10.1074/jbc.M512757200.
522. Matunis, M. J., Zhang, X. D. & Ellis, N. A. SUMO: The Glue that Binds. *Developmental Cell* (2006) doi:10.1016/j.devcel.2006.10.011.
523. Alandijany, T. *et al.* Distinct temporal roles for the promyelocytic leukaemia (PML) protein in the sequential regulation of intracellular host immunity to HSV-1 infection. *PLoS Pathog.* (2018) doi:10.1371/journal.ppat.1006769.
524. Everett, R. D., Parsy, M.-L. & Orr, A. Analysis of the Functions of Herpes Simplex Virus Type 1 Regulatory Protein ICP0 That Are Critical for Lytic Infection and Derepression of Quiescent Viral Genomes. *J. Virol.* (2009) doi:10.1128/jvi.02593-08.
525. Boutell, C., Orr, A. & Everett, R. D. PML Residue Lysine 160 Is Required for the Degradation of PML Induced by Herpes Simplex Virus Type 1 Regulatory Protein ICP0. *J. Virol.* (2003) doi:10.1128/jvi.77.16.8686-8694.2003.
526. Cuchet-Lourenco, D., Vanni, E., Glass, M., Orr, A. & Everett, R. D. Herpes Simplex Virus 1 Ubiquitin Ligase ICP0 Interacts with PML Isoform I and Induces Its SUMO-Independent Degradation. *J. Virol.* (2012) doi:10.1128/jvi.01145-12.
527. Everett, R., O'Hare, P., O'Rourke, D., Barlow, P. & Orr, A. Point mutations in the herpes simplex virus type 1 Vmw110 RING finger helix affect activation of gene expression, viral growth, and interaction with PML-containing nuclear structures. *J. Virol.* (1995) doi:10.1128/jvi.69.11.7339-7344.1995.
528. Everett, R. D. & Maul, G. G. HSV-1 IE protein Vmw110 causes redistribution of PML. *EMBO J.* (1994) doi:10.1002/j.1460-2075.1994.tb06835.x.
529. O'Rourke, D. & O'Hare, P. Mutually exclusive binding of two cellular factors within a critical promoter region of the gene for the IE110k protein of herpes simplex virus. *J. Virol.* (1993) doi:10.1128/jvi.67.12.7201-7214.1993.
530. Hattersley, N., Shen, L., Jaffray, E. G. & Hay, R. T. The SUMO protease SENP6 is a direct regulator of PML nuclear bodies. *Mol. Biol. Cell* (2011) doi:10.1091/mbc.E10-06-0504.
531. Dallaire, F., Blanchette, P., Groitl, P., Dobner, T. & Branton, P. E. Identification of Integrin α3 as a New Substrate of the Adenovirus E4orf6/E1B 55-Kilodalton

E3 Ubiquitin Ligase Complex. *J. Virol.* (2009) doi:10.1128/jvi.00089-09.
532. Babiss, L. E. & Ginsberg, H. S. Adenovirus type 5 early region 1b gene product is required for efficient shutoff of host protein synthesis. *J. Virol.* (1984) doi:10.1128/jvi.50.1.202-212.1984.
533. Pilder, S., Moore, M., Logan, J. & Shenk, T. The adenovirus E1B-55K transforming polypeptide modulates transport or cytoplasmic stabilization of viral and host cell mRNAs. *Mol. Cell. Biol.* (1986) doi:10.1128/mcb.6.2.470.
534. Chow, K. H., Elgort, S., Dasso, M., Powers, M. A. & Ullman, K. S. The SUMO proteases SENP1 and SENP2 play a critical role in nucleoporin homeostasis and nuclear pore complex function. *Mol. Biol. Cell* (2014) doi:10.1091/mbc.E13-05-0256.
535. Duheron, V., Nilles, N., Pecenko, S., Martinelli, V. & Fahrenkrog, B. Localisation of Nup153 and SENP1 to nuclear pore complexes is required for 53BP1-mediated DNA double-strand break repair. *J. Cell Sci.* (2017) doi:10.1242/jcs.198390.
536. Cutt, J. R., Shenk, T. & Hearing, P. Analysis of adenovirus early region 4-encoded polypeptides synthesized in productively infected cells. *J. Virol.* (1987) doi:10.1128/jvi.61.2.543-552.1987.
537. Smiley, J. K., Young, M. A. & Flint, S. J. Intranuclear location of the adenovirus type 5 E1B 55-kilodalton protein. *J. Virol.* (1990) doi:10.1128/jvi.64.9.4558-4564.1990.
538. Öhman, K., Nordqvist, K. & Akusjärvi, Gö. Two adenovirus proteins with redundant activities in virus growth facilitates tripartite leader mrna accumulation. *Virology* (1993) doi:10.1006/viro.1993.1234.
539. Muller, D. *et al.* Functional Cooperation between Human Adenovirus Type 5 Early Region 4, Open Reading Frame 6 Protein, and Cellular Homeobox Protein HoxB7. *J. Virol.* (2012) doi:10.1128/jvi.00222-12.
540. Dallaire, F. *et al.* The Human Adenovirus Type 5 E4orf6/E1B55K E3 Ubiquitin Ligase Complex Enhances E1A Functional Activity. *mSphere* (2016) doi:10.1128/msphere.00015-15.
541. O'Connor, R. J. & Hearing, P. The E4-6/7 Protein Functionally Compensates for the Loss of E1A Expression in Adenovirus Infection. *J. Virol.* (2000) doi:10.1128/jvi.74.13.5819-5824.2000.
542. Schaley, J. E., Polonskaia, M. & Hearing, P. The Adenovirus E4-6/7 Protein Directs Nuclear Localization of E2F-4 via an Arginine-Rich Motif. *J. Virol.* (2005) doi:10.1128/jvi.79.4.2301-2308.2005.
543. Psakhye, I. & Jentsch, S. Protein group modification and synergy in the SUMO pathway as exemplified in DNA repair. *Cell* (2012) doi:10.1016/j.cell.2012.10.021.
544. Jentsch, S. & Psakhye, I. Control of nuclear activities by substrate-selective and protein-group SUMOylation. *Annual Review of Genetics* (2013) doi:10.1146/annurev-genet-111212-133453.
545. Zunino, R., Schauss, A., Rippstein, P., Andrade-Navarro, M. & McBride, H. M. The SUMO protease SENP5 is required to maintain mitochondrial morphology and function. *J. Cell Sci.* (2007) doi:10.1242/jcs.03418.
546. Nayak, A., Viale-Bouroncle, S., Morsczeck, C. & Muller, S. The SUMO-specific isopeptidase SENP3 regulates MLL1/MLL2 methyltransferase complexes and controls osteogenic differentiation. *Mol. Cell* (2014) doi:10.1016/j.molcel.2014.05.011.

547. Vereb, G., Nagy, P. & Szöllosi, J. Flow cytometric FRET analysis of protein interaction. *Methods Mol. Biol.* (2011) doi:10.1007/978-1-61737-950-5_18.
548. Kumar, A. & Zhang, K. Y. J. Advances in the development of SUMO specific protease (SENP) inhibitors. *Computational and Structural Biotechnology Journal* (2015) doi:10.1016/j.csbj.2015.03.001.
549. Chen, S., Dong, D., Xin, W. & Zhou, H. Progress in the discovery of small molecule modulators of desumoylation. *Curr. Issues Mol. Biol.* (2020) doi:10.21775/cimb.035.017.

Acknowledgements

Zuerst möchte ich mich bei meinem Doktorvater Thomas Dobner dafür bedanken, dass er mir die Möglichkeit gegeben hat in der Abteilung für virale Transformation meine Doktorarbeit anzufertigen. Weiterhin danke ich ihm für die Sammlung kleiner Kunstwerke die während unserer Projektbesprechungen entstanden sind, sie werden mich auch in Zukunft an die tolle Zeit am HPI erinnern.

Vielen Dank auch an Wolfram Brune für die Übernahme des Zweitgutachtens, Julia Kehr für die Übernahme des Vorsitzes der Prüfungskommission und an Joachim Hauber und Giada Frascaroli für die Mitwirkung in der Prüfungskommission.

Außerdem möchte ich Timothy Soh für die Übernahme des Sprachgutachtens danken.

Ein ganz besonders großes Dankeschön geht an Wing-Hang Ip für das Lesen und die Korrektur dieser Arbeit und natürlich die Unterstützung und Hilfe während des gesamten Projekts. An dieser Stelle möchte ich mich auch bei Tina Meyer, Britta Wilkens, Sören Pfitzner, Laura Seddar, Konstantin von Stromberg, Renke Brixel und Andreas Gehrmann für Lesen und Korrektur der Arbeit bedanken. Euch, sowie Edda Renz, Gabi Dobner, Willi Ching und Bernd Hartz möchte ich außerdem für die tollen Jahre am HPI danken, die vielen Diskussionen, Kaffeepausen, Weihnachtsfeiern, Konferenzen, Labor Ausflüge und Abende in unserer Küche haben die Zeit unvergesslich gemacht. Hier möchte ich mich auch bei meinen ehemaligen Laborkollegen Vicky Kolbe, Steween Krone, und Michael Melling bedanken. Außerdem möchte ich mich bei meinem Master Studenten Francis Nkrumah für sein außergewöhnliches Engagement bedanken.

Zuletzt möchte ich noch ein großes Dankeschön an meine Freunde, Familie und meinen Freund Andreas aussprechen. Vielen lieben Dank für Eure Hilfe und Unterstützung, ohne die ich manchmal verzweifelt wäre.